Etude de l'état de santé des écosystèmes côtiers sud méditerranéensanthropisés par application des modèles du réseau trophique planctonique et des indicateurs écologiques en situation de contamination chronique & pulsée

Oumayma Chkili

Normandie Université

UNIVERSITÉ CAEN NORMANDIE

THÈSE

Pour obtenir le diplôme de doctorat

Spécialité PHYSIOLOGIE ET BIOLOGIE DES ORGANISMES - POPULATIONS - INTERACTIONS

Préparée au sein de l'Université de Caen Normandie

En cotutelle internationale avec Université de Carthage , TUNISIE

Etude de l'état de santé des écosystèmes côtiers sud méditerranéens anthropisés par application des modèles du réseau trophique planctonique et des indicateurs écologiques en situation de contamination chronique & pulsée.

Présentée et soutenue par
OUMAYMA CHKILI

Thèse soutenue le 12/07/2023 devant le jury composé de		
M. ZAHER DRIRA	Maître de conférences HDR, Faculté des Sciences de Gafsa	Rapporteur du jury
M. TELESPHORE SIME-NGANDO	Directeur de recherche, UNIVERSITE CLERMONT FERRAND 1 AUVERGNE	Rapporteur du jury
MME MALIKA BEL HASSEN	Professeur, INSTM Tunis	Membre du jury
M. OLIVIER PRINGAULT	Directeur de recherche, Université de Toulon	Membre du jury
M. EZZEDDINE MAHMOUDI	Professeur, Université de Carthage	Président du jury
MME NATHALIE NIQUIL	Directeur de recherche, Université de Caen Normandie	Directeur de thèse
MME HLAILI ASMA SAKKA	Professeur, Université de Carthage	Co-directeur de thèse

Thèse dirigée par NATHALIE NIQUIL (Biologie des organismes et ecosystèmes aquatiques (Caen)) et HLAILI ASMA SAKKA

ED 497 NBISE
Normande de Biologie Intégrative, Santé, Environnement

BOREA
Biologie des organismes et écosystèmes aquatiques

Avant propos

Les travaux de recherche de la thèse ont été réalisés au sein du laboratoire de Phytoplanctonologie & de Biologie Végétale à la Faculté des Sciences de Bizerte, Université de Carthage, et le Laboratoire de Biologie des Organismes et Ecosystèmes Aquatiques, Université de Caen Normandie sous la direction du Pr Asma SAKKA HLAILI et la co-direction du Pr Nathalie NIQUIL.

La première partie du travail a été effectuée dans le cadre d'un projet de coopération scientifique « ***Marine Ecosystem Response to the Input of contaminants in the coastal zone*** « MerMex-MERITE » (Responsable : Pr Marc TEDETTI) et fait aussi partie du programme de recherche du Laboratoire Mixte International LMI CoSysMED (***COntaminants et écoSYStèmes marins côtiers sud MEDiterranéens***) qui s'inscrit dans le cadre du partenariat Nord-Sud Méditerranéen soutenu par l'IRD et le MESRS.

Les données obtenues au cours de ce travail ont fait l'objet de :

- Quatre articles :

Oumayma Chkili, Marouan Meddeb, Kaouther Mejri Kousri, Sondes Melliti Ben Garali, Nouha Makhlouf Belkhahia, Marc Tedetti, Marc Pagano, Nathalie Niquil, Asma Sakka Hlaili. *Influence of Nutrient Gradient on Phytoplankton Size Structure, Primary Production and Carbon Transfer Pathway in a Highly Productive Area (SE Mediterranean).* **Ocean Sciences Journal**. https://doi.org/10.1007/s12601-023-00101-6 **(IF = 1,042).**

Chkili O., Saint Béat B., Mejri Kousri K., Meddeb M., Gauvin P., David V., Sakka Hlaili A., Niquil N. *The typology of planktonic food web and its emergent properties as indicators of the ecological status of a permanently disturbed Gulf*. Soumis dans **Journal of Marine Systems (IF = 3,01).**

Grami B., Chkili O., Melliti Ben Garali S., Mejri Kousri K., Meddeb M., Chouba L., Niquil N., Sakka Hlaili. Field study on natural phytoplankton throughout "Bizerte City" oil spill on the south-western Cost of the Mediterranean Sea Soumis dans **Archive of Environmental Contamination and Toxicologie (IF = 3,692)**.

Chkili O., Melliti Ben Garali S., Mejri Kousri K., Meddeb. M. Niquil N., Sakka Hlaili A. Novel insight into the oil impact on the protozooplankton, trophic interactions and food web structure: field and modelling study. Cet article est en cours de soumission dans **Science of The Total Environment Journal (IF = 10,754)**.

- Des communications dans des congrès et des manifestations scientifiques :

2019-2020 Participation aux journées scientifiques organisées à l'Institut National des Sciences et Technologies de la Mer (INSTM) avec une communication orale « **Dynamique spatiale de la production primaire et de son transfert trophique dans le Golfe de Gabès en automne 2017** ».

2019-2020 Participation aux journées LMI COSYS-MED organisée à Tunis avec un Poster intitulé **« dynamique spatiale des producteurs et des consommateurs primaires & de leurs interactions trophiques dans le Golfe de Gabès en automne 2017 ».**

2021-2022 Participation aux journées doctoriales Vallée de Seine 2021 à Caen avec un Poster intitulé « **Dynamique spatiale de la production primaire et de son transfert trophique dans le Golfe de Gabès en automne 2017 ».**

2021- 2022 Participation aux journées scientifiques BOREA organisée à l'université de Caen Normandie, avec une communication orale « **Étude de l'état de santé des écosystèmes côtiers sud méditerranéens anthropisés à partir du fonctionnement du réseau trophique planctonique : modélisation des indicateurs écologiques en situation de contamination chronique ou pulsée** ».

2021-2022 Participation à la 59 ème conférence internationale **ECSA**, organisée en Espagne à Sain sébastien de 5-8 septembre 2022 avec un Poster intitulé « **Influence du gradient de nutriments sur la structure de taille du phytoplancton, la production primaire et la voie de transfert du carbone dans une zone hautement productive (SE Méditerranée) »**

À ma raison d'être, ma Mère …
À un Père exceptionnel …
Tout ceci a été possible grâce à vous et je ne vous remercierai jamais assez

« La plus belle chose que nous puissions éprouver, c'est le côté mystérieux de la vie. C'est le sentiment profond qui se trouve au berceau de l'art et de la science véritable »

Albert Einsten.

Remerciements

Etre chercheur, ce n'est pas un choix de carrière, c'est un choix de vie. Ce travail de thèse a marqué le fil conducteur d'une tranche de ma vie et me mène ce jour à la pointe de la maturité scientifique. Nombreuses personnes, que je voudrais bien les remercier, ont accompagné Oumayma la doctorante durant ces années de persévérance pour la connaissance et pour la Science.

J'aimerais tout d'abord commencer par remercier, Mme **Asma Sakka Hlaili**, Professeur à la faculté des Sciences de Bizerte qui m'a encadré durant mon stage de deuxième année Master et mon doctorat. Aucun mot ne peut exprimer mes remerciements et ma gratitude pour votre aide précieuse et votre soutien continu. Les conseils, la confiance en soi que vous m'avez accordé pour travailler et avancer sur ce sujet de thèse sont prépondérants pour la bonne réussite de ce présent travail. Merci pour votre patience, votre grande disponibilité pour les discussions scientifiques, vos corrections précieuses et vos remarques éclairées.

Un grand MERCI du fond du cœur à ma codirectrice de thèse Mme **Nathalie Niquil**, directrice de recherche à l'université de Caen Normandie d'avoir acceptée de codiriger cette thèse en me faisant confiance avant même me bien connaître. Je n'oublie jamais l'aide que vous m'avez accordé depuis mon premier jour en France jusqu'aujourd'hui. Le premier accueil chez vous, votre accompagnement administratif pour les papiers de logement, de séjour et ceux de l'Université de Caen reste bien ancré dans mon esprit. Grace à votre façon de présenter les choses, et à l'indépendance que vous m'avez apporté, j'ai appris à trouver et explorer mes propres idées. Votre gentillesse et vos encouragements m'ont énormément touchée et aidée. Un grand merci également de m'avoir permis de participer à de nombreux journées scientifiques congrès et écoles d'été nationaux et internationaux malgré l'exigence de Covid-19.

Merci aux membres de mon comité de suivi individuel de thèse, Mrs **Behzad Mostajir**, **Ezzeddine Mahmoudi** et Mmes **Sylvie Chevalier** et **Marion Rouge** pour leurs regards extérieurs et leurs conseils sur mon travail de doctorat.

Je souhaite exprimer mes remerciements chaleureux à l'ensemble des membres du jury, qui m'ont fait l'honneur de bien vouloir étudier avec attention mon travail : Mr **Télesphore Sime-Ngando** et Mr **Zaher Drira** pour avoir accepté d'être rapporteurs de cette thèse; Mr **Olivier**

Pringault, et Mme **Malika Bel Hassen** pour leurs qualités d'examinateurs et enfin Mr **Ezzeddine Mahmoudi** pour m'avoir fait l'honneur d'accepter de présider ce jury.

Merci aussi à tout le personnel de l'Université de Caen qui m'a permis de faire de l'enseignement dans de bonnes conditions.

Je remercie également le Laboratoire de Biologie des Organismes et des Ecosystèmes Aquatiques (BOREA) pour son accueil et pour m'avoir permis de travailler en toute sérénité et indépendance durant ces deux ans et demi. Malgré les perturbations liées à la crise épidémique du COVID-19, le laboratoire m'aura permis, dans le respect des règles sanitaires, de continuer à travailler. Je tiens donc à remercier la direction du laboratoire et particulièrement Mme **Céline Zatylny-Gaudin** ainsi que tout le personnel de BOREA pour leur accueil, leur aide, leur gentillesse et pour m'avoir permis de réaliser cette thèse dans de bonnes conditions.

Merci à Mme **Juliette Fauchot** pour son bon cœur, son écoute, sa confiance et pour le contrat d'ingénieur d'étude qui m'a offert durant cette dernière année de thèse. Ce contrat m'a permet de développer de nouvelles compétences qui me permettront d'évoluer dans mon parcours professionnel.

J'adresse mes vifs remerciements à Mme **Valérie David** maitre de conférence à l'université de Bordeaux pour avoir pris le temps de m'aider durant mon deuxième chapitre de thèse, ses conseils et ses encouragements ont eu un impact non négligeable sur la suite de mes travaux, et je ne peux que la remercier assez pour cela.

Je tiens à remercier tous les chercheurs avec qui j'ai pu discuter la méthode de modélisation numérique et l'analyse inverse en particulier **Quentin** et **Blanche**. Merci **Blanche** de m'avoir appris les bases de la modélisation. Grâce à ta façon d'expliquer et de présenter les choses, par la suite tout a paru si simple et si compréhensible.

Merci **Boutheina** pour avoir pris le temps de m'aider à l'analyse de données et la rédaction d'une partie de mon cinquième chapitre de thèse, avec rigueur, dynamisme, professionnalisme et enthousiasme.

Je tiens à exprimer toute ma gratitude aux membres du laboratoire de phytoplanctonologie et de biologie végétale notamment **Marouan**, **Kouka**, **Soulaima**, **Ines** et **Sondes**.

Remerciements

Merci **Kouka** d'être toujours présente pour répondre à mes questions quand je me sens bloquée. Tu m'es venu en aide alors que j'en avais vraiment besoin. Merci à **Soulaima** sur qui j'ai pu compter pour mes dernières procédures administratives qui n'étaient pas évidentes avec la distance. Merci également **Marouan** pour ton aide durant ces années de thèse.

Comment ne pas remercier l'extraordinaire **Sondes**, pour qui je porte une admiration sans failles. Merci d'avoir toujours répondu présent quand j'avais besoin de tes conseils. Je ne t'ai jamais considéré une simple collègue de laboratoire. En toi, j'ai trouvé une meilleure amie, une sœur, une confidente et une inspiration. Tes conseils et tes encouragements m'ont beaucoup aidé à arriver là où je suis aujourd'hui.

Un grand merci aux doctorants et à mes collègues de bureau à BOREA: **Fabian**, **Claire**, **Elise**, **Natacha**, **Laurie**, **Anna**, **Hélène**, **Marie**, **Alexandre** et **Paula** (qui faisait partie du bureau aussi). Merci pour tous les bons moments de franche rigolade au labo et en dehors. Un grand merci également pour avoir été là dans les moments difficiles.

Je tiens également à remercier tous mes amis, ceux que j'ai pu me faire à Caen comme **Sidney**, **Céline**, **Akram, Yassin, Ahmed, Oussama, Saida, Vincent et Gomria.** La folle **Gomria** ! Merci d'avoir été l'amie qui vaut une vraie sœur. Je te remercie d'avoir été toujours là pour m'écouter, m'apaiser, m'encourager, me soutenir quand j'en avais besoin et à me tirer vers le haut durant les périodes difficiles et parfois douloureuses. Sans oublier mon amie tunisienne **Amira**, qui n'a jamais cessé de me soutenir et d'avoir mes nouvelles malgré que je n'ai pas mal négligé ces temps-ci. Je remercie également à la belle **Sabrina**, **Anissa, Houssem** et **Ehsen** d'être les amis que j'apprécie beaucoup.

Et pour en finir avec affection, mon cher **Mahdi,** je ne te remercierai jamais assez pour ton soutien indéfectible et tes encouragements. Merci d'être toujours à côté de moi surtout pendant les moments de faiblesse. Je t'aime !

Et non, en fait ce n'est pas fini, car à la fin, il y a toujours la famille. Je suis redevable à mes parents, ma reine **Houda** et mon héro **Habib Chkili**, pour leur amour, leur soutien et leur confiance indéfectibles tout au long de mon parcours. **Hadhouda**, ma super maman, tes prières, ta présence et tes encouragements sont pour moi les piliers fondateurs de ce que je suis et de ce que je fais. Je t'adore maman !

Merci mes sœurs **Chayma**, **Hadil**, **Maryem**, pour avoir été là quand ça n'allait pas et que j'avais le plus besoin de vous. Merci également à mon oncle **Zied** qui m'a soutenu durant tout mon parcours universitaire.

Ma nièce **Lina** et mon neveu **Jade**, je vous admire !

Pour tous ceux que j'oublie il faudra excuser l'épuisement, l'oubli n'est que temporaire..

R É S U M É

Les écosystèmes côtiers méditerranéens sont considérés parmi les zones les plus perturbées vu qu'elles sont soumises à une importance pression anthropique, qui a conduit à leur eutrophisation et leur contamination par divers types de polluants chimiques. Ces perturbations ont des conséquences sur le fonctionnement de ces écosystèmes, leur état écologique et ultimement sur leurs capacités d'exportation de carbone et de productivité. C'est dans ce contexte que ce travail a été mené visant à étudier l'état de santé des deux écosystèmes côtiers sud méditerranéens anthropisés en caractérisant les réseaux trophiques planctoniques (RTPs) et en appliquant des indicateurs écologiques. Cette étude a concerné le Golfe de Gabès qui est caractérisé par une forte hydrodynamique et une contamination chronique due principalement aux industries du complexe Gannouche-Gabès et le Canal de Bizerte qui a été soumis à une contamination pulsée causée par une fuite de pétrole.

Dans le Golfe de Gabès, la dynamique spatiale du RTP a été étudiée en automne 2017 lors de la campagne MERMEX-MERITE dans quatre stations situées à différentes distances de la principale source de contamination. Des échantillonnages et des incubations *in situ* ont été conduits à chaque station pour déterminer les conditions environnementales, et nutritives entre autres, les biomasses carbonées des composantes du réseau [carbone organique particulaire et dissous, bactérioplancton, picophytoplancton (< 2 µm), nanophytoplancton (2-10 µm), microphytoplancton (> 10 µm), protozooplancton et métazooplancton (> 200 µm)] et certains flux de carbone (production bactérienne et phytoplanctonique, consommation du protozooplancton et du métazooplancton et sédimentation des particules). Les flux estimés à partir des données de terrain ont été utilisés dans une analyse inverse de Monte Carlo en Chaîne de Markov (LIM-MCMC) pour calculer les flux manquants afin de construire des modèles du RTP de chaque station. Cette analyse inverse était suivie par une analyse des indicateurs écologiques (ENAs et ratios de typologie) afin de dégager les propriétés structurales et fonctionnelles des RTPs. Les résultats ont montré que la circulation hydrodynamique complexe dans le Golfe semble induire un gradient nord-sud et côte-large des concentrations nutritives conduisant à des variations spatiales dans la structuration en taille et la production du phytoplancton ainsi que dans les interactions trophiques. Par conséquent différentes voies trophiques ont été distinguées en fonction du stress nutritif. Le réseau microbien dominait à la station la moins riche en nutriments (la plus au nord) et se caractérisait par la production primaire et l'activité les plus faibles, mais par l'ascendance la plus élevée, reflétant une importante organisation et stabilité. Le système à la station la plus eutrophe (la plus au sud) fonctionnait comme un réseau herbivore et était le plus actif avec une forte production primaire et débit total de carbone, mais restait le moins organisé et le moins stable. Dans les deux autres stations, un réseau multivore s'est développé et était le plus organisé grâce à une importante détritivorie par rapport à l'herbivorie, un fort recycle et une ascendance élevée.

Dans le Canal de Bizerte, les effets d'une marée noire, survenue en octobre 2018, sur les communautés du phytoplancton et du protozooplancton ainsi que leurs interactions trophiques ont été évalués dès les premiers jours suivant le déversement du pétrole et après quelques semaines. L'évolution du RTP au cours des différents jours suivant le déversement a été aussi décrite. Des échantillonnages et des incubations *in situ* ont été conduits les 1^{ier}, 4ème, 8ème et 18ème jours après la fuite du pétrole. On a noté la présence d'une nappe de pétrole du 1^{ier} au 8ème jour avec une contamination des eaux par les hydrocarbures aromatiques polycycliques (HAPs), principalement le chrysène. Le phytoplankton a montré des différentes réponses au fil du temps. À court terme (du 1^{ier} au 8ème jour), la croissance et la biomasse du picophytoplancton ont augmenté, alors que celles du nano- et du microphytoplancton ont diminué, probablement en raison de la sensibilité des certaines grandes espèces aux HAPs. À plus long terme (18ème jour),

la dispersion du pétrole et la réduction de son effet négatif se sont accompagnées par une prolifération des grandes cellules avec un changement dans leur composition taxinomique et une forte accumulation de la biomasse du picophytoplancton, causée par la diminution de leur broutage par le protozooplancton. En conséquence, la structure en taille du phytoplancton a évolué tout au long de l'exposition au pétrole, passant d'une prédominance du microphytoplancton après quelques jours à une dominance à long terme du picophytoplancton. La structure de la communauté du protozooplancton a également changé au fil des jours vers une dominance des dinoflagellés mixotrophes (principalement *Heterocapsa*) au détriment d'une diminution des dinoflagellés hétérotrophes (i.e. *Gyrodinium* and *Protoperidinium*). Les ciliés (principalement *Strombidium*) ont montré une diminution à court terme mais une récupération au 18ème jour, tandis que les nanoflagellés hétérotrophes étaient plus vulnérables à la toxicité du pétrole et ont disparu à partir du 8ème jour. Les taux de production des différentes fractions de taille du phytoplancton ainsi que leurs taux de consommation par le protozooplancton ont largement varié entre les différents jours. L'intégration de ces taux modifiés par la contamination pétrolière dans des modèles linéaires inverses de flux de carbone et le calcul des indicateurs écologiques ont montré un changement clair dans la structure et le fonctionnement du RTP, de la voie herbivore (au 1^{ier} jour), au réseau multivore (4ème et 8ème jour) jusqu'un réseau microbien spécial (au 18ème jour), ce qui implique différentes efficacités dans l'exportation du carbone tout au long de l'évolution de la marée noire.

Cette étude met en évidence l'importance de coupler la typologie des RTPs et les indicateurs écologiques pour mieux décrire l'état écologique des écosystèmes soumis soit à une contamination permanente ou pulsée. Ces approches intégratives peuvent fournir des outils efficaces pour gérer et évaluer la santé des écosystèmes anthropisés.

A B S T R A C T

Mediterranean coastal ecosystems are considered to be among the most disturbed zones, as they are subject to considerable anthropogenic pressure, which has led to their eutrophication and contamination by various types of chemical pollutants. These disturbances have consequences for the functioning of these ecosystems, their ecological status and ultimately their carbon export and productivity capacities. It is against this backdrop that this study was carried out to investigate the state of health of two anthropized southern Mediterranean coastal ecosystems by characterizing planktonic food webs (PFWs) and applying ecological indicators. The study focused on the Gulf of Gabès, which is characterized by strong hydrodynamics and chronic contamination due mainly to the industries of the Gannouche-Gabès complex, and the Bizerte Channel, which was subjected to pulsed contamination caused by an oil spill.

In the Gulf of Gabès, the spatial dynamics of the PFWs were studied in autumn 2017 during the MERMEX-MERITE campaign at four stations located at different distances from the main source of contamination. Sampling and in situ incubation were conducted at each station to determine environmental and nutrient conditions, including carbon biomass of food webcomponents [particulate and dissolved organic carbon, bacterioplankton, picophytoplankton (< 2 µm), nanophytoplankton (2-10 µm), microphytoplankton (> 10 µm), protozooplankton and metazooplankton (> 200 µm)] and certain carbon fluxes (bacterial and phytoplankton production, protozooplankton and metazooplankton consumption and particulate sedimentation). The fluxes estimated from the field data were used in an inverse Markov Chain Monte Carlo (LIM-MCMC) analysis to calculate the missing fluxes in order to build models of the PFW for each station. This inverse analysis was followed by an analysis of ecological indicators (ENAs and typology ratios) to identify the structural and functional properties of the PFWs. The results showed that the complex hydrodynamic circulation in the Gulf appears to induce a north-south and coast-offshore gradient in nutrient concentrations, leading to spatial variations in phytoplankton size structuring and production, as well as trophic interactions. As a result, different trophic pathways were distinguished as a function of nutrient stress. The microbial food web dominated at the least nutrient-rich station (northernmost) and was characterized by the lowest primary production and activity, but the highest ascendancy, reflecting a high degree of organization and stability. The system at the most eutrophic station (southernmost) functioned as an herbivorous food web and was the most active with high primary production and total carbon flow, but remained the least organized and stable. At the other two stations, a multivorous food web developed and was the most organized thanks to high detritivory compared with herbivory, strong recycling and high ascendancy.

In the Bizerte Channel, the effects of an oil spill, which occurred in October 2018, on phytoplankton and protozooplankton communities and their trophic interactions were assessed from the first days after the oil spill and after a few weeks. In situ sampling and incubation were carried out on days 1, 4, 8 and 18 after the oil spill. The presence of an oil slick was noted from days 1 to 8, with water contamination by polycyclic aromatic hydrocarbons (PAHs), mainly chrysene. Phytoplankton showed different responses over time. In the short term (days 1-8), picophytoplankton growth and biomass increased, while those of nano- and

microphytoplankton decreased, probably due to the sensitivity of certain large species to PAHs. In the longer term (day 18), the dispersal of oil and the reduction of its negative effect were accompanied by a proliferation of large cells with a change in their taxonomic composition and a strong accumulation of picophytoplankton biomass, caused by reduced grazing by protozooplankton. As a result, the size structure of phytoplankton evolved throughout oil exposure, from a predominance of microphytoplankton after a few days to a long-term dominance of picophytoplankton. The structure of the protozooplankton community also changed over the days towards a dominance of mixotrophic dinoflagellates (mainly Heterocapsa) at the expense of a decrease in heterotrophic dinoflagellates (i.e. Gyrodinium and Protoperidinium). Ciliates (mainly Strombidium) showed a short-term decrease but recovery by day 18, while heterotrophic nanoflagellates were more vulnerable to oil toxicity and disappeared by day 8. The production rates of the various phytoplankton size fractions and their consumption rates by protozooplankton varied widely among days. Integrating these oil contamination-modified rates into linear inverse carbon flux models and calculating ecological indicators showed a clear shift in PFW structure and function, from the herbivorous pathway (at day 1), to the multivorous food web (days 4 and 8) to a special microbial food web (at day 18), implying different carbon export efficiencies throughout the evolution of the oil spill.

This study highlights the importance of coupling PFW typology and ecological indicators to better describe the ecological state of ecosystems subjected to either permanent or pulsed contamination. These integrative approaches can provide effective tools for managing and assessing the health of anthropized ecosystems.

Table des matières

Liste des Figures

Chapitre I

Chapitre II

Chapitre III

Chapitre IV

Chapitre V

Liste des Tableaux

Chapitre II

Chapitre III

Chapitre IV

Chapitre V

Liste des abbréviations

PIC: Picophytoplancton
NAN: Nanophytoplancton
MIC: Microphytoplancton
BAC: Bactérioplancton
PRO: Protozooplancton
MET: Métazooplancton
NFHs : Nanoflagellés hétérotrophes
DET: Détritus
MOD : Matière Organique Dissoute
MOP : Matière Organique Particulaire
LIM: Linear Inverse Modelling
LIM MCMC: LIM Markov Chain Monte Carlo
ENA: Ecological Network Analysis
A/DC: Ascendance relative
AMI : Information mutuelle moyenne
FCI : Indice de recyclage de Finn
APL : Longueur moyenne du chemin
TST : Débit total du système
D/H : Détritivorie / Herbivorie
ANOVA : Analyse des variances
ACC : Une analyse canonique des correspondances
ACP : Une analyse en composantes principales
AFM : Une analyse factorielle multiple
MDS : Une ordination par échelle multidimensionnelle

Introduction Générale

Les écosystèmes aquatiques sont des systèmes sensibles aux changements environnementaux et aux stress anthropiques qui déclenchent à la fois des problèmes locaux et globaux (Worm et al., 2006; Eastwood et al., 2007; Michán et al., 2021). Les pressions exercées sur les systèmes marins provoquent donc des réponses qui pourraient être rapidement visibles, ou enregistrables, ce qui en fait des milieux sentinelles intéressants. Aujourd'hui, chercheurs et gestionnaires s'interrogent sur le devenir à long terme de ces écosystèmes. Ainsi, la compréhension du fonctionnement et de la dynamique de ces systèmes est primordiale pour pouvoir comprendre leur évolution et évaluer leur "état de santé" pour les mieux les gérer.

La Commission Européenne a mis en place la Directive-Cadre pour l'Eau (DCE) en 2000 et la Directive-Cadre Stratégie pour le Milieu Marin (DCSMM) en 2008 permettant d'établir un cadre d'action communautaire dans le domaine de la politique pour l'eau et le milieu marin dans les pays de l'Union Européenne. Ces directives ont pour principal objectif que toutes les mesures nécessaires soient prises pour réaliser ou maintenir un "Bon Etat Ecologique, BEE" à l'horizon 2026. Elles ont permis de centraliser plus de 30 directives régionales différentes, comme la Convention de Barcelone en Méditerranée (1976), l'OSPAR en Atlantique Nord-Est (1992) ou l'HELCOM en Mer Baltique (1992). Par définition, un écosystème possédant un « BEE » et qui ne présente pas de "syndrome de stress" est un système stable, durable, actif et qui maintient son organisation et son autonomie dans le temps (Costanza et al., 1992). Des travaux effectués dans le cadre de la DCSMM ont mis en évidence l'importance de prendre en considération des différents processus éco-systémiques et de développer des indicateurs intégratifs axés sur ces processus (tels que les indicateurs du réseau trophique, les ENA) afin d'établir le « BEE » (Rombouts et al., 2013; Niquil et al., 2014a). Ces indicateurs fonctionnels et holistiques permettent de décrire l'activité et le niveau d'organisation et de maturité des réseaux trophiques et fournissent des informations utiles sur le degré de stress et de stabilité des écosystèmes (Christensen, 1995; Bodini & Bondavalli, 2002; Grami et al., 2008; Heymans et al., 2014; Saint-Béat et al., 2015; Pezy et al., 2017). Par conséquent, les indicateurs fonctionnels sont fréquemment utilisés pour évaluer l'impact des pressions naturelles et anthropiques sur les écosystèmes marins côtiers (Belgrano et al., 2005; Niquil et al., 2014a; Piroddi et al., 2015; Chaalali et al., 2016) et peuvent donc être appliqués par les gestionnaires des écosystèmes aquatiques (Arroyo et al., 2019; Fath et al., 2019; Safi et al., 2019). En outre, la DCSMM a

retenu le "réseau trophique marin" comme descripteur de l'état écologique du système (Cardoso et al., 2010; European Commission, 2010), puisque le fonctionnement global de l'écosystème dépend énormément de la structure et des caractéristiques de son réseau trophique. L'étude des réseaux trophiques présente donc un grand intérêt écologique et pratique, car elle constitue une étape essentielle dans l'évaluation des réponses de l'écosystème aux différentes perturbations (Gotwals & Songer, 2010; Lewis et al., 2022).

En raison de leur structure de taille, leur grande abondance et leur diversité taxonomique et fonctionnelle, les organismes planctoniques (i.e. bactérioplancton, phytoplancton, protozooplancton et métazooplancton) jouent un rôle prépondérant dans les flux de matière et d'énergie au sein des écosystèmes aquatiques grâce à leurs activités de production de biomasse, de consommation, d'excrétion, de minéralisation, etc. (Azam et al., 1983; Legendre & Rassoulzadegan, 1995; Sime-Ngando et al., 1995; Sakka et al., 2000; Arrigo, 2005; Sime-Ngando, 2012). De ce fait, la caractérisation des réseaux trophiques planctoniques (RTPs) semble être très utile pour évaluer l'état des écosystèmes aquatiques (Araignous, 2017). Différentes structures trophiques planctonique existent, incluant la boucle microbienne, le réseau herbivore, le réseau microbien, le réseau multivore, le réseau multivore-bactérien et les réseaux poly- ou phyto-microbiens (Azam et al., 1983; Legendre & Rassoulzadegan, 1995; Sakka Hlaili et al., 2014; Meddeb et al., 2019). Ces structures trophiques ont des différentes capacités de production de carbone, de recyclage et d'exportation et ils contrôlent les flux de carbone vers les consommateurs supérieurs (Legendre & Rassoulzadegan, 1995, 1996), influençant ainsi la productivité de l'écosystème et ses propriétés structurales et fonctionnelles en général (Mazumder et al., 2017). Le type de réseau peut changer à des échelles spatiale et saisonnière en réponse à tout changement des conditions environnementales (hydrologiques, nutritives, climatiques, contamination, etc.). Il est donc primordial de déterminer le type de réseau pour évaluer comment les écosystèmes réagissent faces aux perturbations environnementales et anthropiques et les impacts de ces forçages sur eux. Malgré leur pertinence, les RTPs restent peu proposés comme potentiels indicateurs de santé des écosystèmes (Fath et al., 2019; Safi et al., 2019).

La détermination des réseaux trophiques planctoniques, entre autres, nécessite la connaissance des flux de carbone entre leurs compartiments, qui ne peuvent pas toujours être mesurés sur le terrain, à cause des limitations techniques et financières. Le recours à la modélisation des flux de carbone peut fournir des informations concises sur les flux de matière et d'énergie dans le système (Forest et al., 2011; Thompson et al., 2012; Meddeb et al., 2019).

La modélisation des réseaux trophiques est considérée comme l'une des méthodes les plus utiles dans l'étude de l'état des écosystèmes marins (Niquil et al., 2011; Pacella et al., 2013; Taffi et al., 2015; Hines et al., 2018). Elle permet d'estimer l'incertitude des flux et des indices des propriétés structurelles et fonctionnelles du réseau trophique (De Laender et al., 2010; Grami et al., 2011; Niquil et al., 2011; Saint-Béat et al., 2013; Chaalali et al., 2015; Hines et al., 2018). Les flux calculés par modélisation permettent de déterminer la typologie et le fonctionnement du réseau trophique qui à leur tour permettent de quantification des degrés d'organisation, de stabilité et de stress des écosystèmes (Christensen, 1995; Thomas & Christian, 2001; Ulanowicz et al., 2009). Par exemple, les modèles des réseaux trophiques ont été appliqués pour évaluer l'impact du changement climatique, pour la bioaccumulation des polychlorobiphényles (PCB) et même pour les impacts cumulatifs tels que les parcs éoliens offshore combinés au changement climatique (Forest et al., 2011; Taffi et al., 2015; Nogues et al., 2021).

Dans le bassin Sud méditerranéen, le Golfe de Gabès est classé en Méditerranée parmi les mers à forte productivité avec une grande importance socio-économique, assurant 64% de la production halieutique nationale. Paradoxalement, cet écosystème est considéré comme un «hot spot» de contamination chimique avec un problème crucial dû aux industries chimiques d'acide phosphorique. Les caractéristiques biologiques et hydrodynamiques du Golfe ont fait l'objet de plusieurs études, ainsi que son niveau de contamination et d'eutrophisation et leur impact sur les organismes sont de plus en plus connus (Bel Hassen et al., 2009; Ben Ltaief et al., 2015). Par ailleurs, des modèles de réseau pélagiques sur le plateau continental du Golfe de Gabès ont permis d'incorporer différentes sources d'information provenant d'études physiques, bio-géochimiques et biologiques pour caractériser la distribution des communautés pélagiques au sein de réseau trophique (Hattab et al., 2013; Halouani et al., 2016). Toutefois, la dynamique des réseaux trophiques planctoniques sont peu étudiés vue que peu de données existent à ce jour sur les interactions entre les compartiments planctoniques et sur les flux de carbone. En outre, l'impact des forçages anthropique sur les propriétés fonctionnelles de l'écosystème reste à appréhender. De plus les contaminants peuvent avoir une influence irréversible sur cet écosystème dont la capacité de résilience est peu connue.

La Lagune de Bizerte, incluant le Canal de Bizerte, constituent un pôle de conchyliculture et de pêche en Tunisie. Ces écosystèmes se trouvent aussi sous une anthropisation accrue, conduisant à leur eutrophisation et contamination chimique par divers polluants (Lafabrie et al., 2013; Barhoumi et al., 2014; Saidi et al., 2019; Pringault et al., 2016, 2021) qui ont impacté les communautés marines et les microorganismes planctoniques. La modélisation des flux de

carbone a montré que la structure et le fonctionnement trophique de ces écosystèmes changent en réponse à une perturbation par les sédiments contaminés et que leur capacité de recyclage augmente aussi. Ceci a révélé la forte capacité de résilience de la Lagune et du Canal qui sont continuellement soumis à des perturbations, dues surtout à une contamination chimique qui ne diminue pas. Ces écosystèmes ont été affrontés à une contamination soudaine en 2018 provoquée par une fuite de pétrole brute causant une marée noire. Malheureusement, la capacité de résistance de ces écosystèmes face à cet évènement majeur de perturbation pulsée reste à vérifier.

Ces lacunes d'ordre fonctionnel au niveau du Golfe de Gabès et du Canal de Bizerte, nous a conduit à mener ce travail de thèse dont les objectifs principaux sont **(i)** évaluer les impacts d'une contamination chronique ou pulsée sur les RTPs et les propriétés structurales, fonctionnelles et émergentes des deux systèmes et **(ii)** proposer des indicateurs écologiques spécifiques aux deux pressions pour décrire l'état de santé de chaque écosystèmes. Les indicateurs sélectionnés peuvent être mis à la disposition des gestionnaires comme des outils efficaces pour une gestion durable de l'environnement marin.

Afin d'atteindre ces objectifs, différents types d'approches ont été utilisées, incluant des échantillonnages dans les deux sites d'étude, des incubations et expérimentations *in situ* et des analyses de modélisation.

Le manuscrit de la thèse est organisé en différents chapitres :

► **Chapitre I**: Ce chapitre est dédié à la revue bibliographique qui présente une synthèse sur le fonctionnement des écosystèmes avec les différents types de réseaux trophiques planctoniques, l'impact de la contamination sur le fonctionnement et la structuration des réseaux ainsi que sur la modélisation numérique et l'analyse d'indicateurs écologiques.

► **Chapitre II** : Ce chapitre présente le « Matériel et Méthodes » utilisés pour accomplir le travail de la thèse avec des descriptions des stratégies d'échantillonnage, des dispositifs expérimentaux, des protocoles analytiques utilisés, de la modélisation inverse LIM-MCMC, de l'analyse ENA et des rapports écologiques ainsi que des analyses statistiques.

► **Chapitre III** : Ce chapitre présente les données de terrain collectées dans le Golfe de Gabès au niveau de quatre stations situées le long d'un gradient de contamination (pression nutritive). Ces données ont concerné le phytoplancton (biomasse, composition, structure en taille, croissance et production primaire), le protozooplankton (abondance et

composition), le métazooplancton (abondance et composition), les interactions trophiques (broutage du phytoplancton par le proto- et métazooplancton) et les taux de sédimentation (flux verticaux des particules de carbone organique). Ces données de terrain ont permis de conceptualiser des voies de transfert de carbone. Ce chapitre était écrit sous forme d'un article scientifique «**Influence of Nutrient Gradient on Phytoplankton Size Structure, Primary Production and Carbon Transfer Pathway in a Highly Productive Area (SE Mediterranean)**» qui est publié dans le journal «*Ocean Sciences Journal*», Chkili et al. (2023) 58:6. https://doi.org/10.1007/s12601-023-00101-6

► **Chapitre IV** : Dans ce chapitre, les modèles des réseaux trophiques planctoniques ont été mis en place par la méthode inverse améliorée (LIM-MCMC) pour les quatre stations du Golfe de Gabès. Cette méthode a été couplée à une analyse des réseaux afin de dégager des indices écologiques permettant de décrire les propriétés structurales et fonctionnelles de chaque réseau et pour aussi une comparaison inter-système. Ces deux outils numériques ont été appliqués pour la première fois sur le réseau trophique planctonique du Golfe de Gabès. Les résultats de ce chapitre étaient rédigés sous forme d'un article scientifique «**Typology of planktonic food webs and associated emerging properties as indicators of the ecological status of a permanently disturbed Gulf**» qui est soumis dans la revue « *Progress in Oceanography* ».

► **Chapitre V** : Ce chapitre présente les résultats du monitorage réalisé dans le Canal de Bizerte à la suite de la marée noire et qui ont concerné la réponse à la contamination pétrolière, à court et à long terme, de la communauté naturelle du phytoplancton, de la communauté du protozooplancton et son activité de broutage ainsi que les conséquences sur la structure et le fonctionnement du réseau trophique planctonique. Ces résultats ont fait l'objet de deux articles :

Article 3 : «**Field study on natural phytoplankton throughout "Bizerte City" oil spill on the south-western Cost of the Mediterranean Sea**» qui est soumis dans le journal « *Archive of Environmental Contamination and Toxicologie* ».

Article 4: «**Novel insight into the oil impact on the protozooplankton, trophic interactions and food web structure: field and modelling study**» qui est en cours de soumission dans la revue «*Science of The Total Environment*».

Une discussion générale présente tous les résultats et met en évidence les changements entre les deux types de contamination, en se basant sur les indices écologiques. Le manuscrit de la thèse se termine par une conclusion générale et les perspectives de recherche sont finalement développées.

Chapitre I.

Revue bibliographique

Fonctionnement des écosystèmes marins

I. Producteurs primaires et consommateurs planctoniques

L'un des principaux défis de l'écologie était de comprendre les moteurs de la structure et de la fonction des écosystèmes (Levin, 1992). Les écosystèmes marins forment des systèmes dynamiques contenant de nombreux composants vivants et non vivants qui interagissent entre eux (Prasad, 2022). Les composants vivants ont besoin de matière et d'énergie pour exécuter leurs fonctions vitales et, ainsi, développer leurs cycles de vie. L'énergie entre dans l'écosystème sous la forme de production primaire, le traverse et est stockée sous forme de biomasse dans les organismes vivants (Tomlinson et al., 2014). Ainsi la production primaire correspond à la production de matière organique végétale (biomasse), issue de la photosynthèse par des organismes autotrophes, les producteurs primaires (P1) qui représentent le premier maillon du réseau trophique. Le stock de carbone organique produit est transféré aux divers consommateurs (C_1, C_2, etc.) qui vont se succéder dans les réseaux trophiques (Figure I. 1).

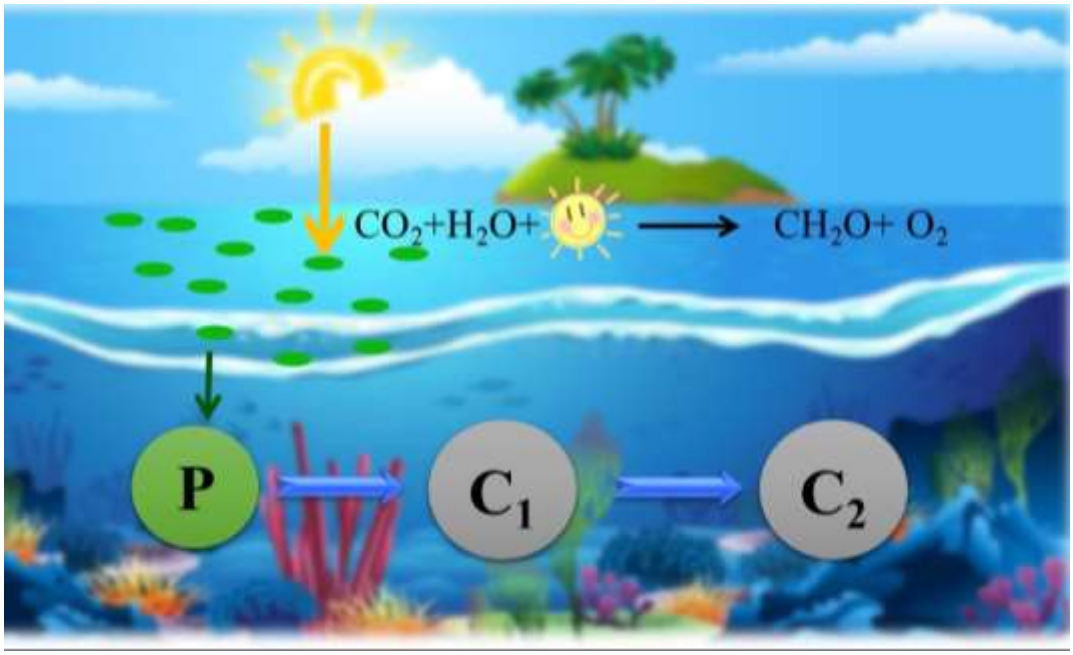

Figure I. 1. Schéma simplifié de la production primaire et son transfert (P : producteurs ; C_1, C_2 : Consommateurs)

1. Producteurs primaires

Le phytoplancton constitue les producteurs primaires des écosystèmes marins, dont la productivité dépend énormément du taux de la production phytoplanctonique. Ce taux est lui-même lié à la structuration de la communauté phytoplanctonique, surtout à la taille des producteurs (Maranon, 2010; Kang et al., 2020).

Le picophytoplancton (0,2-2 µm) est constitué par les pico-cyanobactéries procaryotes et pico-eucaryotes photosynthétiques (notamment des représentants des chlorophytes) (Stockner & Antia, 1986; Riemann & Christoffersen, 1993). Le picophytoplancton forme une faible fraction de la biomasse carbonée du phytoplancton (10%) mais pourrait contribuer à 75% de la chlorophylle *a* dans certaines régions (Stockner & Antia, 1986; Magazzu & Decembrini, 1995). Il est capable d'utiliser les faibles ressources plus efficacement que les grosses cellules grâce à sa petite taille (Raven, 1986). Cette particularité de taille lui permet d'être plus abondant et plus compétitif par rapport aux larges algues dans les écosystèmes pauvres en nutriments (Chisholm, 1992; Agawin et al., 2000). Plusieurs études ont montré également que le picophytoplancton joue un rôle très important dans le flux de matière et d'énergie dans le réseau trophique microbien (Šimek et al., 1995; Stockner et al., 2002; Jiao et al., 2005; Sakka Hlaili et al., 2007).

Le nanophytoplancton (2-10 µm ou 2-20 µm) renferme un ensemble d'organismes eucaryotes autotrophes appartenant à différentes classes taxinomiques, tels que les chlorophycées, les prasinophycées, les cryptophycées, les chrysophycées et les petits dinoflagellés et petites diatomées. Ces nano-organismes sont considérés comme les principaux producteurs primaires, dont l'énergie et la matière sont transférées vers les consommateurs protozooplanctoniques (Sherr et al., 1986; Verity et al., 2002). Plusieurs travaux ont montré l'importance quantitative de la fraction nanoplanctonique dans le milieu marin (Sanders et al., 2000; Lovejoy et al., 2002). Cette fraction est parfois responsable de plus de 80% de l'activité photosynthétique (Bruno et al., 1983).

Le microphytoplancton (10-200 µm ou 20-200 µm) est souvent représenté par deux classes (Bougis, 1974; Totti et al., 2005): les diatomées et les dinophycées (ou dinoflagellés). Mais on peut trouver aussi des grandes cellules comme les dictyochophycées, les euglénophycées, les prasinophycées, les nephrophyceae, les pédinophyceae et les chlorophycées. Le microphytoplancton constitue le principal producteur primaire au niveau des écosystèmes marins pélagiques caractérisés par des eaux riches en nutriments, où il peut

présenter des taux élevés de production (Bec et al., 2005; Meddeb et al., 2019). Le microphytoplancton est très abondant dans les eaux néritiques caractérisées par un excès d'éléments nutritifs (Cole et al., 1988; Harrison & Cota, 1991). En terme de biomasse et de productivité, les eaux côtières sont caractérisées par une production élevée, qui est due essentiellement au microphytoplancton (Grami, 2009; Sakka Hlaili et al., 2007; Meddeb et al., 2018).

La taille des producteurs primaires joue un rôle majeur dans la sélection pour les consommateurs planctoniques. Ainsi, il existe une cohérence entre la dominance d'un type d'autotrophes et le type de brouteurs. Lorsque la fraction picoplanctonique domine, ce sont les consommateurs microbivores qui se développent, alors qu'en présence des grosses cellules, c'est souvent les organismes herbivores qui prolifèrent.

2. Consommateurs planctoniques

2.1. Protozooplancton

Le protozooplancton, à travers son broutage, joue un rôle essentiel dans la structuration des communautés planctoniques(Paranjape, 1990; Verity & Paffenhofer, 1996; James et al., 1998) et dans le contrôle de la production phytoplanctonique et bactérienne (Gifford, 1988; Burkill et al., 1995; Cotano et al., 1998; Pecqueur et al., 2022; Kosiba & Krztoń, 2022). Il représente un lien important entre les petits producteurs et les niveau trophiques supérieurs (Montagnes et al., 2010; Sommer et al., 2012; Agasild et al., 2013; Kosiba et al., 2017).

Le protozooplancton est représenté par des organismes unicellulaires planctoniques hétérotrophes et mixotrophes dont la taille ne dépasse pas 200 µm; on y distingue le nanozooplancton et le microzooplancton (Sieburth et al., 1978; Yang et al., 2008). Le nanozooplancton est constitué de petits organismes nanoflagellés hétérotrophes (NFHs) et les petits ciliés, surtout les aloriqué, alors que le microzooplancton regroupe les dinoflagellés et les ciliés loriqués. Les NFHs et les ciliés aloriqués sont des consommateurs microbivores (ou bactérivores) qui se nourrissent par phagotrophie sur les proies pico- et nanoplanctoniques. Le protozooplancton microbivore joue donc un rôle primordial dans les écosystèmes oligotrophes où les petits producteurs dominent en consommant une importante fraction de leurs biomasses (Šimek et al., 1995; Sime-Ngando et al., 1995; Calbet et al., 2000; Bouvy et al., 2006; Drira et al., 2009). Les gros ciliés loriqués et les dinoflagellés sont les principaux consommateurs herbivores dans les eaux, où la production primaire est supportée par le phytoplancton de grande

taille (Sakka Hlaili et al., 2007; Sherr et al., 2009). Ces gros protozoaires peuvent parfois exercer une pression de broutage sur les diatomées plus importante que celle des copépodes et des autres grands consommateurs (Sherr & Sherr, 2007; Meddeb et al., 2018). Les ciliés loriqués, représentés principalement par les tintinnides peuvent ingérer une large portion de la production primaire journalière dans les milieux côtiers et lors des blooms printaniers du gros phytoplancton (Johansson et al., 2004; Sakka Hlaili et al., 2007; Meddeb et al., 2018; Sime-Ngando et al., 1995; Drira et al., 2009). Sherr & Sherr, (1987) ont montré que les ciliés sont des brouteurs majeurs des bactéries, alors que Sime-Ngando et al. (1995) ont les signalé comme consommateurs potentiels des dinoflagellés. Drira et al. (2009) ont émis en évidence le rôle potentiel joué par les ciliés non seulement en tant que prédateurs du phytoplancton, mais aussi en tant que proies pour les copépodes filtreurs dans le Golfe de Gabès. Les dinoflagellés englobent des organismes hétérotrophes stricts dépourvus de pigment photosynthétique, comme les espèces de *Protoperidinium*, et sont les principaux brouteurs herbivores lors des efflorescences des diatomées (Jacobson & Anderson, 1986; Lessard, 1991; Sherr & Sherr, 2007). D'autres dinoflagellés sont mixotrophes, comme les espèces des genres *Gymnodinium*, et *Gonyaulax*, et sont capables soit de réaliser la photosynthèse soit de phagocyter des proies dont la taille dépasse parfois leur propre taille (Jeong et al., 1999; Seong et al., 2006; Calbet et al., 2008).

Le protozooplancton peut également avoir une activité carnivore importante puisqu'il peut se nourrir de dinoflagellés, flagellés et ciliés hétérotrophes, fournissant ainsi une alimentation essentiel au métazooplancton (Calbet & Landry, 1999; Calbet & Saiz, 2005).

2.2. Métazooplancton

Le métazooplancton, qui est composé par les organismes métazoaires planctoniques, constitue un compartiment essentiel des réseaux trophiques marins et des cycles biogéochimiques par son alimentation, sa migration verticale et par la production de pelotes fécales (Banse, 1995; Robinson et al., 2010; Steinberg & Landry, 2017). Ce compartiment trophique est très diverse regroupant les copépodes, les cladocères, les appendiculaires, les nauplii de Cirrhipèdes, les larves de décapodes, les chaetognathes, les annélides, etc. L'activité de broutage du métazooplancton sur les producteurs primaires permet de limiter leur accumulation tout en transférant la matière organique produite vers les niveaux trophiques supérieurs (McQueen et al., 1986). L'activité herbivore du métazooplancton est souvent

associée aux copépodes. Le spectre de taille de ce groupe (copépodes de petite et large tailles) joue un role essentiel dans la filtration et/ou la prédation du microphytoplancton.

Les copépodes de petite taille (200µm) était capable de se nourrir d'une large sélection de proies phytoplanctoniques (Drira et al., 2010). Ce sont des filtreurs (Graeve et al., 1994) qui capturent souvent des nano et micro-phytoplancton dont la taille varie de 5 à 50 µm, comme les diatomées (Mauchline, 1998), les chrysophycées et les cryptophycées (Antajan & Gasparini, 2004). La sélectivité vis-à-vis de la taille des proies est essentiellement liée à la taille et la structure des appendices qui servent à la capture ou à la filtration des proies (Karlson & Bamstedt, 1994). D'autre part, il y'a des copépodes carnivores (Calbet et al., 2007) qui ne filtrent pas l'eau, mais ils capturent les protozoaires, les rotifères, les larves d'autres crustacés ou d'autres copépodes dont la taille est un peu plus grande par rapport aux proies des filtreurs. Parmi les espèces qui possèdent les deux comportements alimentaires, il y a les omnivores qui peuvent consommer du phytoplancton ou du petit zooplancton et même des détritus (Dalsgaard et al., 2003; Arts et al., 2009). Ils peuvent être prédateurs ou filtreurs en fonction des conditions environnementales, la disponibilité, la taille et la valeur nutritive des proies (Adrian & Schneider-Olt, 1999). Le cannibalisme n'est pas rare chez les copépodes (Camus & Zeng, 2009) surtout dans les cas de cultures, ce sont souvent les stades juvéniles des copépodes qui sont les victimes de ce phénomène (Ohman & Hirche, 2001).

II. Transfert trophique et réseaux trophiques planctoniques

La productivité marine dépend tout d'abord de la production primaire et ensuite de l'efficacité de son transfert trophique, qui est en relation étroite avec la structure du réseau trophique planctonique. En fait, la structure du réseau trophique se base principalement sur le type des producteurs primaires qui eux-mêmes définissent le type des consommateurs. Dans les écosystèmes marins, plusieurs structures trophiques peuvent être distinguées (Steele, 1974; Azam et al., 1983; Cushing, 1989; Legendre & Rassoulzadegan, 1995; Sakka Hlaili et al., 2014)

La typologie des réseaux trophique a été décrite la première fois par Steele, (1974). Ce dernier a schématisé le transfert de matière et d'énergie au sein des différentes composantes planctoniques (producteurs et consommateurs) sous forme d'une chaîne alimentaire classique appelée réseau herbivore «***herbivorous food web***». La production primaire dans ce type de réseau trophique est dominée par le microphytoplancton (notamment les diatomées de 10-200 µm) qui assurent l'essentiel de la productivité et qui est ensuite brouté par le

métazooplancton herbivore (copépodes en particulier) (Figure I. 2a). Ce réseau trophique classique, par sa productivité importante, alimente les niveaux trophiques supérieurs pélagiques et assure un transfert trophique efficace du carbone biogène. Il est responsable d'une forte exportation de la matière organique en dehors de la couche euphotique. Généralement, le réseau herbivore domine lors des efflorescences algales surtout des diatomées ou pendant la remontée de nutriments allochtones suivie par une stabilisation de la couche de mélange (Legendre, 1990).

Des études ont ensuite signalé l'importance des autotrophes et hétérotrophes de petite taille dans la structure des réseaux trophiques planctoniques marins (Azam et al., 1983; Sherr & Sherr, 1988; Legendre & Rassoulzadegan, 1995). Azam et al. (1983) ont introduit la notion de boucle microbienne « *microbial loop* », où les bactéries sont ingérées par les nanoflagellés hétérotrophes (NFHs) qui sont eux-mêmes broutés par les ciliés (Figure I. 2b). Sherr & Sherr, (1988) ont suggéré l'existence d'un réseau trophique microbien « ***microbial food web*** » incluant en plus les autotrophes et les hétérotrophes de petite taille, assurant le flux d'énergie nécessaire pour le réseau trophique pélagique (Figure I. 2c). La prédominance de la boucle microbienne ou du réseau microbien est déterminée par l'importance de la quantité d'azote organique dissous (NOD) par rapport à celui du carbone organique dissous (COD). Selon Caron et al. (1988), lorsque le NOD est abondant, les bactéries reminéralisent plus d'ammonium quelles n'en utilisent, cet ammonium étant utilisé par le picophytoplancton ce qui conduit à un réseau microbien (Legendre & Rassoulzadegan, 1995). Par contre, lorsque le NOD est peu abondant, les bactéries hétérotrophes entrent en compétition avec les petits phototrophes pour l'ammonium ce qui conduit à un système presque fermé dominé par la boule microbienne (Legendre & Rassoulzadegan, 1996). Le réseau microbien est moins efficace dans le transfert du carbone vers le domaine pélagique que le réseau herbivore, puisqu'une partie assez importante de la production primaire est oxydée dans la zone euphotique (Legendre & Le Fèvre, 1989; Legendre & Gosselin, 1989; Meddeb et al., 2019). Sakka Hlaili et al. (2014) ont carcatérisé deux sous type du réseau microbien. Le réseau « *phyto-microbien* » dans lequel le protozooplancton se nourrit principalement sur le phytoplancton et le « *réseau poly-microbien* » où le protozooplancton consomme toutes les ressources alimentaires disponibles à savoir phytoplancton, bactérioplancton et détritus. Legendre & Rassoulzadegan (1995) ont défini une voie trophique intermédiaire entre les réseaux herbivore et microbien à savoir le réseau multivore « ***Multivorous food web*** » (Figure I. 2d). Dans ce type de réseau, l'herbivorie et la microbivorie jouent simultanément un rôle crucial dans le transfert du carbone biogène. Le

broutage du gros phytoplancton par les copépodes ainsi que le protozooplancton herbivore favorise l'activité d'excrétion de ces brouteurs, ce qui enrichit le milieu par le COD et NOD et d'ammonium. Du fait de l'abondance du NOD, il y a reminéralisation de l'ammonium par les bactéries et par leurs brouteurs protozoaires. Ce nutriment régénéré favorise la production du petit phytoplancton qui est activement exploité par le protozooplancton microbivore. Récemment, Meddeb et al. (2019) ont identifié un nouveau type de réseau trophique appelé «***Bacterial multivorous food web***» (Figure I. 2e), qui s'ajoute au continuum trophique conventionnel. Cette nouvelle voie trophique a été caractérisée par la co-contribution de phytoplancton et de bactérioplancton ensemble à la production de carbone et par le plus fort recyclage du carbone, ce qui a conduit à une plus grande rétention du carbone dans l'écosystème et une faible efficacité de transfert vers les niveaux supérieurs.

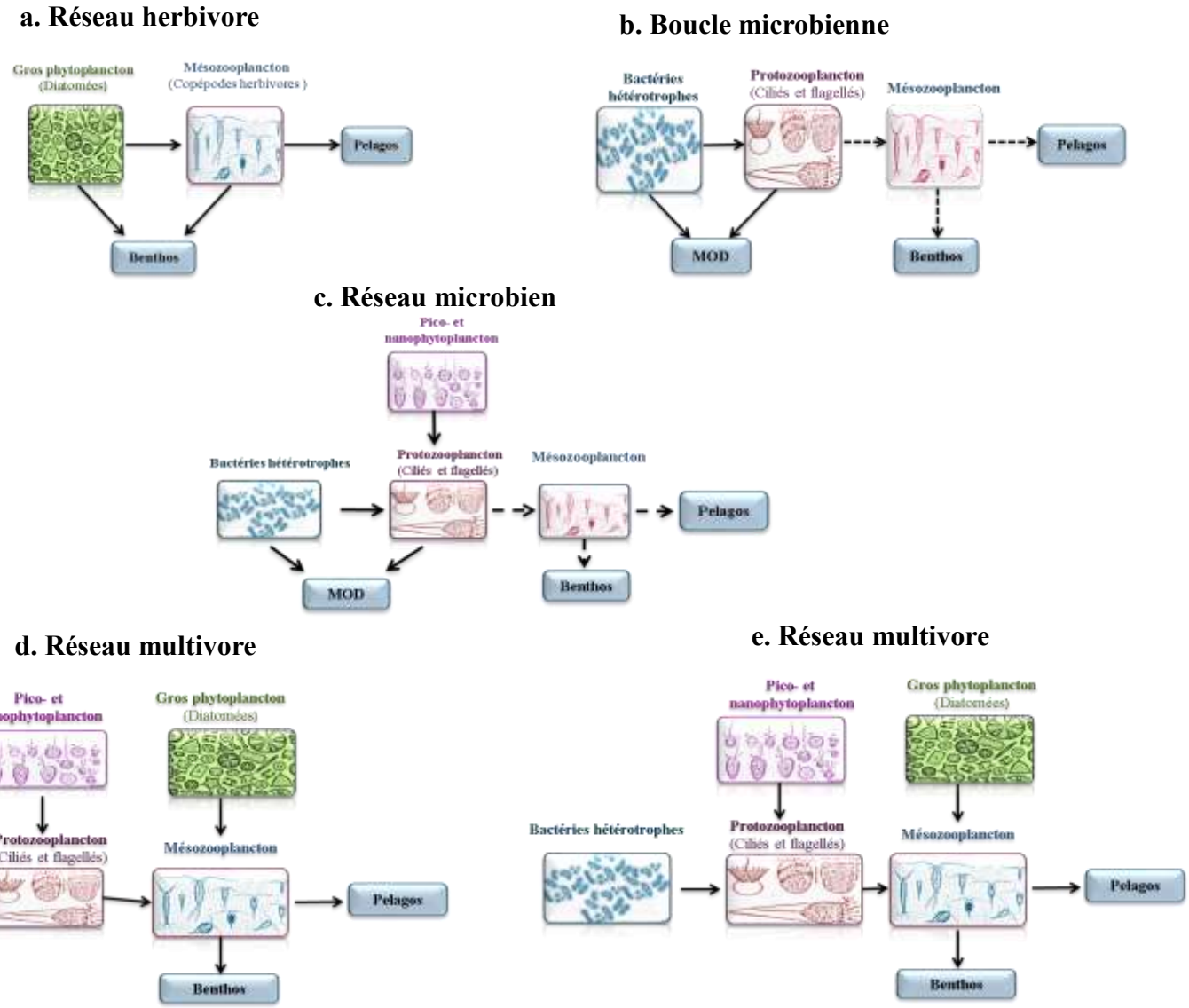

Figure I. 2. Différent types de réseaux trophiques planctoniques marins.

Perturbation des écosystèmes marins et réseaux trophiques planctoniques

Un écosystème est dit "stressé" lorsque sa structure et ses processus naturels sont altérés face à une perturbation. Généralement, les tendances attendues dans un écosystème soumis à un stress comprennent des changements dans la biomasse, la structure et la fonction de la communauté, l'énergétique (respiration, exportation ou désaffectation de la production primaire) et le cycle des nutriments (augmentation du transport horizontal et diminution du cycle vertical des nutriments) (Odum, 1985). La réponse de l'écosystème à un stress dépend du type de stress. Par exemple, un stress chronique qui se prolonge sur une longue période peut avoir un effet différent d'un stress aigu qui est rapidement suivi d'une récupération et d'un retour à un état non stressé (Odum, 1985). Les réseaux trophiques marins sont soumis à différentes types de perturbations anthropiques qui sont susceptibles de modifier leurs structures et fonctionnements. Quel que soit le type de perturbation (naturelle ou anthropique), elle est capable de modifier l'écosystème et donc les communautés qui y constituent (Frontier et al., 2008). Ainsi, la compréhension de la réaction des écosystèmes face aux perturbations est un ancien enjeu de la recherche écologique (MacArthur, 1955; Yodzis, 1988). Des efforts considérables ont été réalisés pour déterminer les caractéristiques structurelles des communautés, à savoir les types d'interaction entre les espèces (Allesina & Tang, 2012) ou la structure du réseau (Rooney et al., 2006; Grilli et al., 2016), qui influencent la capacité de l'écosystème à résister à une perturbation (résistance) et à s'en remettre (résilience).

Les travaux sur la contamination marine traitent les différents types de polluants présents dans les milieux marins, leur devenir dans les systèmes marins ainsi que leurs effets sur les différents niveaux trophiques. La vulnérabilité de cette contamination est d'autant plus visible que les organismes appartiennent à des niveaux trophiques plus élevés. Son effet sur le phytoplancton est discret et n'est remarqué qu'après que les changements qui en résultent se sont transmis en cascade à d'autres niveaux trophiques et sont devenus évidents (D'Costa et al., 2017) . Le phytoplancton, par son cycle de vie court (David et al., 2007), et le zooplancton, par la capacité de certaines espèces à produire des formes de résistance (Guerrero & Rodriguez, 1998), sont d'excellents indicateurs des conditions environnementales et de la santé aquatique, car ils sont sensibles aux changements de la qualité de l'eau. Ils réagissent à de faibles niveaux d'oxygène dissous, à des niveaux élevés

de nutriments, à des contaminants toxiques, à une mauvaise qualité ou abondance de la nourriture et à la prédation.

Les changements produits par les perturbations sur la structure des communautés planctoniques peuvent avoir des conséquences sur la totalité réseau trophique planctonique. Ce dernier, donne une vision claire du fonctionnement des écosystèmes et de sa stabilité à travers l'étude des relations trophiques entre les communautés planctoniques (Ulanowicz, 1986, 1997). Cette stabilité est reconnue comme une propriété efficace de caractérisation de l'écosystème (McCann, 2000). Elle peut être mesurée soit par la résistance (c.à.d. la capacité d'un écosystème à résister à une perturbation) soit par la résilience (McCann, 2000), permettant ainsi d'avoir une information sur l'organisation et la composition modifiée de l'écosystème. Dans le milieu marin, en décrivant la stabilité d'un écosystème, Legendre & Rassoulzadegan (1995) ont déclaré que le réseau alimentaire herbivore qui domine les eaux stressées par les forts apports en nutriments, agit comme un système peu stable, puisqu'il est de nature transitoire. En revanche, les réseaux alimentaires multivores et microbiens, qui dominent les eaux plus au moins oligotrophes, ont une plus grande stabilité et sont donc plus durables et dominent l'environnement pélagique dans la plupart des océans. D'autres propriétés émergentes ont été associées à chaque type de réseau. Le réseau herbivore est défini comme un réseau à forte efficacité trophique (transfert d'énergie vers les hauts niveaux trophiques) et à forte exportation de matière, alors que la boucle microbienne et le réseau microbien engendre par opposition un fort recyclage de la matière et une faible efficacité trophique (Legendre & Rassoulzadegan, 1995).

Les réseaux alimentaires planctoniques présentent un intérêt croissant depuis plus de 40 ans (GOFS, 1986), en raison de leur relation intense avec les cycles biogéochimiques marins et, principalement, avec la régulation de l'augmentation des concentrations de CO_2 dans l'atmosphère. Ces réseaux peuvent être des indicateurs de temps de séjour des éléments et des contaminants dans les eaux de surface en changeant leurs structures (Frost, 1984; Goldman & Caron, 1985; Vézina & Platt, 1987). De plus, il est clair que la productivité secondaire est liée à la production primaire, donc le fonctionnement planctonique affecte directement l'exploitation des ressources naturelles. En outre, les pressions anthropiques croissantes sur la plupart des océans, lacs et lagons du monde confirment l'importance d'examiner les réponses du réseau trophique pour prédire l'avenir de la production secondaire.

Modélisation des réseaux trophiques planctoniques

Par modélisation, nous entendons une projection de la réalité et du fonctionnement d'un système, par un modèle, c'est-à-dire par " *une construction de l'esprit, dans laquelle la réalité est simplifiée, permettant de mieux l'appréhender, avec une intention précise* " (De Brabandere & Iny, 2012). Depuis son implantation (Riley, 1946), la modélisation a permet de développer de nouvelles techniques qui facilitent la compréhension du fonctionnement des écosystèmes marins. La modélisation est une approche mathématique utilisant des équations pour caractériser les processus au sein de l'écosystème.

Plusieurs approches de modélisation ont été développées pour caractériser les réseaux alimentaires marins. Ces modèles peuvent fournir des bases écologiques pour les services écosystémiques et la gestion des systèmes marins naturels (Carpenter et al., 2009; Bagstad et al., 2013; Beske-Janssen et al., 2015). La modélisation du réseau trophique par Ecopath associé à Ecosim (EwE) est une approche principalement utilisée pour étudier les niveaux trophiques supérieurs soumis à la pêche (Pauly et al., 2000; Christensen, 2005; Sreekanth et al., 2021) et pour évaluer l'impact de l'exploitation humaine et des changements environnementaux sur les réseaux trophiques aquatiques (Steenbeek et al., 2018). Le modèle linéaire inverse (LIM), tel que défini par (Vézina & Piatt, 1988), est issu des sciences physiques et est considéré comme l'une des méthodes les plus utiles dans l'étude de l'état des écosystèmes marins (Niquil et al., 2011; Pacella et al., 2013; Taffi et al., 2015; Hines et al., 2018). Cette méthode a été combinée à la technique de la chaîne de Markov Monte Carlo (MCMC) pour devenir la méthode innovante LIM Markov Chain Monte Carlo (LIM-MCMC; Van den Meersche et al., 2009). L'analyse LIM-MCMC estime l'incertitude des flux et des indices des propriétés structurelles et fonctionnelles du réseau trophique (De Laender et al., 2010; Grami et al., 2011; Niquil et al., 2011; Saint-Béat et al., 2013; Chaalali et al., 2015; Hines et al., 2018).

Vu la complexité des réseaux trophiques marins et la diversité des interactions au sein d'eux, la mesure de tous les flux de carbone entre les différents compartiments trophiques est impossible à réaliser. Vézina & Platt (1988) sont les premiers qui ont utilisé l'analyse inverse pour reconstruire les flux de matière inconnus à partir des flux connus (i.e. mesurables sur le terrain) et donc ils ont résolu le problème de l'estimation des flux de carbone manquant dans les réseaux planctoniques. L'avantage de l'analyse inverse est d'obtenir une estimation des divers échanges trophiques entre les compartiments en intégrant

l'ensemble des données existantes sur les processus biologiques et écologique, et de caractériser l'incertitude de ces estimations.

Cette méthode comporte 4 étapes qui sont résumé dans la Figure I. 3. (i) Elle démarre par la mise en place d'un type de modèle conceptuel, le model *a priori*, qui présente les différentes interactions entre les compartiments vivants et non vivants. (ii) Ensuite, on établit des bilans de masse qui correspondent à un équilibre des flux entrants et sortants de chaque compartiment trophique. Les flux entrants correspondent à la production primaire, ou la consommation et à l'importation vers un compartiment donné. Les flux sortants comprennent la respiration, l'excrétion, la prédation et l'exportation du compartiment considéré. (iii) Puis, on ajoute des informations sur les flux mesurés sur le terrain, avec leur intervalle de variation, et sur les flux inconnus à partir de la littérature. Ces informations constituent des inéquations ou contraintes biologiques et permettent d'attribuer des valeurs réalistes à chaque flux. (iv) La dernière étape consiste en calcul des solutions possibles par un échantillonnage de l'espace des solutions aussi appelé polytope (Niquil et al., 2011).

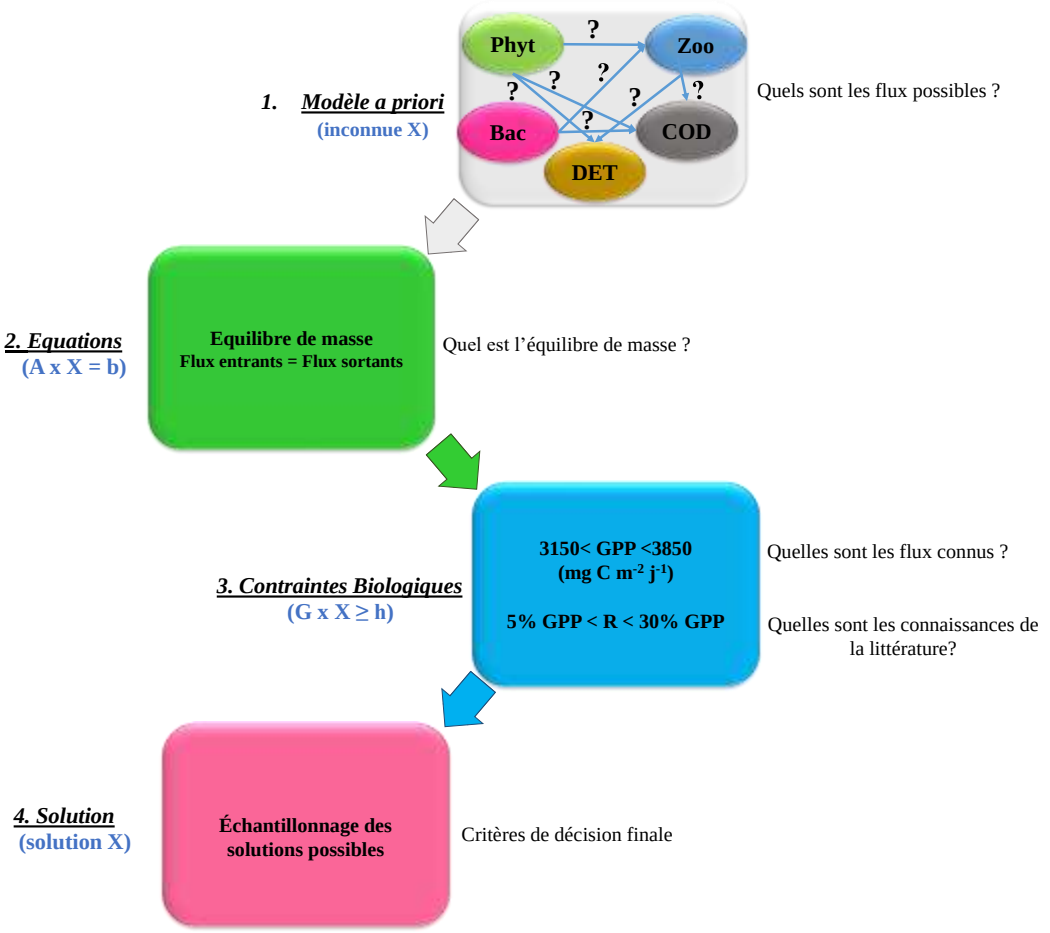

Figure I. 3. Schéma illustrant les différentes étapes de l'analyse inverse (Vézina & Platt, 1988)

Phyt= Phytoplancton ; **Bac**= Bactéries ; **Zoo**= Zooplancton; **COD** = Carbone organique dissous ; **DET**= Détritus ; **GPP phyt**= Production primaire brute du phytoplancton ; **R**= respiration du phytoplancton

Chapitre II

Matériels et Méthodes

Sites d'étude, échantillonnages et méthodes analytiques

I. Description des sites d'étude

1. Golfe de Gabès

Le Golfe de Gabès est situé sur la côte sud-est de la Tunisie. Il représente plus de la moitié du littoral tunisien avec environ 700 km et possède le plus grand plateau continental de la mer Méditerranée. Son contour, mesuré uniquement sur l'isobathe 20 mètres, est de 110 milles nautiques. La profondeur de 50 mètres s'étend à plus de 70 milles nautiques au large des îles *Kerkennah* (Hattour et al., 2010). Le Golfe est caractérisé par une circulation complexe des eaux résultant de la combinaison de courants généraux, de courants de marée, de courants éoliens et/ou de courants de houle ou littoraux, et les marées atteignent l'amplitude la plus élevée en mer Méditerranée (~ 2 m) (Hattour et al., 2010; Othmani et al., 2017). Le Golfe abrite des eaux riches en nutriments en raison des apports des activités anthropiques (M. B. Bel Hassen et al., 2009; Drira et al., 2009b; Khammeri et al., 2018), ce qui contraste avec l'oligotrophie bien connue du bassin méditerranéen oriental (D'Ortenzio & Ribera d'Alcalà, 2009; Ben Brahim et al., 2010). Le Golfe est un écosystème très productif qui abrite une grande biodiversité marine et contribue à hauteur de ~50% à la production nationale de poissons (DGPA, 2015; Béjaoui et al., 2019). Il constitue également un écosystème de nurserie crucial pour la mer Méditerranée (Enajjar et al., 2015; Koched et al., 2015). Cet écosystème a récemment été considéré comme l'une des onze écorégions consensuelles de la mer Méditerranée et est classé comme une région d'eau peu profonde caractérisée par des efflorescences de phytoplancton (Ayata et al., 2018). Néanmoins, le Golfe est identifié comme un hotspot de pressions anthropiques (Reygondeau et al., 2017) car il est fortement impacté par l'industrialisation, notamment les rejets des usines de production de phosphate, principalement le Groupe Chimique Tunisien (Boudaya et al., 2019; Kmiha-Megdiche et al., 2021). La surpêche est également un problème croissant dans le Golfe, entraînant un déséquilibre de l'écosystème et le déclin des ressources halieutiques (Béjaoui et al., 2019).

2. Canal de Bizerte

Le Canal de Bizerte situé au nord de la Tunisie forme un milieu de transition entre la Baie et la Lagune de Bizerte, avec une longueur de 7 km, une largeur de 300 m et une profondeur de 12 m. La rareté des données bibliographiques sur ce milieu, nous permet d'avoir très peu de données sur l'hydrodynamisme dans ce site. Le canal est fortement influencé par la courantologie de la Méditerranée et de la Lagune de Bizerte. L'hydrodynamisme est sous contrôle des houles et des marées. L'action des houles est relativement faible vue la mise en place des brises lames à l'entrée du canal (Furse, 1899; Shaiek et al., 2017). La marée au niveau du Canal dépend de celle de la Lagune et des côtes mais reste généralement faible (Ben Haj, 1992). Le Canal est soumis à une eutrophisation progressive depuis des années, due à d'importants apports d'éléments nutritifs (3,5–32,40 N µM; 1,30–11,5 P µM; 2–11 Si µM), induisant des teneurs élevées en Chl *a* (6,20 mg m^{-3}) (Bouchouicha Smida et al., 2012; Sahraoui et al., 2012*)*. Ainsi, les décharges d'égouts municipaux, le ruissellement d'une grande décharge municipale anarchique sur ses berges (près de la cimenterie), et les rejets de la station d'épuration de Sidi Ahmed, riches en nitrates et en phosphates rend ce milieu un écosystème de plus en plus pollué. Cette contamination est de nature plutôt chimique supportée surtout par les élements traces métalliques (85–228 mg g^{-1} de sédiments secs), les hydrocarbures aromatiques polycycliques (21–772 µg g^{-1} de sédiments secs) et les Polychlorobiphényles (4,39 et 6,62 ng g^{-1} de sédiments secs) (Derouiche et al., 2004; Pringault et al., 2016).

II. Echantillonnages

1. Golfe de Gabès

Une campagne d'échantillonnage a été réalisée du 31 octobre au 3 novembre 2017 au niveau du Golfe de Gabès dans le cadre du projet MERMEX-MERITE. Notre étude a été menée au niveau de quatre stations pertinentes (S1, S2, S3 et S4, Figure. II.1) caractérisées par une distribution hétérogène des nutriments. La station S2 est située en face de l'usine d'acide phosphorique du complexe industriel de Ghannouch-Gabès et a été choisie pour représenter les eaux côtières affectées par la charge de phosphogypse; les stations S1 et S4 sont localisées de part et d'autre de la station S2 (au nord et au sud, respectivement), tandis que la station S3 est une station offshore située en face de la station S1. Les caractéristiques des stations sont présentées dans l'article, ci-après.

Pour chaque station, l'eau a été collectée (en trois repliques) à l'aide d'un échantillonneur en plastique (Hydro-Bios) et ses propriétés physico-chimiques (température, salinité, pH et oxygène dissous) ont été mesurées *in situ* avec un capteur multisondes (Multi 1970i, WTW), au niveau de trois profondeurs (de 0.5 à 14 m), qui ont été choisies selon la bathymétrie de la station et le coefficient d'atténuation verticale de la lumière.

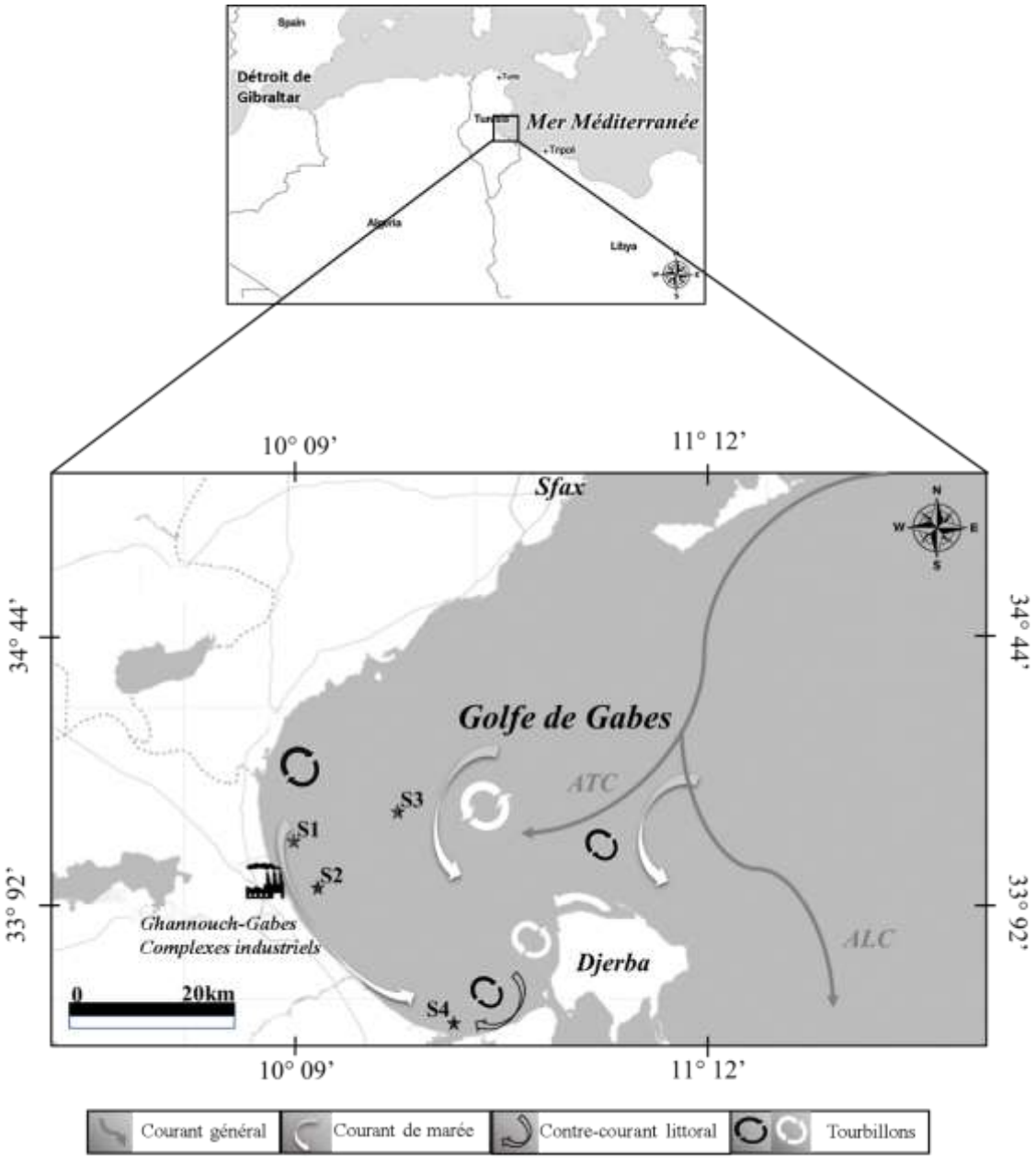

Figure II. 1. Golfe de Gabès :localisation des stations d'échantillonnage et circulation hydrodynamique (courant tunisien atlantique : ATC et Atlantique Lybien : ALC). Modifié d'après Zayen et al., (2020)

Des sous-échantillons (5 mL) ont été immédiatement filtrés sur des filtres en polycarbonates stérilisés (0,2 µm) et congelés à -20°C dans des flacons lavés à l'acide jusqu'à l'analyse du carbone organique dissous(COD). L'eau restante a été filtrée sur un filet Nitex de 200 µm, pour enlever le métazooplancton, et des sous-échantillons ont été pris pour les analyses des nutriments (1000 ml), du carbone organique particulaire (COP)(200ml), du phytoplancton fractionné en taille (picophytoplancton: < 2 µm; nanophytoplancton: 2-10 µm; microphytoplancton: 10-200 µm)(100ml), de la chlorophylle *a* (Chl *a* totale et de différentes fractions de taille)(1000 ml), du bactérioplancton (2 ml) et du protozooplancton (200 ml). En outre, le métazooplancton a été collecté avec un filet à plancton WP2 (200 µm de maille et 28 cm de diamètre) par des traits verticaux depuis le bas vers la surface. Des échantillons d'eau (1000- 1400 ml) collectés par le filet ont servi pour l'analyse du métazooplancton.

2. Canal de Bizerte

Une marée noire était survenue le 4 octobre 2018 dans la Baie de Bizerte à la suite d'une fissure dans le réservoir de la société tunisienne STIR causant une fuite de 7 tonnes de pétrole brute. Les caractéristiques climatiques et hydrodynamiques de la région de Bizerte ont étendu l'impact du déversement pétrolier à 5 Km de la source de la fuite et la nappe de pétrole a été dirigée vers le Canal de Bizerte (Figure.II. 2).

L'échantillonnage a été conduit à une station (profondeur maximale de 7 m) dans le Canal de Bizerte (Figure. II. 2) les 5, 8, 12 et 22 octobre 2018, qui correspondaient, respectivement, aux 1^{ier}, 4ème, 8ème et 18ème jours après la fuite du pétrole. La prospection sur le terrain a montré la présence d'une couche de pétrole à la surface de la station du 1^{ier} au 8ème jour. En fin de l'échantillonnage (18ème jour), l'eau de la station avait retrouvé sa couleur et son odeur d'avant accident.

A chaque jour, trois échantillons d'eau ont été prélevés soit au niveau de trois profondeurs par un échantillonneur (0,5, 2,5 et 5 m), soit sur toute la colonne avec une pompe submersible. Ces échantillons ont été ensuite filtrés sur 200 µm et ont servi pour analyser les nutriments (1000 ml), la Chl *a* (1000 ml), le phytoplancton et le protozooplankton (200ml). La température de l'eau et la salinité ont été enregistrées *in situ* avec un conductimètre à microprocessuer (LF 196, WTW), le pH a été mesuré à l'aide d'un pH-mètre (AB15, Fischer Scientific) tandis que la turbidité de l'eau a été déterminée avec un turbidimètre (TURB 350 IR, WTW)

Au 8ème jour, des échantillons d'eau ont été prélevés manuellement à environ 0,5 m sous la surface d'eau dans des bouteilles en verre pré-nettoyées et stériles et des échantillons de

sédiments ont été collectés avec une benne Van Veen (Hydro-Bios). Ces échantillons (1000 ml) ont servi pour analyser les hydrocarbures aromatiques polycycliques (HAPs), les composés les plus toxiques du pétrole (Jiang et al., 2010).

Figure II. 2. Localisation du site de déversement de pétrole (dans la Baie de Bizerte) et du site d'échantillonnage. Photos des côtes polluées de la plage de Sidi Semlem (1- https://www.webdo.tn/2018/10/05/bizerte-7-tonnes-de-petrole-ont-fuite-dans-la-mer-de-zarzouna/) et du Canal de Bizerte (2- https://directinfo.webmanagercenter.com/2018/10/10/tunisie-les-plages-polluees-par-une-vaste-couche-de-petrole-video/)

Pour les deux sites, le Golfe de Gabès et le Canal de Bizerte, les différentes étapes des échantillonnages ont été illustrées dans la Figure.II. 3.

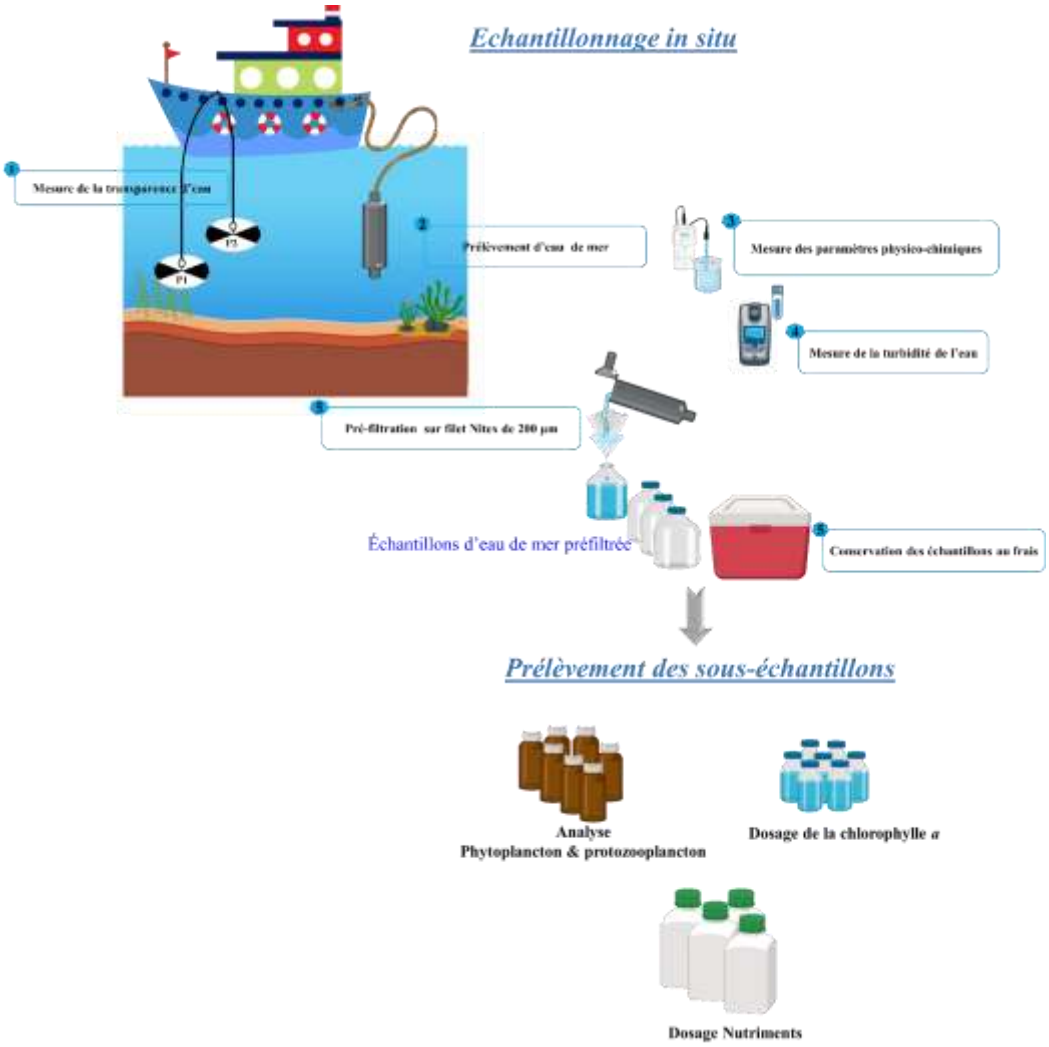

Figure II. 3. Schéma illustrant les différentes étapes réalisées pour l'échantillonnage *in situ* et le prélèvement des sous-échantillons pour les analyses au laboratoire

III. Méthodes analytiques

Les méthodes analytiques utilisées lors de cette étude sont détaillées dans les différents articles. Ici, une brève description est donnée.

Les nutriments inorganiques (NO_3^-, NO_2^-, NH_4^+, PO_4^{3-}, $Si(OH)_4$) et totaux (azote et phosphore) étaient analysés avec un auto-analyseur (Bran et LUEBBE type 3) pour les échantillons du Golfe de Gabès ou avec un spectrophotomètre (JENWAY 6400) (Parsons et al., 1984) pour les échantillons du Canal de Bizerte.

Les HAPs dans l'eau de mer et les sédiments ont été analysés par chromatographie gazeuse FID (Agilent Technologies) selon la technique proposée par UNEP/FAO/IAEA/IOC.1996.

Le COD a été analysé à l'aide d'un autonalyseur Shimadzu TOC-5000A (Sharp et al., 1993), alors que l'analyse du COP s'est basée sur la méthode de combustion élevée et la spectrométrie de masse (Raimbault et al., 2008) (Figure II. 4).

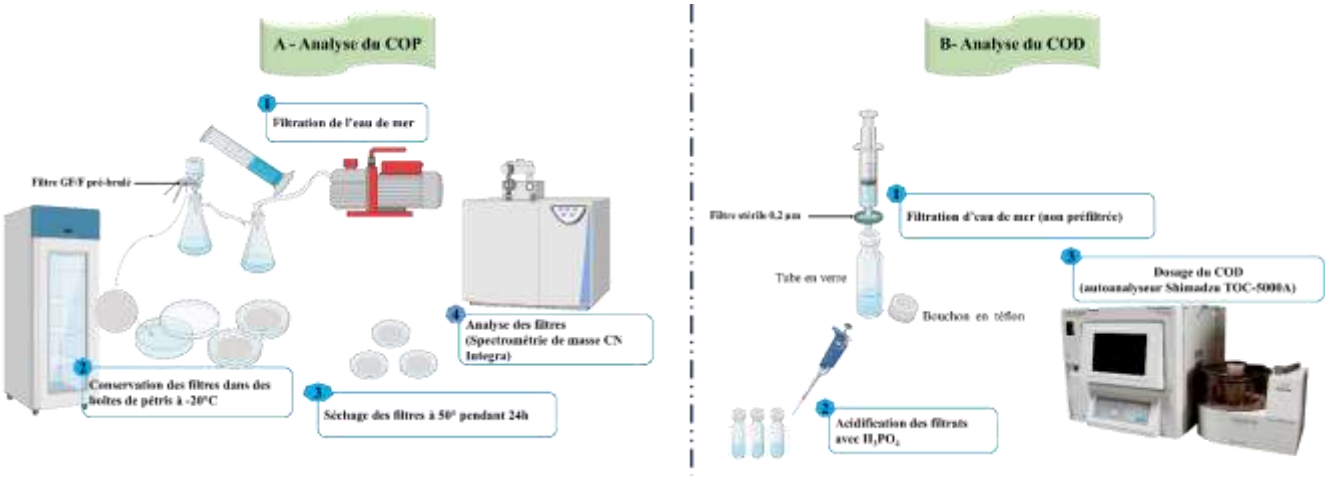

Figure II. 4. Schéma illustrant les différentes étapes d'analyses du COP (1-4) et COD (1-3)

La Chl *a* totale et des trois fractions de taille du phytoplancton était analysée selon la méthode spectrophotométrique (Parsons et al., 1984) (Figure II. 5).

Les abondances cellulaires du bactérioplancton (BAC) et du picophytoplancton (PIC) était déterminées en utilisant un cytomètre en flux (CyFlow® Space , Partec). Le comptage et l'identification du nanophytoplancton (NAN) et microphytoplancton (MIC) ont été réalisés selon la méthode de la microscopie inversée d'Utermöhl, (1931). Le protozooplancton (PRO) était énuméré et identifié aussi sous un microscope inversé (Motic AE31E). Pour le métazooplancton (MET), l'analyse était réalisée à l'aide d'un stéréo-microscope (Leica M 205C) (Figure II. 5).

Les abondances cellulaires (cellules L^{-1}) du bactérioplancton, des trois fractions de taille du phytoplancton et du protozooplancton ont été converties en biomasses carbonées (mg C m^{-3}) en utilisant des facteurs ou des équations de conversion spécifiques au groupe planctonique (Meddeb et al., 2018). La longueur et la largeur des organismes métazoaires ont été mesurées et converties en teneur en carbone en employant des facteurs de conversion ou des formules

correspondant à chaque groupe métazoaire (Meddeb et al., 2018). Les concentrations du COD (mg C m^{-3}) ont été obtenues en considérant que 1 µM de COD correspondait à 12 mg C m^{-3} (Grami et al., 2008). La biomasse (mg C m^{-3}) du carbone organique détritique (DET) a été estimée comme étant le COP moins les biomasses carbonées de tous les organismes planctoniques.

Pour chaque compartiment planctonique, les concentrations en carbone exprimées en mg C m^{-3} ont été intégrées verticalement pour déterminer la biomasse en mg C m^{-2}. Les différents calculs et formules utilisées ont été détaillés dans les articles ci-après.

.

Analyse de la Chl *a* fractionnée

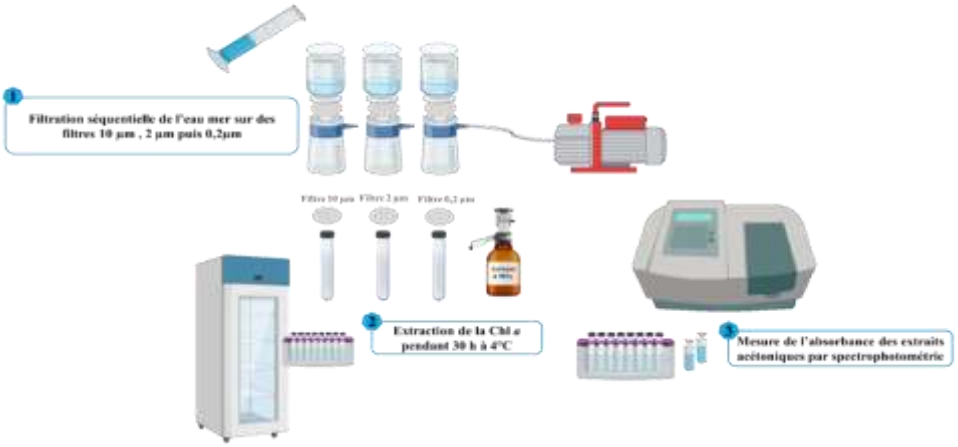

Analyse du nano-/microphytoplancton et du protozooplancton

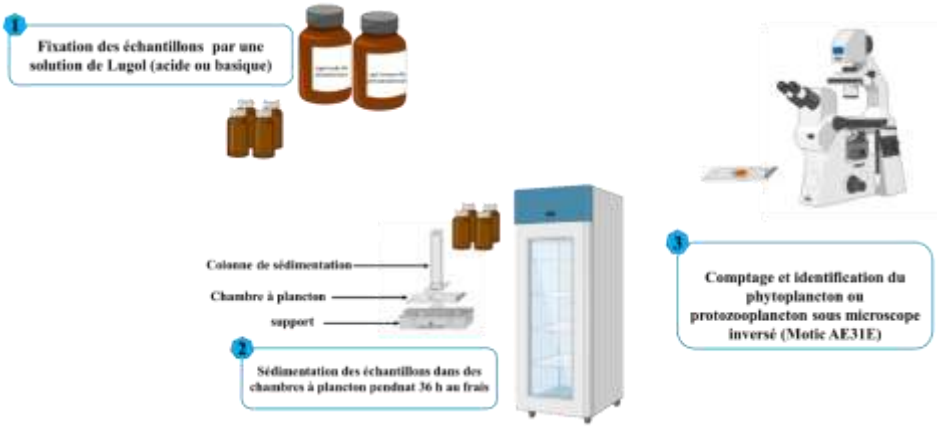

Analyse du métazooplancton

Figure II. 5. Schéma illustrant les différentes étapes des analyses de la Chl *a* fractionnée, du phytoplancton, du protozooplancton et du métazooplancton

Mesure *in situ* des flux de carbone

I. Estimation de la production bactérienne et primaire et leur consommation par le protozooplancton

La production du bactérioplancton et du phytoplancton (i.e. PIC, NAN et MIC) ainsi que leur taux de consommation par le protozooplancton ont été estimées par la méthode de dilution. Cette méthode a été amplement utilisée au cours des dernières décennies dans différents milieux marins et côtiers, y compris les eaux méditerranéennes (Calbet & Landry, 2004; Sakka Hlaili et al., 2007; Grami et al., 2008; Grinienė et al., 2016; Meddeb et al., 2019; Leruste et al., 2019; Pecqueur et al., 2022; Wickham et al., 2022). Cette technique, mise au point par Landry & Hassett (1982), est relativement simple et permet de mesurer simultanément les taux de croissance des proies et leur taux de broutage par les proto-consommateurs. De plus, elle ne nécessite pas beaucoup de manipulations et ainsi les communautés planctoniques sont peu perturbées. En outre, cette technique a montré des taux de production phytoplanctonique similaires à ceux mesurés par la méthode de ^{14}C (Moigis & Gocke, 2003; Meddeb et al., 2018; Dokulil & Qian, 2021).

Au cours de notre étude, des expériences de dilution ont été menées dans le Golfe de Gabès (au niveau des quatre stations) et le Canal de Bizerte (pendant les quatre jours de monitorage) parallèlement aux échantillonnages. La procédure expérimentale, qui est illustrée dans la Figure II. 6, ainsi que les analyses et les calculs sont détaillés dans le chapitre III.

II. Estimation de la consommation du phytoplancton par le métazooplancton

Pendant l'échantillonnage menée dans le Golfe de Gabès, la consommation du phytoplancton par le métazooplancton a été estimée en analysant les pigments des contenus stomacaux des métazoaires (Slaughter et al., 2006). Dans l'analyses, seul le phytoplancton > 2µm a été considéré puisque le métazooplancton (en particulier les copépodes) a une faible efficacité de filtration pour les particules < 5 µm (Bergales et al., 1988). Cette technique est largement utilisée car elle est simple et très utile pour étudier le rôle fonctionnel du métazooplancton dans divers milieux marins (Tseng et al., 2008; Meddeb et al., 2018; He et al., 2021).

Le métazooplancton a été collecté au niveau des quatre stations dans le Golfe par le filet à plancton WP2 (200 µm), comme expliqué, et les échantillons collectés (200 ml) ont été

immédiatement anesthésiés, avec 10% d'eau gazéifiée, pour minimiser le stress et l'évacuation du contenu stomacal (Kleppel & Pieper, 1984), puis congelés dans l'obscurité pour minimiser la production des pelotes fécales (Saiz et al., 1992) (Figure II. 7). Les différentes étapes de l'analyse, le calcul des teneurs en pigment stomacaux ainsi que des taux de consommation sont détaillés dans le Chapitre III.

III. Estimation des Flux verticaux des particules

Les flux verticaux des particules organiques (i.e. phytopplancton, pelotes fécales du métazooplancton et détritus) ont été estimés en employant des pièges à sédiment au niveau des quatre stations dans le Golfe de Gabès. Cette technique a été utilisée dans différentes études pour quantifier et qualifier le flux de matière organique particulaire qui quitte la couche euphotique vers les eaux profondes (Laurenceau-Cornec et al., 2015; Meddeb et al., 2019; Xiang et al., 2022; Kojima et al., 2022).

A chaque station, deux pièges à sédiments (63 cm de hauteur et 9 cm de diamètre) ont été incubés verticalement pendant 24 h laissant à peu près 2 m du fond, telsque illustré dans la Figure II.8 Avant leur déploiement, les pièges ont été remplis d'eau de mer dense (eau filtrée sur 0,2 µm + 5g NaCl L^{-1}) pour créer un gradient de densité et éviter de collecter des particules de surface. A la fin de l'incubation, les pièges ont été fermés *in situ* et gardés au frais dans le laboratoire pendant la nuit pour laisser les particules se déposer. Après avoir enlevé le surnageant, des sous-échantillons (1590 - 3150 ml) ont été pris du matériel piège pour analyser le COP, le phytoplancton (i.e NAN et MIC) et les pelotes fécales des métazoaires. Ces analyses ainsi que le calcul des flux verticaux des particules sont détaillés dans le Chapitre III.

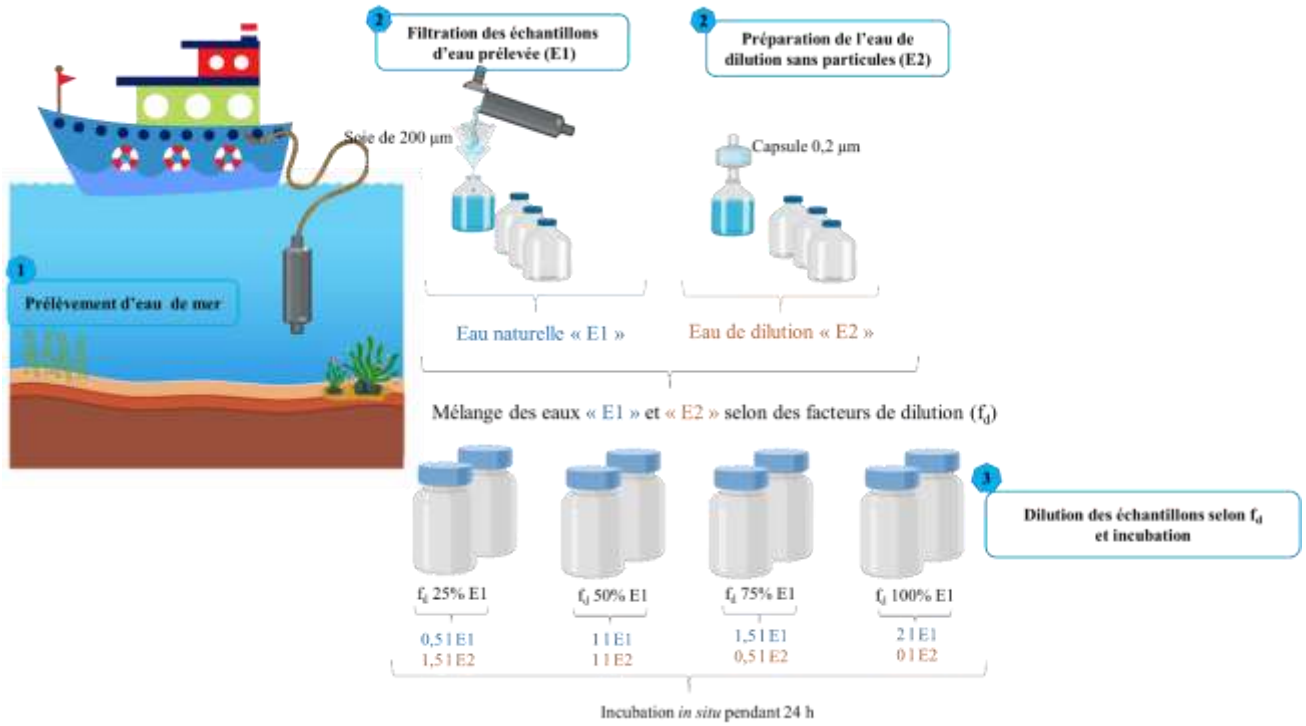

Figure II. 6. Schéma illustrant la procédure expérimentale de l'expérience de dilution

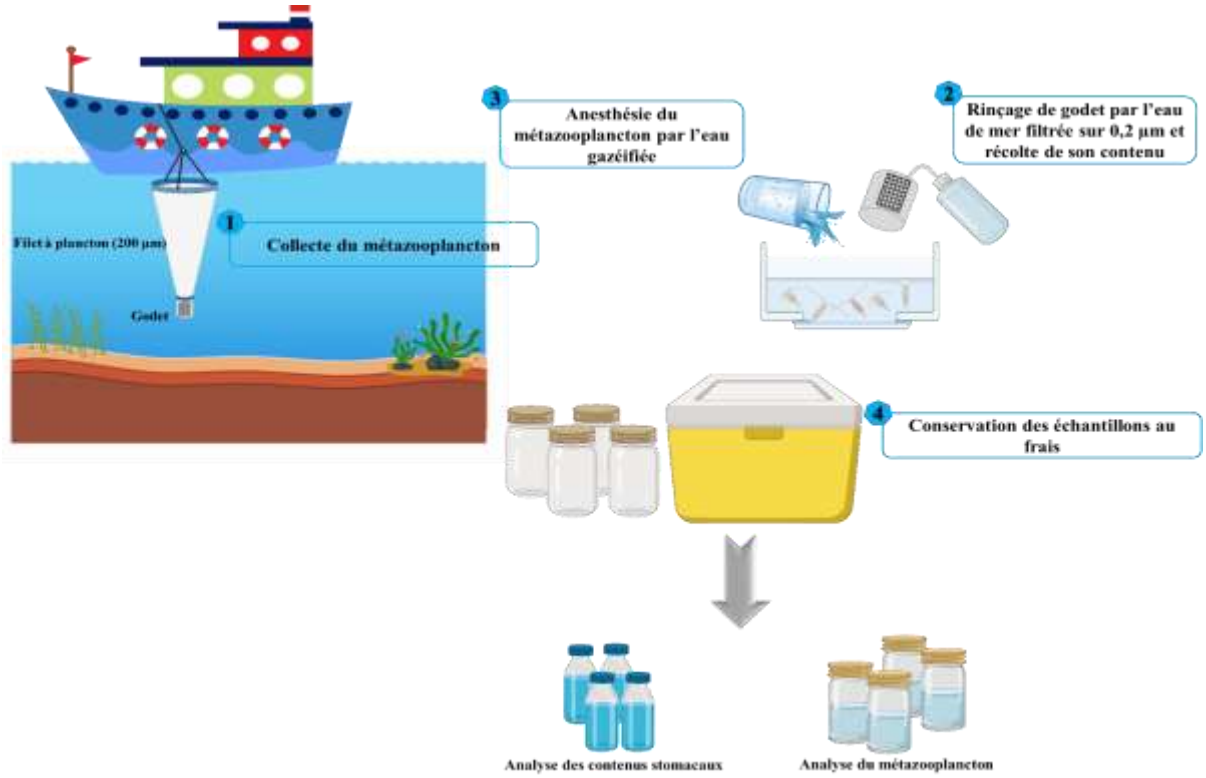

Figure II. 7. Schéma illustrant l'échantillonnage du métazooplancton et la collecte des échantillons pour l'analyse de la communauté et des contenus stomacaux

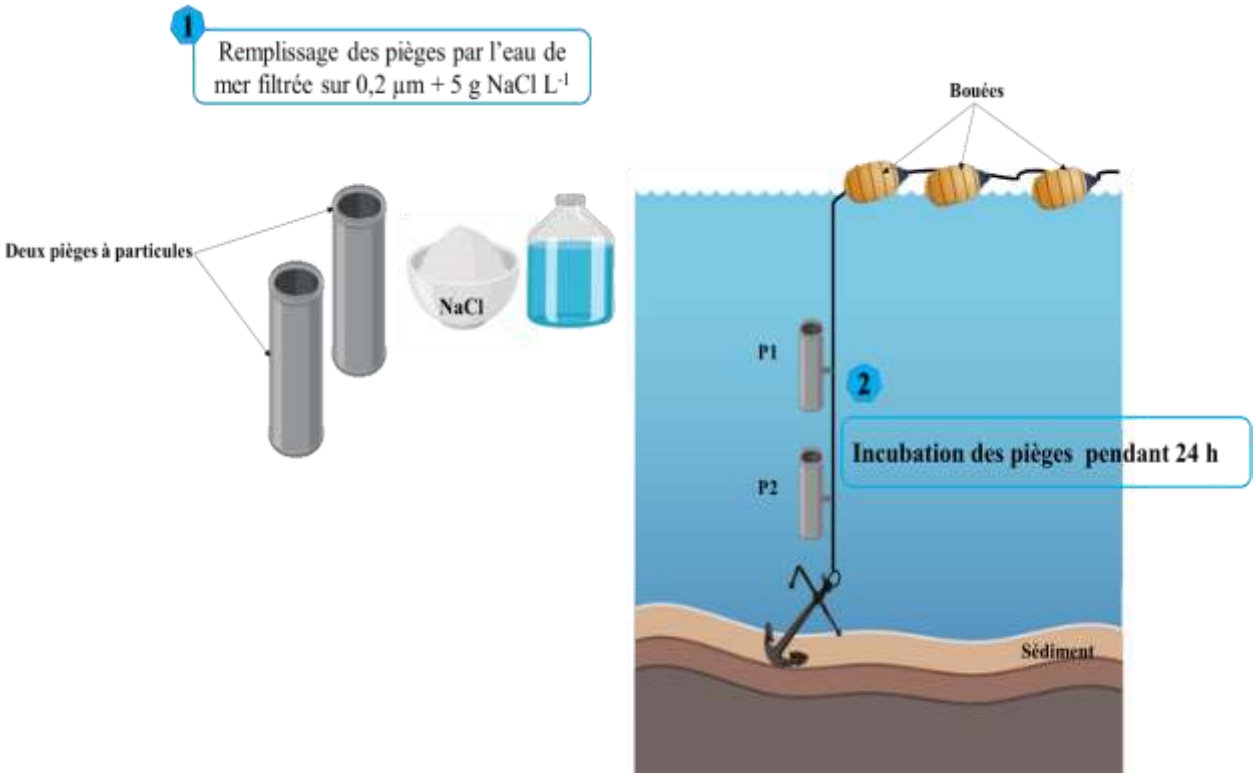

Figure II. 8. Schéma illustrant la procédure de l'incubation *in situ* des pièges à particules

Modélisation des flux de carbone et calcul des indicateurs écologiques (indices de typologie et indices fonctionnels)

I. Modélisation des flux de carbone

Des modèles des réseaux trophiques planctoniques ont été développés dans le Golfe de Gabès au niveau des quatre stations et le Canal de Bizerte pendant les quatre jours prospectées suite à la marée noire. Les flux estimés *in situ* n'ont concerné que quelques processus (comme mentionner ci-dessus). Pour avoir un modèle complet du réseau trophique planctonique la méthode de modélisation linéaire inverse combinée à la technique de Monte Carlo en chaînes de Markov (LIM-MCMC) a été appliquée dans notre étude (Vézina & Piatt, 1988; Van den Meersche et al., 2009). Cette méthode permet d'estimer l'incertitude des flux et des indices des propriétés structurelles et fonctionnelles du réseau trophique planctonqiue (Grami et al., 2011; Niquil et al., 2011; Saint-Béat et al., 2013; Chaalali et al., 2015; Hines et al., 2018). Les modèles ont été construits en appliquant le LIM-MCMC à l'aide de la fonction xsample du paquetage R LimSolve sous le logiciel R studio.

La modélisation inverse est basée sur quatre étapes:

1. **La construction d'un modèle *a priori*** qui inclut les huit compartiments planctoniques (i.e. BAC, PIC, NAN, MIC, PRO, MET, DET et COD) et tous les flux de carbone connus et inconnus possibles entre eux, tels que illustré dans la Figure II.9.

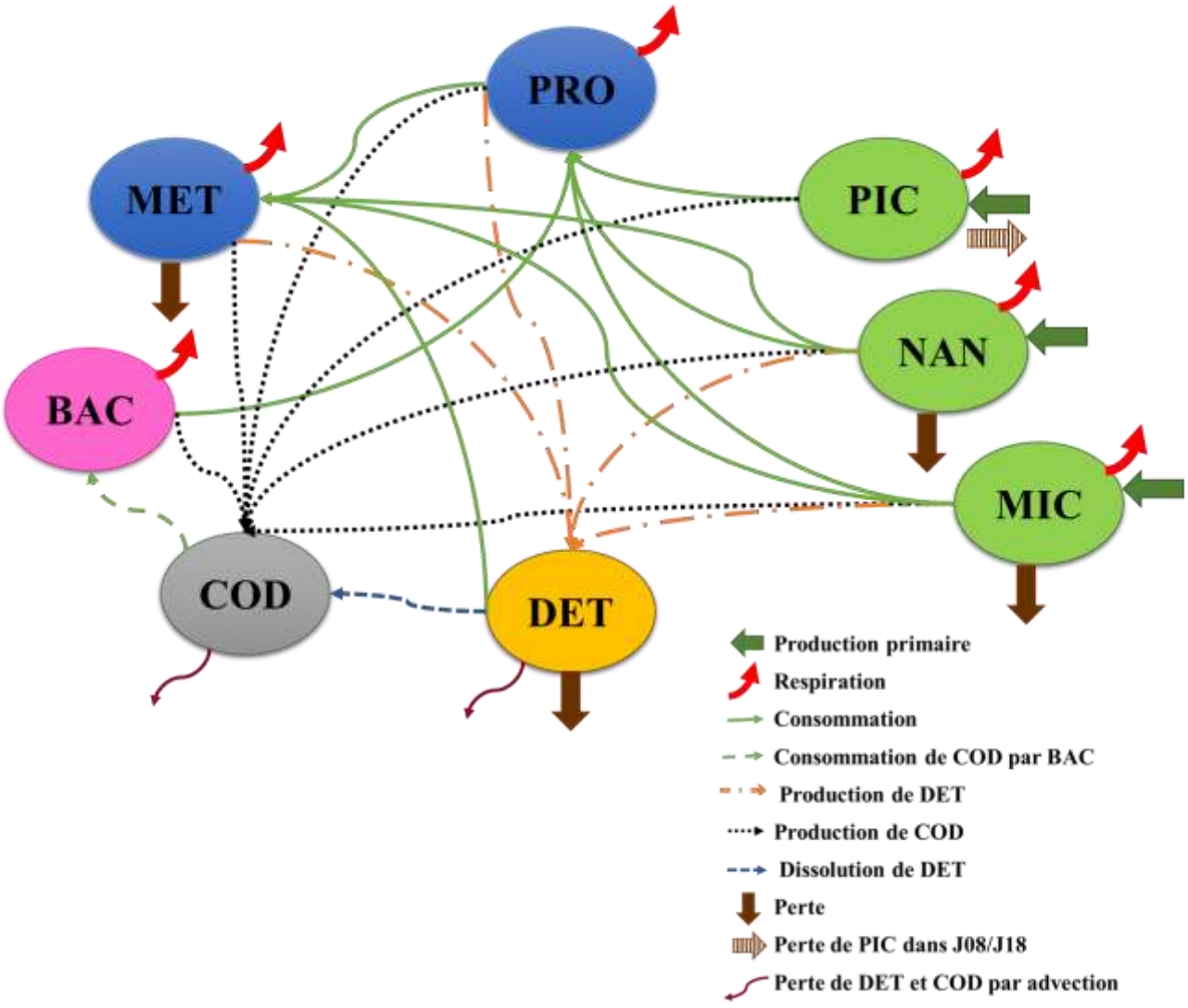

Figure II. 9. Modèle *a priori* utilisé pour construire les réseaux trophiques planctoniques au cours des différents jours suivant la marée noire. Bactéries hétérotrophes = BAC, picophytoplancton < 2 µm = PIC, nanophytoplancton, 2-10 µm = NAN, microphytoplancton 20-200 µm = MIC, protozooplancton < 200 µm = PRO, métazooplancton >200 = MET, carbone organique dissous = COD et détritus = DET

2. La mise en place des égalités : pour chaque compartiment planctonique, on établit un équilibre de masse (i.e. la somme des flux entrant est égale à la somme des flux sortant).

3. La mise en place des inégalités : ces inégalités, obtenue de la littérature, décrivent de façon logique et réelle la relation qui peut exister entre deux phénomènes naturels ou plus.

4. Le calcul des solutions possibles pour chaque flux : la dernière étape de la LIM-MCMC est le calcul de tous les flux définis dans le modèle *a priori*. Les détails de ces différentes étapes sont portés dans les chapitres IV et V.

II. Indice de typologie des réseaux trophiques

En se basant sur nombreux modèles de réseau trophique, Sakka Hlaili et al. (2014) ont défini sept indices opérationnels pour identifier la voie de transfert de carbone dans les systèmes naturels planctoniques. Ces indices de typologie du réseau sont basés sur des ratios de flux de carbone qui peuvent être facilement estimés sur le terrain.

Dans notre étude, quatre ratios de typololgie de réseau trophique ont été calculés à partir des flux fournis par la modélisation pour caractériser et décrire les interactions au sein des réseaux dans le Golfe de Gabès (i.e. au niveau des quatre stations) et le Canal de Bizerte (i.e. pendant les quatre jours suivant le déversement du pétrole). La description de ces ratios, leur interprétation ainsi que les valeurs discriminantes sontportées dans le Tableau II.1.

III. Indices fonctionnels des réseaux trophiques

Une analyse des réseaux écologiques a été appliquée pour décrire le fonctionnement des réseaux trophiques dans le Golfe de Gabès et le Canal de Bizerte à partir des flux obtenus par l'approche LIM-MCMC. Ces indices fonctionnels (indices ENA) décrivent les propriétés structurales et fonctionnelles (Ulanowicz, 1986; Fath & Patten, 1999; Tecchio et al., 2015; Meddeb et al., 2019). Le calcul de ces indices est détaillé dans le chapitre IV.

Dans notre étude un certain nombre d'indice ENA a été considéré (Tableau II. 2)

Tableau II. 1. Ratios de flux de carbone pour la détermination des types de réseaux trophiques planctoniques (ou ratios de typologie trophqiue, Sakka Hlaili et al., 2014) dans le Golfe de Gabès et de Canal de Bizerte

Ratio	Valeur de discrimination et signification	Formule	Description	Interprétation trophique
Ratio 4 (R4)		Pnetpht*/D2**	Production nette totale de phytoplancton divisée par la production nette de nourriture potentielle de PRO	Contribution du phytoplancton à la production des proies du protozooplancton
Ratio 6 (R6)		(PnetDET + PnetDOC)/D2	Production nette de COD et de DET divisée par la production nette de nourriture PRO potentielle	Contribution de la matière organique non vivante à la production des proies du protozooplancton
Ratio 7 (R7)	R7 ≤ 0.1 : Herbivore 0,1<R7<0,6 : Multivore R7 ≥ 0,1 : Microbien	PnetPIC/Pnetpht	Production nette de PIC divisée par la production nette totale de phytoplancton	Contribution du picophytoplancton à la production primaire nette totale
Ratio 8 (R8)	R8 > 0,5 : Protozooplancton R8 < 0,5 : Metazooplancton	pht-PRO/(pht-PRO + pht-MET)	Taux de consommation du phytoplancton total par PRO divisé par le taux de consommation du phytoplancton total par PRO et MET	Importance du protozooplancton dans la consommation du phytoplancton total

Tableau II. 2. Indices fonctionnels ENAs utilisés pour les modèles du Golfe de Gabès et du Canal de Bizerte.

Nomenclature des symboles utilisés dans les formules de calcul des indices: i : flux sortant du système en provenant de i , i=1,... n ; j : flux entrant dans le système en direction de j, j=1.... n; Ti : flux total sortant du compartiment i ; Tj : flux total entrant dans le compartiment j ; et Tij : flux en provenance du compartiment i vers le compartiment j. TSTc est le flux total recyclé : Flux du compartiment i vers le compartiment j. TSTc est le flux total recyclé. DET_MET : consommation de détritus par le métazooplancton et DOC_BAC : consommation de carbone organique dissous par les bactéries.

Indices ENA	Interprétation	Formule de calcul	Unité	Références
Débit total de système (**TST**)	Quantifie l'activité totale du système	$TST = \sum_{i=1,j=1}^{n} T_{ij}$	mg C m^{-2} d^{-1}	Kay et al. (1989)
Information mutuelle moyenne (**AMI**)	Mesure l'organisation des échanges entre les compartiments.	$AMI = \sum_{i=1,j=1}^{n} T_{ij} Q_i \log\left(\frac{T_{ij}}{\sum_{k=1} T_{kj} Q_k}\right)$	mg C m^{-2} d^{-1}	Latham & Scully (2002)
Ascendance relative (**A/C**)	Définit le degré d'organisation et de développement de l'écosystème.	$A/C = \frac{AMI * T..}{-\sum_{ij} t_{ij} \log\left(\frac{t_{ij}}{T}\right)}$	%	Baird & Ulanowicz, (1989); Baird et al. (1991)
Indice de recyclage de Finn (**FCI**)	Quantifie la fraction de tous les flux impliqués dans le recyclage.	$FCI = \sum TST_{ci} / TST_{flux}$	%	Finn (1976)
Longueur moyenne du chemin (**APL**)	Représente une mesure de la capacité de rétention de l'écosystème.	$APL = \frac{TST_{flux}}{\sum_{i=1}^{n} z_i}$	Sans unité	Kay et al. (1989)
Détrivorie/Herbivorie (**D/H**)	Mesure l'importance de consommation du phytoplancton par rapport à la consommation de carbone détritique.	$D/H = \frac{DET\_MET + DOC\_BAC}{Flux\ de\ consommation\ de\ phyt\ par\ PRO\ et\ MET}$	Sans unité	Kay et al. (1989)

Analyses statistiques des données

Les analyses statistiques ont été réalisées avec le logiciel SPSS version 18.0 pour Windows, le logiciel MVSP v3.22, XLSTAT v.Trial et le logiciel R-studio v4.1.0. Les traitements statistiques de base (valeurs moyennes et écarts types) ont été appliqués à chaque variable abiotique ou biotique mesurée.

Une analyse de variance (ANOVA) a été utilisée pour tester l'importance des variations spatiales et temporelles de la biomasse planctonique. L'ANOVA a été utilisée pour comparer les taux estimés (g' et k) entre les fractions de taille du phytoplancton et pour comparer lestaux de broutage estimés. La normalité des distributions des données (test de KolmogorovSmirnov) ainsi que l'homogénéité des variances (test de Bartlett-Box) ont été vérifiées.

La corrélation de Spearman a été utilisée pour mesurer la relation linéaire entre les paramètres phytoplanctoniques (concentrations en Chl *a* et abondance du phytoplancton) et les facteurs physicochimiques au cours de la période d'étude. Le coefficient de corrélation de Spearman « r » a été calculé à partir des données des variables numériques. Une valeur positive (maximum = +1) indique une variation simultanée dans le même sens, une valeur négative (minimum = - 1) indique une variation simultanée en sens inverse.

Une analyse canonique des correspondances (ACC; Braak, 1986) a été réalisée pour relier la distribution spatiale des communautés du plancton aux paramètres environnementaux (nutriments inorganiques et organiques) dans le Golfe de Gabès (**Chapitre III**). L'ACC a également permis d'élucider la relation entre la biomasse fractionnée du phytoplancton et les différents groupes zooplanctoniques.

Une analyse factorielle multiple (AFM) a été réalisée pour identifier les interrelations entre différents indicateurs écologiques (ratios de typologie et indices ENA) ainsi que des variables environnementales (nutriments inorganiques et organiques) et certains des flux calculés (GPP de PIC, NAN et MIC, production bactérienne et flux verticaux de NAN, MIC et MET) aussi bien dans le Golfe de Gabès (**Chapitre IV**) que dans le Canal de Bizerte (**Discussion générale**).

Une analyse en composantes principales (ACP) a été appliquée afin d'évaluer la variabilité dans le temps des données environnementales et des facteurs individuels recueillis dans le Canal de Bizerte (**Chapitre V**).

Les indices de diversité du phytoplancton (richesse en espèces, S ; indice de diversité de Shannon-Wiener, H' ; régularité, J) ont été calculés pour la communauté phytoplanctonique échantillonnée pendant les différents jours après la marée noire. Une ordination par échelle multidimensionnelle (MDS) a été réalisée sur les abondances des espèces de phytoplancton afin de détecter les changements dans la composition de la communauté phytoplanctonique au fil du temps. Une analyse de dissimilarité de la distance euclidienne a été utilisée pour déterminer la dispersion entre les communautés à différents moments de l'échantillonnage. L'indice de diversité et les analyses MDS ont été réalisés à l'aide du programme PRIMER (PRIMER 6) (**Chapitre V**).

Chapitre III

Dynamiques spatiales des nutriments, des producteurs primaires, des consommateurs et des voies de transfert de carbone dans le Golfe de Gabès

I. Problématique et Objectif

Le spectre de taille de phytoplancton est un trait écologique important qui influence la quantité de production primaire, contrôle la taille des consommateurs et ultimement régule le transfert de carbone à travers le réseau trophique marin (Decembrini et al., 2009; Ward et al., 2012; Sakka Hlaili et al., 2014; Negrete-García et al., 2022). Il est donc évident que la dynamique du réseau trophique planctonique et la capacité du système marin à exporter la production primaire soient affectées de manière significative par les changements de taille du phytoplancton (Legendre & Le Fèvre, 1989; Sakka Hlaili et al., 2008; Grami et al., 2011). En fait, Legendre & Rassoulzadegan, (1995) ont rapporté une forte relation entre la dynamique du réseau trophique planctonique et celle des nutriments et par conséquent, ont défini un continuum de voies trophiques entre les systèmes eutrophes et oligotrophes, allant du réseau herbivore à un réseau alimentaire multivore, puis à un réseau microbien.

Les conditions nutritives sont eux-mêmes contrôlées par les processus physiques du système qui influencent finalement le spectre de taille du phytoplancton et sa production primaire (Estrada et al., 1999; Cermeo et al., 2006; Ferland et al., 2011). Par exemple, en mer Méditerranée, l'état nutritif des eaux est fortement lié au forçage hydrodynamique qui peut impacter la structure du réseau trophique et la capacité de l'écosystème à exporter du carbone biogénique. Les eaux ouvertes de la Méditerranée sont dominées par le pico- et le nanoplancton et supportent une faible production primaire lors de la stratification de la colonne d'eau (Decembrini et al., 2009). Le carbone biogène se trouve donc transféré aux consommateurs supérieurs *via* le réseau trophique microbien, avec une forte activité de recyclage (Giannakourou et al., 2014; Livanou et al., 2019). Lorsque les nutriments sont apportés à la zone euphotique par le mélange vertical profond ou une remontée d'eau, la structure du phytoplancton change vers une dominance de cellules de grande taille (c'est-à-dire les diatomées), avec une augmentation de la production primaire (Allen et al., 2002). Dans ce cas, un réseau trophique herbivore s'installe, avec un transfert efficace du carbone vers des niveaux trophiques supérieurs (Stibor et al., 2019). Dans les eaux côtières méditerranéennes, les caractéristiques hydrodynamiques peuvent aussi influencer la structure des communautés phytoplanctoniques (Caroppo et al., 2006, 2018; Bel Hassen et al., 2009; Geyer et al, 2018; Trombetta et al., 2021), impactant celle du réseau trophique. Par exemple, Decembrini et al. (2020) ont montré que l'advection latérale d'eau riche en nutriments dans le Golfe d'Augusta (côte de la Sicile, Mer Ionienne) a provoqué des changements dans le spectre de taille du

phytoplancton et de la production primaire, avec un effet écologique important sur le réseau trophique planctonique. Outre le forçage hydrodynamique, les concentrations nutritives dans les eaux côtières, qui sont généralement eutrophes, sont influencées par les différents apports anthropiques. Ces derniers peuvent perturber le lien entre le phytoplancton et les consommateurs, modifiant ainsi les voies trophiques (Smith et al., 2006; Decembrini et al., 2021). Il serait donc intéressant de prendre en compte les interactions entre l'hydrodynamique et les apports de nutriments pour décrire la structure du réseau trophique marin dans les écosystèmes côtiers (Liu et al., 2018; Decembrini et al., 2021).

C'est dans ce contexte que ce travail a été réalisé dans le Golfe de Gabès, caractérisé par une hydrodynamique importante et des eaux relativement peu profondes, un mélange printanier alterné par des periodes de stratification thermique estivale et riches en nutriments, provenant principalement des industries d'acide phosphorique (Bel Hassen et al., 2009; Khedhri et al., 2014; El Kateb et al., 2018; Zayen et al. 2020). La circulation d'eau complexe dans le Golfe provoque des transports de la côte (dans la partie Nord) vers le large et du Nord vers le Sud, entraînant des gradients de particules et d'éléments dissous (tels que les nutriments) qui s'accumulent dans la partie Sud du Golfe (Cigleneki et al., 2020; Mansouri et al., 2020). Les recherches antérieures dans le Golfe ont rapporté que la dynamique spatiale du phytoplancton était fortement influencée par les conditions nutritionnelles et aux caractéristiques physiques de l'eau (Bel Hassen et al., 2008, 2009; Drira et al., 2009, 2014). Les distributions spatiales des communautés du protozooplancton et des copépodes ont également été reliées à l'interaction entre les charges anthropiques et les conditions hydrodynamiques (Hannachi et al., 2008; Drira et al., 2009, 2017; Makhlouf Belkahia et al., 2021). Bien que les apports en nutriments et la circulation hydrodynamique soient reconnus comme des moteurs majeurs influençant la dynamique du plancton dans le Golfe (Béjaoui et al., 2019), leur effets sur les liens entre le phytoplancton et le zooplancton ainsi que les rôles fonctionnels de ces communautés restent peu connus.

L'objectif de cette étude était donc de décrire les principales caractéristiques de la voie de transfert du carbone dans le Golfe de Gabès (i.e. au niveau des quatre stations) en analysant le spectre de taille du phytoplancton et de sa production ainsi que les interactions trophiques entre le phytoplancton et le zooplancton. En particulier, notre recherche vise à démontrer comment la voie de transfert de carbone change le long d'un gradient spatial de nutriments dans le Golfe. Le travail permettra également de vérifier si le "continuum de voies trophiques" décrit par

Legendre & Rassoulzadegan (1995) pouvait se trouver dans des eaux très productives caractérisées un gradient de conditions eutrophiques.

II. Résumé

Les teneurs en nutriments, les concentrations en Chl *a* (~2-6 µg L^{-1}) et les taux de la production primaire (1816-3674 mg C m^{-2} d^{-1}) mesurés lors de notre étude ont indiqué un statut eutrophe du Golfe, le contrastant avec l'oligotrophie du bassin oriental de la Méditerranée.

Nos résultats s'alignaient avec ceux des études précédentes, montrant que les apports anthropiques combinés avec la circulation hydrodynamique complexe au sein du Golfe ont induit un gradient spatial nutritif ascendant (du Nord vers le Sud et de la partie Côte(Nord) vers le large). En effet, les concentrations en nutriments les plus faibles ont été enregistrés dans la station la plus au Nord (4,27 µM N, 0,91 µM P et 4,90 µM Si). Ces teneurs augmentaient jusqu'à atteindre des maxima (8,93 µM N, 2,2 µM P et 8,98 µM Si) à la station la plus au Sud. Les concentrations dans la station située au large étaient plus élevées que dans la station côtière la plus au Nord, mais inférieures à celles de la station la plus au Sud. Ces gradients nutritifs ont influencé la distribution spatiale de la communauté phytoplanctonique. La biomasse et la production du phytoplancton étaient les plus faibles (1,65 mg Chl *a* m^{-3}; 780 mg C m^{-2}; 1816 mg C m^{-2} j^{-1}) dans la station la plus au Nord, et étaient principalement soutenues par le picophytoplancton (33- 78 %; respectivement). Parallèlement, les petits ciliés aloricates (*Strombidium* spp.) étaient dominants (56%), conduisant à une forte microbivorie. Inversement, une biomasse et une production plus élevées ont été mesurées vers le Sud (6,06 mg Chl *a* m^{-3}; 1624 mg C m^{-2}; 3889 mg C m^{-2} j^{-1}) et au large (5,90 mg Chl *a* m^{-3}; 1300 mg C m^{-2}; 2773 mg C m^{-2} j^{-1}), avec une prédominance de phytoplancton de plus grande taille (nanophytoplancton et/ou microphytoplancton) qui était dominé par des diatomées. Le protozooplancton herbivore (les dinoflagellés et les ciliés loriqués) et le métazooplancton herbivores (copépodes dominés par *Oithona*) étaient plus abondants dans ces zones, ce qui a entraîné une augmentation de l'herbivorie. Le flux vertical de particules de carbone (562 - 1891 mg C m^{-2} j^{-1}) a également suivi un gradient ascendant Nord-Sud et côte-large, avec une contribution accrue du phytoplancton et des pelotes fécales du zooplancton à ce flux dans la zone la plus au Sud (611 et 38 mg C m^{-2} j^{-1} , respectivement).

Ces changements, provoqués par les gradients nutritifs, dans la structure en taille et la production du phytoplancton ainsi que dans les interactions trophiques pourraient conduire à

diverses voies trophiques (microbienne, herbivore et multivore) dans les différentes stations, ce qui implique une efficacité variable dans l'exportation du carbone. Nos résultats ont mis en évidence la présence d'un « continuum de voies trophiques » même dans les eaux eutrophes.

Influence of nutrient gradient on phytoplankton size structure, primary production and carbon transfer pathway in a highly productive area (SE Mediterranean)

Oumayma Chkili[1,2,5] · Marouan Meddeb[1,2] · Kaouther Mejri Kousri[1,4] · Sondes Melliti Ben Garali[1,2] · Nouha Makhlouf Belkhahia[2·] Marc Tedetti[3] · Marc Pagano[3] Amel Belaaj Zouari[4] · Malika Belhassen[4] · Nathalie Niquil[5] · Asma Sakka Hlaili[1,2*]

(Publié dans Ocean Sciences Journal)

Influence of nutrient gradient on phytoplankton size structure, primary production and carbon transfer pathway in a highly productive area (SE Mediterranean)

Ocean Science Journal (2023) 58:6
https://doi.org/10.1007/s12601-023-00101-6

Online ISSN 2005-7172
Print ISSN 1738-5261

ARTICLE

Influence of Nutrient Gradient on Phytoplankton Size Structure, Primary Production and Carbon Transfer Pathway in a Highly Productive Area (SE Mediterranean)

Oumayma Chkili[1,2,5] · Marouan Meddeb[1,2] · Kaouther Mejri Kousri[1,4] · Sondes Melliti Ben Garali[1,2] · Nouha Makhlouf Belkhahia[2] · Marc Tedetti[3] · Marc Pagano[3] · Amel Belaaj Zouari[4] · Malika Belhassen[4] · Nathalie Niquil[5] · Asma Sakka Hlaili[1,2]

Received: 16 July 2022 / Revised: 30 November 2022 / Accepted: 5 December 2022

Abstract
We assessed the spatial variability in the size structure of phytoplankton, community composition, primary production and carbon fluxes through the planktonic food web of the Gulf of Gabès (GG; Southeastern Mediterranean Sea) in the fall of 2017 during the MERMEX-MERITE cruise. High concentrations in nutrients, chlorophyll *a* (~2–6 µg L^{-1}) and primary production (1816–3674 mg C m^{-2} d^{-1}) revealed an eutrophic status of the studied stations in the GG. In accordance with hydrodynamic features, inorganic nutrients showed increases in concentrations from North to South and from coast to offshore, these nutrient gradients impacting the spatial distribution of phytoplankton community. Size-fractioned phytoplankton biomass and production were the lowest in the northernmost zone where they were mainly sustained by pico-sized fraction. Concomitantly, in this area, small aloricate ciliates were dominant leading to a high microbivory. Conversely, higher biomass and production were measured towards the South and offshore with prevalence of larger phytoplankton (nano- and/or micro-sized fractions) supported by diatoms. The herbivorous protozooplankton and metazooplankton were more abundant in these zones, resulting in an increase of the herbivory. The vertical particulate organic carbon flux followed also a north–south and coast-offshore increasing gradient, with a higher contribution of phytoplankton, and zooplankton fecal pellets to the sinking organic matter in the southernmost area. Our results suggest that even in nutrient-rich and highly productive waters, a continuum of trophic pathways, ranging from microbial to multivorous and herbivorous food webs, may exist, which implies different efficiencies in carbon export and carrying capacity within the ecosystem.

Keywords Phytoplankton size-structure · Primary production · Zooplankton grazing · Planktonic food web · Mediterranean gulf

1 Introduction

The phytoplankton, through its biomass, diversity and productivity, has a key role in the functioning of marine ecosystems. The size structure of phytoplankton is an important planktonic trait that affects the magnitude of primary production, controls the size of grazers and hence regulates the carbon transfer through the marine food web (Decembrini et al., 2009;

Negrete-García et al., 2022; Sakka Hlaili et al., 2014; Ward et al., 2012). Any shift in the size of phytoplankton may largely influence the planktonic food web dynamics and the overall efficiency of the marine system to export primary production (Legendre and Le Fèvre, 1989; Legendre and Rassoulzadegan, 1996).

In general, large phytoplankton (mainly micro-sized cells) is consumed by herbivorous zooplankton (mainly copepods), and primary production is efficiently transferred to higher consumers through the herbivorous food web. At the opposite, small phytoplankton (mainly pico-sized cells) and microbivorous protozooplankton (heterotrophic nanoflagellates and aloricate ciliates) are involved in the microbial food web that channels less carbon to higher consumers, as most of primary production is remineralized in the euphotic zone (Legendre and Le Fèvre, 1989; Meddeb et al., 2018). More complex carbon pathways may be present in marine ecosystems. The multivorous food web, in which large and small phytoplankton, as well as herbivorous and microbivorous zooplankton play all together significant roles, can be efficient in carbon transfer (Legendre and Rassoulzadegan, 1995). The bacterial-multivorous food web, in which phytoplankton and bacterioplankton contribute together to carbon production, was recently identified and reported to be less efficient in carbon transfer because of the recycling of the latter (Meddeb et al., 2019). Legendre and Rassoulzadegan (1995) reported that the dynamics of planktonic food web was related to that of nutrients and thus described a continuum of trophic pathways between eutrophic and oligotrophic systems, going from herbivorous to multivorous and microbial food webs.

The nutrient conditions are controlled by physical processes that ultimately influence the size structure of phytoplankton and the primary production (Estrada et al. 1999; Cermeño et al. 2006; Ferland et al. 2011). Previous studies in the Mediterranean Sea have shown that trophic status driven by hydrodynamic forcing can impact the structure of food webs and promote the ecosystem's ability to export biogenic carbon. In highly stratified oligotrophic open waters,

where primary production is low, pico- and nano-sized cells dominate the phytoplankton community (Decembrini et al., 2009). Most carbon is then channeled to higher consumers through microbial food web, with a high recycling activity (Giannakourou et al., 2014; Livanou et al., 2019). Changes in the food web structure can occur when vertical deep mixing or upwelling supply nutrients to the euphotic zone that promote large-sized phytoplankton (i.e., diatoms) and substantially increase primary production (Allen et al., 2002). In that case, the food web shifts to an herbivorous pathway that efficiently transfers carbon to upper trophic levels (Stibor et al., 2019).

In the Mediterranean coastal systems, hydrodynamic features (mesoscale structures, tides…) may influence the hydrological and biogeochemical parameters (salinity, temperature, nutrients…) that finally impact the size structure and composition of phytoplankton (Caroppo et al. 2006, 2018; Geyer et al. 2018; Trombetta et al. 2021). Decembrini et al. (2020) have recently shown that the lateral advection of nutrient-rich water in the Gulf of Augusta (Eastern Sicilian coast, Ionian Sea) triggered a change in the size structure of phytoplankton and primary production with a significant ecological effect on the planktonic food web. Besides physical forcing, continental nutrient inputs from anthropogenic activities can influence the phytoplankton structure and alter the relationship between the latter and grazers, with possible changes in trophic pathways (Decembrini et al., 2021; Smith et al., 2006). The coastal Mediterranean environments are typically mesotrophic or eutrophic systems, with relatively high nutrient concentrations and dominance of large-sized phytoplankton (MedECC 2020). Yet, the herbivorous food web is not usually observed and other trophic pathways (such as microbial or multivorous food webs) can occur at spatial and seasonal scales (Decembrini et al., 2021; Grami et al., 2008; Meddeb et al., 2018; Trombetta et al., 2022), probably due to the influence of the hydrological properties of the system. Therefore, the interactions between hydrodynamics and nutrient inputs must be taken into account to describe the structure of marine food web in eutrophic coastal ecosystems (Decembrini et al., 2021; Liu et al., 2018).

Although much interest has been given to primary production and its trophic transfer in the Mediterranean Sea (Moran and Estrada 2001; Casotti et al. 2003; Psarra et al. 2005; Decembrini et al. 2009; Kovač et al. 2018; Mayot et al. 2020), data acquired in its Southern basin are scarce (Grami et al., 2008; Meddeb et al., 2018; Sakka Hlaili et al., 2008). Furthermore, little effort has been dedicated to describe how nutrient inputs and physical features affect the phytoplankton community structure and food web dynamics. In the Southeastern Mediterranean Sea, the Gulf of Gabès (hereafter refers to as GG) is a highly dynamical coastal ecosystem, characterized by a large continental shelf with relatively shallow well-mixed and rich-nutrient waters (Bel Hassen et al., 2009; Zayen et al., 2020), which is in contrast to the oligotrophic status of the Eastern Mediterranean basin. The nutrient enrichment results mainly from the anthropogenic inputs (mostly by phosphoric acid industries) (El Kateb et al., 2018; Khedhri et al., 2014) and the atmospheric deposition through Saharan dust (Khammeri et al. 2018) . The GG is also characterized by a complex water circulation, which results from the combination of the general thermohaline circulation (Bel Hassen et al. 2009), the anticyclonic winds and the strong tides (Sammari et al., 2006, Hattour et al. 2010; Othmani et al. 2017) (see details below). This circulation induces North-South and coast-offshore transports, which induce a gradient of particles and dissolved elements (such as nutrients) with accumulation in the Southern part of the GG (Ciglenečki et al., 2020; Mansouri et al., 2020). Previous studies have actually shown that phytoplankton dynamics within the GG was related to the nutrient conditions and water physical properties (Bel Hassen et al., 2008; Bel Hassen et al., 2009; Drira et al., 2014, 2009). Spatial distributions were also documented for protozooplankton and copepod communities and were shown to be linked to the combination of hydrodynamic conditions and anthropogenic loads (Drira et al., 2017, 2009; Hannachi et al., 2008; Makhlouf Belkahia et al., 2021). Although nutrient inputs and water circulation are recognized as major drivers in influencing the dynamics of phytoplankton and zooplankton in

the GG (Béjaoui et al. 2019), the link between these communities and their functional roles are not well known.

The aim of this study is to analyze the size structure of phytoplankton and the size-fractionated primary production, as well as trophic interactions between planktonic components in order to define the main characteristics of carbon transfer pathway. In particular, our work aims to demonstrate how food web structure changes along a nutrients spatial gradient in a highly dynamical environment like the GG. The study will also allow verifying whether the "continuum of trophic pathways" reported by Legendre and Rassoulzadegan (1995) could be found in highly productive waters characterized by a gradient of eutrophic conditions.

2 Materials and Methods

2.1 Hydrodynamic features of the study area

The GG is a relatively shallow ecosystem which is strongly influenced by hydrodynamic forcing, mainly driven by the general Mediterranean circulation, the anticyclonic winds and the high tide effects (Hattour et al., 2010; Othmani et al., 2017). The Atlantic Tunisian Current (ATC) is a surface current originating from the Atlantic Ocean. It crosses the Sicilian-Tunisian Channel, flows along the Tunisian continental shelf southward, and splits into two branches (Fig. 1). One coastal branch of the ATC enters the GG and creates an anticyclonic circulation in its Southern part (Ben Ismail et al., 2012; Boukthir et al., 2019). The other branch flows on southeastward along the Libyan shelf, giving rise to the Atlantic Libyan Current (ALC) (Ben Ismail et al., 2015). Furthermore, the hydrodynamics of the GG is deeply influenced by barometric tides (Sammari et al. 2006), which have the highest range of the Mediterranean Sea with a maximal amplitude (~ 2 m) in the Southern region (Abdennadher and Boukthir, 2006; Othmani et al., 2017). Concomitantly with our work, Zayen et al. (2020) investigated the hydrodynamic circulation in the GG, and reported an average littoral current flowing North to

South and two eddies in the middle of the GG that induce a counter current on the littoral in its Southern part (Fig. 1).

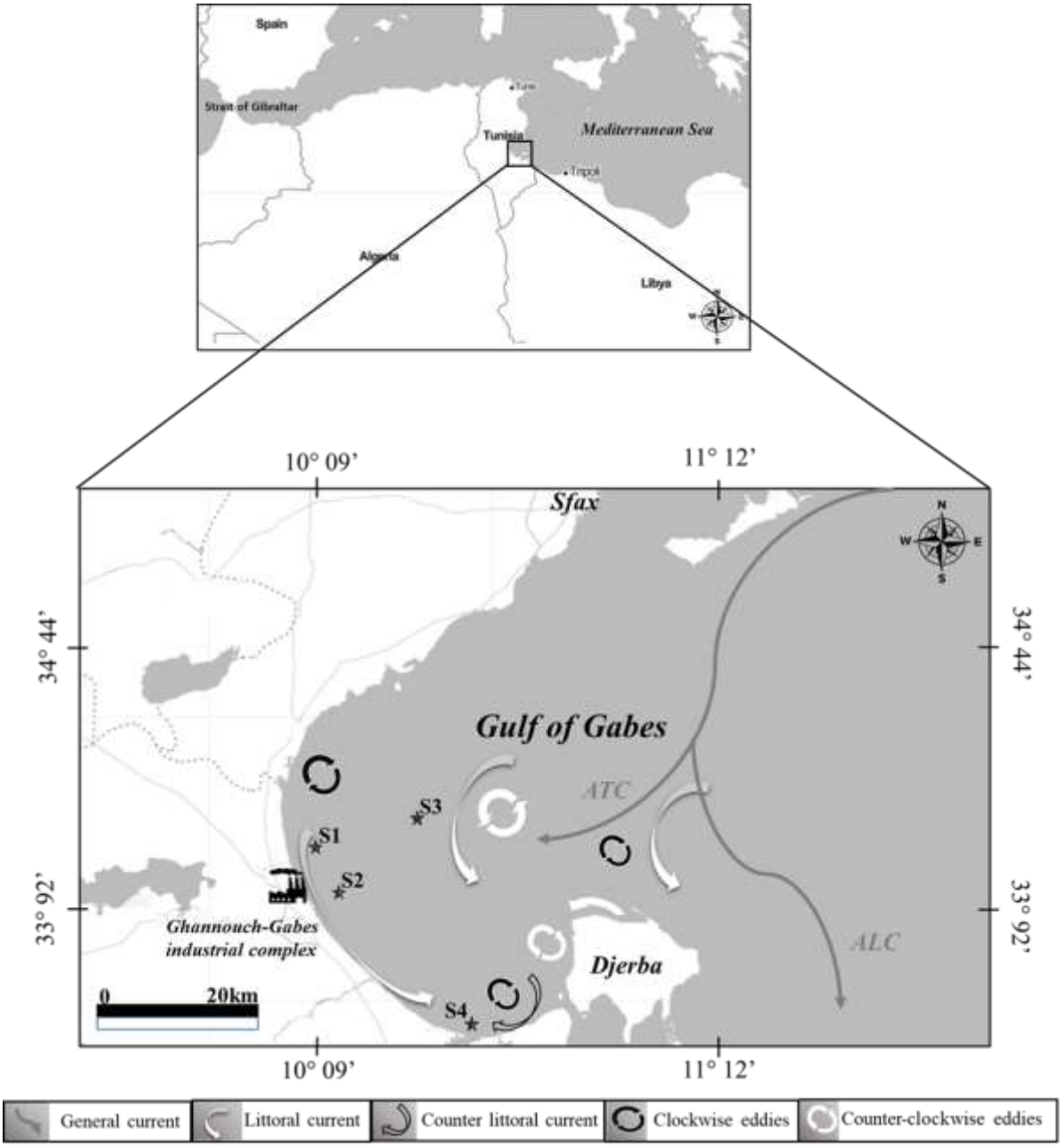

Figure III. 1 Gulf of Gabès: localization of the sampling stations and hydrodynamic circulation (Atlantic Tunisian Current: ATC and Atlantic Lybian Current: ALC). Modified from Zayen et al. (2020)

2.2 Choice of study stations and sampling

The study was carried out within the framework of the MERMEX-MERITE project (*Marine Ecosystems Responses In The Mediterranean Experiment)* campaign from 31 Oct. to 3 Nov. 2017. We investigated the overall function of plankton communities based on sampling

and field experiments carried out simultaneously, which was not easy to achieve in several stations. Therefore, to meet our objective, we chose to explore several key processes in plankton communities in four relevant stations within the GG (S1, S2, S3 and S4; Figure III. 1). The choice of the stations was based on a preliminary work emphasizing a heterogeneous distribution of nutrients in the study region, with increased concentrations from North to South and from the coast to offshore (Figure III . S1 in Supplementary Material).

Station S2 was located in front of the phosphoric acid plant of the Ghannouch-Gabès industrial complex and was chosen as to represent coastal waters impacted by phosphogypsum loading; Stations S1 and S4 were located on either side of station S2 (North and South, respectively), while S3 was an offshore station in front of S1 (Fig. 1). The characteristics of the stations and sampling are reported in Table 1.

In each station, seawater was collected using 2.5 L plastic water sampler (Hydro-Bios), and water temperature, salinity, pH and dissolved oxygen (O_2) were measured *in situ* with a multi-probe sensor (Multi 1970i, WTW) at three depths (between 0.5 and 14 m) depending on the maximal water depth of the stations (Table 1). The collected water was filtered through a 200 µm mesh screen to remove large zooplankton, and three subsamples from each depth were taken for nutrients, chlorophyll *a* (Chl *a*), phytoplankton and protozooplankton analyses. At each station, metazooplankton (> 200 µm organisms) was collected with a 28 cm diameter WP2 200 µm net by vertical hauls from the bottom to the surface. A flow meter was used to determine the water volume filtered during the net tow.

Table 1. Main characteristics, environmental parameters and phytoplankton biomasses of the sampling stations within the Gulf of Gabès during the fall 2017

Physico-chemical variables and Chl *a* concentrations are depth-averaged values; carbon biomasses are depth-integrated values

		S1	**S2**	**S3**	**S4**
Coordinates	Latitude (N)	34° 01.767'	33° 56.545'	34° 01.491'	33° 52.346'
	Longitude (E)	10° 06.295'	10° 08.939'	10° 19.940'	10° 11.803'
Sampling date		30/10	01/11	01/11	03/11
Tide condition / height (m)		High / 1.6	High / 1.9	Low / 0.7	Low / 0.8
Maximum water depth (m)		13.5	12.1	18.8	13.6
Sampled depths (m)		0.5; 2.5; 5	2.5; 4; 7	2; 8; 14	2; 6; 10
Water temperature (ºC)		22.55 ± 0.64	22.90 ± 0.37	22.89 ± 0.21	24.18 ± 0.52
Salinity		39.43± 0.85	39.56± 0.37	39.48± 0.25	39.42± 0.54
pH		8.31 ± 0.005	8.24 ± 0.028	8.27 ± 0.01	8.25 ± 0.017
Dissolved O_2 (mg L^{-1})		8.20 ± 0.05	8.25 ± 0.02	8.23 ± 0.04	8.15 ± 0.11
N_{inorg} (µM)		4.27 ± 0.36	7.63 ± 0.43	5.12 ± 0.31	8.93 ± 2.11
N_{org} (µM)		12.29 ±2.42	9.20 ± 0.27	6.50 ± 0.11	5.03 ± 0.49
P_{inorg} (µM)		0.91 ± 0.27	1.77 ± 0.44	1.52 ± 0.08	2.20 ± 0.05
P_{org} (µM)		8.23 ± 1.93	16.95 ± 2.42	11.45 ± 0.18	18.32 ± 0.02
$Si(OH)_4$ (µM)		4.90 ± 0.22	5.34 ± 0.40	6.40 ± 0.30	8.98 ± 0.76
Chl *a* (µg L^{-1})		1.65 ± 0.06	3.68 ± 1.63	5.90 ± 1.12	6.06 ± 0.24
% of total Chl *a*					
Microphyt.		35 ± 3	30 ± 2	49 ± 5	74 ± 5
Nanophyt.		28 ± 5	43 ± 6	30 ± 4	15 ± 5
Picophyt.		37 ± 6	27 ± 5	21 ± 4	11 ± 1
Carbon biomass (mg C m^{-2})		780.22 ± 65.60	854.50 ± 90.19	1300.3 ± 44.28	1624.57 ± 134.80
% of carbon					
Microphyt.		54 ± 2	71 ± 3	74 ± 1	75 ± 1
Nanophyt.		9 ± 1	8 ± 1	7 ± 1	16 ± 3
Picophyt.		38 ± 3	21 ± 2	20 ± 1	9 ± 1

2.3 Nutrient, Chl *a* and plankton analyses

Inorganic nitrogen (N_{inorg}: $NO_2^- + NO_3^- + NH_4^+$), inorganic phosphorus (P_{inorg}: PO_4^{3-}) and silicates ($Si(OH)_4$), as well as total nitrogen (N_{total}) and phosphorus (P_{total}) were analyzed with

a BRAN and LUEBBE type 3 autoanalyzer (Bran + Luebbe Co, Germany). The precision for all nutrient analyses was ≤ 1%. Organic nutrients (N_{org} and P_{org}) were estimated as the difference between total and inorganic elements.

For Chl *a* analysis, water samples (1 L) were successively filtered through 10, 2 and 0.2 µm polycarbonate membranes to determine size-fractionated Chl *a* (> 10, 2-10 and ≤ 2 µm). Filtrations were performed under low vacuum pressure (< 100 mm Hg) and low light intensity. Chl *a* concentrations were estimated using the spectrophotometric method after 24 h extraction in 90% acetone at 4 °C in the dark (Parsons et al., 1984). Total Chl *a* concentration was estimated as the sum of the three size-fractioned Chl *a* concentrations.

To enumerate picophytoplankton (≤ 2 µm cells), 2 mL samples were immediately fixed after sampling with 20% paraformaldehyde solution, then placed at 4 °C in the dark for 15 min, and finally frozen at -80 °C in liquid nitrogen until analysis with a CyFlow® Space flow cytometer (Partec). Prior to analysis, the samples were filtered on 30 µm pore size filters and enriched with fluorescent beads of 1 and 2 µm in diameter (Polysciences, Inc) as internal cell size standards. Trucount™ beads were also added to accurately estimate the volume of each sample (BD-Biosciences). Picoprokaryotes and picoeukaryotes were identified and counted on the basis of their relative forward scatter (FSC) and phycoerythrin orange fluorescence (at 488 nm) and Chl *a* red fluorescence (at 638 nm), respectively. Cell volumes were determined using equivalent diameters estimated from flow cytometry. The biovolumes (picoprokaryotes: 1.77 μm^3; picoeukaryotes: 4.19 μm^3) were converted into carbon content using the following conversions: 0.357 pg C μm^{-3} for picoprokaryotes, and 0.433 x $(\mu m^3)^{0.863}$ for picoeukaryotes (Verity et al., 1992). The cell carbon contents were multiplied by the abundances to estimate the carbon biomass of picophytoplankton (mg C m^{-3}). Depth-integrated biomass (mg C m^{-2}) was obtained from the carbon biomasses estimated for the three depths.

Phytoplankton samples (nano-: 2-10 µm; micro-phytoplankton: > 10 µm) were preserved in 3% acidic Lugol's solution and stored at room temperature in the dark (Parsons et al., 1984).

The identification and counting of cells (at least 500 *per* sample) were determined using the Motic AE31E inverted microscope on 100 mL settled volume (Lund et al., 1958; Utermöhl, 1931). Cell dimensions of phytoplankton taxa were measured using a calibrated ocular micrometer and biovolumes were determined by applying standard geometric formulae to each taxon (Hillebrand et al. 1999). Then, the biovolumes were converted into carbon content using specific conversion factors or formulae (Menden-Deuer and Lessard, 2000; Putt and Stoecker, 1989) for diatoms, autotrophic flagellates and ciliates, as detailed in Meddeb et al. (2018). The carbon biomass of phytoplankton (mg C m^{-3}) was then determined by multiplying the carbon content of different taxa by their specific abundances. Carbon biomasses from the three sampled depths were used to calculate the depth-integrated biomass (mg C m^{-2}).

Protozooplankton samples (100 mL) were fixed with 4% basic Lugol's solution (Sherr and Sherr, 1993), and organisms were identified and counted (at least 200 cells *per* sample) according to the inverted microscopy technique of Utermöhl (1931). Protozooplankton was composed of heterotrophic nanoflagellates and ciliates including loricate and aloricate species, but also of dinoflagellates (most of which are phagotrophic). Within dinoflagellates, mixotrophic and heterotrophic organisms were distinguished according to several works (Boutrup et al., 2016; Jeong et al., 2010a; Sakka Hlaili et al., 2007). The ebridian flagellate *Hermesinium sp.* was also considered as a micrograzer since its mixotrophy had been confirmed (Hargraves, 2002; Jafari et al., 2015).

Samples of metazooplankton (250 mL) were fixed with a 5% borate-buffered formalin solution. Metazoan organisms were counted and identified in the whole sample using a Leica M 205C stereo microscope.

2.4 *In situ* dilution experiment

The dilution method (Landry and Hassett, 1982) was used to estimate the growth rate of phytoplankton and its grazing rate by protozooplankton at each station and at the same sampling date. Water samples were collected over the water column (5 m for S1, 7 m for S2, 14 m for S3

and 10 m for S4) with a submersible pump and then filtered through 200 µm mesh screen (to remove meso- and macroplankton). This screened seawater was diluted with free-particle seawater to achieve four dilutions (25, 50, 75 and 100% of 200 µm screened seawater). The diluting seawater was obtained by gravity filtration using a 0.22 µm sterile filter capsule (polycap 75 AS). Triplicate 2 L polycarbonate bottles (Nalgene®) were used for each dilution, and all bottles were incubated *in situ* for one day (t = 1 d). The GG is a nutrient-rich environment where nutrients are considered as available throughout the year (Béjaoui et al., 2019; Bel Hassen et al., 2008). Therefore, nutrients were not added to our dilution bottles to avoid the overestimation of growth rates. Furthermore, several authors have found that growth rates in nutrient-enriched bottles were not significantly different from those estimated without nutrients during dilution experiments conducted in nutrient-rich systems (Olson and Strom 2002; Sakka Hlaili et al. 2007; Pecqueur et al. 2022). Subsamples were taken from each dilution bottle at the beginning and the end of incubation to determine initial and final phytoplankton carbon biomasses (C_0 and C_t ; respectively). As protozoans have a prey size-selective feeding activity (Sakka Hlaili et al., 2007; Zhang et al., 2017), size-fractioned biomass of phytoplankton was determined (i.e., pico-: ≤ 2 µm, nano-: 2-10 µm, and microphytoplankton: > 10 µm). The apparent growth rate of each size fraction prey (R) was calculated from the changes in carbon biomass during the incubation period as:

$$R(d^{-1}) = \ln\left({C_t}/{C_0}\right) \times t^{-1}$$

The coefficients R were plotted against the dilution factor, and a model I linear regression was used to estimate growth rates k (d^{-1}) (i.e., the y-intercept that represented growth in 100% dilution in the absence of grazers) and the grazing coefficient g (d^{-1}) (i.e., the slope of the regression line) (Landry and Hassett, 1982). For each size fraction in all stations, the regression lines were tested as significant by Student's t-test ($p < 0.05$) and were represented in the Supplementary Material (Figure III . S2).

For each phytoplankton size fraction, production rates (P_1) and consumption rates by protozooplankton (G_{p1}) were calculated according to several authors (Grattepanche et al., 2011; Meddeb et al., 2018) as:

$$P_1\ (mg\ C\ m^{-3}\ d^{-1}) = k \times C_0\left[e^{(k-g)t} - 1\right]/(k - g \times t)$$

and

$$G_{p1}\ (mg\ C\ m^{-3}\ d^{-1}) = g \times C_0\left[e^{(k-g)t} - 1\right]/(k - g \times t)$$

The P_1 and G_{p1} data were multiplied by the sampling depth to get depth-integrated rates of production (P, mg C m^2 d^{-1}) and consumption (G_p, mg C m^2 d^{-1}), respectively. Depth-integrated production rates for the three size fractions were added to obtain production rate for total phytoplankton. The percentage of production consumed *per* day was estimated as:

$$\%Pgrazed\ d^{-1} = \left({}^{G_p}/_{P}\right) \times 100$$

2.5 Metazooplankton gut fluorescence analysis

The grazing of metazooplankton on phytoplankton was estimated using the gut fluorescence method (Slaughter et al., 2006). Zooplankton was collected as indicated above. To account for vertical migration of zooplankton likely to affect its feeding activity, sampling was carried out around sunset, when zooplankton perform a vertical ascension. Three 500 mL subsamples of the cod content were immediately narcotized with 10% carbonated water (final concentration, v/v) to minimize stress and gut evacuation by zooplankton (Kleppel and Pieper, 1984) and were kept frozen in the dark to minimize fecal pellet production by the organisms (Saiz et al., 1992). The zooplankton subsamples were thawed and washed with filtered seawater to remove adhering algae and debris, and filtered onto 47 mm diameter GF/F membranes that were extracted in 10 mL of 90% acetone solution maintained at 4 °C in the dark. After overnight extraction, each solution was centrifuged, and the supernatant absorbance was measured using a Jenway spectrophotometer before and after acidification with 10% hydrochloric acid solution (Parsons et al., 1984).

The gut pigment content (GP) was calculated according to Slaughter et al. (2006) as:

$$GP(mg\ pigment\ m^{-3}) = (GP_{sub} \times v)/(F \times V_{net}),$$

where GP_{sub} (mg pigment m^{-3}) is the phaeopigment concentration in the subsample, v (m^3) is the volume of the subsample, F is the fraction of subsample processed for gut pigment content, and V_{net} (m^3) is the total volume of seawater filtered during the net tow.

Consumption of > 2-µm phytoplankton by metazooplankton was calculated as:

$$G_m(mg\ C\ m^{-2}\ d^{-1}) = [GP \times CR \times C{:}Chla] \times D,$$

where D is the depth of the net tow (m), C:Chl *a* is the depth-averaged C:Chl *a* ratio determined for > 2 µm phytoplankton at each station, and CR is the gut clearance rate of metazooplankton (d^{-1}). The CR was obtained from the gut clearance rate constant (GCRC) *vs.* temperature (T) relationship (GCRC = 0.0117 + 0.001794T) (Dam and Peterson, 1988; Irigoien, 1998; Mauchline, 1998).

The impact of metazooplankton grazing on the standing stock and production of phytoplankton were calculated as:

$$\%Chla\ grazed\ d^{-1} = (GP \times CR \times 100)/SC$$

$$\%P\ grazed\ d^{-1} = \left({}^{G_m}/_{P}\right) \times 100,$$

where SC is the depth-averaged concentration of Chl *a* and P is the production rate of nano- and micro-phytoplankton, estimated by the dilution method.

2.6 Vertical carbon fluxes

Sediment traps were used to estimate the vertical flux of particles, including phytoplankton, metazooplankton fecal pellets, and detritus. This technique was performed by several authors (Kojima et al., 2022; Laurenceau-Cornec et al., 2015; Xiang et al., 2022) because it is very useful for estimating the particle sinking and gives details in the composition of the sinking fluxes. At each station, two sediment traps (63 cm high, 9 cm internal diameter)

were incubated vertically two meters from the bottom. Prior to deployment, the traps were filled with dense seawater (0.2 µm filtered seawater + NaCl 5 g L^{-1}) to create a density gradient and avoid collecting surface particles. After 24 h incubation, the traps were closed *in situ*, returned to the laboratory and stored at 5 °C overnight to let particles settle. The supernatant was removed from each trap and the bottom contents of the two traps were mixed. Subsamples were taken from the trapped material for further analyses of particulate organic carbon (POC), phytoplankton and fecal pellets.

For POC, ~ 500 mL seawater samples were filtered onto precombusted glass fiber filters (450 °C, 24 h) (Whatman GF/F, 25 mm). The filters were oven dried at 50 °C for 24 h and stored in clean glass vials in a desiccator. POC was determined by the high combustion method and mass spectrometry according to Raimbault et al. (2008).

Phytoplankton (> 2 µm cells) was enumerated on 500 mL subsamples fixed with acidic Lugol's solution (final concentration 4%), and cell abundances were converted into carbon biomasses as described above.

Subsamples (200 mL) were preserved in buffered formaldehyde (final concentration 7%) for counting fecal pellets using an inverted microscope (× 100 magnification). Differently shaped pellets were distinguished (cylindrical, conical; ovoid and round), and their dimensions were measured using a calibrated ocular micrometer.

The vertical fluxes of phytoplankton (F_{phyt}) and detritus (F_{det}) were estimated following Grami et al. (2008):

$$F_{phyt}(mg\ C\ m^{-2}d^{-1}) = {}^{1}/_{2}\left(C_{phyt} \times V_{tr}\right)/S_{tr} \times t$$

$$F_{det}(mg\ C\ m^{-2}d^{-1}) = {}^{1}/_{2}\left(C_{det} \times V_{tr}\right)/S_{tr} \times t,$$

where C_{phyt} is the carbon biomass of nano- and microphytoplankton (mg C m^{-3}) and C_{det} is the detrital carbon estimate, calculated as the POC concentration minus the carbon biomass of all particles. V_{tr} is the volume of trapped material (m^3), S_{tr} is the trap area (m^2) and t is the duration of incubation (d). The vertical flux of phytoplankton was considered to be the phytoplankton

export from the planktonic system towards the benthos, while the vertical flux of detritus was assigned to the sinking flux.

The volume of each pellet shape category (V_{pel}, mm^3 m^{-3}) was estimated from its dimension and abundance. Then, its vertical volume flow (S_{pel}) and vertical carbon flux (F_{pel}) were estimated following Grami et al. (2008):

$$S_{pel}(mm^3 m^{-2} d^{-1}) = {}^1/_2 \left(V_{pel} \times V_{tr}\right)/S_{tr} \times t$$

$$F_{pel}(mg\ C\ m^{-2} d^{-1}) = S_{pel} \times f,$$

where f is a conversion factor (0.057 mg C mm^{-3} for cylindrical/conical pellets and 0.042 mg C mm^{-3} for ovoid/rounded pellets).

2.7 Statistical analyses

An analysis of variance (ANOVA) was used to test the significance of the spatial variation of physico-chemical factors, Chl *a*, plankton concentrations and vertical fluxes. ANOVA was also used to compare (i) environmental factors and plankton concentrations among depths, and (ii) the estimates of rates (k, g, P, G_p, G_m) between phytoplankton size fractions (> 10, 2-10 and < 2 µm) or stations. The assumptions of normality of data distribution (Kolmogorov-Smirnov test) and homogeneity of variance (Bartlett-Box test) were met. Spearman correlations (r_s) were used to test the relationships between different variables: phytoplankton (Chl *a*, carbon biomass, growth rate, production rate) and nutrients; growth (k) and grazing (g) rates; coefficients g and G_p and protozooplankotn abundances; production (P) and consumption rate by protozooplankton (G_p); consumption rate by metazooplankton (G_m) and phytoplankton biomass and metazoans abundances. ANOVA and correlation analyses were performed in SPSS software 18.0 for Windows.

Canonical correspondence analysis (CCA; Ter Braak 1986) was performed to relate the spatial distribution of plankton communities to environmental parameters (P_{org}, P_{inorg}, N_{inorg}, N_{org}, $Si(OH)_4$, pH, temperature and salinity). The CCA also elucidated the relationship between the biomass of size-fractioned phytoplankton and different zooplanktonic groups.

Phytoplankton and zooplankton data were ln (x + 1) transformed. The comparison of the canonical inertia associated with the CCA (constrained ordination) and the inertia of the classical correspondence analysis (CA, unconstrained ordination) indicated the extent to which the environmental variables explained the spatial structure of communities. Permutation tests (n = 999) were performed to identify the significant axis and to test the significance of the correlations between environmental factors and plankton distribution.

3 Results

3.1 Environmental conditions

Sampling stations were located in the continental shelf of the GG, which is characterized by a shallow (< 20 m) well-mixed water column. Environmental factors showed no significant variations between sampling depths (ANOVA $p > 0.05$), and hence data were presented as depth-averaged values (Table 1). Water temperature (22.6-24.2 °C), salinity (39.42-39.56), pH (8.25-8.31) and dissolved O_2 (8.15-8.25 mg L^{-1}) varied little among stations, while nutrient concentrations exhibited significant spatial variations (ANOVA, $p < 0.05$). In S1, inorganic nutrients presented the lowest values (4.27 µM N, 0.91 µM P and 4.90 µM Si) and increased up to 8.93 µM N, 2.2 µM P and 8.98 µM Si in S4. Inorganic nutrient concentrations recorded in S3 were higher than in S1, but lower than the southernmost station (S4). The highest and lowest levels of organic nitrogen (N_{org}: 5.03-12.29 µM) were recorded in S1 and S4, respectively. An opposite trend was observed for organic phosphorus (P_{org}: 8.23-18.32 µM).

3.2 Spatial distribution of planktonic communities

Phytoplankton. The depth-averaged Chl *a* concentrations and the depth-integrated carbon biomasses were different among stations (ANOVA, $p < 0.05$; Table 1), increasing gradually from S1 (1.7 µg Chl *a* L^{-1}, 780 mg C m^{-2}) to S4 (6.07 µg Chl *a* L^{-1}, 1,624 mg C m^{-2}). Positive correlations were found between inorganic N, P and Si and Chl *a* concentrations

(r_s = 0.64-0.84, $p < 0.01$) and carbon biomass (r_s = 0.67-0.78, $p < 0.01$). Microphytoplankton was the main source of Chl *a* in S4 (74%) and contributed to ~50% of it in S3. The contribution of picophytoplankton to Chl *a* was higher in S1 (37%) than in the other stations (11-27%), while nanophytoplankton contributed to a large fraction of Chl *a* in S2 (43%) (Table 1). In terms of carbon biomass, micro-sized fraction (418-1207 mg C m^{-2}) formed the most of phytoplankton (54-75%), while nano-sized fraction (70-265 mg C m^{-2}) contributed only by 9-16%. The pico-sized fraction (152-292 mg C m^{-2}), which formed only 9% of phytoplankton carbon in S4, showed increased contributions in S2 and S3 (20-21%) and mostly in S1 (38%).

The composition of > 2 µm phytoplankton community changed also among stations. Diatoms showed different contributions to the community according to the station, and their biomass was positively correlated with inorganic N, P and Si (r_s = 0.79-0.67, $p < 0.01$). Diatoms were dominant in S2, S3 and S4, showing depth-averaged contribution of 73-88% (Figure III . 2a). They were mainly represented by *Leptocylindrus minimus* (30-60% of diatoms) in the three stations. Large chains of *Skeletonema costatum* and *Rhizosolenia setigera* showed increased contribution to diatoms (18-28%) only in S3 and S4 (Figure III . 2b). The small phytoplagellates were particularly abundant in S1 (45%; Figure III . 2a), and were represented by nano-sized Cryptophyceae (*Hillea fusiformis* and *Rhodomonas marina*). Within the phytoflagellates, the micro-sized Dictyochophyceae (i.e., *Dictyocha fibula*) were more important in S3 and S4 than in the other stations (Fig. 2c). In all stations, photosynthetic ciliates (*Mesodinium rubrum*) and dinoflagellates (*Prorocentrum gracile*) only accounted for 2-13% of the > 2 µm phytoplankton community (Figure III 2a).

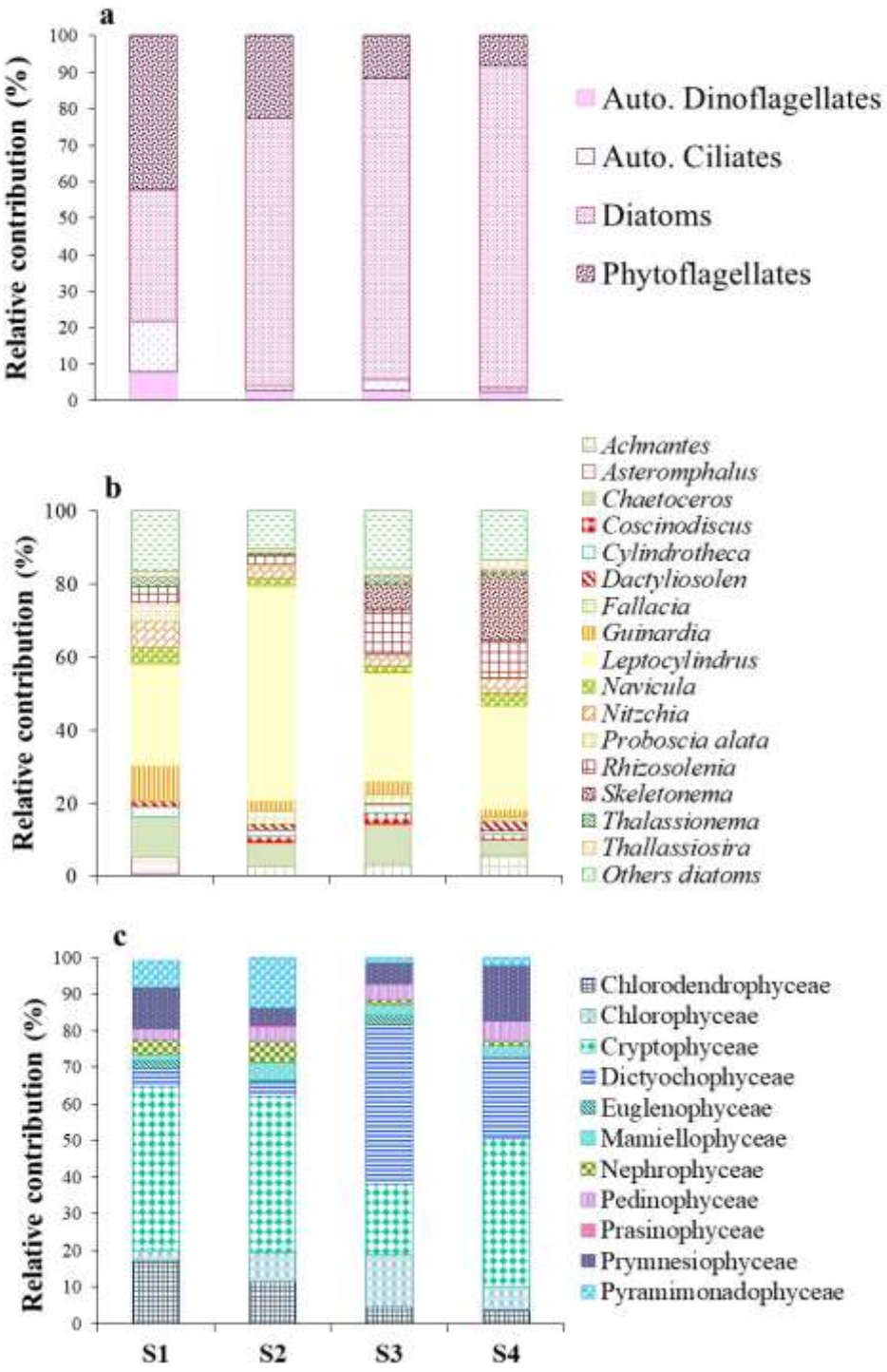

Figure III. 2 Composition of > 2 µm phytoplankton (**a**), diatoms (**b**) and phytoflagellates (**c**) in the sampling stations during fall 2017. (Values are the means of the three depths at each station)

Protozooplankton. The depth-averaged abundance of total protozooplankton was significantly different between stations (ANOVA, $p < 0.05$), varying from 43×10^3 cells L^{-1} (in S3) to 123×10^3 cells L^{-1} (in S1) (Figure III. 3a). Aloricate ciliates, mainly composed of *Strombidium* spp. (Figure III. 3b), were dominant in S1 (~60%; 70×10^3 cells L^{-1}). Loricate ciliates displayed a relatively low abundance ($1.5\text{-}6 \times 10^3$ cells L^{-1}) and were most abundant in S4, where *Tintinnopsis*, *Helicostomella* and *Amphorellopsis* occurred (Figure III. 3b). Dinoflagellates were abundant in S2, S3 and S4 ($20\text{-}55 \times 10^3$ cells L^{-1}), contributing to 48-64% of protozooplankton. Mixotrophic dinoflagellates including *Gymnodinium*, *Heterocapsa*, *Karenia* and *Neoceratium* (Figure III. 3c) were dominant in S2 (59% of dinoflagellates), whereas large heterotrophic dinoflagellates (mainly *Protoperidinium*) mostly occurred in S4 (60%). The heterotrophic nanoflagellate *Commation cryoporinum* ($0.75\text{-}5.78 \times 10^3$ cells L^{-1}) and the ebridian flagellate *Hermesinium sp.* ($8.7\text{-}26.7 \times 10^3$ cells L^{-1}) contributed 2-12% and 15-37% to protozooplankton, respectively (Figure III. 3a).

Metazooplankton. Metazooplankton abundance significantly varied among stations (ANOVA, $p < 0.05$) from 11×10^2 ind. m^{-3} in S1 to 20×10^2 ind. m^{-3} in S4 (Figure III. 4a). Copepods ($7.5\text{-}12.5 \times 10^2$ ind. m^{-3}) were dominant in all stations, forming 53-86% of total metazooplankton (Figure III. 4a). Calanoida (*Centropages*, *Clausocalanus*, *Paracalanus* and *Phaenna*) and Cyclopoida (*Oithona*) contributed to the majority of copepods, but with different percentages according to the station (Figure III. 4b). The harpacticoid *Euterpina* was relatively abundant in S3 (12%). Cladocerans (*Penilia sp.*) mainly occurred in S4 (forming 16% of metazoans), while decapod, polychaete and crab larvae as well as, crustacean nauplii were observed at moderate concentrations in S2, S3 and S4. Other metazoan groups, e.g., chaetognaths, appendicularians, nematodes and siphonophores were observed in all stations, but at much lower densities.

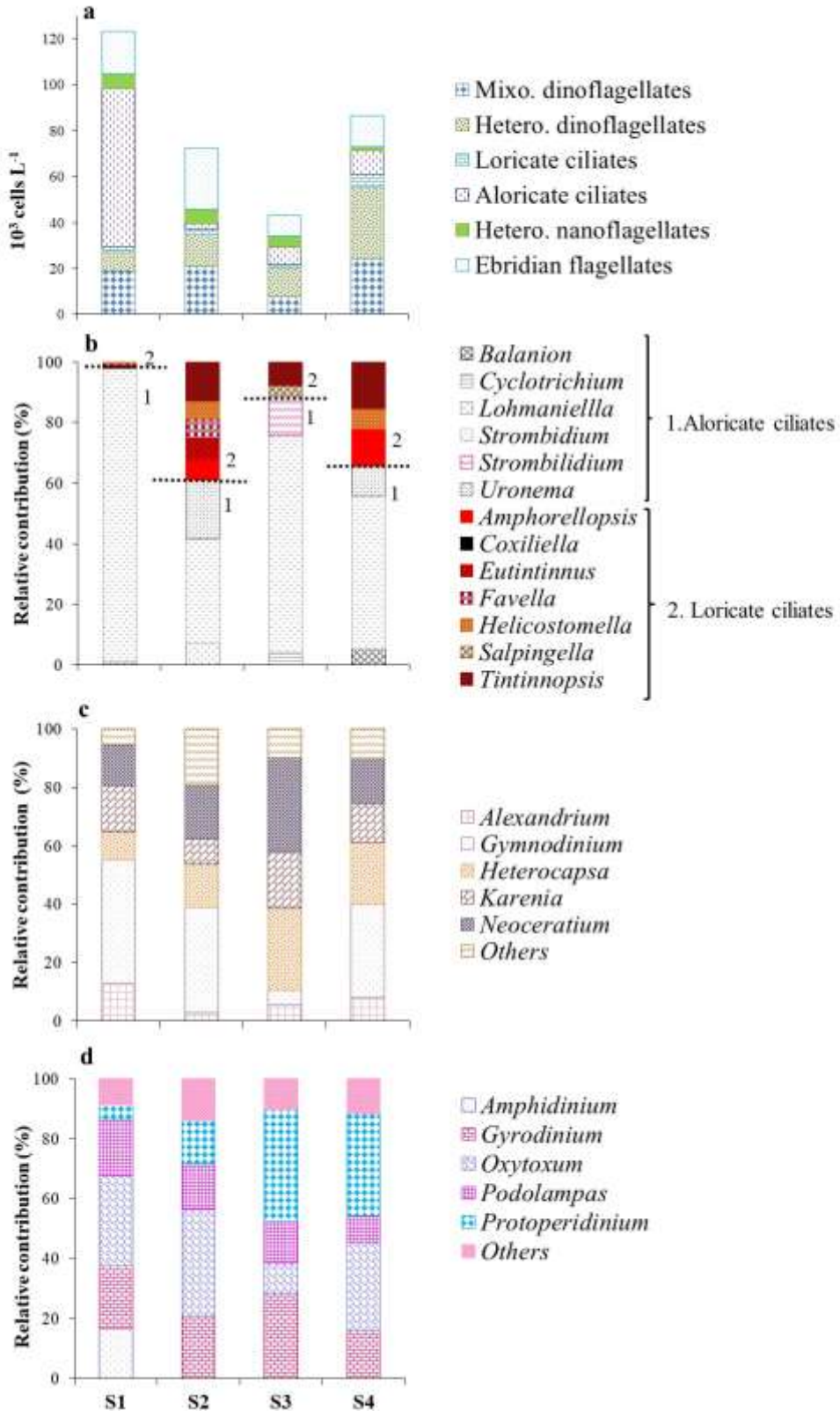

Figure III. 3 Abundance and composition of protozooplankton (**a**), and specific structure of the main protozoan groups (**b-d**) in the sampling stations during the fall 2017. (Values are the means of the three depths at each station)

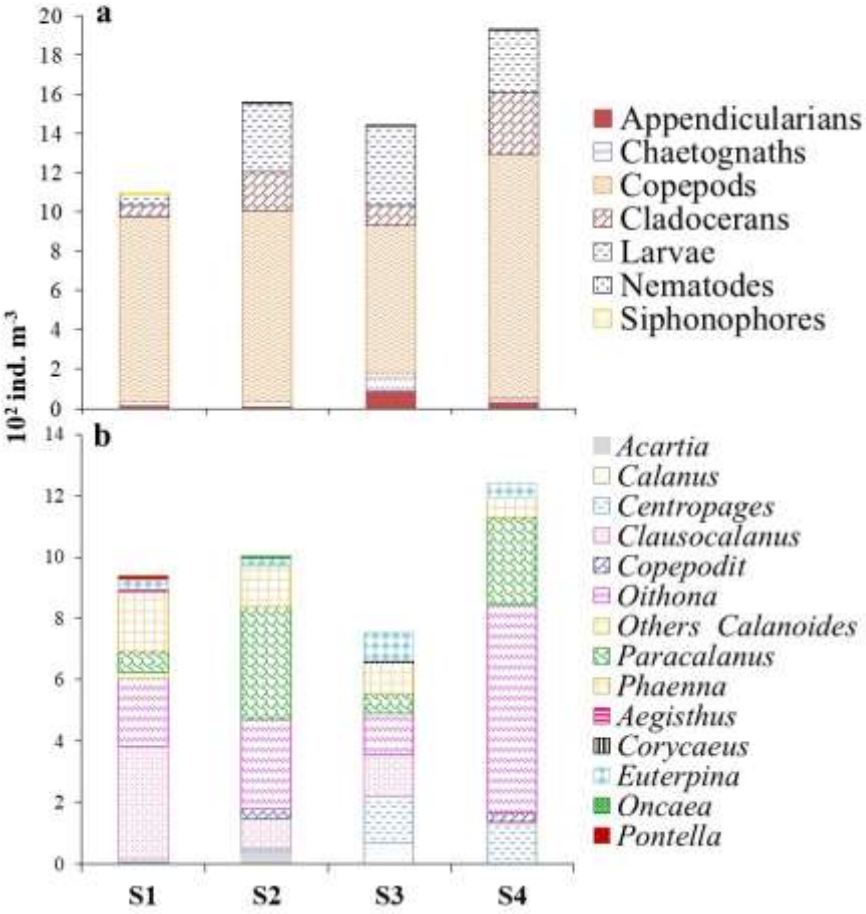

Figure III. 4 Abundance and composition of total metazooplankton (**a**), and taxonomic structure of copepods (**b**) in the sampling stations during the fall 2017

Relationship between environmental conditions and plankton communities. The influence of physico-chemical factors on phytoplankton (the three size fractions) and zooplankton distribution, as well as relationships between phytoplankton and zooplankton were summarized by the CCA. The first two canonical components extracted 69% of the canonical variance (Figure III. 5). A Monte Carlo permutation test showed that all canonical axes were highly significant ($p < 0.0001$). The positive pole of axis 1 was correlated with salinity (0.53, $p < 0.05$) and organic nitrogen (0.73, $p < 0.01$), while the negative pole was correlated with temperature (-0.51, $p < 0.05$), inorganic phosphorus (-0.61, $p < 0.05$), inorganic nitrogen (-0.50,

p < 0.05), silicates (-0.61, p < 0.05) and organic phosphorous (-0.65, p < 0.05). Axis 2 was positively correlated with the pH (0.53, p < 0.05).

The CCA discriminated two groups. The first axis positively selected picophytoplankton with abiotic variables such as salinity and organic nitrogen, while nano- and microphytoplankton were related to organic and inorganic phosphorus, silicates, inorganic nitrogen, and temperature. The CCA also showed that pico-sized cells were associated with aloricate ciliates, as well as heterotrophic and ebridian nanoflagellates. In contrast, nano- and microphytoplankton prevailed when dinoflagellates (mixo- and hetero-trophic organisms), loricate ciliates, copepods and cladocerans largely occurred. Dinoflagellates, loricate ciliates and copepods showed a positive correlation with temperature but were negatively correlated to salinity. Loricate ciliates and flagellates protozoans followed, however, the opposite trend.

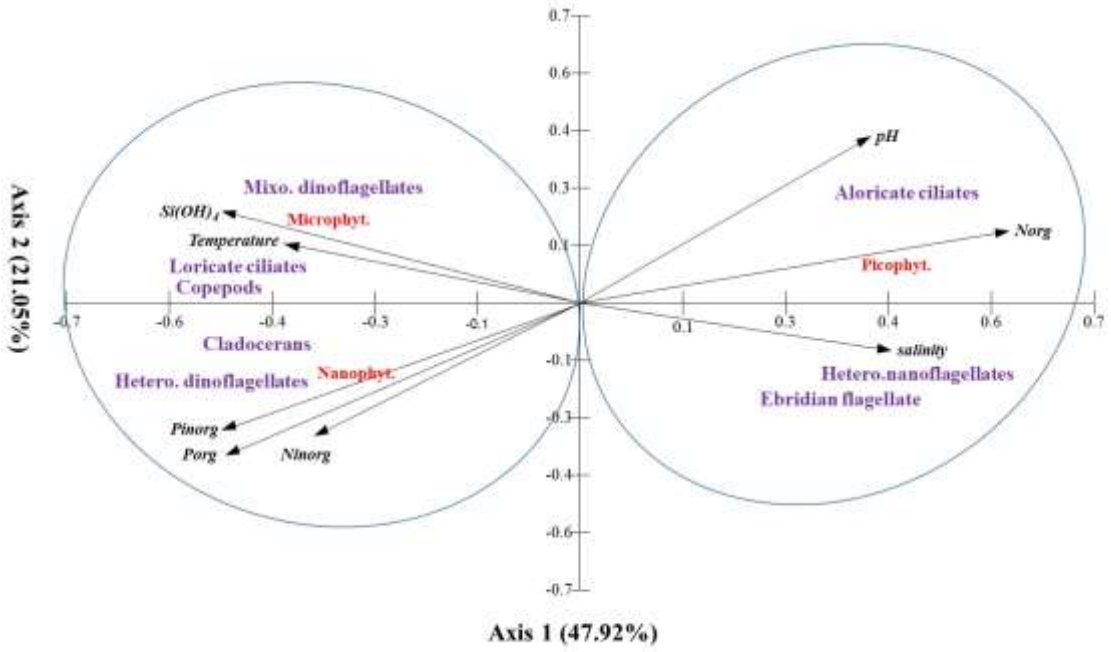

Figure III. 5 Canonical correspondence analysis (CCA) ordination diagram showing the relationship between phytoplankton (the three size classes), zooplankton, and physico-chemical factors

3.3. Phytoplankton growth and production

The growth rates varied significantly (ANOVA, $p < 0.01$) among stations and size fractions (micro-: 0.41-1.52 d^{-1}; nano-: 1.09-1.89 d^{-1}; pico-phytoplankton: 1.01-1.89 d^{-1}) (Figure III. 6a). The highest rate for the pico-sized fraction was recorded in S1, whereas for nano- and micro-phytoplankton, the highest rates were observed in S4. The growth rate of microphytoplankton was positively correlated with inorganic N and P (r_s = 0.73-0.76, $p < 0.01$), while that of picophytoplankton showed negative correlations with these nutrients (r_s = -0.62 - 0.73, $p < 0.01$).

Production rates for size fractioned and total phytoplankton varied significantly among stations (ANOVA, $p < 0.05$; Figure III. 6b). Picophytoplankton displayed a very high production rate in S1 (1412 mg C m^{-2} d^{-1}) in comparison to other stations (300-496 mg C m^{-2} d^{-1}). Microphytoplankton showed an opposite trend, with higher production rates in S2, S3 and S4 (1160-2075 mg C m^{-2} d^{-1}) than in S1 (188 mg C m^{-2} d^{-1}). The production rate for the micro-sized fraction was positively correlated to diatom biomass (r_s = 0.83, $p < 0.01$). Production rate for nanophytoplankton was low in S1 and S3 (188-215 mg C m^{-2} d^{-1}). Higher value was observed in S2 (452 mg C m^{-2} d^{-1}) and the highest in S4 (1301 mg C m^{-2} d^{-1}). Production rate for total phytoplankton showed an increasing trend from S1 (1816 mg C m^{-2} d^{-1}) to S4 (3873 mg C m^{-2} d^{-1}), and was positively correlated to all inorganic nutrients (r_s = 0.68-0.81, $p < 0.01$). In S2, S3 and S4, microphytoplankton was the main carbon producer (55-78%), whereas in S1 picophytoplankton provided 78% of total carbon production. Nanophytoplankton contributed only 7-12% of produced carbon in S1 and S3, and 21-34% in S2 and S4.

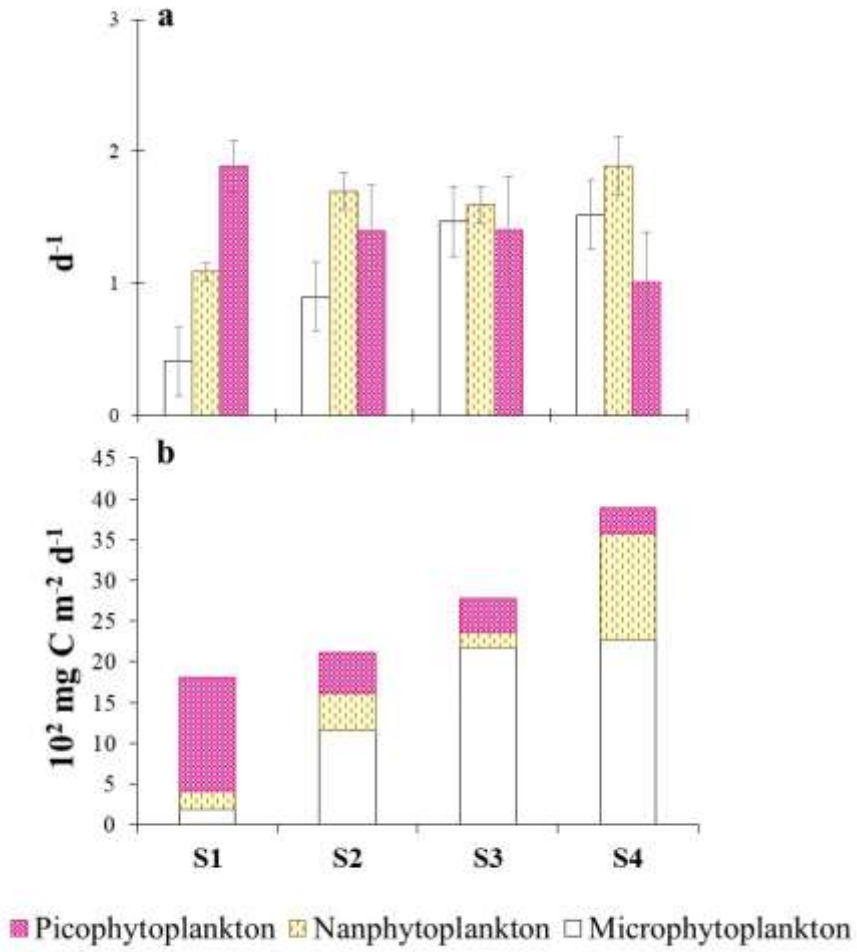

Figure III. 6 Growth (**a**) and production (**b**) rates of the three phytoplankton size fractions (picophytoplankton: < 2 µm, nanophytoplankton: 2-10 µm, microphytoplankton: > 10 µm) in the sampling stations during the fall 2017

3.4 Phytoplankton grazing

Grazing by protozooplankton. The grazing and consumption rates by protozooplankton varied significantly among size fractions and across stations (ANOVA, $p < 0.01$; Table 2). Picophytoplankton was grazed at higher rates (0.82-1.30 d^{-1}) than the other size fractions (micro-: 0.18-0.54 d^{-1}; nano-phytoplankton: 0.51-1.01 d^{-1}) in stations S1, S2 and S3. However, microphytoplankton was the most grazed in S4 (0.84 d^{-1}). The highest consumption rate for

picophytoplankton was recorded in S1 (762.96 mg C m^{-2} d^{-1}) and the lowest in S4 (137 mg C m^{-2} d^{-1}). In the opposite, nano- and micro-phytoplankton were consumed at low rates in S1 (92 and 71 mg C m^{-2} d^{-1}, respectively). Their consumption increased in other stations, particularly in S4 (318 and 1049 mg C m^{-2} d^{-1}, respectively). For each size fraction, the consumption rates showed positive correlations to the production rates (r_s = 0.73-0.95, $p < 0.05$). The consumption rate for micro-sized fraction was positively correlated with the abundances of heterotrophic dinoflagellates (r_s = 0.85, $p < 0.01$) and loricate ciliates (r_s = 0.60, $p < 0.05$). Protozooplankton removed a substantial fraction of daily production for picophytoplankton in most stations (~60% P grazed d^{-1}), except in S4 (40% P grazed d^{-1}). The protozooplankton grazing corresponded to daily remove of 23-62% of nanophytoplankton production. Protozooplankton grazing impact on microphytoplankton was higher in S4 (47% P grazed d^{-1}) than in the other stations (22-41% P grazed d^{-1}). Furthermore, microbivory (carbon from picophytoplankton) contributed to carbon ingestion of protozooplankton by only 9% in S4, but by 24-34% in S2 and S3, and up to 82% in S1. Conversely, herbivory played a significant role in the feeding of protozooplankton in the other stations, as microphytoplankton alone represented 54-70% of their diet (Table 2).

Grazing by metazooplankton. The grazing rate and the impact of metazooplankton were significantly different among stations (ANOVA, $p < 0.01$; Table 3). The consumption rate of phytoplankton by metazooplankton showed the lowest value in S1 (76 mg C m^{-2} d^{-1}) and the highest in S4 (794 mg C m^{-2} d^{-1}). This rate was positively correlated with nano- and microphytoplankton biomass (r_s = 0.70-0.78, $p < 0.01$), and with copepod and cladoceran abundances (r_s = 0.62-0.76, $p < 0.05$). Metazooplankton removed 10-24% of phytoplankton production and 22-38% of phytoplankton standing stock (Table 3).

Table 2 Grazing rates by protozooplankton (g), consumption rates of phytoplankton (G_p), grazing impact on phytoplankton and protozooplankton diet in the sampling stations within the Gulf of Gabès during the fall 2017

	S1	S2	S3	S4
G (D^{-1})				
MICROPHYT.	0.18 ± 0.07	0.54 ± 0	0.38± 0.09	0.84 ± 0.03
NANOPHYT.	0.88 ± 0.21	0.51 ± 0.15	0.71 ± 0.10	0.65 ± 0.21
PICOPHYT.	1.30 ± 0.04	0.88 ± 0.48	0.82 ± 0.80	0.68 ± 0.11
G_P (MG C M^{-2} D^{-1})				
MICROPHYT.	71.07 ± 17.46	463.79 ± 6.96	461.91 ± 103.73	1048.77 ± 48.25
NANOPHYT.	91.74 ± 12.49	102.12 ± 29.80	119.45 ± 46.56	317.73 ± 16.81
PICOPHYT.	762.96 ± 6.35	293.91 ± 39.01	204.79 ± 30.00	137.50 ± 16.73
%P GRAZED D^{-1}				
MICROPHYT.	35 ± 15	40 ± 5	22 ± 4	47 ± 7
NANOPHYT.	42 ± 5	23 ± 7	62 ± 20	40 ± 15
PICOPHYT.	60 ± 1	57 ± 6	56 ± 13	40 ± 4
DIET (%)				
MICROPHYT.	8 ± 3	54 ± 8	63 ± 27	70 ± 7
NANOPHYT.	10 ± 3	12 ± 1	14 ± 8	21 ± 6
PICOPHYT.	82 ± 7	34 ± 7	24 ± 19	9 ± 1

Table 3 Phytoplankton (nano- and micro-sized fractions) consumption rates by metazooplankton and grazing impact in the sampling stations within the Gulf of Gabès during the fall 2017

	S1	S2	S3	S4
G_m (mg C m^{-2} d^{-1})	76.26 ± 0.65	313.36 ± 6.58	225.84 ± 2.40	794.28 ± 72.20
% P grazed d^{-1}	19 ± 1	20 ± 1	10 ± 5	24 ± 6
% Chl *a* grazed d^{-1}	22 ± 1	38 ± 3	32 ± 1	37 ± 4

3.5 Vertical fluxes of particulate organic matter

The vertical fluxes of particles varied significantly among stations, from 561 mg C m^{-2} d^{-1} in S1 to 1891 mg C m^{-2} d^{-1} in S3 (ANOVA, $p < 0.05$; Figure III. 7). These fluxes only accounted for 30% of primary production in S1, but reached 43-45% in S2 and S4, and 70% in S3. Detritus was the dominant sinking flux from S1 (78%) to S3 (79%), but contributed less to the vertical carbon flux of S4 (62%). The phytoplankton carbon exported towards the benthos followed an increasing trend from S1 (111 mg C m^{-2} d^{-1}) to S4 (611 mg C m^{-2} d^{-1}). Zooplankton fecal pellets were non-significant in S1, S2 and S3, and made only 2% of the vertical carbon flux in S4 (38 mg C m^{-2} d^{-1}).

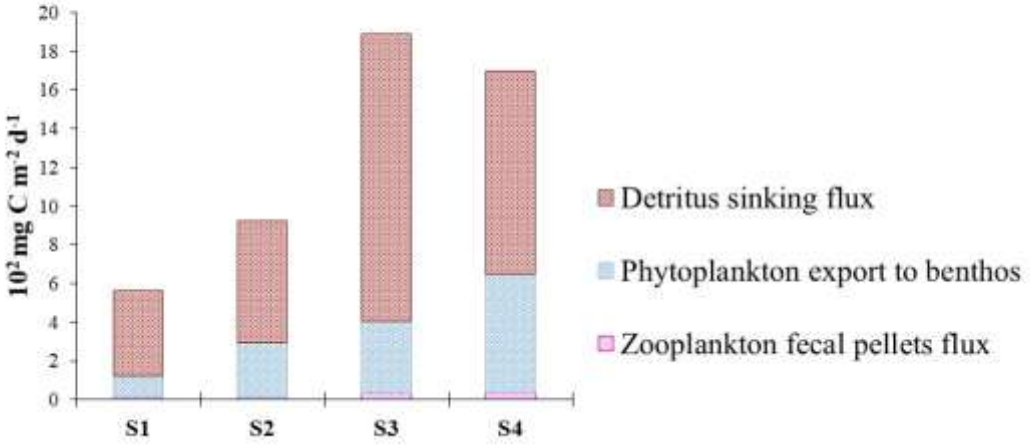

Figure III. 7 Vertical fluxes of particulate organic carbon in the sampling stations during the fall 2017

3.6 Planktonic interactions

Based on data of size-fractionated production, prey-grazers relationships and carbon vertical flux, conceptual diagrams of planktonic interactions were established for all sampling stations (Figure III. 8). The importance of the zooplankton microbivory and herbivory in the carbon transfer (i.e., total consumption by proto- and meta-zooplankton) were considered in each station.

In station S1, the primary production (1816 mg C m^{-2} d^{-1}) was lower than in the other stations, and mainly sustained by picophytoplankton (78%). These small producers were under strong grazing pressure by protozooplankton, which was dominated by aloricate ciliates. Consequently, a large amount of carbon (763 mg C m^{-2} d^{-1}) entered the food web *via* the microbivory of protozooplankton, which represented 76% of carbon transfer. However, > 2 µm phytoplankton (i.e., nano- and microphytoplankton), which was mainly composed by nano-sized phytoflagellates and to a lesser extent by diatoms, participated weakly to primary production (22%). Moreover, protozooplankton grazing on > 2 µm phytoplankton supplied small amounts of carbon to higher consumers (163 mg C m^{-2} d^{-1}). Metazooplankton had also

low feeding on nano- and microphytoplankton (76 mg C m^{-2} d^{-1}). Consequently, herbivory of proto- and metazooplankton together represented only 24% of channeled carbon. Similar to primary production, the amount of carbon particles that settled down and could reach benthos was low (562 mg C m^{-2} d^{-1}).

In comparison to station S1, stations S2 and S3 had an increased production of > 2 µm phytoplankton, particularly of microphytoplankton forming more than 70% of the total primary production, simultaneously to an increase of the diatom abundance. This was accompanied by an increase in the herbivory of protozooplankton (48-60% of carbon transfer), which was dominated by mixotrophic and heterotrophic dinoflagellates and ebridian flagellates. Thus, a high amount of > 2 µm phytoplankton production (566-660 mg C m^{-2} d^{-1}) fueled the food web. Conversely, grazing impact of protozooplankton has decreased for picophytoplankton, which contributed moderately to primary production (15-24%), and hence protozooplankton microbivory (205-294 mg C m^{-2} d^{-1}) supplied 20-25% of carbon to food web. Herbivory of metazooplankton was relatively important (226-313 mg C m^{-2} d^{-1}), corresponding to 20-27% of carbon transfer. Similarly, vertical flux of particles increased in both stations to reach higher value (924-1891 mg C m^{-2} d^{-1}) than in S1.

In station S4, the production of picophytoplankton had further decreased, compared to other stations, to reach the lowest rate (8% of total PP) in detriment of an increase of the production of > 2 µm phytoplankton, which was characterized by the abundance of large diatoms (such as *Rhizosolenia setigera* and *Skeletonema costatum*). Therefore, herbivorous protozoans, such as the diatom-consumer *Protoperidinium*, were abundant, leading to increased herbivory for proto- (59%) and meta-zooplankton (35%), which supplied substantial quantities of carbon (1367 and 794 mg C m^{-2} d^{-1}, respectively) to food web. A significant carbon flux towards benthos was also observed in this station (1700 mg C m^{-2} d^{-1}).

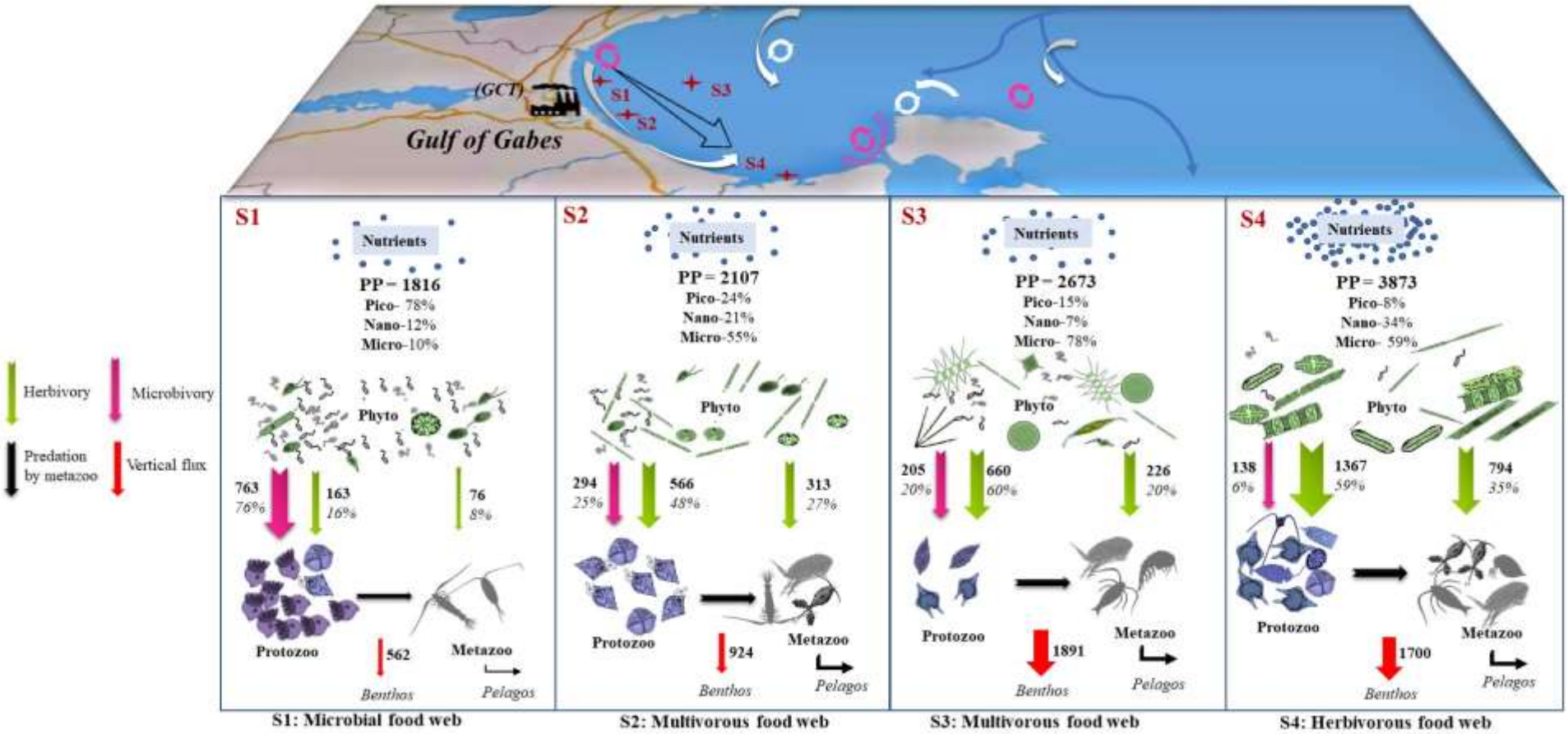

Figure III. 8 Primary production (PP, mg C m^{-2} d^{-1}), trophic relationships and carbon transfer pathways within the planktonic systems of the sampling stations in link with the nutrient spatial gradient and hydrodynamic circulation in the Gulf of Gabès during the fall 2017. Percentage contributions of phytoplankton size fractions to PP are indicated. Values with arrows show the amount of channeled biogenic carbon (mg C m^{-2} d^{-1}) and percentages represent the contribution of zooplankton microbivory or herbivory to carbon transfer. Width of arrow is proportional to the carbon flow

4 Discussion

4.1 Productivity and nutrient richness

Although the primary production levels are well documented for several Mediterranean regions (Psarra et al. 2005; Kovač et al. 2018), information remains scarce for the Southern Mediterranean (Meddeb et al., 2018; Sakka Hlaili et al., 2008) and even deficient for the GG. Here we provide primary production estimates in the GG based on dilution experiments. This technique has been already used in various marine systems, and has shown production rates that are similar to those measured by ^{14}C method (Moigis and Gocke 2003; Meddeb et al. 2018; Dokulil and Qian 2021). Nutrients were not added to dilution bottles, assuming high nutrient concentrations in the GG during our study period. The estimated growth rates were relatively high for most size fractions ($k \geq 1$ d^{-1}; Figure III. 6a), indicating that nutrients were non-limiting for phytoplankton growth. Furthermore, our estimates of growth rates for different size fractions (0.4-1.9 d^{-1}) are in the range of values reported for fractioned phytoplankton from dilution experiments (with or without nutrient addition) in other coastal ecosystems (Grami et al. 2008; Wickham et al. 2022). Furthermore, Boudriga et al. (2022) recently reported similar growth rate (0.38-1.7 d^{-1}) for phtytoplankton to our study. Therefore, the growth coefficients and subsequently the calculated production rates measured in the present work are considered as realistic.

Previous observations have suggested that the high fish production of the GG was related to a high primary production (Béjaoui et al., 2019; Halouani et al., 2016). Our study reveals indeed high total phytoplankton production rates (130-370 mg C m^{-3} d^{-1} or 1816-3674 mg C m^{-2} d^{-1}), which were comparable with estimates from dilution technique in other coastal waters, including Mediterranean ecosystems (Grami et al., 2008a; Marquis et al., 2007; Moigis and Gocke, 2003). However, the primary production levels determined in the GG, located in the

oligotrophic Eastern Mediterranean, far exceed rates currently reported for ecosystems within the same basin, as Ionian Sea, Aegean Sea and Gulf of Trieste (Christaki et al. 2011; Šolić et al. 2010; Cibic et al. 2018). This suggests the influence of anthropogenic nutrient inputs, in addition to natural sources, in the GG leading to its high productivity. Our estimates of Chl *a* concentrations (1.65-6.06 µg L^{-1}) also surpassed values reported in Mediterranean open sea areas (Raveh et al., 2015; Salgado-Hernanz et al., 2019), but were in the range found in other coastal waters (Meddeb et al. 2018; Morsy et al. 2022). Our Chl *a* levels were higher than those recorded by previous studies in the offshore part of GG (< 1 µg L^{-1}; Bel Hassen et al. 2009; Hamdi et al. 2015), which can be due to several environmental features, such as hydrological conditions, nutrient content, season, and phytoplankton community composition. Most of previous works have been conducted during the summer-stratification period (July-September) or during the transition period from the mixed to the stratified water (May-June), when nutrients were in shortage (< 3 N µM, < 1 P µM) resulting in low Chl *a* concentrations. Furthermore, > 2 µm cells dominated the total Chl *a* in all stations (63-89%) and microphytoplankton alone formed ≥ 50% in S3 and S4 (Table 1). Moreover, large diatoms (*Leptocylindrus*, *Skeletonema* and *Rhizosolenia*) were dominant during our sampling period (Figure III. 2a, b). All these observations may explain the higher Chl *a* concentrations measured during our study compared to previous works, which reported the dominance of pico- and nano-sized phototrophs and the scarcity of diatoms (Bel Hassen et al. 2009; Hamdi et al. 2015; Khammeri et al. 2020).

The high primary production and Chl *a* concentrations in the GG were associated to high nutrient concentrations (Table 1), mainly due to the large supply from anthropogenic discharges and also to tide-induced sediment resuspension and atmospheric deposition (Drira et al. 2016; Khammeri et al. 2018). The GG is exceptionally enriched in inorganic and organic P (Table 1) since it continuously receives large amounts of phosphogypsum (1,000 to 13,000 t *per* day since the 1970's) from the phosphoric acid plant (Béjaoui et al., 2004; Khedhri et al., 2014). The P_{inorg}

concentrations measured in all stations exceed those usually observed in Mediterranean coastal waters, like the lagoons of Bizerte (0.15 µM; Meddeb et al. 2018) and Thau (0.18 µM; Courboulès et al. 2021), and the Gulf of Lion (0.06-0.12 µM; Ross et al. 2016). The continuous nutrient enrichment caused by anthropogenic inputs could lead to enhanced eutrophication of the GG, causing ecosystem imbalance in the future. Signs of eutrophication, such as occurrence of harmful algal blooms, have indeed been often reported (Feki- Sahnoun et al. 2017; Ayata et al. 2018).

In the GG, a North-South and coast-offshore gradient of nutrients (Figure III. S1) and organic matter with accumulation in the Southern part has been already observed (Ciglenečki et al., 2020; Mansouri et al., 2020). This spatial pattern can be related to the hydrodynamics of the GG, which is characterized by the presence of a stationary southward current, two great eddies in the middle, and a counter current in the Southern part (Figure III. 1; Zayen et al. 2020). During our study, nutrients also showed increasing concentrations from the North (S1) to the South (S4) and from the coast (S1) to offshore (S3). Phytoplankton variables (i.e., production, carbon biomass and Chl *a*) followed the same spatial distribution patterns than nutrients, confirming that spatial distribution of Chl *a* is closely related to nutrient concentrations in the GG (Bel Hassen et al. 2009).

4.2 Spatial dynamics of phytoplankton

There was a clear spatial variability in the size structure of phytoplankton. The dominance of fast-growing picophytoplankton in S1 (Table 1, Figure III. 6a, b) confirmed its main functional role in this station. In general, the picophytoplankton is dominant in oligotrophic Mediterranean open sea, such as the Northern Adriatic Sea, the Levantine Basin, the Southern Tyrrhenian Sea and the Southern Adriatic Sea (Cerino et al., 2012; Decembrini et al., 2009; Tanaka et al., 2007; Totti et al., 2005). Our results reveal that picophytoplankton can be an

important component within the phytoplankton community in coastal Mediterranean waters, with relatively important nutrient concentrations (i.e., in S1). Unlike S1, large phytoplankton characterized the other stations, even the offshore station (i.e., S3). The micro-sized fraction contributed most of the primary production (55-78%) and carbon biomass (71-75%) in S2, S3 and S4, and dominated the Chl *a* (49-74%) in S3 and S4 (Table 1, Figure III. 6b). The nutrient spatial gradient induced by hydrodynamic features has likely influenced the spatial distribution of phytoplankton size fractions. This was evidenced by a positive correlation between the growth rate of micro-sized fraction and inorganic nutrients, and a negative correlation for the pico-fraction growth rate. The CCA showed also that large phytoplankton was associated with all inorganic nutrients while an opposite trend was found for the picophytoplankton (Figure III. 5). Jyothibabu et al. (2015) have reported a clear impact of the hydrodynamics (summer monsoon current and associated eddies) on the evolution of nutrients and phytoplankton size structure in the Bay of Bengal (Northeastern Indian Ocean). Recently, Decembrini et al. (2020) have showed that the circulation within the Gulf of Augusta (Western Ionian Sea) allowed the advection of nutrient-rich waters that modified the size structure of phytoplankton and triggered an increase of the micro-sized fraction.

The > 2 µm phytoplankton community also displayed a spatial variation in species composition. Generally, nano-sized phytoflagellates, mainly represented by cryptophyceae, dominated in biomass in S1, typified by the least rich waters of the majority of nutrients (lowest concentrations of P_{inorg}, $P_{org,}$ and $Si(OH)_4$). Conversely, the contribution of diatoms increased from S1 (37%) to S4 (88%) concomitantly with the nutrient increase. Diatom biomass showed a positive correlation with all inorganic nutrients (r_s = 0.79-0.67, $p < 0.01$). It is well known that small phototrophs with high surface-to-volume ratio require lower nutrient concentrations for their growth than large cells, which grow well under more nutrient enriched waters (Duarte et al., 2000; Varkitzi et al., 2020). This may explain the high contribution of nano-sized cells to

the > 2 µm phytoplankton community and the dominance of picophytoplankton in S1. The high contribution of nano-sized cells, such as chlorophyceae, cryptophyceae and prymnesiophyceae, to phytoplankton community was previously reported in the GG during a period characterized by reduced nutrient supply (Bel Hassen et al. 2009; Ben Ltaief et al. 2015; Rekik et al. 2015). Nano-sized phytoflagellates are typical of waters with low nutrient concentrations, such as Mediterranean open sea areas (Vidussi et al., 2000; Decembrini et al., 2009). In contrast, blooms of diatoms are commonly observed in coastal Mediterranean environments, particularly during late winter-spring (d'Alcalà et al., 2004; Mayot et al., 2017; Leblanc et al., 2018), when the stratification of the water column follows the vertical mixing, thus favoring the growth of small species (such as *Chaetoceros*) (Peters et al., 2006; Trombetta et al., 2021). Other authors have rather reported the presence of diatoms in Mediterranean waters during the period of turbulence (i.e., autumn), with high proliferation of large species (Decembrini et al., 2009; Margalef, 1978; Vascotto et al., 2021). This agrees with our finding showing that micro-sized diatoms (*Leptocylindrus*, *Skeletonema* and *Rhizosolenia*) were dominant during our study period.

The decrease of picophytoplankton contribution to total primary production and Chl *a* content from S1 to S4, and the increase of micro-sized contribution and diatom proliferation would greatly influence the size and the type of grazers, as well as their feeding activity, suggesting a significant change in carbon transfer pathways between stations. These effects are detailed in the following sections.

4.3 Spatial variation of top-down control by metazooplankton

Copepods were dominant in the GG (Figure III. 4a), as previously observed in this area (Drira et al., 2017; Makhlouf Belkahia et al., 2021) and in other Mediterranean ecosystems (Ben Lamine et al., 2015; Gueroun et al., 2020; Sakka Hlaili et al., 2008). The abundance of copepods found here (0.939-1240 × 10^3 ind m^{-3}) compared also well with previous reports in the GG (Ben

Ltaief et al., 2017; Drira et al., 2017) and in other Mediterranean systems, i.e., Lagoons of Bizerte, Venice and Berre (Riccardi 2010; Siokou-Frangou et al. 2010; Marques et al. 2015; Gueroun et al. 2020). Our study assessed the feeding impact of metazooplankton on phytoplankton using the gut fluorescence method. This simple technique has been widely used for more than several decades because it is useful for revealing the functional role of metazooplankton in various marine environments (Tseng et al. 2008; Meddeb et al. 2018; He et al. 2021). The results show that metazooplankton had an important control on phytoplankton, by consuming 10-24% of the primary production. This feeding effect exceeded that reported in other world oceanic regions (12%, Calbet et al. 2000), but compared with estimates from the gut fluorescence method in other Mediterranean ecosystems (8-30% P grazed d^{-1} in the Lagoon of Bizerte and 9-20% P grazed d^{-1} in the Alboran Sea) (Gaudy et al., 2003; Meddeb et al., 2018). The impact of metazooplankton on phytoplankton biomass (22-38% Chl *a* d^{-1}) was also in the range of percentages found by other authors (using the gut content technique) in coastal ecosystems, such as Gironde estuary, and Gulf of Mexico (Sautour et al. 2000; Landry and Swalethorp 2021). The significant percentages of phytoplankton biomass and production daily consumed by metazooplankton suggested the importance of the metazoan grazers in channeling carbon to higher trophic level in the GG.

The consumption by metazooplankton varied significantly among stations (Table 3), in relation with spatial variations of metazoan abundance (r_s = 0.62-0.76, $p < 0.05$) and prey biomass (r_s = 0.70-0.78, $p < 0.01$). Besides, change in size structure of phytoplankton seemed to influence the feeding of metazooplankton. Consumption rates of phytoplankton measured from S2 to S4 were 3-10 folds higher than that in S1, where the phytoplankton production was dominated by the pico-sized fraction, which is inefficiently consumed by copepods (Berggreen et al. 1988; Morales et al. 1993; Callieri and Stockner 2002). Conversely, the highest feeding activity of metazooplankton was observed in the southernmost station (S4), where large

phytoplankton dominated the Chl *a* and primary production (Table 1, Figure III. 6b). This coincided with a high proliferation of herbivorous copepods (e.g., *Centropages*, *Clausocalanus* and *Paracalanus*) and herbivorous cladocerans (e.g., *Penilia*, Katechakis et al. 2004) (Figure III. 4a). The CCA also showed a clear association between the two metazoan groups and nano- and microphytoplankton (Figure III. 5), which might be due to trophic relationships. As explained, the complex circulation in the GG favoured the accumulation of particles towards the South – among which zooplankton and phytoplankton – leading to increased trophic interactions between the two planktonic components. Similarly, a recent work highlighted the role of hydrodynamics in the retention of metazooplankton in the Southern area of the GG and in the enhancement of its potential control of phytoplankton (Makhlouf Belkahia et al., 2021).

4.4 Spatial variation of top-down control by protozooplankton

Our study examined the impact of protozooplankton grazing on phytoplankton using the standard dilution method. This simple technique, which gives simultaneous estimations of growth and grazing rates, has been used over the past decades in open and coastal environments, including Mediterranean systems (Calbet and Landry 2004; Calbet et al. 2008; Grinienė et al. 2016; Leruste et al. 2019; Pecqueur et al. 2022; Wickham et al. 2022). However, the dilution method has been employed to a lesser extend for the estimation of protozooplankton grazing in the Southern Mediterranean (Grami et al., 2008; Meddeb et al., 2018; Sakka Hlaili et al., 2008). Furthermore, the functional role of protozooplankton is poorly documented in the GG, although previous studies have reported high abundances of ciliates, heterotrophic and mixotrophic flagellates (Ben Ltaief et al., 2017; Drira et al., 2008; Hamdi et al., 2015; Hannachi et al., 2008; Kchaou et al., 2009; Rekik et al., 2021).

Different size fractions of phytoplankton were measured in our dilution bottles rather than total phytoplankton in order to give an insight into the size-selective protozooplankton feeding.

The dilution experiments provided statistically significant grazing estimates for different phytoplankton size fractions in all stations (Figure III. S2 in Supplementary Material). Grazing rates may be over-estimated, if nutrient limitation occurs during experiment (Landry and Hassett, 1982). In our work, although nutrients were not added, the phytoplankton growth was kept under unlimited conditions. Moreover, our estimates of grazing rates for pico-sized fraction were in the range of values reported from dilution experiments (with or without nutrients) in other coastal waters (Dong et al. 2021; Pecqueur et al. 2022). Using the same method, several authors have also found grazing rates for nano- and microphytoplankton (Sakka Hlaili et al., 2007; Dong et al., 2021) comparable to our estimates (Table 2).

In general, there is a close and a positive trophic interaction between the growth of prey and their grazing by protozooplankton (Chen et al., 2020; Dopheide et al., 2011; Martin-Cereceda et al., 2003; Shinada et al., 2000). Indeed, for each size-fraction, significant and positive correlations were found between prey production and protozooplankton consumption rates. Several studies have shown that protozoan organisms were able to modify their growth according to the availability of their potential prey and that the change in phytoplankton size structure may influence the community composition of protozooplankton and its grazing pressure (Sherr and Sherr 2007; Mansano et al. 2014; Horn et al. 2020; Corradino and Schnetzer 2022; Li et al. 2022). The high proliferation of picophytoplankton in S1 was associated with a clear dominance of small aloricate ciliates (20-50 µm *Strombidium* spp.; Figure III. 3a), which are known to have large predation on pico-sized cells (Rassoulzadegan et al. 1988; Sakka 2000; Meddeb et al. 2018). Heterotrophic nanoflagellates (*Commotion cryoporinum*) and ebridian flagellates (*Hermesinium sp.*), which can actively consume pico-sized prey (Berglund et al., 2007; Calbet and Landry, 2004; Hargraves, 2002), were well represented in S1 (Figure III. 3a). The CCA analysis showed likewise a strong association, likely through feeding links, between picophytoplankton biomass and the abundances of all these microbivorous consumers (Figure

III. 5). Accordingly, the protozooplankton displayed high consumption rate and grazing impact on the pico-sized fraction in S1 (60% P grazed d^{-1}), testified by the large contribution of the picophytoplankton to the protozoan diet (82%) (Table 2). Our result is consistent with the finding of high grazing pressure of protozooplankton on picophytoplankton in other Mediterranean coastal systems, such as the Bizerte Channel (84% P grazed d^{-1}) and Thau Lagoon (71% P grazed d^{-1}) (Bec et al. 2005; Meddeb et al. 2018). Grazing and consumption rates for the pico-sized fraction showed a decreased trend from S1 to S4, where the protozooplankton community has clearly changed towards a dominance of heterotrophic and mixotrophic dinoflagellates (Figure III. 3a), concomitantly to the increase of large phytoplankton proliferation (Table 1, Figure III. 6). In S4, heterotrophic dinoflagellates were dominated by species of *Protoperidinum* and *Oxytoxym* (Figure III. 3d), which are known as potential grazers of chain-forming diatoms and small diatoms, respectively (Girault et al., 2013; Kase et al., 2021; Seong et al., 2006). Mixotrophic dinoflagellates were dominated by *Heterocapsa* and *Gymnodinium* (Figure III. 3c) that can feed on small diatoms and nano-sized cells (Du Yoo et al., 2009; Jeong et al., 2010a). The loricate ciliates, mainly *Tintinnopsis, Helicostomella* and *Amphorellopsis,* which commonly feed on large algae (Dolan et al., 2012; Yang et al., 2019), were more abundant in S4 than in other stations (Figure III. 3a). All these herbivorous protozoans seemed to be tightly associated, probably *via* feeding links, to nano- and micro-phytoplankton (CCA analysis, Figure III. 5). Thus, the highest consumption rates for nano- and micro-sized fractions were recorded in S4. In this station, the protozoan's diet mainly relied on microphytoplankton (70%), which accordingly was under the greatest protozooplankton grazing effect (~50% P grazed d^{-1}) (Table 2). In S4, although metazoans displayed increased abundance and very high consumption rates (Table 3; Figure III. 4), their grazing impact (24% P grazed d^{-1}) remained lower than that of protozooplankton, which daily consumed 48% of the > 2-µm phytoplankton production. Our finding is in good agreement with

several authors stating that protozooplankton is the major grazer of phytoplankton in productive waters dominated by large phytoplankton (Aberle et al. 2007; Vargas et al. 2007; Meddeb et al. 2018; Yang et al. 2022). In S2 and S3, nano- and micro-sized fractions formed large proportions of phytoplankton production and biomass (Chl *a* and carbon). The contribution of picophytoplankton was not as low, reaching ~20% of biomass and production of phytoplankton (Table 1; Figure III. 6a). Accordingly, microbivorous protozoans (i.e., aloricate ciliates, heterotrophic nanoflagellates and ebridian flagellates) and herbivorous organisms (i.e., dinoflagellates) were both important components of the protozooplankton in both stations (Figure III. 3). This resulted in significant protozooplankton top-down control on large and small phytoplankton in S2 and S3 (Table 2).

4.5 Implication for carbon transfer pathway

Anthropogenic nutrient inputs coupled with a complex hydrodynamic circulation in the GG led to a clear spatial gradient in nutrients, associated with spatial changes in composition and size structure of phytoplankton and selective zooplankton grazing. Microbivory and herbivory would therefore have different roles in carbon transfer (Figure III. 8), inducing different trophic structures among stations.

In the northernmost station (S1), characterized by less nutrient-rich waters, the high contribution of picophytoplankton (78%) to the primary production was associated with a high microbivory of protozooplankton, representing 76% of carbon transfer. Therefore, the feeding of the microbivorous protozoans played the main role in carbon transfer to upper consumers (76%), as the herbivory of proto- and meta-zooplankton contributed together only 24% of the channeled carbon. These trophic interactions suggest the prevalence of the microbial food web in S1 (Legendre and Rassoulzadegan, 1995; Sakka Hlaili et al., 2014), which is different from the traditional view regarding the presence of the microbial pathway in oligotrophic waters.

Nevertheless, there is increasing evidence that microbial food web can be significant for eutrophic coastal areas (Grami et al., 2008; Paklar et al., 2020; Viñas et al., 2013). The situation has changed in S2 and S3, evidenced by the increased contribution of microphytoplankton to primary production (55-78%), albeit the pico-sized cells remained as substantial contributor to carbon production (15-24%). Parallel to the increase of large phytoplankton production, the herbivory of proto- and metazooplankton increased, forming 75-80% of biogenic carbon channeling. The consumption of picophytoplankton allowed 20-25% transfer of biogenic carbon. Therefore, pico-, nano- and micro-phytoplankton potentially contributed to the production of biogenic carbon, which reached higher consumers through the microbivory and the herbivory of zooplankton. This suggests that a multivorous food web (Legendre and Rassoulzadegan, 1995) was present in both stations. The multivorous pathway was already observed in other productive waters (Masclaux et al., 2015; Meddeb et al., 2018; Siokou-Frangou et al., 2010; Vargas and González, 2004). In the southernmost nutrient-rich station (S4), the herbivorous food web seemed to be dominant, since the high primary production was mainly sustained by microphytoplankton (~60%) and the biogenic carbon was mainly channeled to higher trophic levels through the proto- and meta-zooplankton herbivory, which represented 94% of total carbon transfer. The herbivorous pathway was reported in several coastal waters with high trophic level and abundant diatoms (Sakka Hlaili et al. 2008; Masclaux et al. 2015; Meddeb et al. 2018; D'Alelio et al. 2022). The co-existence of different and contrasted planktonic food webs during the same period in a highly productive system (i.e., the GG) diverges from the traditional view that large phytoplankton and herbivorous pathway usually dominate in nutrient-rich waters.

The spatial variability in planktonic food webs has an ecological implication, as biogenic carbon can be exported with different efficiency to pelagos and benthos (Legendre and Rassoulzadegan, 1995; Sakka Hlaili et al., 2014). The microbial food web is known to be

inefficient in exporting organic matter, as most of the carbon is recycled and a small amount of carbon can be exported to higher consumers or outside euphotic system (Decembrini et al., 2009; Legendre and Rassoulzadegan, 1995). This was consistent with the low vertical carbon flux found in S1, which only accounted for 30% of total primary production. In the other stations, the increase of primary production and of the dominance of large phytoplankton was associated with the increase of vertical flux of organic particles (43-70% of primary production). Furthermore, phytoplankton and zooplankton fecal material showed increased contribution to the carbon flux toward the benthos (Figure III. 7). This confirms that more biogenic carbon is exported towards multivorous and herbivorous food webs (Legendre and Rassoulzadegan, 1995; Meddeb et al., 2019). The highest phytoplankton export to benthos was observed in S4, coinciding with the largest contribution of microphytoplankton to primary production. Conversely, the highest detritus sinking flux was not measured in S4 but in S3. This indicates that some of the sinking detrital material in S3 could be transported from elsewhere.

The hydrodynamic and hydrological features of this area change across seasons, which can impact the plankton dynamics (Bel Hassen et al., 2008; 2009; Makhlouf Belkahia et al., 2021) as well as planktonic interactions within the ecosystem. Thus, it is important to consider the seasonal variations in further investigations to better understand the overall functioning of this high dynamical and productive Mediterranean area.

5 Conclusion

Our study provides a detailed analysis of the plankton communities and the trophic links between size fractionated phytoplankton and proto/metazooplankton in a nutrient-rich and highly productive Mediterranean system, the GG. The complex hydrodynamic circulation within the GG seemed to induce a spatial gradient in nutrient concentrations driving a spatial changes in size structure and production of phytoplankton and trophic interactions, ultimately

leading to various food webs structure with different efficiency in carbon export. Our results allows changing our traditional view concerning the dominance of the herbivorous pathway in highly productive areas and evidencing the presence of a trophic pathway continuum, with other types of planktonic food webs. Our study gives relevant insight on the functional roles of phytoplankton size fractions, proto- and meta-zooplankton and proposes a first description of carbon transfer pathways in the Southeastern Mediterranean area, where such information is deficient. These results can improve the understanding of the dynamics of marine food webs, particularly in ecosystems strongly impacted by anthropogenic nutrient inputs and strong hydrodynamics.

Références (voir références bibliographiques)

Annexes

Figure III. S1. Spatial distribution of nitrate, phosphate and silicate concentrations in the study region within the Gulf of Gabès (unpublished data)

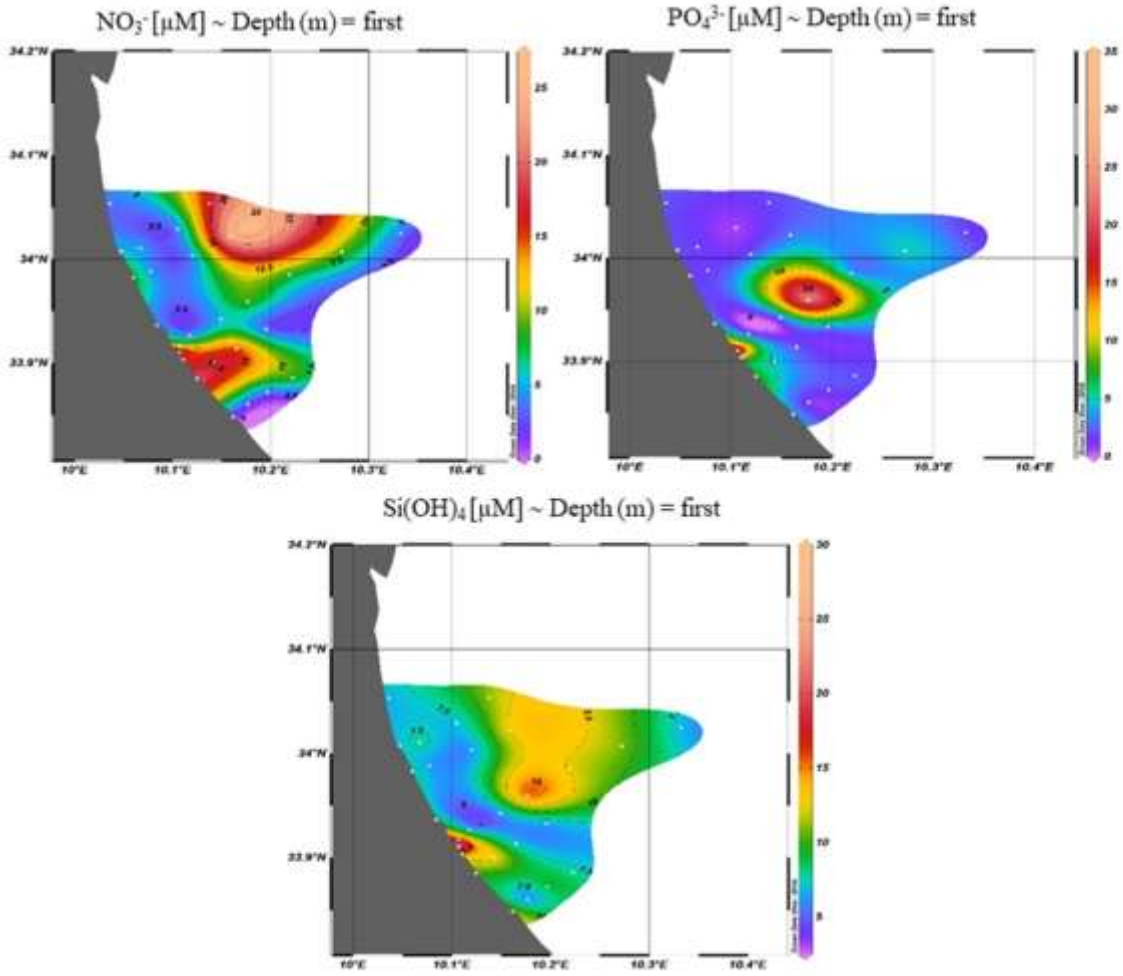

Figure III. S2. Relationship between dilution factor and apparent growth rate (R, d-1) of biomass for pico-, nano- and microphytoplankton in each study station

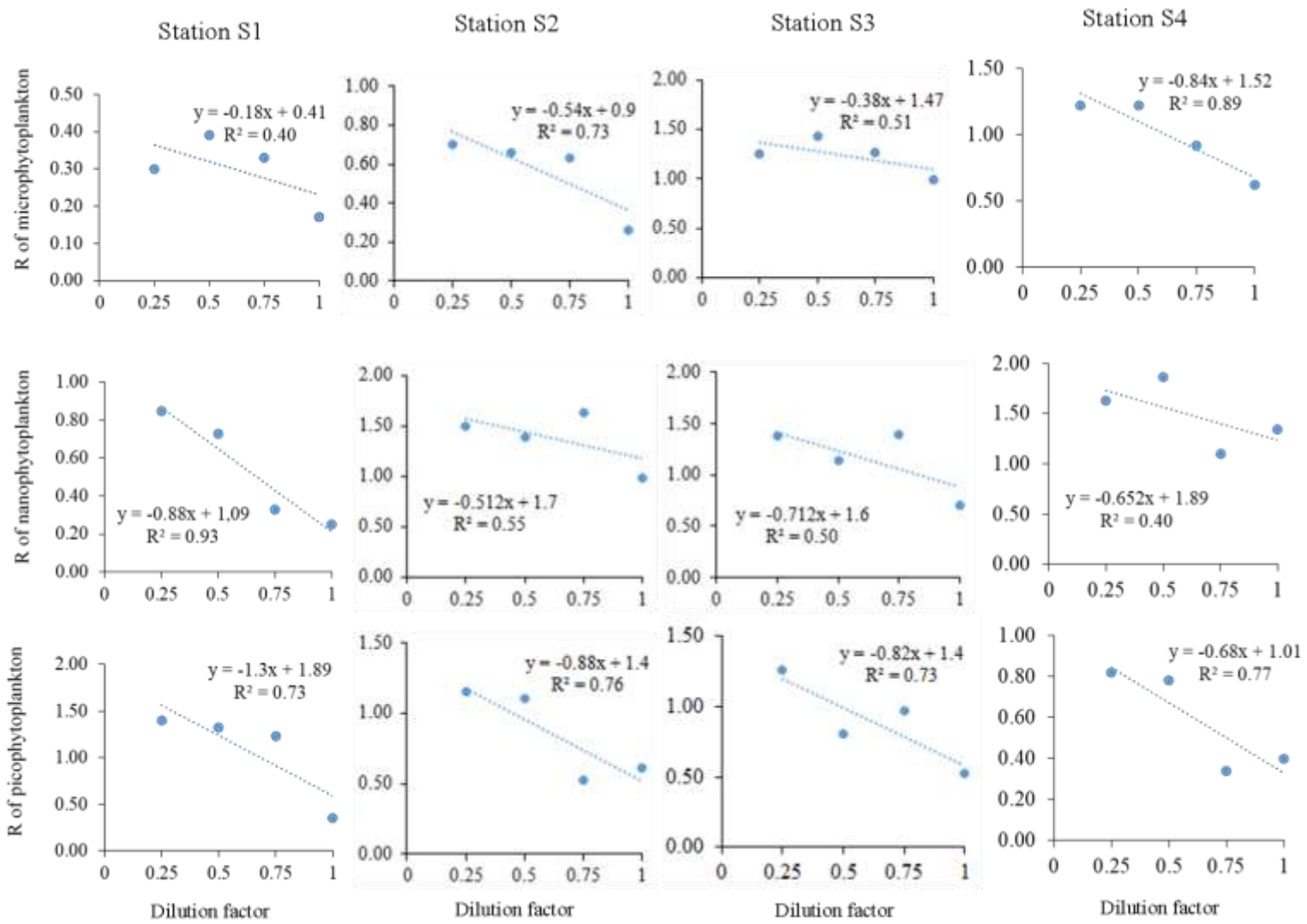

Chapitre IV

Typologie des réseaux trophiques planctoniques & propriétés émergentes comme indicateurs de l'état écologique d'un écosystème sous perturbation chronique

I. Problématique et objectif

L'identification du type de réseau trophique marin est d'une importance écologique et pratique majeure, étant donné qu'il forme une étape clé pour décrire le fonctionnement des écosystèmes et comprendre les flux de matière et d'énergie au sein des communautés planctoniques marines. A titre d'exemple, la détermination du type de réseau trophique peut donner une idée précise sur le potentiel du système à soutenir l'activité de pêche (Hill et al., 2006; Gaichas, 2008; Knights et al., 2013; Subramaniam et al., 2022). Ces informations sont utiles pour une exploitation et une gestion efficaces. Comprendre le réseau trophique marin est une première étape cruciale pour savoir comment les écosystèmes réagissent aux perturbations anthropiques et naturelles (Gotwals et Songer, 2010; Lewis et al., 2022). À l'heure actuelle, les efforts de gestion des écosystèmes marins se concentrent fortement sur les réseaux alimentaires. La « DCSMM » a retenu le "réseau trophique marin" en tant que description de l'état écologique du système (Cardoso et al., 2010; Commission européenne, 2010). Cela signifie que l'un des principaux critères du "bon état écologique" est basé sur les réseaux alimentaires et donc sur leur typologie. En outre, l'analyse des réseaux écologiques fournit des indicateurs écologiques (appelés indices ENA) qui caractérisent le fonctionnement de l'écosystème, comme par exemple son activité, sa capacité de rétention, son organisation et sa maturité (Ulanowicz, 1986; Christensen, 1995; Christian et al., 2009; Bodini et al., 2012a; Pezy et al., 2017; De Jonge & Schückel, 2021). Les effets des stress anthropiques et naturels sur les écosystèmes marins côtiers sont généralement évalués à l'aide d'indicateurs ENA (Belgrano et al., 2005; Niquil et al., 2014; Piroddi et al., 2015; Chaalali et al., 2016). Ces indicateurs fonctionnels fournissent également des données utiles sur la stabilité des réseaux trophiques et le niveau de stress auquel ils sont soumis (Grami et al., 2008; Heymans et al., 2014; Saint-Béat et al., 2015).

Bien que l'état écologique des écosystèmes méditerranéens ait été largement étudié (Méndez et al., 2008; Liquete et al., 2016; Meddeb et al., 2019; Danovaro et al., 2020; Decembrini et al., 2021), les recherches sur la structure et la fonction du réseau trophique et sur la santé des écosystèmes font encore défaut. Par exemple, le groupe MerMex a montré que l'appauvrissement de la biomasse aux niveaux trophiques élevés, la simplification des réseaux alimentaires et les changements de biomasse et de productivité aux niveaux trophiques inférieurs sont des indications fréquentes de la détérioration écologique des écosystèmes marins méditerranéens (Durrieu de Madron et al., 2011). En outre, des recherches récentes ont fourni un ensemble d'indicateurs ENA que les gestionnaires d'écosystèmes pourraient utiliser pour

analyser l'état de santé des milieux marins (Fath et al., 2019; Safi et al., 2019). Dans le sud de la Méditerranée, Meddeb et al., (2018) ont montré l'utilité des modèles inverse de réseaux trophiques et des indicateurs ENA pour identifier les changements de l'état environnemental et les influences anthropiques au niveau de la Lagune, le Canal et la Baie de Bizerte. Selon plusieurs études, un certain nombre d'écosystèmes méditerranéens, notamment les eaux côtières, sont soumis à une pression anthropique importante qui perturbe leurs populations et leur biodiversité et met en péril leurs fonctions éco-systémiques (Templado, 2014; Danovaro, 2003; Bevilacqua et al., 2021). Il est donc essentiel d'utiliser une approche holistique pour prédire comment les perturbations anthropogéniques peuvent affecter le fonctionnement des écosystèmes méditerranéens.

L'objectif de cette étude est donc d'étudier la structure du réseau trophique et ses propriétés émergentes dans le Golfe de Gabès, un site méditerranéen soumis à une perturbation chronique causé principalement par le Groupe Chimique Tunisien (TCG), qui y déverse de grandes quantités de phosphogypse, apportant beaucoup de nutriments et de métaux (Ayadi et al., 2015; El Zrelli et al., 2015; Drira et al., 2018). Notre étude vise également à fournir des indicateurs écologiques utiles pour évaluer l'état de santé de l'écosystème, à prendre en compte par les gestionnaires de l'environnement.

Dans la présente étude, nous avons utilisé les données sur les stocks et les flux de carbone du plancton déterminées au cours de l'étude précédente au niveau des quatre stations (chapitre IV), et nous avons mesuré les stocks de carbone organique dissous (COD) et de carbone organique particulaire (COP). Ensuite, l'approche LIM-MCMC a été appliquée pour caractériser les réseaux trophiques planctoniques et les propriétés structurelles et fonctionnelles dans les différentes stations. Nous avons spécifiquement abordé les questions suivantes : i) comment le type de réseau trophique planctonique change-t-il en fonction des variations spatiales de la pression des nutriments et de spectre de taille du phytoplancton ; ii) comment les ratios de typologie et les indices ENA peuvent-ils être appliqués pour décrire au mieux l'état écologique d'un écosystème soumis à des perturbations permanentes; et iii) quelles sont les applications pour les gestionnaires en termes de surveillance de l'état de santé ?

II. Résumé

Notre étude souligne l'importance de combiner la typologie du réseau trophique planctonique et les caractéristiques émergentes afin de décrire l'état écologique d'un écosystème

soumis à des perturbations permanentes, notamment dues à l'industrie du phosphate. Des modèles linéaires inverses ont été construits pour décrire le fonctionnement trophique des quatre stations dans le Golfe de Gabès, qui étaient soumises à différentes pressions de contamination (i.e. pression nutritive). Les flux de carbone estimés par la méthode LIM-MCMC ont ensuite été utilisés pour calculer les ratios de typologie des réseaux trophiques et réaliser une analyse des réseaux écologiques, permettant de calculer des indices ENA. En se basant sur les ratios de typologie, trois réseaux trophiques planctoniques avec différents indices fonctionnels ont été distingués en fonction du stress nutritif. Le réseau trophique microbien a dominé dans l'environnement le moins riche en nutriments (R7 = 0.73>0.6). Ce réseau était alimenté principalement par la production du picophytoplancton (<2 µm) (R4>R6) qui était principalement transférée par la microbivorie élevée du protozooplancton (R8 = 0.92). En revanche, le réseau trophique herbivore s'était développé dans l'environnement le plus riche en nutriments (R7 = 0.06 < 0.1), où le carbone biogène était principalement produit par le microphytoplancton (> 10 µm) (R4>R6) et transféré vers les niveaux trophiques supérieurs principalement par le protozooplancton herbivore et secondairment par le métazooplancton (R8 = 0.66). Dans les deux autres stations - des systèmes modérément riches en nutriments - le système fonctionnait comme un réseau multivore (0.1<R7= 0.11-0.21 <0.6). Le phytoplancton (fractions de petite et grande taille) et les composants non vivants (détritus et COD) ont joué un rôle important dans la production du carbone (R4~R6) qui se trouvait acheminé sourtout par le le protozooplancton puis le métazooplancton (R8=0.74). Les indices ENA ont révélé que le réseau herbivore, avec un débit total du système (TST) le plus élevé (10,966 mg C m^{-2} d^{-1}) et une ascendance relative (A/C) et un recyclage les plus faibles (0.32- 0.05 %, respectivement), était le système le plus actif, mais aussi le moins organisé et le moins stable. En revanche, le réseau microbien, avec le flux total le plus faible (5,386 mg C m^{-2} d^{-1}) et l'ascendance relative la plus élevée (41%), était le moins actif mais plus organisé que le réseau herbivore. Le réseau multivore, avec des valeurs élevées du rapport détritivorie/herbivorie (1.22-1.36), du recyclage et de l'ascendance relative (13-16 % ; 36- 46 %, respectivement), était le système le plus organisé avec un fort recyclage. Cette étude montre que la typologie des réseaux alimentaires combinée à des indices écologiques peut constituer un outil efficace pour l'évaluation de la santé des écosystèmes, ainsi que pour l'étude de l'occurrence de la pression anthropogénique.

Typology of planktonic food webs and associated emerging properties as indicators of the ecological status of a permanently disturbed Gulf

Oumayma Chkili[1,2,3], Blanche Saint Béat[4], Kaouther Mejri Kousri[1], Marouan Meddeb[1,2], Paula Gauvin[5], Valerie David[5], Asma Sakka Hlaili[1,2], Nathalie Niquil[3*].

(En révision dans JOURNAL OF MARINE SYSTEMS)

Track your submission

This is a new submission-tracking service.

Thank you, could you tell us more?

Peer review status

Typology of planktonic food webs and associated emerging properties as indicators of the ecological status of a permanently disturbed Gulf

- Reviews completed: 2
- Review invitations accepted: 2
- Review invitations sent: 2+

Required Reviews Complete

Last review activity: 23rd May 2023

Watch to learn what we're doing behind the scenes

Journal:
Journal of Marine Systems

Corresponding author:
Nathalie Niquil

First author:
Oumayma Chkili

Date of submission:
10th March 2023

Manuscript number:

MARSYS-D-23-00072

Need more help?

Please visit our Journal Article Publishing Support Center

Typology of planktonic food webs and associated emerging properties as indicators of the ecological status of a permanently disturbed Gulf

Oumayma Chkili[1,2,3], Blanche Saint Béat[4], Kaouther Mejri Kousri[1], Marouan Meddeb[1,2], Paula Gauvin[5], Valerie David[5], Asma Sakka Hlaili[1,2], Nathalie Niquil[3*].

✉ Nathalie Niquil
nathalie.niquil@unicaen.fr

[1] Université de Carthage, Faculté des Sciences de Bizerte, Laboratoire de Biologie Végétale et Phytoplanctonologie, Bizerte, Tunisie

[2] Université de Tunis El Manar, Faculté des Sciences de Tunis, Laboratoire des Sciences de l'Environnement, Biologie et Physiologie des Organismes Aquatiques LR18ES41, Tunis, Tunisie

[3] Université de Normandie, UNICAEN, UMR BOREA (MNHN, CNRS-8067, Sorbonne Universités, Université Caen Normandie, IRD-207, Université des Antilles), CS 14032, Caen, France

[4] Ifremer-Plouzané- DYNECO-PELAGOS, France

[5] Université de Bordeaux, UMR EPOC, CNRS, 5805, France

Abstract

This study highlights the importance of coupling the typology of planktonic food webs and their emerging properties to better describe the ecological status of an ecosystem under permanent disturbance mainly caused by phosphate industry. Linear inverse models were built to describe four stations under various levels of nutrient pressure, using the Markov Chain Monte Carlo method to estimate known and unknown carbon flows, later used to calculate food web typology ratios. Ecological network analysis (ENA) was used to describe the structural and functional properties of each food web. Based on the food web typology ratios, three planktonic trophic pathways (PTP) with different functional indices were distinguished according to nutrient stress. The microbial food web dominated in the least nutrient-rich environment. It mainly relied on phytoplankton production (picophytoplankton < 2 µm) that was mainly transferred by the high microbivory of protozooplankton. In contrast, the herbivorous food web developed in the most nutrient-rich environment, where biogenic carbon was mainly produced by large phytoplankton (microphytoplankton > 10 µm) and mainly channeled to higher trophic levels by herbivorous protozooplankton and metazooplankton. In the other two stations – moderately nutrient-rich systems – the PTP acted as a multivorous food web. Phytoplankton (small and large size fractions) and non-living components (detritus and dissolved organic carbon) played a significant role in carbon production, and protozooplankton and metazooplankton competed with each other in its channel. ENA indices revealed that the herbivorous food web, with the highest total system throughput and lowest relative ascendancy and cycling, was the most active but the least organized and stable system. In contrast, the microbial food web, with the lowest total system flux and high relative ascendancy, was least active but more organized than the herbivorous food web. The multivorous food web, with high values of the detritivory-to-herbivory ratio, cycling and relative ascendancy, was the most recycling and organized system. This study shows that typology of food webs combined with ecological indices can provide an effective tool for managing and assessing ecosystem health, and for investigating the occurrence of anthropogenic pressure.

Keywords: Food-web modeling, ecological network analysis, typology ratios, Mediterranean coastal ecosystem, anthropogenic pressure.

1. Introduction

In marine waters, primary production can reach higher consumers through different types of food webs. The size structure of phytoplankton is the most relevant functional trait driving carbon transfer pathways. Small phytoplankton is mainly involved in microbial food webs, dominated by protozooplankton (PRO) grazing, while large phytoplankton is mainly consumed by metazooplankton (MET) (e.g., copepods) leading to herbivorous food webs. In-between these two contrasting food webs, the trophic continuum includes multivorous pathways in which microbial and herbivorous trophic patterns both play significant roles (Legendre and Rassoulzadegan, 1995a, 1996a). These food webs channel biogenic carbon to higher consumers with different efficiencies. Consequently, changes in the size structure of phytoplankton in response to any environmental variation leads to a shift in the food web structure that ultimately influences the ability of the ecosystem to export or recycle biogenic carbon (Decembrini et al., 2009; Legendre and Le Fèvre, 1989; Meddeb et al., 2019).

Determining marine food web types is of great ecological and practical interest, since it is the main step toward characterizing ecosystem functioning and understanding the flows of material and energy within marine planktonic communities. For example, in the fisheries sector, identifying the type of food web can provide a clear idea of the capacity of the system to support the fishing activity, and this helps for proper exploitation and management (Hill et al., 2006; Gaichas, 2008; Knights et al., 2013; Subramaniam et al., 2022). In ecosystems subject to natural and anthropogenic disturbances, knowledge of the marine food web is an essential step in assessing ecosystem responses to these disturbances (Gotwals and Songer, 2010; Lewis et al., 2022). Food webs are currently in the foreground in marine ecosystem management programs. Furthermore, the European Marine Strategy Framework Directive has retained the “marine food web” as a descriptor of the ecological status of the system (Cardoso et al., 2010; European Commission, 2010). This means that one of the major criteria for "good environmental status" is based on the typology of food webs, highlighting the usefulness of identifying the structure and functioning of food webs in marine ecosystems.

Several modeling approaches have been developed to characterize marine food webs. These models can provide ecological underpinnings for ecosystem services and the management of natural marine systems (Carpenter et al., 2009; Bagstad et al., 2013; Beske-Janssen et al., 2015). Ecopath with Ecosim (EwE) food web modeling is an approach mainly used to study upper trophic levels subject to fishing (Pauly et al., 2000; Christensen et al., 2005;

Sreekanth et al., 2021) and to assess the impact of human exploitation and environmental changes on aquatic food webs (Steenbeek et al., 2018). The linear inverse model (LIM), as defined by Vézina and Platt (1988), is derived from the physical sciences and is considered among the most useful methods in the study of the state of marine ecosystems (Niquil et al., 2011; Pacella et al., 2013; Taffi et al., 2015; Hines et al., 2018). This method has been combined with the Markov Chain Monte Carlo (MCMC) technique to become the innovative LIM Markov Chain Monte Carlo (LIM-MCMC; Meersche et al., 2009). LIM-MCMC estimates uncertainty in flows and indices of structural and functional properties of the food web (De Laender et al., 2010; Grami et al., 2011; Niquil et al., 2011; Saint-Béat et al., 2013; Chaalali et al., 2015; Hines et al., 2018).

Food web determination and modeling requires knowledge of carbon flows, which cannot always be measured in the field. Therefore, several researchers have provided operational criteria to identify and describe food web types, based on ratios calculated from carbon stocks or fluxes easy to estimate in the field (Legendre and Rassoulzadegan, 1995; Mousseau et al., 2001; Sakka Hlaili et al., 2014). Based on a list of numerous LIM models of plankton food webs, Sakka Hlaili et al. (2014) proposed seven food web typology ratios, which can be used as indicators of the type of trophic pathways in natural planktonic systems.

Food web modeling is often associated with ecological network analysis (ENA). ENA provides ecological indicators that characterize ecosystem functioning in terms of activity, retention capacity, organization and food web maturity (Ulanowicz, 1986; Christensen, 1995; Christian et al., 2009; Bodini et al., 2012a; Pezy et al., 2017; de Jonge and Schückel, 2021). ENA indicators are frequently used to assess the impact of natural and anthropogenic pressures on coastal marine ecosystems (Belgrano et al., 2005; Niquil et al., 2014a; Piroddi et al., 2015; Chaalali et al., 2016). They also provide useful information on the degree of stress and stability of food webs (Grami et al., 2008; Heymans et al., 2014; Saint-Béat et al., 2015). In addition, recent studies have presented a set of ENA indices that are most appropriate for studying the health status of ecosystems and could be applied by ecosystem managers (Fath et al., 2019; Safi et al., 2019).

Although much effort has been undertaken to assess the ecological state of Mediterranean ecosystems (Méndez et al., 2008; Liquete et al., 2016; Meddeb et al., 2019; Danovaro et al., 2020; Decembrini et al., 2021), studies on the food web structure and function and on ecosystem health remain scarce. For example, MerMex group reported that common indicators of ecological degradation of Mediterranean marine ecosystems are biomass depletion at high trophic levels, simplification of food webs, and shifts in biomass and productivity to lower

trophic levels (Durrieu de Madron et al., 2011). Meddeb et al. (2018) showed that LIM-MCMC food web models combined with ENA indicators are a powerful approach to detect changes in the environmental status and anthropogenic impacts in southwestern Mediterranean ecosystems. Several Mediterranean ecosystems, particularly coastal waters, are under strong anthropogenic pressure that causes an imbalance in their communities and biodiversity, with a serious threat on their ecosystem services (Templado, 2014; Danovaro, 2003; Bevilacqua et al., 2021). Therefore, predicting the consequences of anthropogenic disturbances on ecosystem functioning by a holistic approach is very relevant. The present study aims to investigate the structure of the trophic food web and its emerging properties in a Mediterranean site under permanent anthropogenic pressure (the Gulf of Gabès). It also aims to provide useful ecological indicators for assessing the health status of the ecosystem, to be considered by environmental managers. The Gulf is highly impacted by the Tunisian Chemical Group (TCG), which discharges high quantities of phosphogypsum into the sea that bring a lot of nutrients and metals and lead to chronic disruption of the ecosystem (Ayadi et al., 2015; El Zrelli et al., 2015). Our previous study in the Gulf (Chkili et al., 2023) was conducted in four stations located at different distances from the TCG complex (Figure IV A.1). It showed a spatial nutrient gradient causing significant spatial variations in the size structure and production of phytoplankton. This was followed by a spatial change in the community composition of PRO and MET, zooplankton grazing and particle sinking. In the present study, we used data of plankton carbon stocks and flows determined during our previous study, and we measured dissolved organic carbon (DOC) and particulate organic carbon stocks (POC). Then, the LIM-MCMC approach was applied to characterize the planktonic food webs and the structural and functional properties in different stations. We specifically addressed the following questions: i) how does the type of planktonic food web change according to the spatial variations in nutrient pressure and in the size structure of phytoplankton?; ii) how can food web typology ratios and ENA indices be applied to best describe the ecological status of an ecosystem under permanent disturbance?; and iii) what are the applications for managers in terms of health monitoring?

2. Materials and Methods

2.1. Study Site

The Gulf of Gabès is located on the south-eastern coast of Tunisia (Figure IV A.1). It represents more than half of the Tunisian coastline with about 700 km and has the largest continental shelf in the Mediterranean Sea. Its outline measured only on the 20-metre isobath is 110 nautical

miles. The 50-metre depth extends to more than 70 nautical miles off Kerkennah Islands (Hattour et al., 2010). The Gulf is characterized by a complex water circulation resulting from the combination of general currents, tidal currents, wind-driven currents and/or swell or littoral currents, and tides reach the highest range in the Mediterranean sea (~ 2 m) (Hattour et al., 2010; Othmani et al., 2017). The Gulf hosts nutrient-rich waters as a result of inputs from anthropogenic activities (M. B. Bel Hassen et al., 2009; Drira et al., 2009a; Y. Khammeri et al., 2018), in contrast with the well-known oligotrophy of the Eastern Mediterranean Basin (D'Ortenzio and Ribera d'Alcalà, 2009; Ben Brahim et al., 2010). The Gulf is a highly productive ecosystem supporting a high marine biodiversity and contributing up to ~50% of the national fish production (DGPA 2015; Béjaoui et al., 2019). It also constitutes a crucial nursery ecosystem for the Mediterranean sea (Enajjar et al., 2015; Koched et al., 2015). This ecosystem was recently considered as one out of eleven consensus eco-regions in the Mediterranean Sea and is classified as a shallow-water region characterized by phytoplankton blooms (Ayata et al., 2018). Nevertheless, the Gulf is identified as a hotspot of anthropogenic pressures (Reygondeau et al., 2017) because it is strongly impacted by industrialization, notably discharges from phosphate production plants, mainly the TCG (Boudaya et al., 2019; Kmiha-Megdiche et al., 2021). Overfishing is also an increasing problem in the Gulf, leading to an imbalance of the ecosystem and the decline of fisheries resources (Béjaoui et al., 2019).

2.2. Sampling and water analyses

Sampling was conducted in the fall of 2017 at four stations selected on either side of the main source of contamination (TCG) (Figure IV A.1). Station S2 was located in front of the phosphoric acid facility and was suspected to be most affected by phosphogypsum loading; stations S1 and S4 were also located in the marine coastal zone, north and south of S2, respectively, and S3 was an offshore station in front of S1. Chkili et al. (2023) showed that anthropogenic nutrient loading coupled with the complex hydrodynamic circulation within the Gulf create north-south (from S1 to S4) and coast-offshore (from S1 to S3) ascending gradients of nutrients.

Water was collected at three depths at each station (between 0.5 and 14 m depending on the maximum water depth of the station) using an acid-washed water sampler (HydroBios). Subsamples (5 mL) were immediately filtered on sterilized 0.2-µm polycarbonate filters and frozen in acid-washed vials at -20 ^{o}C until DOC analysis using a Shimadzu TOC-5000A autoanalyser (Sharp et al., 1993). The remaining water was pre-filtered through a 200-µm mesh screen to remove MET, and several subsamples were taken to analyze nutrients, POC, bacterioplankton (BAC), size-fractioned phytoplankton (picophytoplankton, PIC: < 2 µm; nanophytoplankton, NAN: 2-10 µm;

microphytoplankton, MIC: 10-200 µm) and protozooplankton (PRO). Most of these analyses are described in Chkili et al. (2023). Briefly, inorganic nutrients (N_{inorg}: NO_2^- + NO_3^- + NH_4^+; P_{inorg}: PO_4^{3-}; $Si(OH)_4$) and organic nitrogen (N_{org}) and phosphorus (P_{org}) were measured using a BRAN & LUEBBE type 3 autoanalyzer (Bran + Luebbe Co., Germany). Subsamples for POC determination were filtered on pre-combusted (450 °C, 24 h) GF/F filters (21 mm) and analyzed by the high combustion method and mass spectrometry (Raimbault et al., 2008). The subsamples were fixed with 20% paraformaldehyde solution, placed at 4 °C in the dark for 15 min, and finally frozen at -80 °C in liquid nitrogen until analysis with a CyFlow® Space flow cytometer (Partec) to determine BAC and PIC abundances, according to Khammeri et al. (2020, 2018). The samples for NAN and MIC analyses were fixed with acid Lugol solution (4% final concentration), while the samples for PRO analysis were fixed with alkaline Lugol solution at 5% final concentration (Parsons et al., 1984; Sherr and Sherr, 1993). The cell abundances and species compositions of these planktonic groups were determined under an inverted microscope (Motic AE31E, 100×objective) (Utermöhl, 1931). To determine MET abundance and composition, a WP2 200-µm mesh net, with ring diameter of 28 cm, was used. The net was pulled vertically at a speed of 1 m s^{-1} from depths 10m at S1, 11m at S2 and S4 and 12m at S3 to the surface. A flow meter was used to determine the volume of water filtered during the towing of the net.

2.3. Plankton data

Data about planktonic carbon stocks and carbon fluxes were sourced from Chkili et al. (2023). Biovolumes of BAC, PIC, NAN, MIC and PRO were converted into carbon contents using specific conversion factors or formulae (Table 1 in Meddeb et al., 2018). The length and width of MET organisms were measured and converted to carbon contents using conversion factors or formulae corresponding to each taxonomic group (Table 1 in Meddeb et al., 2018). The cell carbon of each plankton community was multiplied by its abundance to get its carbon concentration. DOC concentrations were obtained considering that 1 µM of DOC was equal to 12 mg C m^{-3} (Grami et al., 2008b). Detrital organic carbon (DET) was estimated as POC minus the carbon biomasses of all organisms. Finally, for each planktonic compartment, carbon concentrations (mg C m^{-3}) from the three depths were vertically integrated to get carbon stocks (mg C m^{-2}).

Production rates (mg C m^{-2} d^{-1}) of BAC and size-fractioned phytoplankton (PIC, NAN and MIC) as well as their grazing rates by PRO (mg C m^{-2} d^{-1}) were estimated using the dilution technique (Landry and Hassett, 1982; Dokulil and Qian, 2021). The experimental procedure, the analysis and the rate estimation are detailed in Chkili et al. (2023). Grazing of phytoplankton (NAN

and MIC) by MET (mg C m^{-2} d^{-1}) was assessed by the gut fluorescence method (Meddeb et al., 2018; Tseng et al., 2008) The experimental procedure and the calculations are detailed in Chkili et al. (2023). Sinking fluxes were estimated by collecting organic particles (NAN, MIC, DET and MET fecal pellets) that settle down along the water column in sediment traps moored at two meters from the bottom of each station. The deployment of sediment traps, the analyses of their contents and the calculation of the vertical fluxes of each type of particle are described in Chkili et al. (2023).

2.4. Model development

Field data provide a limited number of known fluxes. To have a complete model of planktonic food webs, the LIM-MCMC method (Van den Meersche et al., 2009) was used to construct carbon fluxes between planktonic compartments at the four stations. This approach is based on four steps: (i) constructing an *a priori* model, (ii) setting the equalities, (iii) setting the inequalities, and (iv) calculating possible solutions for each flux.

2.4.1. *A priori* model

The *a priori* model included planktonic compartments and all possible known and unknown carbon fluxes between them. In each station, the model included eight compartments: BAC, PIC, NAN, MIC, PRO (mainly protozoans < 200 µm: heterotrophic nanoflagellates, dinoflagellates and ciliates), MET (mainly metazoans > 200 µm), DOC and DET. The model encompassed thirty-five fluxes between the compartments and their outside (Figure IV. 1). Gross primary production (GPP) of the three phytoplankton size fractions (PIC, NAN and MIC) was the only source of carbon input to the network. Some of this carbon was lost by respiration (RES) by all living compartments, sinking (SINK) of most compartments (except BAC, PIC and PRO) and DOC export (EXP). It was assumed that the very small size of PIC and BAC did not allow them to generate a sinking flux. Dissolution of detritus, exudation by phytoplankton and excretion by zooplankton (PRO and MET) contribute to DOC formation. BAC were the only users of DOC since other potential DOC consumers such as choanoflagellates were absent in our samples (Chkili et al., 2023). All living compartments but PIC and BAC contributed to generate DET through mortality, production of faecal pellets by MET and sloppy feeding by zooplankton. Concerning trophic interactions, BAC and all phytoplankton size fractions were consumed by PRO, while MET only consumed NAN and MIC because smaller cells (BAC and PIC) are inefficiently captured by MET (Fortier et al., 1994). PRO and DET also contributed to a food source for MET.

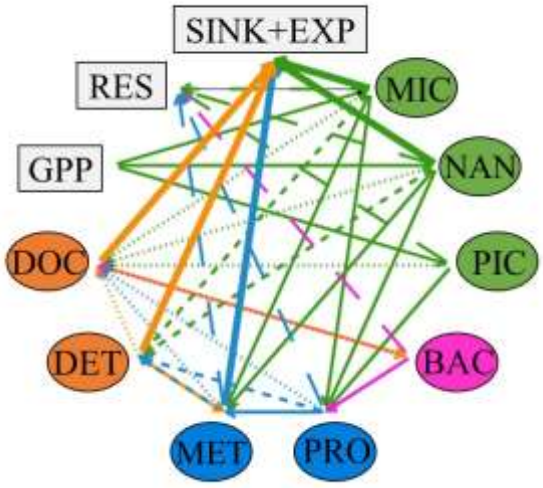

Figure IV. 1. *A priori* food web model for the four stations. Colored circles represent internal compartments. Green, primary producers (PIC = picophytoplankton < 2 µm, NAN = nanophytoplankton 2-10 µm, MIC = microphytoplankton 20-200 µm); pink, bacterioplankton (BAC); blue, consumers (PRO = protozooplankton, MET = metazooplankton); orange, non-living carbon (DET = detritus, DOC = dissolved organic carbon). Gray boxes correspond to external connections: carbon inputs (gross primary production, GPP) and outputs (respiration, RES; particle vertical sinking, SINK; DOC export, EXP). The arrow color of each flow refer to its source.

2.4.2. Equalities and inequalities

The setting up of the equalities is an essential phase for establishing the mass balances of the network. If the mass of the compartment is constant during the period under consideration, the sum of the ingoing fluxes should be equal to the sum of the outgoing fluxes. However, the daily variations in biomass with respect to the daily flux values were neglected. A mass balance equation was written for each compartment (Table IV. A.1). The subsequent step was to impose ecological limits (maximum and/or minimum) for each unknown flux to reduce the range of possible solutions. The inequalities represented two types of ranges. The first range considered the average values of the fluxes measured in the field (i.e., production rates of BAC, PIC, NAN and MIC; grazing rates by PRO and MET, and vertical sinking of particles). Based on these average values, the model only estimated the fluxes with uncertainty. For this reason, we proposed to define the minimum and maximum values for each flux by calculating a confidence interval around the field data, i.e., by using the minimum and maximum of the mean value of each flux. Thirteen inequalities derived from field measurements were considered for every

station (Table IV. A.2). A second group of constraints was adopted from the literature to constrain the unknown fluxes (Vézina and Piatt, 1988b; Steinberg et al., 2000; Vézina and Pahlow, 2003). These inequalities included the lower and/or upper limits of several processes such as respiration of all living compartments; DOC production by phytoplankton, PRO, MET and BAC; production and dissolution of DET; growth efficiency of BAC, PRO and MET, and assimilation efficiency of PRO and MET. For preferential ingestion by MET, we used diet constraints, which are based on the assumption that MET feeding depends on the availability of their prey, i.e., the abundance of a prey relative to other prey (Haraldsson et al., 2018). The availability (A, as a fraction) of prey compartment *i* to consumer compartment *j* was calculated based on the specific diet data about each species *k* in the consumer compartment:

$$A_{ij} = \sum_{k=0}^{n} \left(\frac{prey_{ijk} \times SC}{\sum prey_{ijk}} \times \frac{consum_{jk}}{\sum consum_{jk}} \right)$$

where prey and consum are the biomasses of the prey and consumer, respectively, SC is the selection coefficient (= 1 when there was no selection, = 1.4 when there was assumed positive selection, and = 0.6 when there was negative selection) (Table IV. A.3). Twenty-six inequalities from this second group were applied in the model to the four stations (Table IV. A.3).

2.4.3. Solutions

The calculation of the unknown fluxes was the last step of the inverse analysis. The LIM-MCMC method based on the mirror technique defined by Meersche et al. (2009) estimates each unknown flux. A jump value of 10 mg C m^{-2} d^{-1} and 300,000 iterations were adopted to run the models and optimize the coverage of all possible solutions.

2.5. Food web typology ratios

To describe the different interactions between compartments and identify the type of trophic pathway, Sakka Hlaili et al. (2014) provided seven operational criteria based on carbon flux ratios that can be easily estimated in the field. In our study, four food web typology ratios were calculated from the flux data yielded by the models (Table IV. 1). Ratio R4 (total net phytoplankton production divided by the net production of potential food for PRO) determined the relative importance of phytoplankton production, while ratio R6 (net production of DOC

and DET divided by the net production of potential food for PRO) expressed the significance of production by non-living compartments. Ratio R7 (picophytoplankton net production divided by total phytoplankton net production) discriminated between herbivorous ($R7 \leq 0.1$), multivorous ($0.1 < R7 < 0.6$) and microbial food ($R7: \geq 0.6$). Ratio R8 (consumption rate of total phytoplankton by PRO divided by the consumption rate of total phytoplankton by PRO and MET) identified the main phytoplankton grazers (i.e., PRO when $R8 > 0.5$ or MET when $R8 < 0.5$).

Table IV. 1. Carbon flow ratios for the determination of planktonic food web types (Sakka Hlaili et al., 2014).

Ratio	Formula	Description	Trophic interpretation
Ratio 4 (R4)	Pnetpht*/D2**	Total net phytoplankton production divided by net production of potential PRO feed	Phytoplankton contribution to production of potential protozooplankton feed
Ratio 6 (R6)	(PnetDET + PnetDOC)/D2	Net production of DOC and DET divided by net production of potential PRO food	Contribution of non-living organic matter to production of potential PRO feed
Ratio 7 (R7)	PnetPIC/Pnetpht	Net PIC production divided by total net phytoplankton production	PIC contribution to total net phytoplankton production
Ratio 8 (R8)	pht-PRO/(pht-PRO + pht-MET)	Consumption rate of total phytoplankton by PRO divided by consumption rate of total phytoplankton by PRO and MET	Importance of PRO in the consumption of total phytoplankton

*Pnet = Net production, pht = Total phytoplankton
**D2= Pnetpht + PnetBAC + PnetDET + PnetDOC

2.6. Ecological network analysis (ENA)

An ecological network analysis (ENA) was applied to describe the functioning of the ecosystem from the flux values obtained by the LIM-MCMC approach. ENA examines the food web structure within the ecosystem and its emerging properties (Ulanowicz, 1986; Fath and Patten, 1999; Tecchio et al., 2015; Meddeb et al., 2019). A number of calculated indices were considered to compare and characterize the stations:

- *Total system throughput (TST):* The total system throughput is the sum of all fluxes through all compartments (Kay et al., 1989). The TST is interpreted as an indicator of the system activity (Rutledge et al., 1976; Latham, 2006) and is calculated as:

$$TST = \sum_{i=1,j=1}^{n} T_{ij}$$

Where Tij is the flux from compartment i to compartment j. The size of the system is associated with growth, which is determined by the number of compartments and the magnitude of the fluxes (Bodini et al., 2012; Ulanowicz, 1986).

- *Average mutual information (AMI):* This index measures the efficiency with which materials are transported through the network. It describes the organization of exchanges between compartments (Latham and Scully, 2002; Ulanowicz, 2004) and is expressed as follows:

$$AMI = \sum_{i=1,j=1}^{n} T_{ij} Q_i \log\left(\frac{T_{ij}}{\sum_{k=1} T_{kj} Q_k}\right)$$

with T_{ij} is the flux from compartment i to compartment j; Q_i is the probability of a unit of energy passing through i; and T_{kj} and Q_k represent the total flux of j and the probability of a unit of energy passing through other compartments. Low values of AMI indicate that the system is evolving towards a web-like food web, while high values show an increase in specialization/constraints (Ulanowicz, 1997, 2004).

- Ascendancy/development capacity (*A/C) ratio:* The A/C ratio shows the degree of organization of the food web (Ulanowicz et al., 2009). Ascendancy (A) represents the organized part of the ecosystem and is more informative when expressed in relation to the development capacity (relative ascendancy, A/C). It is calculated as follows:

$$A/C = \frac{AMI * T..}{-\sum_{ij} t_{ij} \log\left(\frac{t_{ij}}{T}\right)}$$

- *Finn cycling index (FCI):* The FCI (Finn, 1976) represents the fraction of the total flux through the system that is cyclic, i.e., the proportion of the flux that revisits the same node several times before exiting the system. The recycled flux from node i (TSTci) can be calculated from the following equation:

$$TST_{ci} = \left({}^{(n_i i - 1)}/_{n_i i}\right) T_i$$

Thus, the FCI can be calculated by dividing the total cycling flux (TST_{ci}) by the total system throughput (TST):

$$FCI = \sum {}^{TST_{ci}}/_{TST_{flux}}$$

- *Average path length (APL):* The APL is the mean number of compartments crossed by a carbon unit from its entry to its exit from the system. It is an indicator of the amount of system activity (TST_{flow}) generated by each unit input into the system (Finn, 1976). It is calculated as follows:

$$APL = \frac{TST_{flux}}{\sum_{i=1}^{n} z_i}$$

Jørgensen et al. (2000) interpreted this index as an indicator of the growth and development of the system, which they renamed network aggradation since it forms an indicator of the organization of the system and its capacity to do more work with given resources (the input limit).

- *Detritivory/herbivory (D/H) ratio:* The D/H ratio measures the importance of grazing of phytoplankton relative to detrital carbon consumption. It is a simple ratio where detritivory represents the DET-MET and DOC-BAC fluxes and herbivory represents phytoplankton consumption fluxes by PRO and MET (Kay et al., 1989; Ulanowicz, 1992; Baird et al., 2009).

2.7. Statistical analyses

2.7.1. Multiple factor analysis (MFA)

A multiple factor analysis (MFA) was performed to identify the interrelationships between different ecological indicators (food web typology ratios and ENA indices) as well as environmental variables (inorganic and organic nutrients) and some of the calculated fluxes (GPP of PIC, NAN and MIC, bacterial production and sinking of NAN, MIC and MET). Each station was considered as a group, which by definition included variables measured at the same date. The objective was to find a common or representative structure for all groups. Unlike individual principal component analysis, MFA can integrate groups of variables (at different sampling dates) in a single analysis, and analyzes the relationship within each group and over time (Escofier and Pagès, 1990).

The calculated indices as well as the environmental and biological data determined in the water column were organized in a matrix where the rows (individuals) represented the 50 randomly chosen values of LIM solutions and the columns (identified variables) were the parameters determined in each station. There were 200 individuals (or rows) in total, and 21 variables were used for each sample. The analysis consisted of a principal component analysis for each table, weighted by dividing each variable by its PCA eigenvalue for the final analysis. Four tables were considered: ENA indices, typology ratios, primary and bacterial production, and export.

All modeling and statistical analyses were performed in R software with LIM libraries for linear inverse modeling, NetIndices for ENA calculation as well as FactomineR, Ade4 and vegan for digital analyses of the results.

2.7.2. Cliff's δ test for comparing network indices between stations

The Cliff's δ test was used to statistically test ENA index differences between models (Tecchio et al., 2016). This method is necessary for large sample sizes (in our case 300,000 values for each stream). Four pairwise comparisons were performed for each ENA index. Then, the following values were used to define small, medium, and large effects (small, $|\delta| >= 0.11$; medium, $|\delta| >= 0.28$; large, $|\delta| >= 0.43$; (Vargha and Delaney, 2000; Romano et al., 2006).

3. Results

3.1. Input, output and throughput flows

We calculated 34 carbon flows in each station using LIM-MCMC analysis (Table IV. 2). Phytoplankton gross primary production (GPP) was the only carbon input in the food web. Total GPP followed an ascending gradient from S1 (1,838.5 mg C m^{-2} d^{-1}), then S2, S3 (2,240.2 - 2,954 mg C m^{-2} d^{-1}) up to S4 (4,110.1 mg C m^{-2} d^{-1}) (Figure IV. 2 A). The contribution of each phytoplankton size fraction to total GPP varied among stations (Figure IV. 2 B). PIC was the main producer in S1 (76%), *versus* MIC in the other stations (56-80%). The contribution of NAN was low (7-21%), but reached 33% in S4.

Table IV. 2. Mean values of the fluxes estimated by the LIM-MCMC for each station in the Gulf of Gabès.

Flow description	Symbol	Mean value (mg C m^{-2} d^{-1})			
		S1	**S2**	**S3**	**S4**
Microphytoplankton gross primary production	GPP-MIC	206.40	1258.00	2359.00	2451.00
Nanophytoplankton gross primary production	GPP-NAN	228.10	481.00	195.70	1365.00
Picophytoplankton gross primary production	GPP-PIC	1404.00	501.20	339.30	294.10
Microphytoplankton respiration	MIC-RES	11.24	78.49	151.70	167.70
Microphytoplankton dissolved organic carbon exudation	MIC-DOC	20.35	144.77	333.20	268.00
Microphytoplankton net production	MIC-DET	0.91	175.88	1259.60	72.48
Microphytoplankton grazing by protozooplankton	MIC-PRO	64.78	441.70	310.90	994.00
Microphytoplankton grazing by metazooplankton	MIC-MET	58.07	281.80	209.80	650.50
Microphytoplankton sinking	MIC-LOS	51.03	135.00	93.60	298.50
Nanophytoplankton respiration	NAN-RES	19.67	39.65	21.41	131.43
Nanophytoplankton dissolved organic carbon exudation	NAN-DOC	29.01	69.71	30.58	182.43
Nanophytoplankton detritus production	NAN-DET	72.82	247.80	14.12	632.50
Nanophytoplankton grazing by protozooplankton	NAN-PRO	88.33	100.93	116.70	315.20
Nanophytoplankton grazing by metazooplankton	NAN-MET	16.40	22.54	12.72	102.71
Nanophytoplankton sinking	NAN-LOS	1.92	0.37	0.14	0.49
Picophytoplankton respiration	PIC-RES	298.23	76.28	96.51	81.57
Picophytoplankton dissolved organic carbon exudation	PIC-DOC	332.50	120.73	88.99	65.67
Picophytoplankton grazing by protozooplankton	PIC-PRO	773.10	304.10	213.80	146.90
Protozooplankton respiration	PRO-RES	464.70	374.10	352.60	547.60
Protozooplankton dissolved organic carbon excretion	PRO-DOC	146.80	248.00	248.60	277.90
Protozooplankton detritus production	PRO-DET	323.60	244.00	197.40	307.70
Protozooplankton consumption by MET	PRO-MET	317.30	484.70	406.90	684.70
Metazooplankton respiration	MET-RES	147.34	353.00	203.50	575.90
Metazooplankton dissolved organic carbon excretion	MET-DOC	63.31	234.50	125.25	270.20
Metazooplankton detritus production	MET-DET	93.79	228.80	105.15	324.00
Metazooplankton sinking	MET-LOS	125.20	313.90	201.90	541.70
Bacterial respiration	BAC-RES	219.30	308.50	338.00	302.70
Bacterial dissolved organic carbon production	BAC-DOC	112.94	250.65	263.24	100.02
Bacterial grazing by protozooplankton	BAC-PRO	326.10	504.00	564.00	361.90
Dissolved organic carbon uptake by bacteria	DOC-BAC	658.30	1063.20	1165.00	764.60
Dissolved organic carbon output	DOC-LOS	54.55	29.10	38.05	460.30
Detritus dissolution	DET-DOC	8.03	26.91	113.50	60.77
Detritus consumption by metazooplankton	DET-MET	37.88	338.10	6.35	273.90
Detritus sinking	DET-LOS	445.30	531.50	1456.00	1002.00

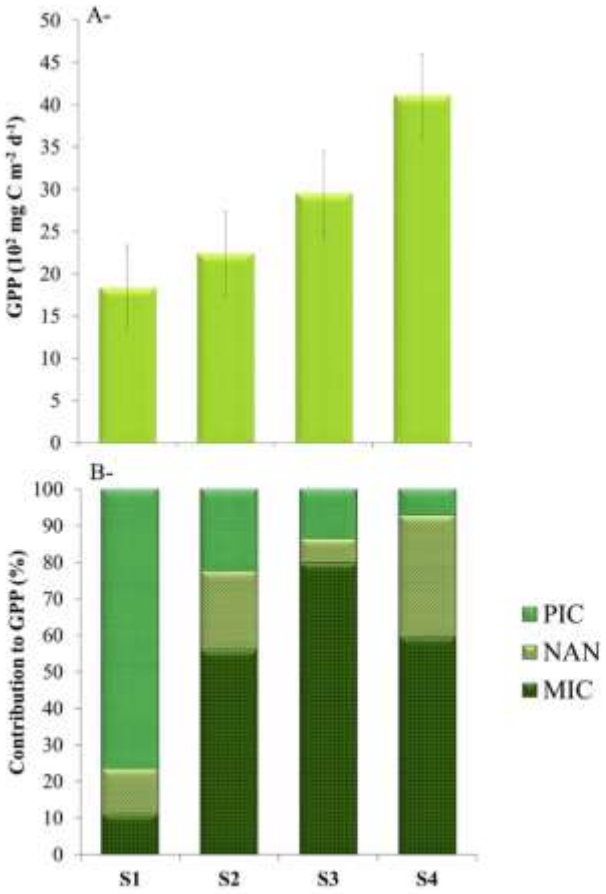

Figure IV. 2. Total gross primary production (GPP) (A), and contribution of each phytoplankton size fraction to GPP (B). PIC, picophytoplankton; NAN, nanophytoplankton; MIC, microphytoplankton.

The output flows were represented by respiration of all living organisms, DOC export, and particle vertical sinking of MIC, NAN, MET and DET. These outputs differed among stations (Table IV. 2, Figure IV. 3 A). Respiration represented the main carbon output in S1 (63%) and S2 (55%) and to lesser extent in S3 and S4 (39-44%) (Figure IV. 3 A). Carbon loss through respiration was about 2-32% of GPP in S2, S3 and S4, and 1-40% in S1. PRO, MET and BAC altogether contributed 77-84% of respiration in S2, S3 and S4, while the total contribution of phytoplankton was ≤23%. In S1, the contribution of phytoplankton to this output increased (~30%) due to the enhancement of PIC respiration (Figure IV. 3 B). DOC export was low, except in S4 where it formed 11% of the carbon output. Particle sinking provided 34-45% of total carbon loss in S1, S2 and S4, and 59% in S3 (Figure IV. 3 A). Particle sinking formed the second main source of carbon output (43-59%). MET and MIC represented most of the

living sinking particles: they represented 12-32% and 5-16% of carbon loss, respectively (Figure IV. 3 C).

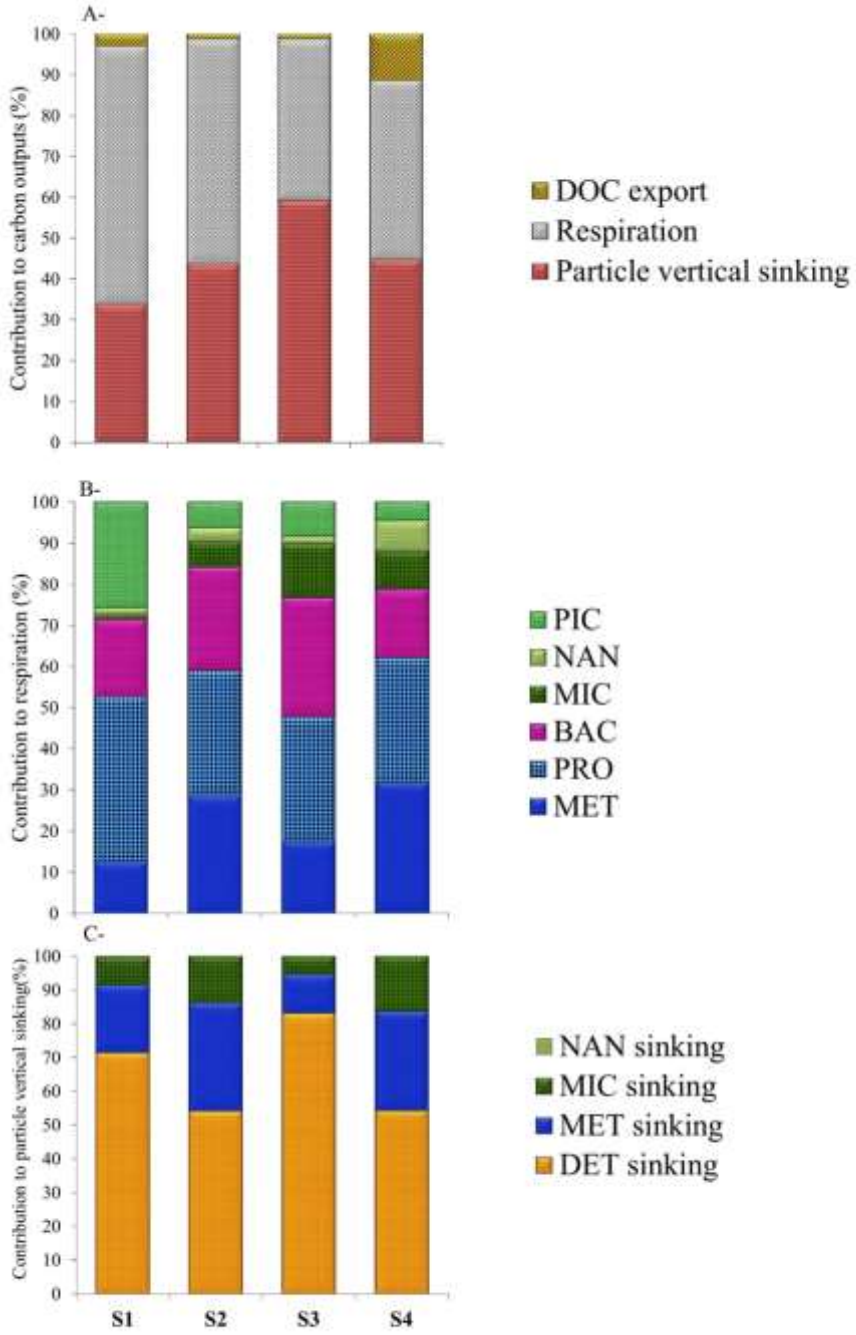

Figure IV. 3. Composition of total carbon outputs (A), contributions of living compartments to respiration (B) and contributions of living and non-living compartments to carbon sinking (C) in four stations in the Gulf of Gabès. PIC, picophytoplankton; NAN, nanophytoplankton; MIC, microphytoplankton; BAC, bacterioplankton; PRO, protozooplankton; MET, metazooplankton; DET, detritus; DOC, dissolved organic carbon.

Throughput was defined as the sum of carbon flows coming into or leaving a compartment. The throughput of each compartment varied among stations (Figure IV. 4). In S1, PIC and PRO showed the highest value of carbon throughput (1,401 and 1,256 mg C m^{-2} d^{-1}, respectively), while both living compartments (MIC, BAC, PRO and MET) and non-living compartments (DET and DOC) showed similar carbon throughputs in S2 (896-1,258 mg C m^{-2} d^{-1}). However, MIC had the highest throughput (2,451 mg C m^{-2} d^{-1}) in S3 and S4, largely above its throughputs in S1 and S2. BAC, PRO, DET and DOC had relatively high throughputs in S3 (1,165-1,576 mg C m^{-2} d^{-1}), while MET and PRO had higher values (1,712-1,818 mg C m^{-2} d^{-1}) than DET and DOC (1,337-1,225 mg C m^{-2} d^{-1}) in S4.

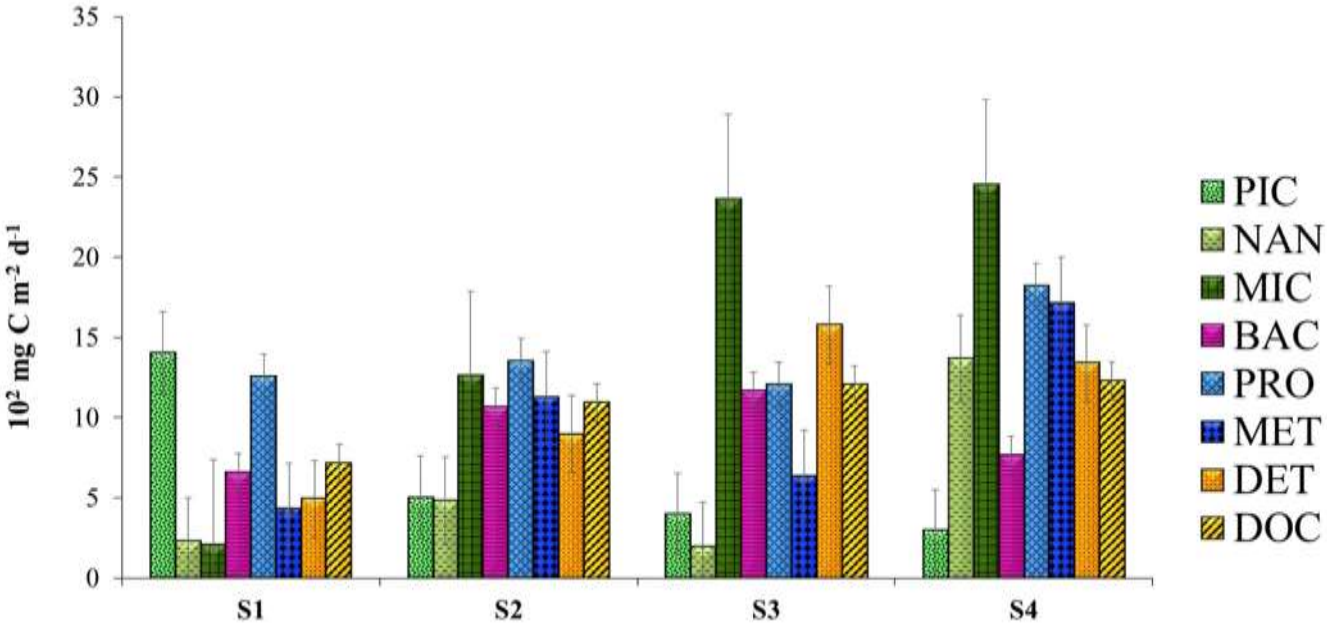

Figure IV. 4. Throughput of each compartment for the four models of four stations in the Gulf of Gabès. PIC, picophytoplankton; NAN, nanophytoplankton; MIC, microphytoplankton; BAC, bacteria; PRO, protozooplankton; MET, metazooplankton; DET, detritus; DOC, dissolved organic carbon.

Error bars, 95% confidence intervals calculated from the probability of distribution of each flow and for 300,000 solutions *per* flow.

3.2. Protozooplankton and metazooplankton diets

The diets of PRO and MET were expressed as the contribution of each food source to the carbon consumed by grazers. The diets of both zooplankton compartments varied among stations (Figure IV. 5). PRO mainly fed on PIC (62%) followed by BAC (26%) in S1. In S2 and S3, the diet of PRO was roughly divided between BAC (37-47%) and phytoplankton

(mainly MIC: 33-26% and PIC: 23-18%). Conversely, phytoplankton was the main food source of PRO in S4; MIC alone formed 54% of its diet (Figure IV. 5A).

In S1, MET was mainly carnivorous, since PRO formed 74% of its diet, while phytoplankton only provided 17%. In S2, PRO and DET were the main food source of MET, forming 43% and 30% of its consumed carbon, respectively. In S3, the diet of MET mainly relied on PRO (64%), and MIC contributed 33%. In S4, the contribution of phytoplankton (mainly MIC) to MET diet increased to 44%. PRO formed 40% of MET diet, while DET only represented 16% in this station (Figure IV. 5 B).

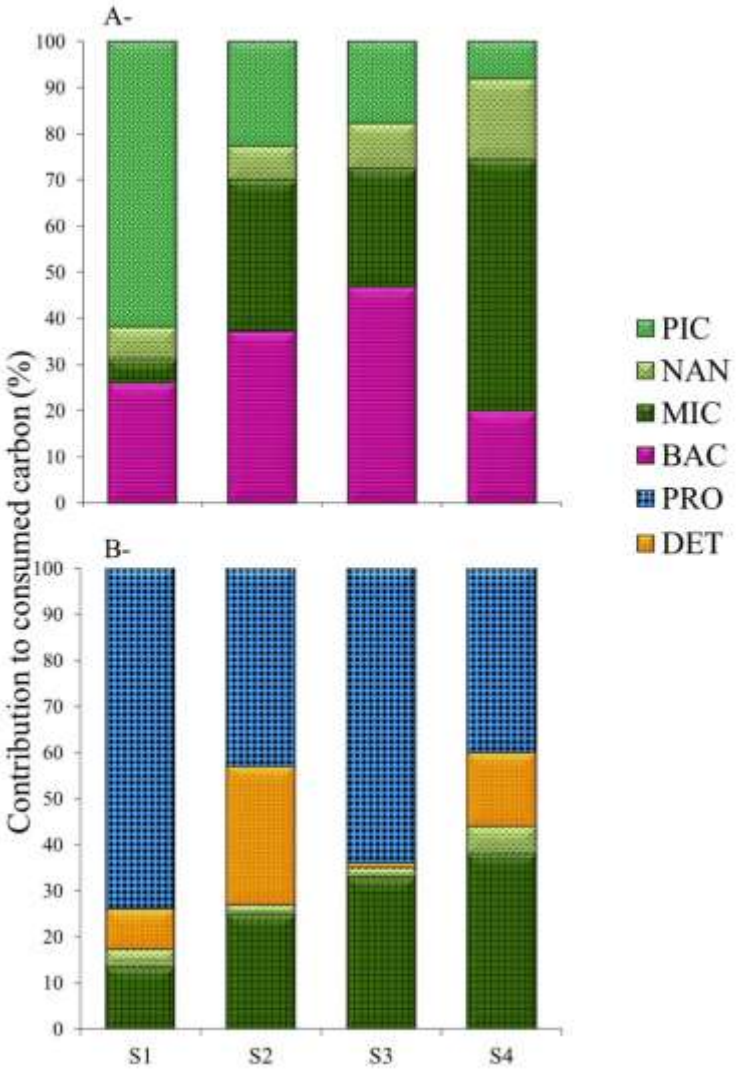

Figure IV. 5. Diets of protozooplankton (A) and metazooplankton (B) in four stations in the Gulf of Gabès. PIC, picophytoplankton; NAN, nanophytoplankton; MIC, microphytoplankton; BAC, bacterioplankton; PRO, protozooplankton; DET, detritus

3.3. Food web typology ratios

The stations presented distinct carbon circulations through the food webs. The typology ratios varied significantly among stations according to Cliff's δ test (Table IV. 3, Figure IV. 6). Ratio R4 significantly differed among stations, with higher values in S4 (0.55) and S1 (0.48) than in S2 and S3 (0.43 and 0.42, respectively) (Figure IV. 6 A). R6 followed an opposite trend, with lower values in S1 and S4 (0.39 and 0.38, respectively) than in S2 and S3 (0.41 and 0.44, respectively) (Figure IV. 6 B). R7 and R8 were very high in S1 (0.73 and 0.92, respectively) and decreased in S2 (0.21 and 0.74) and S3 (0.11 and 0.74) to reach their lowest values in S4 (0.06 and 0.66) (Figure IV. 6 C, D).

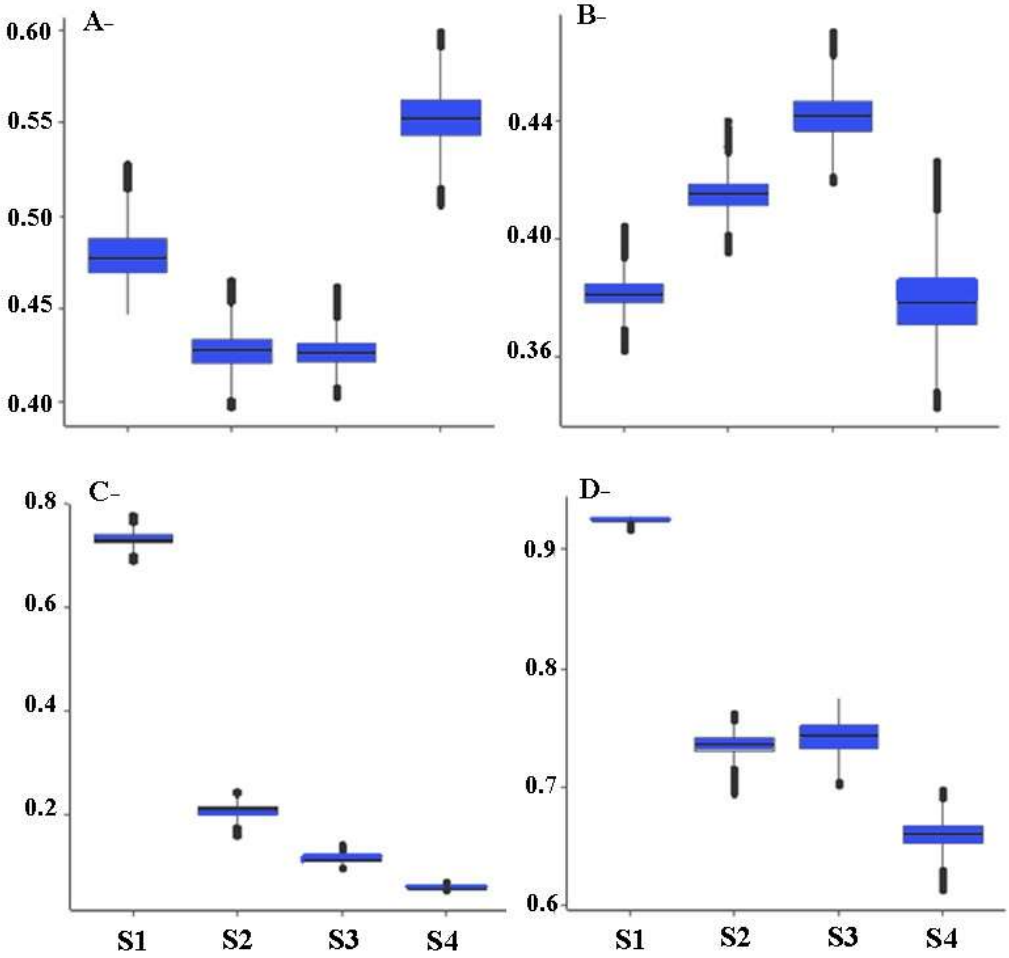

Figure IV. 6. Spatial variation of the food web typology ratios.
R4 = Pnetpht/D2 (A), R6 = (PnetDET + PnetDOC)/D2 (B), R7 = PnetPIC/Pnetpht (C) and R8 = pht-PRO/(pht-PRO + pht-MET) (D)
Pnet, net production; pht, total phytoplankton; D2, Pnetpht + PnetBAC + PnetDET + PnetDOC; pht-PRO, consumption of pht by PRO; pht-MET, consumption of pht by MET.

3.4. Ecological network analysis (ENA) indices

Ecological network analysis (ENA) indices define emerging properties of the food web. They clearly distinguished the functioning of each station; all indices varied significantly and showed large differences among stations according to Cliff's δ test (Table IV. 3, Figure IV. 7). The total system flux (TST) was higher in S4 (10,966 mg C m^{-2} d^{-1}) than in S2, S3 (7,770- 8,740 mg C m^{-2} d^{-1}) and S1 (5,386 mg C m^{-2} d^{-1}) (Figure IV. 7 A). Conversely, the lowest relative ascendancy (A/C) was found for the food webs of S4 (32 %) in comparison with the other stations (36- 46 %) (Figure IV. 7 B). Average mutual information (AMI) followed a similar trend to that of A/C, with higher values in S1, S2 and S3 (1.72-1.86 bits) than in S4 (1.60 bits) (Figure IV. 7 C). The average path length (APL) and Finn cycling index (FCI) showed similar spatial variations, with the highest values in S2 (3.46 and 16%, respectively) and the lowest ones in S4 (2.67 and 5%, respectively) (Figure IV. 7 D, E). Finally, the D/H ratios in S2 and S3 (1.22-1.36) significantly exceeded those in S1 (0.70) and S4 (0.47) (Figure IV. 7 F)

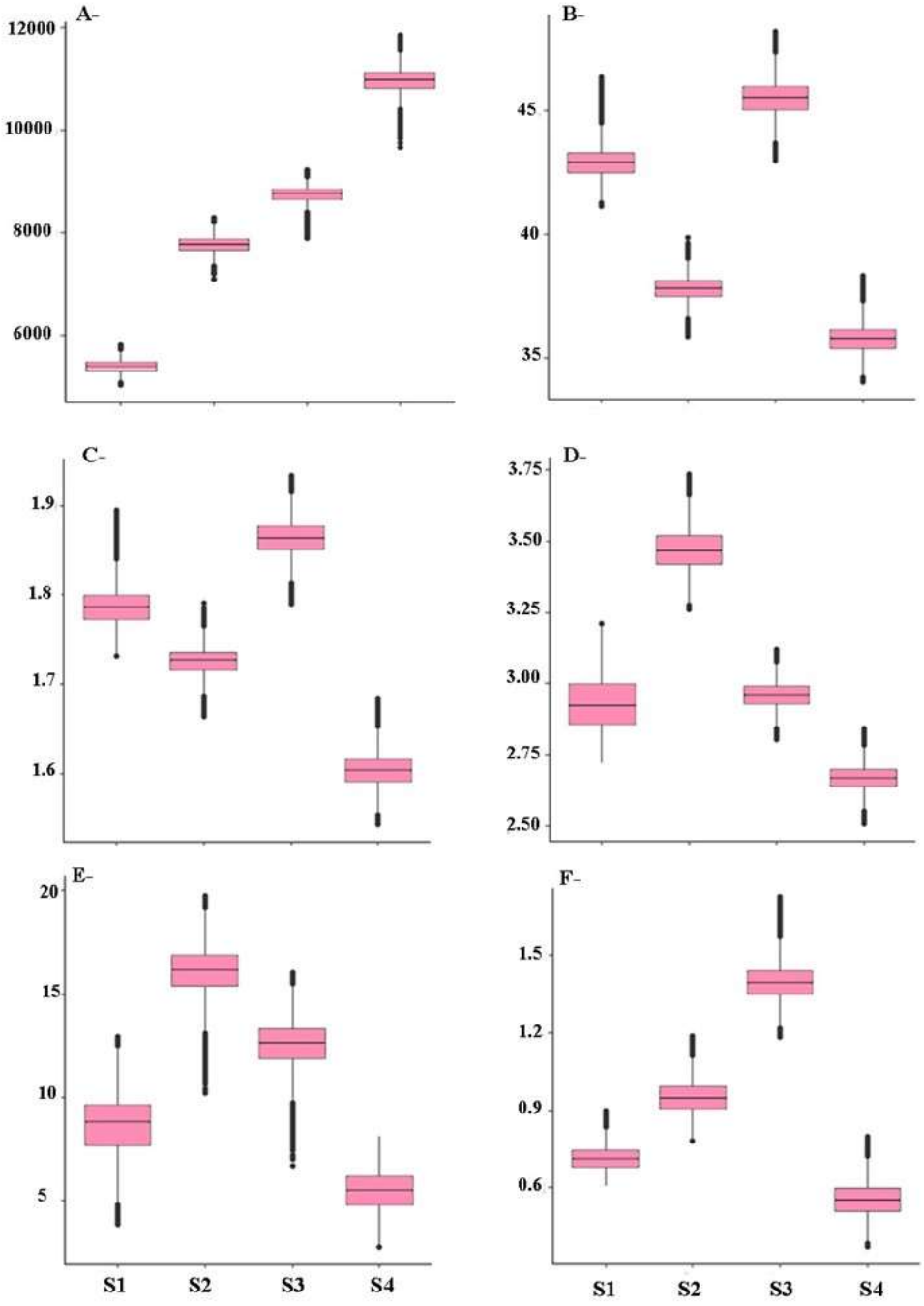

Figure IV. 7. Spatial variation of ENA indices calculated for the planktonic food webs in four stations of the Gulf of Gabès. Total system throughput (TST; mg C m−2 d−1) (A), relative ascendancy (A/C; %) (B), average mutual information (AMI; bits) (C), average path length (APL) (D), cycling index (FCI; %) (E), and detritivory to herbivory (D/H) (F).

Table IV. 3. Results of Cliffs'δ test applied to ecological network indices and typology ratios calculated for four stations of the Gulf of Gabès.
The following values were used to define the size of the effects: |δ| >= 0.43, large; ***, large.

	S1/S2	S1/S3	S1/S4	S2/S3	S2/S4	S3/S4
TST	-1 (***)	-1 (***)	-1 (***)	-1 (***)	-1 (***)	-1 (***)
A/C	1 (***)	-1 (***)	1 (***)	-1 (***)	1 (***)	1 (***)
AMI	1 (***)	-1 (***)	1 (***)	-1 (***)	1 (***)	1 (***)
APL	-0.93 (***)	0.93 (***)	1 (***)	1 (***)	1 (***)	1 (***)
FCI	-1 (***)	-1 (***)	0.73 (***)	0.99 (***)	1 (***)	1 (***)
D/H	-1 (***)	-1 (***)	1 (***)	-0.93 (***)	1 (***)	1 (***)
R4	1 (***)	1 (***)	-1 (***)	0.67 (***)	-1 (***)	-1 (***)
R6	-1 (***)	-1 (***)	0.66 (***)	-1 (***)	1 (***)	1 (***)
R7	1 (***)	1 (***)	1 (***)	1 (***)	1 (***)	1 (***)
R8	1 (***)	1 (***)	1 (***)	-0.89 (***)	1 (***)	1 (***)

3.5. Relationships between ENA indices, typology ratios, input and output flows and environmental variables

Multiple factor analysis (MFA) was applied to the four stations on ENA indices, carbon flux ratios, inorganic and organic nutrients, size-fractioned GPP, bacterial production and particle sinking (Figure IV. 8). The first two axes of the MFA explained 47.84% and 35.98% of the total variance, respectively.

On the first axis of the MFA, the TST index (5%), GPP of NAN (6%) and MIC (6%), sinking of MIC (7%) and MET (7%) and nutrients (N_{inorg} 3%, P_{org} and P_{inorg} 3-4%, Si_{inorg} 4%) were projected onto its positive pole. Its negative pole was determined by the A/C index (2%), ratios R7 (6%) and R8 (8%), GPP of PIC (6%), sinking of NAN (6%) and N_{org} (4%) The positive pole of the second axis was related to several ENA indices (D/H 6%, FCI 4%, APL 2%, AMI 2%, and A/C 2%), R6 (10%) and bacterial production (23%), while its negative pole was related to R4 (7%) (Figure IV. 8 A).

Stations S1 and S4 were discriminated on the first axis. S1 projected on the negative pole of the axis was characterized by high values of PIC GPP and ratios R7 and R8, but hosted low concentrations of inorganic N, P and Si and low TST, indicating a poorly rich nutrient system dominated by small producers. S4 was at the opposite of S1. It was characterized by high values of GPP for MIC and NAN, inorganic nutrient concentrations, TST and sinking of MIC and MET. Stations S2 and S3 occupied the center of axis 1, indicating that the factors represented on axis 1 were not discriminating for these stations. However, S2 and S3 were projected on the positive pole of axis 2 and were characterized by high values of BAC production, D/H and FCI indices and R6, but a low R4 (Figure IV. 8 B).

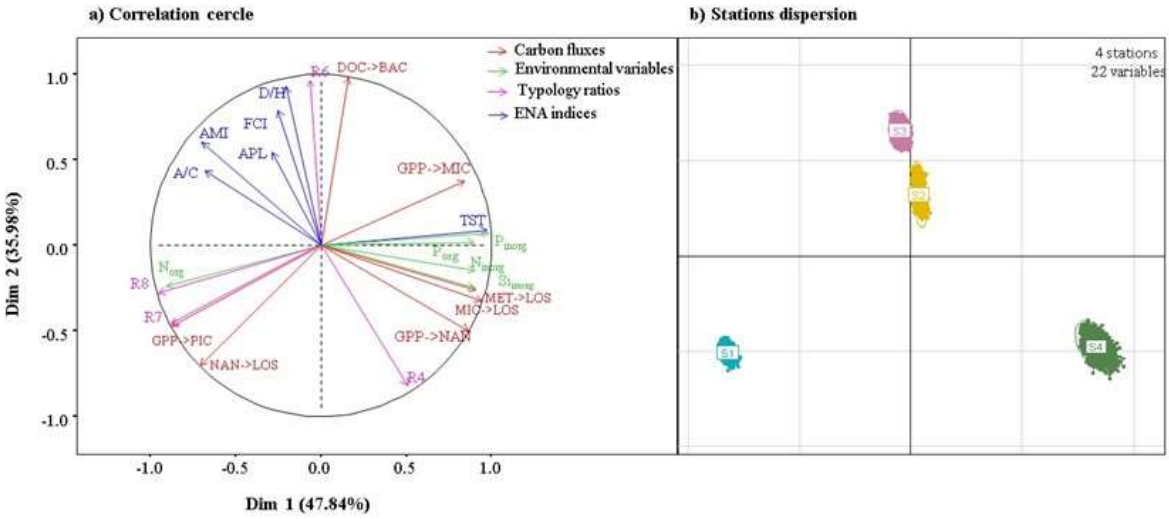

Figure IV. 8. Multiple factor analysis (MFA) ordination diagram showing the relationships between ecological indicators (food web typology ratios and ENA indices), environmental variables (inorganic and organic nutrients: N_{inorg}, P_{inorg}, Si_{inorg}, N_{org}, P_{org}) and carbon flows [GPP of PIC (GPP->PIC), NAN (GPP->NAN) and MIC (GPP->MIC), bacterial production (DOC->BAC) and sinking of NAN (NAN->LOS), MIC (MIC->LOS) and MET (MET->LOS)].

4. Discussion

4.1. Spatial change in planktonic food web characteristics

The complex hydrodynamic circulation in the Gulf of Gabès coupled with anthropogenic nutrient inputs created a north-south and coast-offshore ascending gradient of nutrients that induced a spatial change in the size community structure of phytoplankton (Chkili et al., 2023).

As expected, the present study also showed a clear spatial variation of primary production, in quantity (Figure IV. 2 A) and composition (Figure IV. 2 B). Nutrients are always considered as the main factor controlling the size structure of primary producers, which in turn influence the food web organization (Legendre and Rassoulzadegan, 1995; Sakka Hlaili et al., 2008; Filiz et al., 2020; Hardikar et al., 2021). It is well admitted that identifying the dominant phytoplankton size fractions could play a crucial role in predicting food web types (Richardson and Jackson, 2007). For example, (Bellinger et al., 2006) and (Hardikar et al., 2021) highlighted that the size fraction of producers, i.e., small *versus* large phytoplankton, could be used as a robust indicator of the trophic level of the system and the carbon transfer pathway. In our study, nutrients appeared as significant environmental discriminant factors of the stations, in which small and large phytoplankton played different roles in biogenic carbon production (MFA, Figure IV. 8). PIC production was high in S1 (78% of total GPP; Figure IV. 2 B), and showed a negative relationship with most nutrient concentrations (Figure IV. 8 A). In S2 and S3, the contribution of MIC (55-78% of GPP) increased at the expense of PIC (~20%), while MIC and NAN productions were dominant in S4 (60 and 34%, respectively) (Figure IV. 2 B). MIC and NAN productions were clearly associated to the high level of nutrients (Figure IV. 8 A).

Changes in the phytoplankton size structure could influence selective zooplankton grazing. In S1, the diet of PRO mainly relied on the dominant phytoplankton size fractions PIC (69%) and BAC (26%). In this station, the microbivory of PRO (PIC-PRO and BAC-PRO: 1,099.2 mg C m^{-2} d^{-1}) played a significant role in carbon transfer, whereas the herbivory of PRO (NAN-PRO and MIC-PRO: 153.11 mg C m^{-2} d^{-1}) and MET (NAN-MET and MIC-MET: 74.47 mg C m^{-2} d^{-1}) were low (Table IV. 2). In S2 and S3, the feed of PRO was supported almost equally by small prey (PIC and BAC: 60-65%) and large cells (NAN and MIC: 35-40%) (Figure IV. 5 A). Furthermore, large phytoplankton contributed 27-35% of the diet of MET (Figure IV. 5 B). Therefore, the microbivory of PRO (S2: 808.1 mg C m^{-2} d^{-1}, S3: 777.8 mg C m^{-2} d^{-1}) and the herbivory of PRO and MET (S2: 847.03 mg C m^{-2} d^{-1}, S3: 650.12 mg C m^{-2} d^{-1}) were both main processes in channeling carbon in these stations. Conversely, biogenic carbon mainly entered the food web of S4 *via* the herbivory of zooplankton (2,332.42mg C m^{-2} d^{-1}). In this station, MIC and NAN formed a significant fraction of the diets of PRO (72%) and MET (44%) (Figure IV. 5). By looking at the size structure of phytoplankton, production, and the microbivory and herbivory of zooplankton, we can suggest that various food webs with different efficiencies in carbon export exist in the four stations. Going further with digital tools, we can identify the types of food web and characterize the emerging properties of each type.

4.2. Application of typology ratios and ENA indices to a description of the structure and function of planktonic trophic pathways

Typology ratios based on the size structure of the planktonic community as well as the interactions between the different compartments are useful to distinguish planktonic trophic pathway (PTP) types in marine systems (Sakka Hlaili et al., 2014).

In our study, all typology ratios showed significant spatial change (Table IV. 3, Figure IV. 6), suggesting variation in the structure of PTP among stations (Figure IV. 9). The spatial change in R7 (Figure IV. 6 C) evidenced a modification of the food web type among stations. In accordance with the range of R7 values given by (Sakka Hlaili et al., 2014) and describing the importance of PIC in total carbon production, the microbial food web dominated in S1 (R7 = 0.7 > 0.6), while multivorous pathways prevailed in S2 and S3 (0.1 < R7 = 0.2-0.12< 0.6), but the food web in S4 acted as a herbivorous type (R7 = 0.06 < 0.1) (Figure IV. 9). This is in agreement with our observations of a high microbivory in S1, a shared role between microbivory and herbivory in carbon transfer in S2 and S3, and a strong herbivory in S4. In addition, PIC formed the most active compartment in S1, followed by PRO, while MIC was the most active compartment in the other stations, followed by PRO and MET (Figure IV. 4). This suggests an important role of these communities as producers (PIC and MIC) and grazers (PRO and MET). Furthermore, R8, which distinguished the main grazers in carbon channeling (i.e., PRO *versus* MET) corroborated R7. The high R8 in S1 (~1) indeed denoted that the main phytoplankton grazers in the microbial food web were PRO, while the lower values (0.66-0.74) found in the other stations (Figure IV. 6 D) indicated that PRO and MET altogether played an important role in carbon transfer when the dominant food web was herbivorous or multivorous. In addition, the relative importance of phytoplankton or non-living matter (DOC and DET) relatively to carbon production was specified by two other typology ratios – R4 and R6. Higher R4 than R6 values suggest that the system mainly relies on phytoplankton production, while the opposite means that non-living matter is important in circulating carbon production (Sakka Hlaili et al., 2014). These two ratios evolved differently among stations (Table IV. 3, Figure IV. 6 A, B), showing that phytoplankton and/or non-living matter played different roles in carbon production across the three observed PTP. The higher R4 compared to R6 in S1 indicated that the microbial food web was more based on phytoplankton (mainly PIC) than on non-living matter. This coincides with a higher throughput of phytoplankton (1,838.5 mg C m^{-2} d^{-1}) than DOC and DET (1,204.05 mg C m^{-2} d^{-1}) in this station (Figure IV. 4). In the herbivorous pathway of S4, phytoplankton (mainly MIC) also played a more important role

(R4>R6) and had a higher throughput (4,110.1 mg C m^{-2} d^{-1}) than non-living compartments did (2,561.7 mg C m^{-2} d^{-1}) (Figs. 4, 6 A, B). For the multivorous food web observed in S2 and S3, these same R4 and R6 values suggested that the systems were based on phytoplankton as well as on non-living matter. In both stations, non-living carbon throughputs (1,988.74-2,779.63 mg C m^{-2} d^{-1}) were close to phytoplankton throughputs (2,240.2-2,954 mg C m^{-2} d^{-1}) (Figure IV. 4). Unfortunately, despite the importance of these ratios, their application is rather limited in the literature. Therefore, it would be interesting to use these criteria more extensively by comparing them with those of other ecosystems.

ENA indices were also used to characterize PTPs, as they are powerful tools for understanding carbon circulation through the whole food web (Ulanowicz, 1986; Ulanowicz et al., 2009). In fact, both ecological indicators (typology ratios and ENA indices) could be discriminant in the description of the food web structure (Figure IV. 8). However, coupling ENA indices and typology ratios required selecting complementary indices (Figure IV. 9).

ENA indices are potentially powerful tools when assessing ecosystem health (Niquil et al., 2014a) and are sensitive to different impacts on marine ecosystems (Baird et al., 2009; Tecchio et al., 2016; Pezy et al., 2017). However, they can only partially capture the anthropogenic or natural stress levels of different types of food webs in aquatic ecosystems (Tecchio et al., 2016). Therefore, food web types can also be used as an indicator of the stress level in the ecosystem and its carbon transfer capacity (Legendre and Rassoulzadegan, 1995a; Siokou-Frangou et al., 2010). For example, when a microbial food web exists, particularly in oligotrophic environments, primary production is maintained through recycled nutrients and is mostly lost through remineralization (Goldman et al., 1987; Legendre and Rassoulzadegan, 1995a; Meddeb et al., 2018). This may demonstrate stress of the system, which has become inefficient in carbon transfer (López-Abbate et al., 2019). In contrast, when herbivorous or multivorous food webs dominate, primary production is based on nutrient inputs and significantly transferred to large consumers or efficiently exported to deep waters (Michel et al., 2002; Turner, 2002). Herbivorous food webs are known for their strong capacity to channel carbon to higher pelagic and benthic consumers: low carbon is recycled (Legendre and Rassoulzadegan, 1995a; Meddeb et al., 2019), indicating a stable ecosystem (Meddeb et al., 2019). Based on these statements, our study highlights the links between ecosystem typology and properties derived from ENA indices that characterize the system's activity, stability, maturity and organization.

The TST index is a measure of ecosystem activity and is considered as a basic index of food web models used to discriminate food webs (Finn, 1976; Ulanowicz, 1986; Borrett and Scharler, 2019). Several works have showed that high TST values correspond to productive ecosystems, such as coastal areas influenced by nutrient-rich upwelling or riverine inputs and productive continental shelves (Coll et al., 2007; Grami et al., 2008b; Corrales et al., 2015; Meddeb et al., 2018). TST varied significantly among the three PTPs found in our study (Table IV. 3, Figure IV. 7 A). This can obviously be linked to the variations in GPP and in the eutrophic degree of the stations. Like GPP, TST followed an increasing gradient from the least nutrient-rich station dominated by the microbial food web (S1) to the highly eutrophic station governed by the herbivorous pathway (S4). Our results corroborate other studies showing that the herbivorous food web is more active than the microbial and multivorous food webs (Meddeb et al., 2019; Decembrini et al., 2021b).

Relative ascendency (A/C) is an indicator of the degree of ecosystem organization (Ulanowicz, 1997; Patrício et al., 2004) that negatively correlates to the degree of maturity (Christensen et al., 2005). The highest A/C value was recorded in S3 (Figure IV. 7 B), indicating that the multivorous pathway in this station was more organized than the food webs of the other stations. More particularly, A/C was lowest in contrast to TST in S4 and its herbivorous pathway, indicating a more active but less organized system. The AMI index is a measure of flow specializations within a system (Ulanowicz, 1986). It yields lower values at the early stages of ecosystem development (when the system is immature) and higher values under pristine conditions (least disturbed ecological functioning). In our study, AMI followed the same trend as A/C, i.e., highest in S3 and lowest in S4 (Figure IV. 7 C). This means that higher fluxes of BAC and DET, in parallel to MIC, may allow a greater fraction of the total system flux to pass through specialized pathways in the multivorous food web of S3. Other ENA indices that reflect stability, maturity and organization varied significantly according to the different PTPs (Table IV. 3). The FCI index is an important indicator of changes in system functioning (Fath et al., 2019a; Safi et al., 2019) and gives information about carbon cycling in the ecosystem (Finn, 1976; Saint-Béat et al., 2018). This index can indicate the degree of maturity, resilience and stability of the ecosystem (Vasconcellos et al., 1997; Duan et al., 2009; Niquil et al., 2012). Recycling can indeed reduce the impact of stress on the ecosystem by acting as a buffer. Therefore, increased recycling can give better resilience and stability to the system (Saint-Béat et al., 2015). In addition, the APL index – which measures the retention capacity of the system (Fath et al., 2019; Kay et al., 1989) – is expected to be high in systems with high

degrees of flow diversity and cycling (Christensen, 1995; Thomas and Christian, 2001). Both indexes showed similar spatial evolution, i.e., lower values in S4 than in the other stations (Figure IV. 7 D, E), indicating that the herbivorous food web observed in S4 was less stable than the multivorous and microbial pathways observed in the others stations. This is in agreement with Legendre and Rassoulzadegan, (1995) and Meddeb et al., (2019), who reported lower stability of the herbivorous food web in comparison to the microbial and multivorous ones. The highest values of FCI and APL coincided with the multivorous food web in S2 – the station most exposed to the source of disturbance in the Gulf – TCG (Figure IV A.1). Thus, the increase in recycling and flow diversity seemed to endow the system with a certain resistance to the strong disturbance that the PTP underwent in S2. According to the MFA results, the APL seemed to be less structuring in the system since its contribution was not significant on the first two axes. In this case, considering the first two axes of the MFA, FCI seemed to be more efficient in the stability analysis.

The detritivory/herbivory ratio (D/H), which was initially adapted from (Odum, 1969), was applied to show the importance of detritivory compared to herbivory. Several authors have used this index to provide information on carbon transfer to consumers *via* detritus and/or autotrophs (Kay et al., 1989; Ulanowicz, 1992; Chrystal and Scharler, 2014; Niquil et al., 2014b; Fath et al., 2019b; Safi et al., 2019). High D/H values reflect an ecosystem where detritus plays an important role in carbon recycling, while low D/H values indicate an ecosystem where primary producers play a vital role as food for the second level (Chrystal and Scharler, 2014; Luong et al., 2014). During our study, the ratio indeed showed significant spatial variation (Table IV. 3, Figure IV. 7 F), indicating a shift from systems based on the primary production pathway in S1 and S4 (D/H: 0.7 and 0.5, respectively) to systems based on phytoplankton and the detrital energy pathway, which played an important role in S2 and S3 (D/H ~ 1). This is consistent with the fact that R6 and R4 were similar in S2 and S3 (Figure IV. 6 A, B). Therefore, both phytoplankton and non-living carbon production played an important role for the multivorous food web observed in these stations. The lowest D/H value coincided with the herbivorous food web acting in the most eutrophic station S4. This is in agreement with the results of (Luong et al., 2014), who reported that nutrient-rich environments favor herbivory over detritivory.

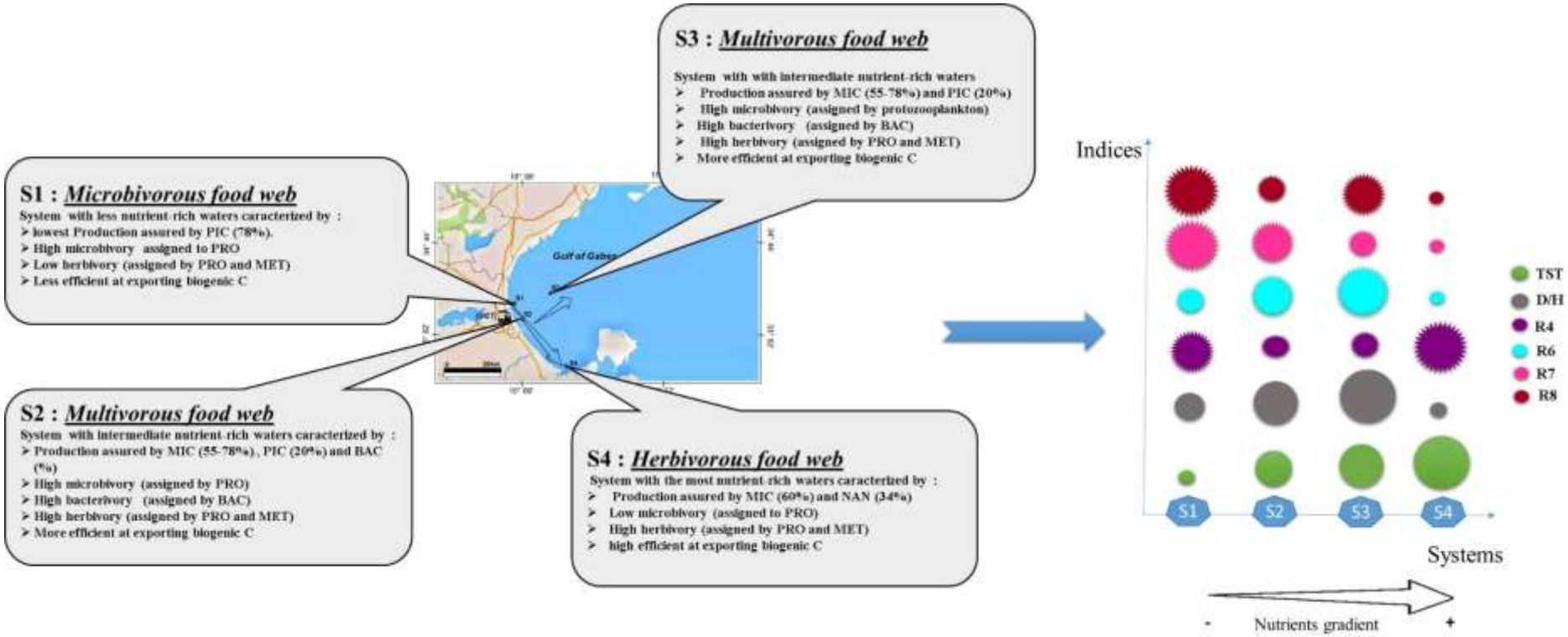

Figure IV9. Characteristics of the four planktonic food webs and most discrete ecological indicators of the ecosystem.

4.3. Importance of coupling ENA and typology ratios for ecosystem health monitoring and management perspectives

A representation of ecosystem dynamics based on the coupling of typology with ENA indicators may be considered as an effective tool for environmental managers. ENAs are sensitive tools for characterizing the ecosystem health status that have been repeatedly used to assess the impact of natural and anthropogenic pressures on coastal marine ecosystems (Niquil et al., 2014b; Pezy et al., 2017; Tecchio et al., 2016; de la Vega et al., 2018a, 2018b; Safi et al., 2019; Fath et al., 2019b).

ENA indices were selected within the framework of regional sea conventions, such as the DCSMM, OSPAR and the Barcelona Convention (Safi et al., 2017, 2019; McQuatters-Gollop et al., 2022). These conventions form the main tools anchored in the community management of marine ecosystems aiming at defining and implementing a strategy to maintain their good ecological status (Rombouts et al., 2013; Safi et al., 2017, 2019; Arroyo et al., 2019). The OSPAR 2017 intermediate assessment (OSPAR IA 2017) provides an update of the OSPAR 2010 assessment and presents some new biodiversity indicators and assessment methodologies to identify changes in ecosystem biodiversity (McQuatters-Gollop et al., 2022). Despite the importance of these conventions in the selection of plankton and food web indicators, their interventions in the typology of planktonic food webs are generally lacking. Therefore, we applied an approach that combined ENA and typology ratios to better understand the functioning of different planktonic food web structures. As a complement to ENA, we can propose researchers and managers new criteria (based on the typology ratios of (Sakka Hlaili et al., 2014)) to be taken into account, that they could use to quantitatively identify the different planktonic food web structures. The advantage of these ratios is that if we consider some of them, we can directly access the specific flows without having to calculate all the flows of the whole network, as we have to for ENA. ENA results lead to a better understanding of the functioning of different planktonic food web structures under anthropogenic pressure. Among the indicators used in this study, some are more discriminating and could be proposed as food web indicators. According to the MFA, it appears that TST, D/H, R4, R6, R7 and R8 were the most structuring in the studied systems (Figure IV. 8). Thus, from a planktonic perspective, the two indices TST and D/H ratio recommended by several authors (Ulanowicz, 2004; Bodini et al., 2012; Fath et al., 2019; Safi et al., 2019) could be coupled with R4, R6, R7 and R8 of (Sakka Hlaili et al., 2014). For example, R4 and R6 indicate whether the system is based on non-living matter (DET, DOC) (low R4 and high R6) or instead on phytoplankton (low R4 and high R6)

(Sakka Hlaili et al., 2014). The D/H index can be used in addition to these typology ratios to determine which of these two sources dominates (Fath et al., 2019). According to the MFA results (Figure IV. 8 A), the anti-correlation between D/H and R6 on the positive pole and R4 on the negative pole of axis 2 indeed reflects different ecosystems (Figure IV. 8 B). The high D/H values can be sustained by a higher R6 than R4, indicating that detritus play an important role in ecosystem recycling, e.g., carbon recycling. Conversely, low D/H values can be maintained by a higher R4 than R6, indicating an ecosystem where primary producers (phytoplankton and/or algae) play a substantial role as feed for consumers (PRO and MET) (Luong et al., 2014).

R7, R8 and TST may be complementary and interact in the description of the primary production of the planktonic food web type and its fate (Figure IV. 8). R7 provides information on the relative contribution of large and small phytoplankton to total primary production (Sakka Hlaili et al., 2014). Thus, it provides indirect information on the amount of primary production in the system, which may have an effect on the ecosystem activity measured by the TST (Finn, 1976; Ulanowicz, 1986; Borrett and Scharler, 2019). In our case, the lowest ecosystem activity, as indicated by the TST, was observed when PIC was the dominant producer (high R7) and primary production was low, indicating a microbial food web. This was supported by the negative correlation of PIC GPP and R7 with TST in the MFA (Figure IV. 8 A). Conversely, the herbivorous food web showed the highest activity (high TST) related to the highest primary production dominated by MIC (low R7). This was supported by the positive correlation of TST and MIC GPP at the positive pole of axis 1 of the MFA (Figure IV. 8 A). Moreover, we can refer to R8 to identify the main grazers of production. Grazers switch from MET (low R8) when herbivorous or multivorous food webs are dominant to PRO (high R8) when microbial pathways prevail (Sakka Hlaili et al., 2014). In general, although ENA indices faithfully characterize carbon circulation within planktonic food webs, they should be complemented with typological indices to make their interpretation easier and describe the main trophic pathways.

Despite efforts in the management of marine ecosystems, there are still gaps in the relationships between planktonic food web levels and benthis/pelagic organisms. The planktonic food web typology approach has only been partially addressed by managers. At the base of the pelagic food web, plankton and the existing fluxes of matter among planktonic compartments largely condition the functioning of the ecosystem because they are a source of primary production, are exported to the benthos or related ecosystems, and condition trophic

efficiency towards the upper links (Legendre and Rassoulzadegan, 1995; Dupuy et al., 1999; Sintes et al., 2004; Leguerrier, 2005; Marquis et al., 2007). As a result, indices of the typology and functioning of the planktonic food web can be linked to the benthos and the higher trophic links from the export estimate. In addition, they can also give an idea of the emerging properties of the whole ecosystem (activity, export, recycling...). Therefore, it is important that EU member states work together to develop a coupling of planktonic food web typology indices with ENA indices.

5. Conclusion

The present study provides an analysis of the food web structure in the permanently disturbed Gulf of Gabès. An approach combining ecological network analysis (ENA) selected on the basis of previous literature and typology reports was tested. The study site was characterized by nutrient inputs (mainly from TCG), whose association with hydrodynamics has created a gradient of nutrient richness. The size structure of primary production, trophic interactions, the food web structure and function differed among the stations. The main results showed that:

- The microbial food web dominated in the least nutrient-rich system S1. It was identified by the highest value of R7 and formed a phytoplankton-based food web (R4>R6) primarily assigned to PRO (higher R8). PRO was inefficient in channeling biogenic carbon. This food web showed the lowest total system throughput (TST), and a low detritivory to herbivory (D/H) ratio, indicating a less active system relying on primary production (phytoplankton).
- In contrast, the herbivorous food web indicated by the lowest value of R7 was identified in the most eutrophic system S4, where large phytoplankton dominated primary production (R4>R6) and was assigned to PRO and MET (lowest R8). These were efficiently exported to higher consumers. Thus, all ecological indicators were lowest in this food web, except TST that was highest. This indicates that the herbivorous food web of the system was more active based on primary production (low D/H) but less organized (low A/C) and less stable (low FCI).
- The multivorous food web, as indicated by R7, dominated in the moderately nutrient-rich systems S2 and S3, and carbon production was based on both phytoplankton and non-living carbon (R4~R6) assigned to PRO and MET (low R8). These can be

efficient in carbon transfer. This food web was characterized by the highest relative ascendency and cycling values (A/C and FCI), and was more organized, specialized and stable. It also showed a higher total system throughput and the highest D/H, reflecting a more active system where detritus play an important role in carbon recycling.

From an ecosystem management perspective, we propose a comprehensive assessment of ecosystem health based on appropriate indicators of food web typology and ENA indices, to be used by managers to assess the structure, functioning, and emerging properties of ecosystems under anthropogenic pressure. We suggest combining typology ratios to identify food web types with ENA indices to distinguish different food web functions across nutrient gradients. This combination can provide an effective tool for managing and assessing ecosystem health, and for investigating the occurrence of anthropogenic pressures. We chose indicators based on nutrient gradient pressure, but it may be interesting to test these indicators under other pressures in order to know if the same couples of indicators are still relevant or if other indices can be applied.

Références (voir références bibliographiques)

Annexes

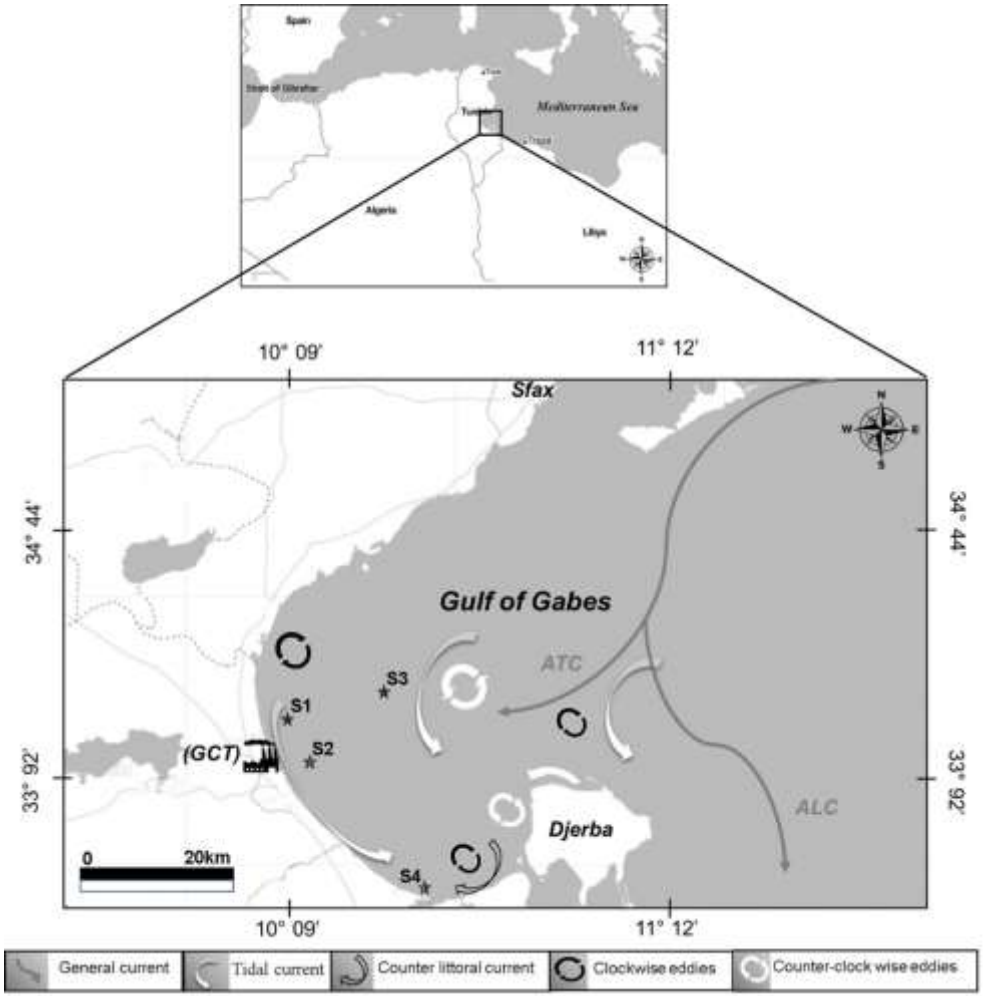

Fig A.1. Location of the sampling stations and hydrodynamic circulation in the Gulf of Gabès, southeastern Mediterranean Sea. (From Chkili et al., 2023)

Table A.1. Mass equilibrium defining the linear equations used for the inverse LIM-MCMC analysis. Each flow is composed of the first three-letter code of the original compartment followed by the first three-letter code of the destination compartment. Abbreviations: GPP, gross primary production; RES, respiration; LOS, loss for the considered system.

Mass balance equation for each compartment	Equations common to the four models
Mass balance for picophytoplankton (PIC)	GPP-PIC – (PIC-RES + PIC-DOC + PIC-PRO) = 0
Mass balance for nanophytoplankton (NAN)	GPP-NAN – (NAN-RES + NAN-DOC + NAN-DET + NAN-PRO + NAN-MET + NAN-LOS) = 0
Mass balance for microphytoplankton (MIC)	GPP-MIC – (MIC-RES + MIC-DOC + MIC-DET + MIC-PRO + MIC-MET + MIC-LOS) = 0
Mass balance for protozooplankton (PRO)	(PIC-PRO + NAN-PRO + MIC-PRO + BAC-PRO) – (PRO-RES + PRO-DOC + PRO-DET + PRO-MET) = 0
Mass balance for metazooplankton (MET)	(NAN-MET + MIC-MET + PRO-MET + DET-MET) − (MET-RES + MET-DOC + MET-DET + MET-LOS) = 0
Mass balance for bacterioplankton (BAC)	DOC-BAC – (BAC-RES + BAC-DOC + BAC-PRO) = 0
Mass balance for dissolved organic carbon (DOC)	(PIC-DOC + NAN-DOC + MIC-DOC + PRO-DOC + MET-DOC + BAC-DOC + DET-DOC) - (DOC-BAC + DOC-LOS) = 0
Mass balance for detritus (DET)	(NAN-DET + MIC-DET + PRO-DET + MET-DET) – (DET-DOC + DET-MET + DET-LOS) = 0

Table A.2. Minimum and maximum flows (mg C m^{-2} d^{-1}) estimated in the field and used as inequalities for the networks of four stations located in the Gulf of Gabès.

Process		Bound	Description	Equation	Reference
Respiration	**PIC NAN MIC**	Upper and lower	Autotrophic respiration ranges between 5% and 30% of their GPP	5% GPP < R < 30% GPP	Vézina and Platt (1988)
	BAC	Lower	Bacterial respiration (R') is higher than 20% of the total uptake of DOC (U_{DOC})	20% U_{DOC} < R'	Vézina and Savenkoff (1999)
	PRO MET	Lower	Zooplankton respiration (R'') is at least 20% of their total ingestion (ΣIng) and does not exceed its maximum specific respiration	20% ΣIng < R''	Vézina and Savenkoff (1999)
DOC production	**PIC NAN MIC**	Upper and lower	Phytoplankton DOC exudation (E) ranges between 10% and 55% of net primary production (NPP)	10% NPP < E < 55% NPP	Vézina and Savenkoff (1999)
	PRO MET	Upper and lower	Zooplankton excretion of DOC (EX) is at least 10% of their total ingestion (ΣIng) and does not exceed its respiration (R'')	10% ΣIng < EX < R"	Vézina and Platt (1988) Vézina and Pace (1994)
	BAC	Upper	Bacterial DOC release (RE) is lower than respiration (R')	RE<R'	Vézina and Pace (1994)
Growth efficiency	**PRO MET**	Upper and lower	Growth efficiency is at least 25% and no more than 50% of total ingestion (ΣIng)	25% ΣIng < ΣIng -(R" + EX +DET) < 50% ΣIng	Vézina and Pahlow (2003)
	BAC	Upper and lower	Growth efficiency of bacterioplankton ranges between 5% and 50% of their total ingestion	0.5 U_{DOC} < U_{DOC} - (r'' + re) < 0.50U_{DOC}	Vézina and Pahlow (2003)
Assimilation efficiency	**PRO MET**	Upper and lower	Assimilation efficiency of zooplankton ranges between 50% and 90% of their total ingestion (ΣIng)	50% ΣIng < Ing -DET < 90% ΣIng	Vézina et al. (2000)
Detritus production	**PRO MET**	Upper and lower	Zooplankton DET production (zoo-DET) is no more than 42% of their combined DET production and respiration (zoo-RES) and is at least 5% of it	5% (zoo-DET + zoo-RES) < zoo-DET < 42% (zoo-DET + zoo-RES)	Steinberg et al. (2000)
Detritus dissolution	**DET**	Upper	The upper bound of DET dissolution (DET-DOC) is 10% of net primary production (NPP)	10% NPP < DET-DOC	Pace et al.(1984)
		lower	DET dissolution (DET-DOC) is at least 10% of DET production	10% DET production <DET-DOC	
Preferential ingestion of MET		Upper	Ingestion of e.g., nanophytoplankton by metazooplankton does not exceed the estimated maximum prey availability	NAN-MET < NANMET.A(t) × Ing-MET MIC-MET < MICMET.A(t) × Ing-MET PRO-MET < PROMET.A(t) × Ing-MET DET-MET < DETMET.A(t) × Ing-MET	Haraldsson et al. (2018)

Table A.3. Constraints used on different planktonic food web networks.

Fluxes	**S1**		**S2**		**S3**		**S4**	
	Min	max	min	max	min	max	min	max
GPP-MIC	169.64	207.34	1042.37	1274.01	1867.90	2282.99	2043.62	2497.76
GPP-NAN	193.58	236.60	406.76	497.15	169.39	207.04	1171.72	1432.10
GPP-PIC	1270.85	1553.26	447.07	546.42	368.56	450.47	284.54	347.78
MIC-PRO	63.96	78.17	417.41	510.17	486.40	594.47	943.90	1153.65
NAN-PRO	82.56	100.91	91.91	112.34	107.50	131.40	285.96	349.51
PIC-PRO	686.66	839.25	264.52	323.31	184.31	225.27	123.75	151.25
MIC-LOS	50.20	61.36	125.06	152.86	203.26	248.43	274.63	335.66
NAN-LOS	1.72	2.11	0.33	0.41	30.29	37.03	0.44	0.53
(MIC+NAN)-MES	68.63	83.88	295.10	360.68	1423.90	1740.33	714.85	873.71
MES-DET	10.56	-	9.01	-	30.29	-	34.29	-
DOC-BAC	543.80	664.64	973.80	1190.20	996.45	1217.89	656.70	802.63
BAC-PRO	323.10	394.90	468.00	572.00	544.00	664.89	340.24	415.85
DET-LOS	437.77	535.05	516.89	631.75	1423.90	1740.33	945.56	1155.68

Chapitre V

Impact du déversement de pétrole sur le phytoplancton, le protozooplancton et la structure du réseau trophique planctonique : évaluation sur le terrain et par modélisation

I. Problématique et objectifs

Les activités pétrolières, notamment la production et le transport du pétrole, entraînent plusieurs marées noires qui ont des effets néfastes sur les écosystèmes marins et peuvent causer des dommages importants, provoquant une perte de biodiversité et une perturbation de l'équilibre environnemental (Kennish, 1996; Gugliermetti et al., 2007; Zhu et al., 2011; Barron, 2012; White et al., 2012).

Pour comprendre les effets de la contamination pétrolière sur les environnements marins, de nombreuses études ont évalué la réponse du phytoplancton à ces accidents, car il constitue la base de la productivité des écosystèmes marins et joue un rôle essentiel dans les cycles des nutriments et du carbone ainsi que dans la pompe biologique (Zehr and Kudela, 2011; Tréguer et al., 2018; Li et al., 2020). Par conséquent, les effets des composés pétroliers toxiques sur ces producteurs primaires peuvent se répercuter en cascade sur les niveaux trophiques supérieurs et avoir un impact sur la structure et la dynamique des réseaux trophiques ainsi que sur les cycles biogéochimiques des écosystèmes marins. En outre, les espèces phytoplanctoniques peuvent réagir rapidement à la contamination marine et aux conditions environnementales, et sont considérées comme un indicateur de la qualité des eaux (Verlecar et al., 2006; Marshall et al., 2006; Feki et al., 2017; Parsons et al., 2021; Song et al., 2022). Néanmoins, les connaissances actuelles sur l'effet du pétrole et de ses composés les plus toxiques (i.e. les hydrocarbures aromatiques polycycliques, HAPs, Jiang et al., 2010) sur le phytoplancton marin sont encore contradictoires. Certaines études ont indiqué que le pétrole avait un effet toxique sur le phytoplancton, provoquant une inhibition de la croissance et l'activité photosynthétique et un dommage au niveau de l'ADN (Aksmann & Tukaj, 2008; Deasi et al., 2010; Bretherton et al., 2019a). De plus, une diminution des diatomées et une augmentation des phytoflagellés ont été observées après des expositions expérimentales au pétrole (Parsons et al., 2015; Fiori et al., 2016; Bretherton et al., 2018). Au contraire, d'autres travaux ont démontré que la présence du pétrole peut stimuler le phytoplancton et que les diatomées ont une grande tolérance aux composés toxiques du pétrole (González et al., 2009; Ozhan et al., 2014; Bretherton et al., 2020). Il apparait que la réponse du phytoplancton au pétrole variait en fonction du type et de la concentration du pétrole, de la composition de la communauté et de la sensibilité des espèces (Huang et al., 2011; Ozhan et al., 2014), qui est liée à la taille des cellules, à la motilité, à la mixotrophie et à la plasticité du métabolisme (Bretherton et al., 2020; Kamalanathan et al., 2021). La réponse du phytoplancton à la contamination par le pétrole et les hydrocarbures peut

également varier si l'on considère les effets à court ou à long terme (Lee et al., 2009; Tang et al., 2019).

La majorité des connaissances sur la réponse du phytoplancton au pétrole viennent des données des expériences d'exposition des cultures mono-spécifiques ou de communautés phytoplanctoniques naturelles (Varela et al., 2006; González et al., 2009; Gemmell et al., 2018; Bretherton et al., 2019, 2020; Putzeys et al., 2022). Cependant, les données de terrain concernant sa réponse dès les premiers stades d'un déversement de pétrole et tout au long de son évolution sont rares car cela nécessite une logistique lourde pour collecte rapidement des échantillons sur le site pollué. Pourtant, les réponses précoces et tardives du phytoplancton à une marée noire sont cruciales pour mieux comprendre comment cet accident peut affecter les communautés marines.

Contrairement au phytoplancton, le protozooplancton a reçu relativement peu d'attention dans les études des marées noires (Almeda et al., 2014b, 2016, 2018). Pourtant, de nombreux auteurs considèrent que la diminution du contrôle « top-down », due à l'effet toxique des hydrocarbures sur les brouteurs sensibles, est un facteur majeur contribuant à l'augmentation de la population et à la diversification du phytoplancton marin à la suite d'une marée noire (Johansson et al., 1980; Hjorth et al., 2007; Gemmell et al., 2018). Récemment, Tang & Buskey (2022) ont conclu aussi que le découplage entre la croissance du phytoplancton et le broutage du protozooplancton à la suite d'une exposition au pétrole brut, peut favoriser la formation d'efflorescences de phytoplancton. Les études ont aussi rapporté des effets contradictoires de la contamination pétrolière sur le protozooplancton. Dans certains cas, l'exposition au pétrole a été suivie d'une stimulation des ciliés tintinnides (Dale, 1987, 1988) et des nanoflagellés bactérivores (Jung et al., 2012), alors que dans d'autres cas, on a observé une diminution des abondances des ciliés (loriqués et non-loriqués), des nanoflagellés hétérotrophes et des dinoflagellés hétérotrophes (Almeda et al., 2014b, 2018 ; Gemmell et al., 2018). Au contraire, la croissance des dinoflagellés mixotrophes peut être non affectée ou stimulée par la présence du pétrole (Almeda et al., 2016, 2018).

Les différents groupes du protozooplancton, ayant des comportements et des préférences alimentaires très variables, sont les principaux brouteurs de la biomasse bactérienne et phytoplanctonique (Poulsen & Reuss, 2002; Calbet & Landry, 2004; Pecqueur et al., 2022; Kosiba & Krztoń, 2022). Ils jouent divers rôles dans les différents réseaux trophiques marins (réseau, microbien, herbivore ou multivore et boule microienne). Par conséquent, tout changement dans l'alimentation et la structure du protozooplancton en réponse à la contamination par les hydrocarbures pétroliers pourrait profondément modifier le devenir du

carbone biogène. Malheureusement, il existe encore des lacunes concernant les effets des marées noires sur les interactions trophiques et les voies de transfert du carbone. Il est donc nécessaire de prendre en compte les réponses du protozooplancton à ces accidents, à l'échelle structurelle et surtout à l'échelle fonctionnelle (i.e. l'activité de broutage), afin de mieux comprendre l'impact écologique de ces événements sur le fonctionnement de l'écosystème.

Les objectifs de ce travail est **(i)** de suivre les réponses *in situ* des communautés naturelles du phytoplancton (biomasse, croissance, structure en taille et diversité) et du protozooplancton (abondance, composition et broutage) au cours d'un déversement de pétrole brute survenu dans les eaux de Bizerte et **(ii)** d'appréhender les impacts de cet accident sur la structure du réseau trophique planctonique, en intégrant les effets du pétrole sur la production du phytoplancton et la consommation du protozooplancton dans des modèles inverses de flux de carbone. Le suivi *in situ* a été réalisé depuis les premiers jours (1^{ier}, 4ème et 8ème jours) jusqu'à quelques semaines (18ème jour) après le rejet du pétrole pour évaluer les réponses à « court terme » et à « long terme », respectivement.

II. Résumé

La prospection sur le terrain a révélé la présence d'une nappe de pétrole du 1^{ier} au 8ème jour avec une contamination des eaux par les HAPs, principalement le chrysène. Au 18ème jour, le pétrole s'est dispersé et les eaux avaient retrouvé leur couleur et leur odeur d'avant accident. Le suivi *in situ*, pendant les différents jours après la marée noire, a montré que le phytoplancton réagissait différemment au fil du temps. À court terme (du 1^{ier} au 8ème jour), la croissance et la biomasse du picophytoplancton ont été stimulées alors que celles du nano- et du microphytoplancton ont diminué probablement due à l'effet direct des HAPs toxiques sur les espèces sensibles et/ou à l'effet indirect de la réduction de la lumière par la nappe de pétrole. À long terme (18ème jour), la dispersion du pétrole et la réduction de son effet négatif semblent favoriser la prolifération du nano- et du microphytoplancton. On a noté aussi une forte accumulation de la biomasse du picophytoplancton qui semble être plutôt liée à une réduction de son broutage. En conséquence, la structure en taille du phytoplancton a évolué tout au long de l'exposition au pétrole, passant d'une prédominance du microphytoplancton après quelques jours à une dominance à long terme du picophytoplancton. La présence du pétrole a aussi affecté la composition du phytoplancton et a réduit les indices de diversité. Les changements les plus marqués ont été surtout observés au 18ème jour, lorsqu'on a observé une prolifération des

diatomées *Chaetoceros* et *Astrionnellopsis glacialis* qui dominaient le nanophytoplancton et le microphytoplancton, respectivement.

La structure de la communauté du protozooplancton a également changé au fil des jours vers une dominance des dinoflagellés mixotrophes (principalement *Heterocapsa*) au détriment d'une diminution des dinoflagellés hétérotrophes (i.e. *Gyrodinium* et *Protoperidinium*). Les ciliés (principalement *Strombidium*) ont montré une diminution à court terme, mais une récupération au 18ème jour, tandis que les nanoflagellés étaient plus vulnérables à la toxicité du pétrole et ont disparu à partir du 8ème jour. L'activité du broutage du protozooplancton a été aussi affectée avec une diminution des taux à court terme pour les trois factions de taille du phytoplancton. A plus long terme, les taux de broutage ont augmenté pour le nano- et le microphytoplancton, mais ont largement chuté pour le picophytoplancton.

Les taux de production des différentes fractions de taille du phytoplancton ainsi que leurs taux de consommation par le protozooplancton ont significativement varié entre les différents jours. L'intégration de ces taux modifiés par la contamination pétrolière dans des modèles linéaires inverses de flux de carbone et le calcul des ratios de typologie ont montré un changement clair dans la structure et le fonctionnement du réseau trophique, de la voie herbivore (au 1^{ier} jour), au réseau multivore (4ème et 8ème jour) jusqu'un réseau microbien (au 18ème jour), ce qui implique différentes efficacités dans l'exportation du carbone tout au long de l'évolution de la marée noire.

Ces résultats apportent des nouvelles données sur les effets de la contamination pétrolière sur les communautés naturelles du phytoplancton et du protozooplancton et renforce l'idée de les utiliser comme bio-indicateurs. L'étude souligne aussi l'intérêt de combiner des suivis *in situ*, des approches expérimentales et la modélisation pour avoir des nouvelles informations sur l'impact de déversement de pétrole sur le fonctionnement trophique des écosystèmes marins.

Field study on natural phytoplankton throughout “Bizerte City” oil spill on the south-western Cost of the Mediterranean Sea

Grami Boutheina [a,b], Oumayma Chkili [a,c,e], Melliti Ben Garali Sondes [a,c], Mejri Kousri Kaouther[a,d], Meddeb Marouan[a], Lassaad Chouba[d], Nathalie Niquil[e], Sakka Hlaili Asma [a,c,*]

(Soumis dans le journal Archive of Environmental Contamination and Toxicologie)

Archives of Environmental Contamination and Toxicology

Field study on natural phytoplankton throughout "Bizerte City" oil spill on the south-western Cost of the Mediterranean Sea

--Manuscript Draft--

Manuscript Number:	
Full Title:	Field study on natural phytoplankton throughout "Bizerte City" oil spill on the south-western Cost of the Mediterranean Sea
Article Type:	Original Research
Keywords:	oil spill phytoplankton diatoms diversity south-western Mediterranean Sea
Corresponding Author:	Asma SAkka Hlaili, Ph.D Universite de Carthage Faculte des Sciences de Bizerte Bizerte, TUNISIA
Corresponding Author Secondary Information:	
Corresponding Author's Institution:	Universite de Carthage Faculte des Sciences de Bizerte
Corresponding Author's Secondary Institution:	
First Author:	Boutheina Grami
First Author Secondary Information:	
Order of Authors:	Boutheina Grami
	Oumayma Chkili
	Sondes Mellit Ben Garali
	Kaouther Mejri Kousri
	Marouan Meddeb
	Lassaad Chouba
	Nathalie Niquil
	Asma SAkka Hlaili, Ph.D
Order of Authors Secondary Information:	
Funding Information:	
Abstract:	Oil spills are recurrent worldwide. Assessing the response of phytoplankton – the basis of marine food webs – at the early stages of an oil spill and throughout its evolution is crucial to improve our understanding of the impact of oil spills on the marine environment. Field data collected 1, 4, 8 and 18 days after the "Bizerte City" oil spill showed that phytoplankton responded differentially over time. In the short term (1-8 days), picophytoplankton biomass and abundance increased, possibly due to reduced grazing. In contrast, nano- and microphytoplankton biomass decreased, probably owing to inhibited growth of sensitive species to polycyclic aromatic hydrocarbons – the most toxic components of oil. After 18 days, the dispersal of oil and its decreasing negative effect were accompanied by outbreaks of all size fractions. Accordingly, the phytoplankton size structure shifted throughout the oil exposure level from a prevalence of microphytoplankton after a few days toward picophytoplankton dominance. Oil pollution influenced the species composition and significantly decreased diversity indexes. In the first days, nanophytoplankton was dominated by cryptophyceae (mainly Hillea fusiformis and H. marina), while microphytoplankton was mostly represented by the pennate diatoms Pseudo-nitzschia and Nitzchia, suggesting

Field study on natural phytoplankton throughout “Bizerte City” oil spill on the south-western Cost of the Mediterranean Sea

Grami Boutheina [a,b], Oumayma Chkili [a,c,e], Melliti Ben Garali Sondes [a,c], Mejri Kousri Kaouther[a,d], Meddeb Marouan[a], Lassaad Chouba[d], Nathalie Niquil[e], Sakka Hlaili Asma [a,c,*]

[a]Université de Carthage, Faculté des Sciences de Bizerte, Laboratoire de Biologie Végétale et Phytoplanctonologie, Bizerte, Tunisie.

[b]Université de Monastir, Institut Supérieur de Biotechnologie de Monastir, Laboratoire de Recherche LR14ES06 "Bioressources : Biologie Intégrative & Valorisation" BIOLIVAL, Monastir, Tunisie.

[c]Université de Tunis El Manar, Faculté des Sciences de Tunis, Laboratoire des Sciences de l’Environnement, Biologie et Physiologie des Organismes Aquatiques LR18ES41, Tunis, Tunisie.

[d]Laboratoire du Milieu Marin, Institut National des Sciences et Technologies de la Mer, La Goulette, Tunisie.

[e]CNRS, Normandie Université, UNICAEN, UMR BOREA (MNHN, CNRS-8067, Sorbonne Universités, Université Caen Normandie, IRD-207, Université des Antilles), CS 14032, Caen, France.

* Corresponding author: Asma SAKKA HLAILI

E-mail address: asma.sakkahlaili@gmail.com

Abstract

Oil spills are recurrent worldwide. Assessing the response of phytoplankton – the basis of marine food webs – at the early stages of an oil spill and throughout its evolution is crucial to improve our understanding of the impact of oil spills on the marine environment. Field data collected 1, 4, 8 and 18 days after the "Bizerte City" oil spill showed that phytoplankton responded differentially over time. In the short term (1-8 days), picophytoplankton biomass and abundance increased, possibly due to reduced grazing. In contrast, nano- and microphytoplankton biomass decreased, probably owing to inhibited growth of sensitive species to polycyclic aromatic hydrocarbons – the most toxic components of oil. After 18 days, the dispersal of oil and its decreasing negative effect were accompanied by outbreaks of all size fractions. Accordingly, the phytoplankton size structure shifted throughout the oil exposure level from a prevalence of microphytoplankton after a few days toward picophytoplankton dominance. Oil pollution influenced the species composition and significantly decreased diversity indexes. In the first days, nanophytoplankton was dominated by cryptophyceae (mainly *Hillea fusiformis* and *H. marina*), while microphytoplankton was mostly represented by the pennate diatoms *Pseudo-nitzschia* and *Nitzchia*, suggesting a better resistance of these genera to oil. Algal recovery after 18 days was associated with high proliferation of nano-sized *Chaetoceros* and micro-sized *Astrionnellopsis glacialis* diatoms. These results improve our knowledge of the impact of oil pollution on coastal phytoplankton communities and reinforce the idea of using them as bio-indicators.

Keywords: oil spill, phytoplankton, diatoms, diversity, south-western Mediterranean Sea.

Oil spills are unintentional releases of petroleum oil or derived oils into the marine ecosystem (Li et al. 2016). They have serious environmental and socio-economic impacts on marine ecosystems and are a persistent threat to human health because of their impact on aquatic food resources (Wirtz and Liu 2006; Penela-Arenaz et al. 2009; El-Fadel et al. 2012). To understand the impact of oil pollution on marine environments, numerous studies have used phytoplankton because it represents the basis of marine ecosystem productivity and plays key roles in the nutrient and carbon cycles and biological carbon pump (Zehr and Kudela 2011; Tréguer et al. 2018; Li et al. 2020). Therefore, the effects of toxic oil compounds on these primary producers can be cascaded to higher trophic levels and impact the structure and dynamic of food webs as well as the biogeochemical cycles of marine ecosystems. Furthermore, phytoplanktonic species can respond quickly to marine contamination and environmental conditions, and are considered as an indicator of water quality (Verlecar et al. 2006; Marshall et al. 2006; Parsons et al. 2021; Song et al. 2022).

Much effort has been dedicated to studying the response of marine phytoplankton to different oil spills, such as the "Volgoneft-248" spill in the Sea of Marmara (1999), the "Prestige" spill along the Spanish coast (2002), the "Montara" spill in the Northwest Shelf of Australia (2009), the "Deepwater Horizon" spill in the Gulf of Mexico (2010) and the "Texas City Y" spill (2014) (Varela et al. 2006; Taş et al. 2011; Sheng et al. 2011; González et al. 2009; Gemmell et al. 2018; Bretherton et al. 2019a, 2020). Nevertheless, current knowledge on the effect of petroleum and its most toxic components – polycyclic aromatic hydrocarbons (PAHs) (Jiang et al. 2010) – on marine phytoplankton is still contradictory. After an oil spill, decreased phytoplankton photosynthesis can be observed as a direct response to the toxic impacts of petroleum compounds or as an indirect effect of less light penetrating into the water column as a result of the presence of oil slick on the sea surface (Goutz et al. 1984; Tomajka 1985; González et al. 2009; Paul et al. 2013). Different negative effects have been observed after oil exposure, such as reduction of phytoplankton growth, DNA damage, and inhibition of photosystem II (Aksmann and Tukaj 2008; Deasi et al. 2010; Bretherton et al. 2019a). In contrast, other studies have reported a stimulation of phytoplankton growth (González et al. 2009; Taş et al. 2011; Bretherton et al. 2019a). Ozhan et al. (2014) reported that crude oil at a low concentration (<1 mg L^{-1}) can stimulate phytoplankton growth, but inhibit it at higher concentrations (> 100 mg L^{-1}). The response of phytoplankton to oil pollution may also vary when considering short- or long-term effects (Lee et al. 2009; Tang et al. 2019). The phytoplankton community can also be impacted indirectly by such incidents *via* the effects of oil on the zooplankton community (González et al. 2009; Almeda et al. 2014). Studies reported

that the increase in phytoplankton biomass following an oil spill can be caused by a decrease in grazing due to PAH toxicity to zooplankton (Hjorth et al. 2007; Tang and Buskey 2022).

Contrasting effects of oil spills on taxonomic groups have also been reported. A decline in diatom biomass and an increase in phytoflagellates have been observed after experimental/laboratoty or *in situ* oil exposure (Harrison et al. 1986; Mishamandani et al. 2015; Fiori et al. 2016), while an opposite impact has been reported in other cases (González et al. 2009; Gilde and Pinckney 2012; Parsons et al. 2015). Ozhan et al. (2014) reported that diatoms showed better tolerance at high oil concentrations but others researchers showed instead the high tolerance of dinoflagellates to oil pollution (Jung et al. 2010; Taş et al. 2011; Gemmell et al. 2018). These results highlight that the response of marine phytoplankton to the hydrocarbon components of oil depends on several factors, such as, the amount and type of oil and the sensitivity of taxonomic groups, since oil toxicity to phytoplankton is widely species dependent (Ozhan et al. 2014). Oil exposure can be lethal for some species, but others can survive and grow at an unaffected or reduced rate. The oil-resisting ability of some phytoplankton species is related to the plasticity of their core metabolism, i.e., reduced extracellular carbohydrate secretion and enhanced flux through the Krebs cycle to conserve and increase energy production and counteract the oxidative stress caused by oil exposure (Kamalanathan et al. 2021, 2022). Physiological traits such as cell size, motility and mixotrophy, are also important in determining the ability of species to survive oil exposure (Bretherton et al. 2020).

Most data on the responses of marine phytoplankton to oil spills have been collected from experimental approaches. These include single species cultures or natural communities in microcosms and mesocosms (Varela et al. 2006; González et al. 2009; Gemmell et al. 2018; Bretherton et al. 2019a, 2020; Putzeys et al. 2022). However, field monitoring data from the early stages of an oil spill and throughout its evolution are rare because i) this requires heavy logistics, and ii) being on site and collecting samples rapidly is a challenge. Data on the early and late responses of natural phytoplankton following an oil spill are crucial to better understand how this event can affect marine communities.

An oil spill accident occurred in the Bay of Bizerte (North of Tunisia, south-western Mediterranean Sea, northern Tunisia) on 4 October 2018 as a result of a crack in a tank of the Tunisian Company. The government of Tunisia announced a leak of 7 tons of crude oil. The climatic and hydrodynamic features of the region extended the impact of the spill up to five km away from the source of the leak. The dykes/breakwaters built at the entrance of the Bizerte channel reduce the sea current intensity, which prevented the oil spreading offshore. Therefore, the oil slick was directed towards the western coasts (Sidi Salem beach) and especially towards

the Lagoon of Bizerte *via* the Channel (Figure.V 1). The Lagoon supports intense fisheries and is considered as the main shellfish farming site in Tunisia. Therefore, this ecological incident can have strong environmental impacts as well as economic and societal consequences. The goal of the present study is to follow the responses of the natural phytoplankton community to an oil spill from the early stages up to a few weeks after the oil release, called "short-term response" and "long-term response" hereafter, respectively. The results will provide valuable information on the dynamics of phytoplankton in response to the oil spill and contribute to a better understanding of the ecological aspects of oil pollution in coastal marine ecosystems.

Materials and Methods

Sampling

Sampling was carried out at one station (maximum depth 7 m) near the northern mouth of the Channel of Bizerte, which was affected by the oil spill (Figure V.1), on 5, 8, 12 and 22 October 2018. These dates corresponded to 1, 4, 8 and 18 days after the oil leak, respectively. The wind was blowing strongly (24 - 60 km h^{-1}) during the oil incident, with a dominant easterly direction propitious to a rapid dispersion of the oil slick towards the coast of the City of Bizerte and the Channel of Bizerte, where the sampling station was located. At each day (D01, D04, D08 and D18), three replicate water samples were collected with a plastic water sampler (Hydro-Bios) at three depths (0.5 m, 2.5 m and 5 m), filtered through a 200 µm-mesh sieve and placed in a cooler until analyses within 2-3 h after sampling. Subsamples for nutrient determination (PO_4^{3-} NO_3^-, NO_2^-, NH_4^+ and $Si(OH)_4$) were filtered through 0.2-µm sterile cellulose acetate filters and stored in microvials at -20°C. Nutrients were analysed following spectrophotometric methods (Parsons et al. 1984). Other samples were taken to analyse the phytoplankton community, i.e., biomass (expressed as Chl *a*), abundance, and species composition. Water temperature and salinity were recorded *in situ* at each sampling depth with a microprocessor conductivity meter (LF 196), the pH was determined using a pH meter (Accumet Basic AB15, Fisher Scientific), while water turbidity was measured with a turbidimeter (WTW, TURB 350 IR).

Figure V. 1. Site sampled during the oil spill in the Bay of Bizerte. Sampling stations in relation to the oil leak location and photographs of the polluted coasts of Sidi Selem beach (1: https://www.webdo.tn/2018/10/05/bizerte-7-tonnes-de-petrole-ont-fuite-dans-la-mer-de-zarzouna/) and of the Channel of Bizerte (2: https://directinfo.webmanagercenter.com/2018/10/10/tunisie-les-plages-polluees-par-une-vaste-couche-de-petrole-video/). White arrows, trajectory of oil dispersal.

Phytoplankton community analysis

Subsamples for Chl *a* measurements were sequentially filtered through 10-µm, 2-µm and 0.2-µm pore-size polycarbonate filters to obtained Chl *a* in three phytoplankton size fractions

(< 2 µm, 2-10 µm and > 10 µm). Concentrations were estimated after overnight dark extraction at 4 °C in 90% acetone, using the standard spectrophotometric method (Parsons et al. 1984). Total Chl *a* was estimated as the sum of the Chl *a* concentrations in the three size fractions. The Chl *a* percentage in each size class was calculated as the Chl *a* concentration of each size class divided by the total Chl *a* concentration.

Picophytoplankton (< 2 µm cells) was counted based on its autofluorescent pigments (MacIsaac and Stockner 1993). Subsamples were fixed with formaldehyde (2% final concentration) and placed in the dark at 4 ºC for 10 min. They were filtered through black polycarbonate filters (Nucleopore, 0.22 µm) and laid over 0.45-mm nitrocellulose backing filters. The filters were mounted on slides using low-fluorescence immersion oil, and stored immediately at -20 ºC. Picophytoplankton was counted under a CETI Topic-T epifluorescence microscope (100×Fluotarobjective), using blue and green excitation and counting at least 200 cells from 30 random squares.

For phytoplankton count and identification (nano-sized cells: 2-10 µm; micro-sized cells: 10-200 µm), subsamples were fixed with acid Lugol's solution (3% final concentration) and stored at 4°C in the dark. Prior to analysis, 50 mL of each subsample were settled for at least 24 h and analysed under an inverted microscope (100× oil immersion objective, CETI) (Utermöhl 1958). At least 500 cells were counted in each subsample.

Hydrocarbon analysis

PAHs – the most toxic compounds of oil (Jiang et al. 2010) – were analysed 8 days after the oil spill. Seawater samples were collected manually approximately 0.5m below the surface using pre-cleaned and sterile glass bottles. Sediment were sampled using using a Van Veen grab (Hydrobios). Analysis of PAHs in water and sediment were performed according to the technique proposed by UNEP/FAO/IAEA/IOC.1996. Appropriate blanks were analyzed with each set of analyses, internal standards and in addition reference material (IAEA 408) with certified concentrations of hydrocarbons was analyzed for quality control purposes.

Recoveries ranged from 72% to 89% for IAEA 408 and the method detection limits ranged from 0.05 to 0.25 ng g^{-1} for PAH. Further quality control was assured through participation in the hydrocarbons intercomparison exercises of IAEA (International Atomic Energy Agency). Quantification was performed by calculation of response factors of individual AH and PAH external standards.

Data analyses

One-way analysis of variance (ANOVA) was performed to test the significance of the variation in physicochemical and phytoplanktonic variables over time. The normality of data distribution and the homogeneity of variance were tested using Shapiro-Wilk's test and Levene's test, respectively.

A principal component analysis (PCA) was applied on the environmental variables to assess variability over time and the relevant factors responsible for the differences. Spearman's correlations were calculated to test for a linear relationship between phytoplankton parameters (Chl *a* concentration and phytoplankton abundance) and physicochemical factors. The ANOVA, PCA and correlation analyses were performed using XLSAT program (XLSTAT 2022 Trial version).

Phytoplankton diversity indices (species Richness, S; Shannon-Wiener's diversity index, H'; evenness, J) were calculated for the phytoplankton community sampled each day. A multidimensional scaling ordination (MDS) was performed on phytoplankton species abundances to detect changes in the phytoplankton community composition over time. A Euclidean distance dissimilarity analysis was used to determine the dispersal between communities at different sampling times. The diversity index and MDS analyses were performed using PRIMER program (PRIMER 6).

Results

3.1. Hydrocarbon contamination

Visual observation showed the presence of oil on the top layer of the sampling station (foam and oil aggregates) on D01, D04 and D08. At the end of sampling (D18), the water at the station had regained its pre-accident colour and smell. Eight days after the oil leak, the station contained toxic oil hydrocarbons, with ~130 ng PAHs L^{-1} measured in seawater and high concentrations in sediment (ΣPAHs: 1222 ng g^{-1} dry sediment). Chrysene was the main hydrocarbon in seawater (89 ng L^{-1}) and sediment (189 ng g^{-1} dry sediment), followed by naphthalene, phenanthrene and fluoranthene. Benzo(b)fluoranthene, benzo(k)fluoranthene and pyrene were only detected in sediment (TableV. 1).

Table V. 1. Concentrations of the main PAHs found in the seawater and sediment of the sampling station (Channel of Bizerte) 8 days after the oil spill incident.

PAH compound	Water solubility ($mg\ L^{-1}$)**	Water ($ng\ L^{-1}$)	Sediment ($ng\ g^{-1}$ dry sediment)
Naphthalene	31.0	18.9	33.17
Acenaphthene	3.9	nd	nd
Fluorene	1.69	nd	nd
Phenanthrene	1.15	13.59	43.26
Anthracene	0.43	nd	nd
Fluoranthene	0.26	7.38	151.52
Pyrene	0.13	nd	144.44
Chrysene*	0.002	87.88	188.85
Benzo(b)fluoranthene*	0.0015	nd	32.15
Benzo(k)fluoranthene*	0.0008	nd	40.27
Benzo(a)pyrene*	0.0016	nd	nd

nd: non detected

*: Considered probable human carcinogens by the US EPA, the European Union, and/or the International Agency for Research on Cancer (IARC) (EFSA, 2008)

**: water solubility values are reported from the literature (Ben Othman et al. 2023)

Environmental data

The sampling station had a shallow (< 7 m) well-mixed water column. Consequently, the environmental and phytoplankton factors showed no significant variations with depth (ANOVA $p > 0.05$, N=12), and the data are presented as depth-averaged values (Table V. 2).

Table V. 2. Environmental factors recorded 1, 4, 8 and 18 days after the oil spill (depth-averaged values ± SD, N = 12).

Sampling day after the oil spill incident	D01	D04	D08	D18
Temperature (°C)	22.00 ± 0.45	24.37 ± 0.31	24.57 ± 0.25	23.27 ± 0.31
Salinity (PSU)	37.20 ± 0.02	37.33 ± 0.05	37.47 ± 0.05	37.30 ± 0.1
pH	8.20 ± 0.10	8.27 ± 0.12	8.26 ± 0.15	8.83 ± 0.11
Turbidity (NTU)	4.22 ± 0.04	3.64 ± 0.04	3.28 ± 0.08	2.27 ± 0.08
NO_2^- (µM)	0.19 ± 0.02	0.12 ± 0.03	0.10 ± 0.01	0.09 ± 0.02
NO_3^- (µM)	0.98 ± 0.02	0.24 ± 0.01	0.35 ± 0.03	0.18 ± 0.01
NH_4^+ (µM)	59.59 ±5.00	33.12 ± 6.23	33.12 ± 6.00	27.43 ± 4.89
PO_4^{3-} (µM)	0.76 ± 0.04	0.67 ± 0.04	0.47 ± 0.04	0.36 ± 0.03
$Si(OH)_4$ (µM)	8.41 ± 1.25	5.75 ± 1.31	5.42 ± 1.30	3.30 ± 1.18
Total Chl *a* (µg l^{-1})	3.01±0.79	3.24 ± 0.41	2.48 ± 0.09	6.61 ± 1.21

Water temperature (22.6-24.57 °C), salinity (37.2-37.47) and the pH (8.2-8.83) varied little over time, while the nutrient and Chl *a* concentrations as well as water turbidity varied significantly (ANOVA, $p < 0.05$, N = 12). The temporal variability of environmental data was confirmed by the PCA, whose axes 1 and 2 explained 65.1% and 26.1% of total variation, respectively. Axis 1 was positively correlated with all inorganic nutrients ($r = 0.793$-0.957, $p < 0.01$, N = 12) and water turbidity ($r = 0.957$, $p < 0.01$, N = 12), but negatively correlated with the total Chl *a* concentration ($r = -0.804$, $p < 0.01$, N = 12). Axis 2 was positively correlated with temperature and salinity ($r = 0.792$-0.841, $p < 0.01$, N = 12). The sampling days were mainly discriminated on axis 1. The first day was characterised by the highest value of turbidity and dissolved nitrogen, phosphorous and $Si(OH)_4$, while the highest total Chl *a* concentration was recorded on the last day, associated to the lowest turbidity and nutrient levels. A cluster including D04 and D08 was distinguished in the middle of the PCA plot and was depicted by intermediate environmental data between D01 and D18 (Table V. 2, Figure V.2).

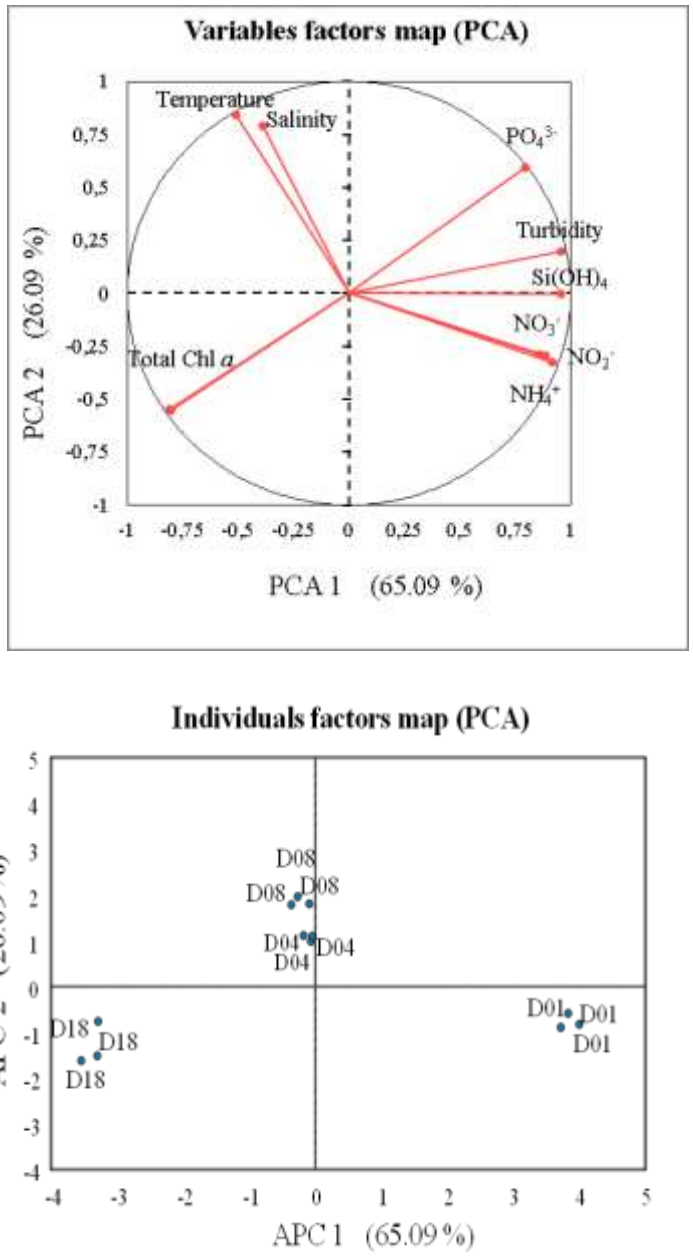

Figure V.2. Principal component analysis of environmental data and individual factors collected from D01 to D18 after the oil spill incident.

Phytoplankton size-fractioned biomass and abundance

The Chl *a* concentrations of the three size fractions showed different responses over time after the oil spill (Figure V.3a). For the pico-sized fraction (< 2 µm), Chl *a* was very low on D01 (< 0.2 µg L^{-1}), increased by 4-5-fold on D04 and D08, and strongly increased on D18 (6-fold relative to D08). Conversely, Chl *a* decreased gradually from D01 to D08 for nano- and microphytoplankton (from 0.93 to 0.53 µg L^{-1} and from 1.84 to 1.37 µg L^{-1}, respectively). However, the biomass of both size fractions significantly increased on D18 (2-fold relative to

D08) (ANOVA, $p < 0.01$, $N = 12$). The size structure of Chl *a* biomass distinctly varied over time. Picophytoplankton, which formed only 7% of total Chl *a* on D01, contributed 32% on D04 and D08, and dominated the biomass (~60%) on D18.

On D01, the abundance of picophytoplankton amounted to 11 10^5 cells L^{-1}, *versus* 0.91 and 1.7 10^5 cells L^{-1} for nano- and microphytoplankton, respectively. The evolution of the abundances of the three size fractions was almost similar to that of size-fractioned Chl *a* (Figure V.3b). The abundance of nano- and microphytoplankton significantly decreased in the short-term (from D01 to D08), while the abundance of picophytoplankton increased. In the long-term, all size fractions bloomed, cell concentrations reaching 3 10^7 cells L^{-1} for picophytoplankton and 2.5 and 4 10^5 cells L^{-1} for nano- and microphytoplankton, respectively (ANOVA, $p < 0.01$, $N = 12$). The abundances and Chl *a* concentrations of the nano- and micro-sized fractions were negatively correlated with nitrogen nutrients (r_s = -0.56 - -0.64, $p<0.05$), phosphorous (r_s = -0.80 - -0.95, $p<0.01$) and silicates (r_s = -0.75 - -0.86, $p<0.01$), while the abundance and biomass of picophytoplankton were not correlated with any nutrient.

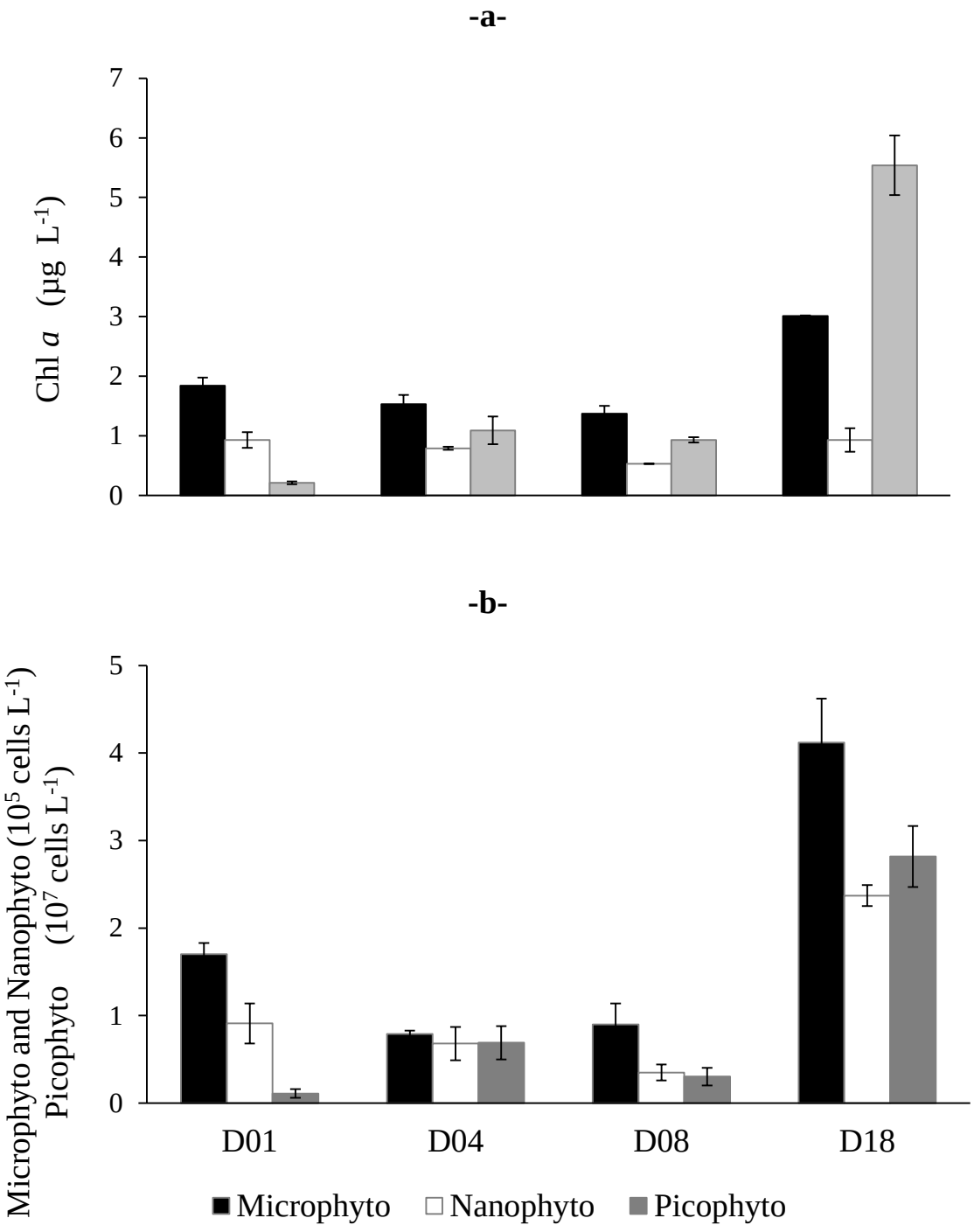

Figure V.3. Evolution of the biomass (a) and abundance (b) of three phytoplankton size fractions following the oil spill incident (depth-averaged values ± SD, N = 12).

Phytoplankton community composition

Microphytoplankton was dominated by diatoms (98-99%) throughout the sampling period. Its community composition changed in the days following the oil spill. Centric diatoms formed 34% of microphytoplankton on D01, but their contribution decreased until D08, when pennate diatoms formed almost all micro-sized cells (91% of microphytoplankton abundance). Centric diatoms became an important component again (40%) on D18 (Figure V.4a). Furthermore, the species composition of each diatom group changed remarkably over time. The pennate diatom community on D01 was mainly represented by *Pseudo-nitzschi*a (42%) and *Nitzscha* (25%) species, and *Asterionellopsis glacialis* and *Thalassionema* spp to a lesser extent (~ 10% each). *Nitzschia* and *Pseudo-nitzschia* species remained important taxa on D04, and the *Nitzshia* genus was dominant on D08 (82%). In contrast, *A. glacialis* bloomed on D18 (2 10^5 cells L^{-1}) and largely dominated the community (87%) (Figure V.4b). The abundance of this species was negatively correlated with the N and Si nutrient concentrations (r_s = -0.643 - -0.699, $p<0.05$). For centric diatoms, *Leptocylindrus* and *Dactyliosolen* formed 66% and 24% of the community on D01, respectively. Then, *Leptocylindrus* grew more and more abundant until they formed almost the entire centric group on D18 (96%) (Figure V.4c).

The community composition of nanophytoplankton also changed over time after the oil spill (Figure V. 5). From D01 to D08, the community was dominated by phytoflagellates (86-92% of nanophytoplankton abundance) – mainly cryptophyceae, mostly represented by *Hillea fusiformis* and *H. marina*. Chrysophyceae (mainly *Micromonas pusilla*) and Prymnesiophyceae (mainly *Imantonia rotunda*) had a relatively important contribution on D01 (12-20%), but decreased to only 1-5% of nanophytoplankton on D08. The 2-10 µm diatoms, represented by centric *Chaetoceros* species, only represented 8-13% of nanophytoplankton from D01 to D08. On D18, these species bloomed (1.3 10^5 cells L^{-1}) and co-dominated the nanophytoplankton community (52%) along with phytoflagellates.

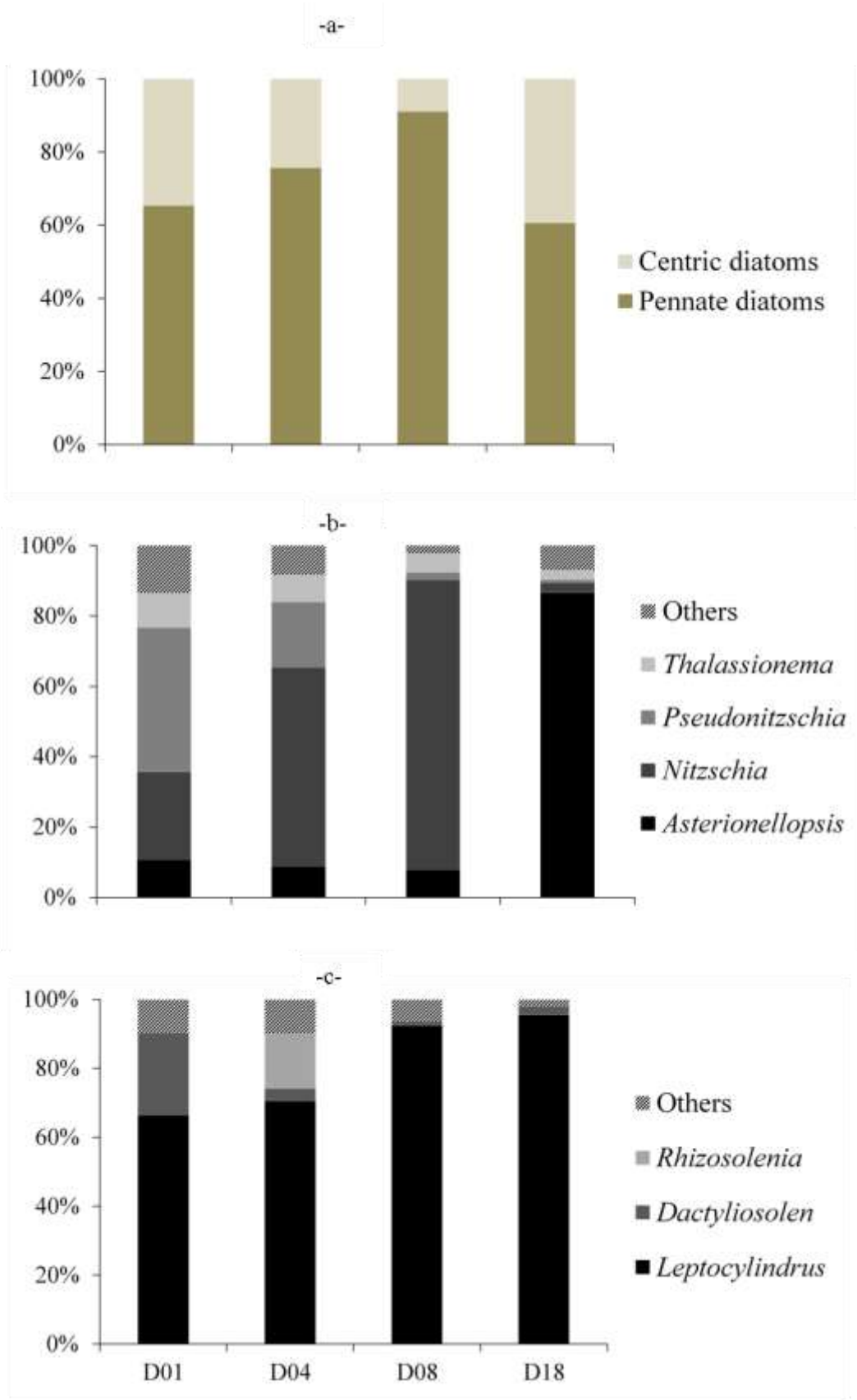

Figure V. 4. Composition of micro-sized diatoms (a), pennate diatoms (b) and centric diatoms (c) in the days following the oil spill.

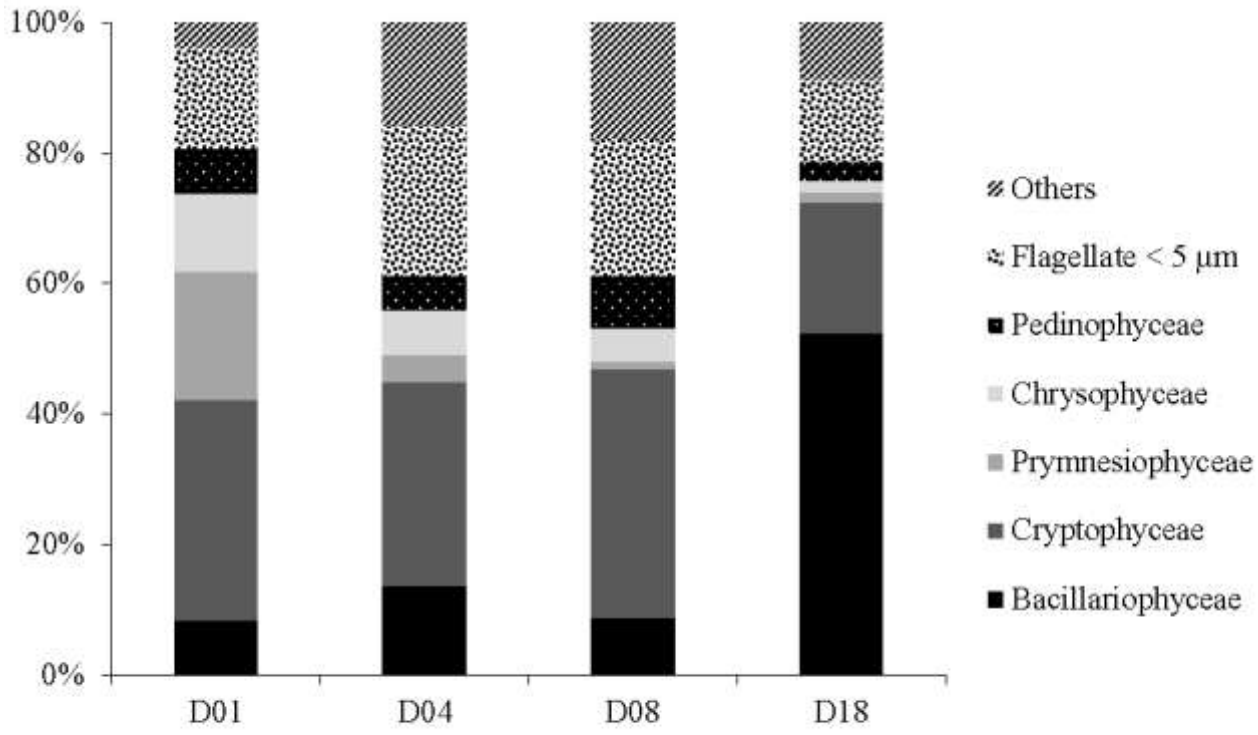

Figure V. 5. Composition of nanophytoplankton in the days following the oil spill.

MDS analysis

The changes in the microphytoplankton and nanophytoplankton communities following the oil spill were confirmed by the NMDS analysis (Figure V. 6). Three clusters were observed for each community. The first cluster grouped all D01replicates, the second was represented by all D04 and D08 replicates, and the last one was composed of the D18 replicates. Moreover, the dissimilarity of communities was low between D04 and D08 (41-44%), but high between D01, D04/D08 and D18 (Table S1).

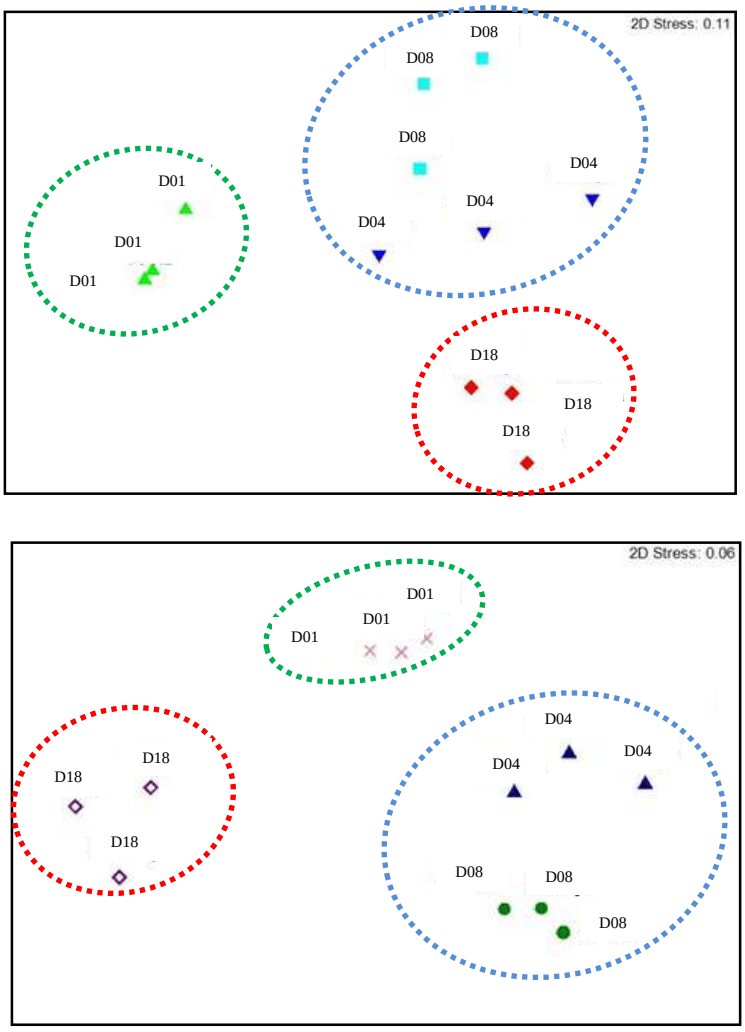

Figure V. 6. Non-metric MDS ordination of nanophytoplankton (a) and microphytoplankton (b) species abundance data collected from D01 to D18 after the oil spill incident.

Diversity indexes

Oil pollution had a marked effect on all diversity indexes 18 days after the accident. The species richness index (S) marked a significant decrease on D18 relatively to the other days (ANOVA, $p<0.01$, N=12) (Figure V. 7a). The Shannon-Wiener index (H') and the evenness (J) recorded on D01 and D04 were not significantly different, but decreased on D08 and were lowest on D18 (ANOVA, $p<0.01$, N=12) (Figure V. 7b, c).

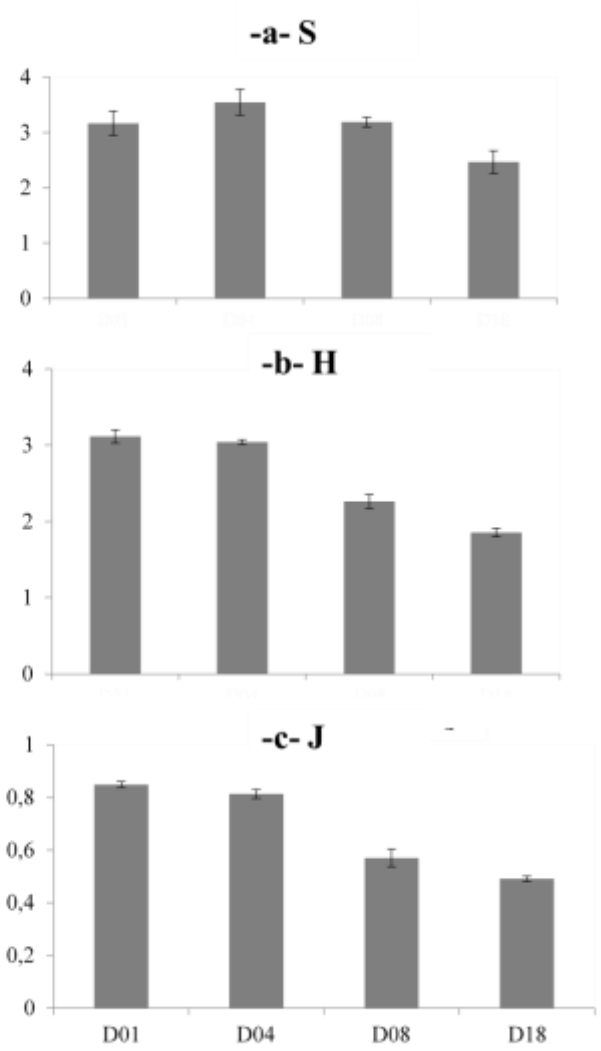

Figure V. 7. Evolution of diversity indexes (a: species richness, S; b: Shannon-Wiener's diversity index, H'; c: evenness, J) calculated for the > 2 µm phytoplankton community from D01 to D18 after the oil spill incident (means ± SD, N=12).

Discussion

Several oil spills have occurred in different marine ecosystems around the world in the last 30 years (Varela et al. 2006; Soto et al. 2014; Duda and Wawruch 2017; Tang et al. 2019). Assessing the effects of these accidents on marine phytoplankton is crucial, considering its basic status in marine food webs and its determining role in material and energy fluxes. Reports on *in situ* phytoplankton community changes at the early stages of an oil spill and throughout its evolution are rare, even if abundant data from experiments with single species or natural communities are available (Varela et al. 2006; González et al. 2009; Bretherton et al. 2019a,

2020; Putzeys et al. 2022). Microbial communities are rapidly altered after an oil spill incident (Gemmell et al. 2018), so that early monitoring is efficient when *in-situ* responses to oil pollution are targeted. Therefore, to improve knowledge on the effects of oil spills, it is important to consider rapid and longer responses of *in situ* phytoplankton following an oil leak. This work presents first field data on the responses of a coastal phytoplankton community to an oil spill from the early stage (the first days) up to a few weeks in the south-western Mediterranean Sea.

The oil leak site was located in the Bay of Bizerte, while the sampling station was located in the Channel of Bizerte (Figure V.1). The wind direction and speed moved the oil slick towards the Bizerte City coast and to the Channel. This was reflected by the presence of PAHs in the sampling station 8 days after the spill. Referring to the WHO 1997 standard (700 ng L^{-1}), seawater was moderately contaminated (ΣPAHs ≈130 ng L^{-1}). Some of the measured PAHs (chrysene, fluoranthene, naphthalene, phenanthrene) could have a toxic effect on phytoplankton even at low concentrations (Echeveste et al. 2010a, 2010b; Ben Othman et al. 2017). The water concentrations of PAHs measured on D08 have certainly been diluted. Therefore, higher levels would have been measured on D01 and D04 if sampled, and phytoplankton was most probably exposed to higher concentrations on D01 and D04 than those measured on D08. PAH levels were much higher in sediment (ΣPAHs = 1222 ng g^{-1} dry sediment, Table V. 1) than in seawater. As a result of their hydrophobic nature, PAHs are known to be sequestered within sediment (Mille et al. 2007; Bradshaw et al. 2012). Historical data showed that the sediment of Bizerte Channel had been exposed to PAH contamination, but at levels much lower than those recorded after this oil spill (394.1 ng g^{-1} dry sediment, Barhoumi et al. 2014).

Impact of oil on the growth of size-fractioned phytoplankton

Phytoplankton is known to respond rapidly to oil pollution and to the most toxic components of oil – PAHs (Ohwada et al. 2003; González et al. 2009; Gemmell et al. 2018). Our results also showed that phytoplankton displayed significant changes in biomass and abundance following the oil spill. However, the three size fractions exhibited different responses, confirming that cell size is important in determining the reaction of phytoplankton to oil and PAH pollution (Echeveste et al. 2010a, 2010b; Ben Othman et al. 2012; Bretherthon et al. 2020). Moreover, the observed changes in biomass and abundance varied over time after the oil spill. The biomasses and abundances of nano- and micro-phytoplankton significantly decreased on D04 and D08 relatively to D01 (Figure V.3a, b). Short-term negative effects of oil and PAHs on large phytoplankton have been reported, and their toxicity on the

photosynthetic activity, growth and biomass of phytoplankton is well documented (Djomo et al. 2004; González et al. 2009; Paul et al. 2013; Ben Othman et al. 2018). PAHs can alter photosystem II functioning and reduce the fluorescence yield in several marine phytoplankton species (Aksmann and Tukaj 2008; Ben Othman et al. 2023). In addition to the toxicity of petroleum hydrocarbons, the presence of an oil slick on the water surface during the first week of sampling (Figure V.1) reduced light penetration and indirectly inhibited phytoplankton growth. Conversely, nearly three weeks after the oil spill (D18), a positive effect was observed on large phytoplankton (> 2 µm), which bloomed and reached high concentrations (2.5-4 10^5 cells L^{-1}, Figure V.3a, b). Our results are in agreement with previous studies reporting a reduced phytoplankton concentration in the short term, but phytoplankton outbreaks (particularly for large species such as diatoms) in the long term (Taş et al. 2011; Sheng et al. 2011; Pan et al. 2012; Ozhan et al. 2014). On D18, the oil in the sampled station had been easily dispersed by the hydrological conditions encountered in mid-autumn (wind, water mass movements), and its negative effect on phytoplankton was ultimately reduced. Therefore, the regrowth of nano- and microphytoplankton on D18 could be mainly due to the return of a long-term favourable situation in the station, particularly light conditions. D18 was indeed characterised by the lowest turbidity (Table V. 2, Figure V.2) and by seawater that had recovered its colour and smell of before the accident. D18 also coincided with the lowest nutrient concentrations (Table V. 2, Figure V.2), which may reflect their absorption during phytoplankton regrowth. Moreover, nano- and microphytoplankton biomasses and abundances were negatively correlated with all nutrients. The recovery of large-sized phytoplankton growth may also have been due to a change in the community structure. Ben Othman et al. (2018) have shown that resumption of phytoplankton growth under PAH contamination coincided with significant change in community composition.

Smaller phytoplankton species are traditionally reported to be more sensitive than large ones to pollutants like oil compounds because of their higher surface-to-volume ratio (Echeveste et al. 2011; Ben Othman et al. 2012), and significant decreases in their abundance and growth are generally reported after PAH exposure (Kottuparambil and Augusti 2018; Ashok and Augusti 2022). On the contrary, the biomass and abundance of picophytoplankton was stimulated after the oil pollution event of Bizerte, even when an oil film covered the surface water of the station (on D04 and D08, Figure V.3). Our results are in agreement with other studies showing proliferation of small phytoplankton after an oil spill incident (González et al. 2009; Huang et al. 2011). Quigg et al. (2021) argued that the dominance of small phytoplankton following an oil spill is related to their higher growth rate than that of large cells. However, the

increase of picophytoplankton could be considered as result of the release from grazing of sensitive grazers, such as heterotrophic nanoflagellates (Johansson et al. 1980; Almeda et al. 2018; Gemmell et al. 2018). Additionally, correlations between picophytoplankton and abiotic factors (nutrients) were absent, suggesting that pico-sized biomass may be more controlled by biotic factors such as zooplankton grazing. Concomitantly with our work, Chkili et al. (submitted) investigated the protozooplanktonic community and its grazing rate, and reported a net decrease in grazing mortality rate of picophytoplankton, with the absence of their potential heterotrophic nanoflagellate grazers from D08.

The different responses of small and large phytoplankton to the oil spill were followed by a shift in the phytoplankton size structure from dominant micro-sized cells on D01 (61% of Chl *a*) to pico-sized cells on D18 (~60% of Chl *a*). This change could influence the grazer community and ultimately the food web structure.

Impact of oil on the phytoplankton community composition

The oil spill had a clear effect on the community composition of nano- and microphytoplankton, which changed differentially in the short and long terms (Figures V. 4, 5, 6).

Short-term impact. In the short term, the compositions of the two communities showed high dissimilarity on D01 relative to D04 and D08 (Table A1). During this short period, the presence of petroleum slick in the station (Figure V.1) was accompanied by a decrease in the abundance and biomass of nano- and micro-sized cells, but some species maintained their growth. This indicates a growth inhibition of sensitive species and a possible selection of pollutant tolerant species following the oil spill in short-term.

As regards microphytoplankton, diatoms were the main species on D01 and remained dominant on D04 and D08 despite the presence of oil in the station. The ability of diatoms to resist oil spills is documented. The presence of the silica frustule can protect them from the lethal effect of oil and confer them a better chance to survive than the naked phytoplankton cells do (Ikavalko 2005; Varela et al. 2006; Hallare et al. 2011; Ozhan et al. 2014; Parsons et al. 2015). Bopp and Lettieri (2007) have demonstrated a down-regulation of genes, which play an important role in the formation of the silica shell of diatoms (e.g. sil3), after exposure to PAH mixtures. However, others researchers showed that diatoms are more affected by oil than phytoflagellates and dinoflagellates (Mishamandani et al. 2015; Taş et al. 2011; Fiori et al. 2016). In fact, the response of coastal diatoms to oil is clearly size-dependent. Small diatoms (<20 mm) are apparently stimulated by oil, whereas large diatoms (>20 µm) are negatively

affected by high oil concentrations (González et al. 2009). Furthermore, when Bretherton et al. (2020) assessed the role of different physiological traits in the response of various phytoplankton taxa to oil, cell size was most important in determining the biomass response to oil. In our study, there was a decrease from D01 to D08 in the abundance of centric diatoms, which were dominated by small *Leptocylindrus* species (mean length/width ratio 35 µm / 3 µm) (Figure V. 4c), at the expense of pennate diatoms whose contribution increased gradually to form almost all microphytoplankton on D08 (~90%; Figure V. 4a). Large *Pseudo-nitzschia* and *Nitzschia* species (length/width ratio ranges 45-108 µm / 3-13 µm) were the main taxa on D01 and D04, and *Nitzschia* spp. formed 91% of pennate diatoms on D08 (Figure V. 4b). Our results are in line with those of Bretherton et al. (2019a) showing the dominance of the *Pseudo-nitzschia* genus after 3 days of oil exposure. The tolerance of pennate diatoms to toxic petroleum products may be explained genetically, since they are known to be more tolerant than other diatoms to oil compounds (Ozhan and Bargu 2014; Bretherton et al. 2019b). Furthermore, Melliti Ben Garali et al. (2021) provided the first evidence that two *Pseudo-nitzschia* species isolated from the Channel and Lagoon of Bizerte could tolerate a 15-PAH mixture by enhancing their biovolume, and were even able to bioconcentrate PAHs and degrade them, probably in synergy with their associated bacteria. Phytoplankton (including diatoms) can release extracellular polymeric substances (EPS) during environmental stress, e.g., oil exposure (Sun et al. 2018; Kamalanathan et al. 2019). The bacteria associated to phytoplankton can influence EPS production, and phytoplankton can in turn alter the bacterial community (Kamalanathan et al. 2019). Therefore, the phytoplankton-bacteria association can undoubtedly play an important role in phytoplankton resistance to oil. A benthic diatom and its associated bacteria isolated from a station close to Bizerte Channel have been found efficient in removing benzo(a)pyrene and fluoranthene (Kahla et al. 2021). All these findings clearly suggest that *Nitzschia* and *Pseudo-nitzschia* species from our study site, where previous PAH contamination has been reported (Lafabrie et al. 2013; Bancon-Montigny et al. 2019) have developed tolerance to PAHs through adaptation mechanisms that make them physiologically able to resist oil pollution. The trophic mode might also influence the sensitivity of phytoplankton to contaminants, including oil compounds. Conversely to autotrophic species, mixotrophic or heterotrophic diatoms can rely on sources of organic carbon to grow and to decrease their dependence on photosynthesis, so that they can better withstand contaminant toxicity (Debenest et al. 2009; Larras et al. 2012; Brethertron et al. 2021). Interestingly, heterotrophy has been reported for some *Peudo-nitzschia* species (Mengelt and Prezelin 2005; Loureiro et al. 2009), including species from the present study site (Melliti Ben Garali et al. 2016). Our results suggest that diatoms are resistant to

hydrocarbons and that certain species – e.g., members of the *Pseudo-nitzschia* and *Nitzschia* genera – may grow under oil contamination conditions. This is of particular interest given the fact that several species within these genera are known to produce the neurotoxin domoïc acid, including strains from the Bizerte waters (Bouchouicha Smida et al. 2014a; Sakka Halili et al. 2016). Blooms of *Pseudo-nitzschia* and *Nitzschia* are a known fact in the Lagoon and Channel of Bizerte (Sahraoui et al. 2012; Bouchouicha Smida et al. 2014b; Melliti Ben Garali et al. 2020). Oil hydrocarbon pollution can promote the growth of these diatoms and could increase the frequency of toxic blooms in these coastal waters, which are chronically prone to this kind of pollution.

As regards nanophytoplankton, cryptophyceae (dominated by *H. fusiformis* and *H. marina)* were the main taxa during the presence of oil silk from D01 to D08 (Figure V. 5). This is not in agreement with the observation of Brussaard et al. (2016), who reported the disappearance of this phytoplankton group after short-term exposure to oil. The major short-term change within nanophytoplankton observed in our study was the decrease of chrysophyceae (mainly *M. pusilla*) and prymnesiophyceae (mainly *I. rotunda*) (Figure V. 5). *M. pusilla* has been found sensitive to oil (Bretherton et al. 2020), or not (Brussaard et al. 2016), and a beneficial effect of oil exposure on chrysophyceae has even been found (Finkel et al. 2020). However, prymnesiophyceae can be a dominant group after an oil spill (Brussaard et al. 2016). In fact, the sensitivity of phytoplankton to oil is largely species dependent, since toxic oil compounds can affect different cellular and molecular targets (Ozhan et al. 2014; Kamalanathan et al. 2021, 2022). Furthermore, species can have differential core metabolism plasticity to counteract oil-induced oxidative stress and thus can modulate their tolerance to oil exposure (Kamalanathan et al. 2021, 2022).

Long-term impact. The community compositions of micro- and nanophytoplankton on D18 greatly differed from those of the other day (Table S1, Figures V. 4, 5, 6). On D18, the wide regrowth of both size fractions (Figure V.3) coincided with significant changes in the community composition, as speculated. For microphytoplankton, centric diatoms were more abundant after 18 days and formed ~40% of the community, although the community structure did not change that much since *Leptocylindrus* spp. remained the dominant taxon (Figure V. 4c). Centric diatoms have been reported to be faster growing species than pennate diatoms after a long post-spill period (Verlecar et al. 2006; Hallare et al. 2011). In the present study, pennate diatoms remained an important component of microphytoplankton, but the community changed deeply: *A. glacialis* had a low contribution from D01 to D08 (8-11%), but proliferated (2 10^5 cells L^{-1}) and became dominant on D18 (87%) (Figure V. 4b). Gallo et al. (2016) reported a

dominance of *A. glacialis* under increased levels of CO_2 in seawater, while Sahu et al. (2022) found that its development can be supported by salinity and a high nitrogen concentration. , the return of favourable environmental factors in our study site in the longer term may be responsible for *A. glacialis* development. The species abundance was negatively correlated with the N and Si concentrations, indicating their utilization during the *A. glacialis* increase.

As regards nanophytoplankton, the *Chaetoceros* spp. bloom (1.3 10^5 cells L^{-1}) was the most significant change observed after 18 days of oil spill (Figure V. 5). The growth of these red tide organisms was recently found stimulated after 10 and 14 days of oil exposure (Lv et al. 2023). Nutrients – phosphorous in particular – are considered the main regulating factors of *Chaetoceros* species growth (Shevchenko et al. 2006; Silkin et al. 2011). During our study, phosphorous seemed to support the proliferation of *Chaetoceros* spp., since the abundance of these organisms was negatively correlated with P concentrations ($rs = -0.699$, $P < 0.05$).

Species succession after an oil spill might also be related to different sensitivity levels to hydrocarbons (Sargian et al. 2007; Huang et al. 2011; Hemmer et al. 2011). Dominant species after several days of oil exposure can be considered more sensitive than species growing in the presence of high amounts of oil. In our study, *A. glacialis* and *Chaetoceros* spp, which can be sensitive to oil pollutants, dominated on D18 and took the place of *Nitzchia* and *Pseudo-nitzschia* species, which can resist to hydrocarbons as discussed above. Another reason might be that *A. glacialis* and *Chaetoceros* spp could outcompete and eliminate other species *via* allelopathic mechanisms, and become more competitive for resources (nutrients, light), hence their better growth. Allelopathy plays a significant role in the dominance, succession, and formation of natural diatom communities (Leflaive and Ten Hage 2009; Zhang et al. 2019). Additionally, the difference in the diatom community composition after long-term oil pollution could be partially due to indirect trophic interactions because herbivorous zooplankton is sensitive to oil compounds (Hjorth et al. 2007; González et al. 2009; Almeda et al. 2014). For one reason or another, our results clearly showed that the oil spill was followed by a profound change in the phytoplankton community composition after 18 days. This modification was accompanied by a significant decrease in the diversity indexes (S, H' and J, Figure V. 7), which reinforces the fact that oil spillage has deep effects on the structure of primary producers. Huang et al. (2010) also observed a drop in biodiversity and in the number and evenness of phytoplankton species after 15 days of crude oil exposure during different seasons.

Conclusion

This study highlights the importance of sampling at different stages of an oil spill because phytoplankton displays various responses throughout the evolution of an oil incident. The size structure and species composition of phytoplankton observed in the days following initial oil exposure were quite different from those in the longer term. Picophytoplankton proliferated, possibly thanks to decreased grazing due to oil poisoning of its potential consumers like heterotrophic nanoflagellates (Chkili et al. submitted). In contrast, large phytoplankton decreased in the short term and bloomed after 18 days. The dominance of pennate diatoms of the genera *Pseudo-nitschia* and *Nitzschia* in the presence of the oil slick could be related to the high tolerance of these species to oil hydrocarbon components. This re-confirms previous observations in the study area that hydrocarbon pollution could increase the likelihood of blooms of toxic diatoms. Our results demonstrate that even small oil spills may have short- and long-term effects on phytoplankton, and their recurrent nature in coastal waters may affect ecosystem functioning. Further research is needed to investigate the chronic impact of oil on coastal ecosystems.

Références (voir références bibliographiques.

Novel insight into the oil impact on the protozooplankton, trophic interactions and food web structure: field and modelling study

Oumayma Chkili[1,2,3], Sondes Melliti Ben Garali[1,2], Kaouther Mejri Kousri[1], Marouan Meddeb[1,2], Nathalie Niquil[3], Asma Sakka Hlaili[1,2*]

(en processus de soumission dans le journal Science of the Total Environment)

Novel insight into the oil impact on the protozooplankton, trophic interactions and food web structure: field and modelling study

Oumayma Chkili[1,2,3], Sondes Melliti Ben Garali[1,2], Kaouther Mejri Kousri[1], Marouan Meddeb[1,2], Nathalie Niquil[3], Asma Sakka Hlaili[1,2*]

✉ Asma Sakka Hlaili
asma.sakkahlaili@gmail.com

[1] Université de Carthage, Faculté des Sciences de Bizerte, Laboratoire de Biologie Végétale et Phytoplanctonologie, Bizerte, Tunisie

[2] Université de Tunis El Manar, Faculté des Sciences de Tunis, Laboratoire des Sciences de l'Environnement, Biologie et Physiologie des Organismes Aquatiques LR18ES41, Tunis, Tunisie

[3] CNRS, Normandie Université, UNICAEN, UMR BOREA (MNHN, CNRS-8067, Sorbonne Universités, Université Caen Normandie, IRD-207, Université des Antilles), CS 14032, Caen, France

ABSTRACT

We examined the effect of oil spill on protozooplankton community structure and feeding activity as well as on size-fractioned phytoplankton in the south-western coast of Mediterranean. Plankton communities were monitored on 1st, 4th, 8th and 18th days of the "Bizerte City" oil leak and dilution experiments were carried out on the same days. Results showed significant decrease in growth and carbon biomass for nano- and microphytoplankton in short term (i.e. 1-8 days) and a regrowth on 18th day. In contrast, picophytoplankton displayed a short-term enhancement of growth and biomass and a high biomass accumulation on 18th day. The protozooplankton community structure has changed throughout the oil spill toward a dominance of mixotrophic dinoflagellates (mainly *Heterocapsa*) in the detriment of a decrease in heterotrophic organisms (such as *Gyrodinium* and *Protoperidinium*). Ciliate (mainly *Strombidium*) showed a short-term decrease but a recovery on 18th day, while heterotrophic nanoflagellates were more vulnerable to oil toxicity and disappeared from 8th day. Grazing rates presented similar temporal evolution as growth rates for nano- and microphytoplankton but there was a de-coupling between both rates for picophytoplankton, promoting the pico-algal biomass. Consequently, rates of carbon production and consumption for the different size fractions of phytoplankton have varied following the oil contamination. The integration of these oil-altered rates into linear inverse models of carbon flux showed a clear shift in food-web structure, from the herbivorous (1st day) to the multivorous (4th and 8th day) until the microbial (18th day) pathways, which implies different efficiencies in carbon export throughout the oil spill. Our study highlights that field sampling and experiments combined with modelling can give new insights on the impact of oil spill on trophic interactions, food-web structure and carrying capacity of the system.

Keywords: Oil spill, phytoplankton, protozooplankton, growth and grazing rates, food-web models, South-western Mediterranean.

1. Introduction

Petroleum activities, particularly oil production and transportation, result in several oil spills, which have adverse effects on marine ecosystems and can cause significant damages resulting in loss of biodiversity and disruption of the environmental balance (Kennish, 1996; Gugliermetti et al., 2007; Zhu et al., 2011; Barron, 2012; White et al., 2012).

Several works have evaluated the impacts of oil spills on planktonic organisms, since they are responsible for the majority of biological processes in marine ecosystems (González et al., 2009; Ozhan et al., 2014; Almeda et al., 2014a, 2016, 2018; Severin et al., 2016; Bretherton et al., 2019; Quigg et al., 2021). Oil can cause both short and long term damages to plankton organisms by its most toxic compounds, i.e. polycyclic aromatic hydrocarbons (PAHs), which soluble fraction remains in seawater for an extended period of time (González et al., 2006; Kryzevicius et al., 2020). Studies on plankton responses to oil spills have focused particularly on phytoplankton, given its basic status of primary producer that provide the energy and matter, *via* its photosynthesis, to marine food webs (Jiang et al., 2012; Ozhan et al., 2014; Almeda et al., 2016; Bretherton et al., 2018; Putzeys et al., 2022). Contrasting results of oil contamination on phytoplankton were obtained. Many studies have reported that oil has a toxic effect on phytoplankton growth and photosynthetic activity, with shift in community structure from diatoms to phytoflagellates dominance (Parsons et al., 2015; Fiori et al., 2016; Bretherton et al., 2018). However, others demonstrated that the presence of oil can stimulate phytoplankton and that diatoms can tolerate the toxic oil compounds (González et al., 2009; Ozhan et al., 2014; Bretherton et al., 2020). Authors stated that phytoplankton oil response varied according to the oil type and concentration, community composition and specie sensitivity(Huang et al., 2011; Ozhan et al., 2014), which is related to cell size, motility, mixotrophy and metabolism plasticity (Bretherton et al., 2020; Kamalanathan et al., 2021). The effects of oil spills on bacteria are also documented (Coral and Karagoz, 2005; Kostka et al., 2011; Bælum et al., 2012; Wanjohi et al., 2015; Bacosa et al., 2015). It has been shown that bacterial community has the ability to rapidly adapt to oil spills through the selective development of oil degraders. Coral and Karagoz, 2005 revealed the use of carbon-rich oil by bacteria to satisfy their cell growth and energy requirements. Wanjohi et al., 2015 reported that hydrocarbon-degrading bacteria can be applied to remediate the oil-contaminated environments. Others studies have also showed that phytoplankton interact strongly with their associated bacteria to co-metabolize PAHs (Severin and Erdner, 2019; Kahla et al., 2021).

Protozooplankton has received comparatively little attention in the oil spill studies (Almeda et al., 2014b, 2016, 2018). Yet, many authors consider that decreased top-down control, due to hydrocarbon poisoning of sensitive grazers, is a major contributing factor to the increase in population and diversification of marine phytoplankton following an oil spill event (Johansson et al., 1980; Hjorth et al., 2007; Gemmell et al., 2018). Recently, (Tang and Buskey, 2022a) reported effectively a de-coupling between phytoplankton growth and protozooplankton grazing following crude oil exposure, which can promote the formation of phytoplankton blooms after oil spill events. Protozooplankton, including heterotrophic ciliates, heterotrophic and mixotrophic dinoflagellates and heterotrophic nanoflagellates (HNF), form a key component of the marine plankton community and are an important grazer of the bacterial and phytoplankton biomasses (Poulsen and Reuss, 2002; Calbet and Landry, 2004; Pecqueur et al., 2022; Kosiba and Krztoń, 2022). Protozooplankton represent an important link between the microbial loop and higher trophic levels (Montagnes et al., 2010; Sommer et al., 2012; Agasild et al., 2013; Kosiba et al., 2017) and has a key role in enhancing the food quality of metazooplankton and fish as essential contributor to the diet of these components (Holt and Holt, 2000; Calbet and Saiz, 2005). Current knowledge of oil contamination effect on protozooplankton are also contradictory. Some studies reported a stimulatory effect of oil exposure on tintinnid ciliates (Dale, 1987, 1988) and bacterivorous nanoflagellates (Jung et al., 2012). In contrast, heterotrophic ciliates, including loricate and aloricates organisms, and heterotrophic dinoflagellates are highly sensitive to crude oil and their abundances decrease with increasing oil concentration(Almeda et al., 2014b; Gemmell et al., 2018), while growth of mixotrophic dinoflagellates is either unaffected or stimulated (Almeda et al., 2016, 2018). Toxic oil compounds may also decrease the abundance of HNF (Almeda et al., 2018). These protozooplankton groups have different feeding behavior and preference and play different roles in marine food webs. Herbivorous organisms, such as dinoflagellates and tintinnid ciliates, are able to consume large phytoplankton and their grazing impact could be higher than metazooplankton, thus constituting major component in the herbivorous food web, with efficient carbon transfer to higher consumers(Sakka Hlaili et al., 2007, 2014; Stibor et al., 2019). Conversely, microbivorous protozooplankton, such as HNF, small dinoflagellates and aloricate ciliates, are important grazers of bacteria and small phytoplankton and play crucial role within the microbial loop and microbial food web, with a high recycling activity and lower amount of channeled carbon (Legendre and Rassoulzadegan, 1996; Meddeb et al., 2018). Herbivorous and microbivorous protozooplankton can simultaneously play efficient role in transferring carbon throughout the multivorous food web (Legendre and Rassoulzadegan, 1996;

Chkili et al., 2023). It's clear that the grazing of protozooplankton is a major ecological process that influence the type of food web structure and hence controls the carbon flow to higher consumers (Grami et al., 2008a; Sakka Hlaili et al., 2014; Meddeb et al., 2019). Shifts in feeding and structure of protozooplankton in response to oil contamination can deeply alter the carbon transfer through marine food webs. Unfortunately, although previous study focused on oil-responses of the abundance and composition of planktonic organisms, there is still gaps about the effect of oil spill on trophic interactions and carbon transfer pathways. Thereby, it is necessary to take into account the responses of protozooplankton to oil spills, at structural scale and especially at the functional scale (i.e. grazing activity), to better understand the ecological impact of these events on the functioning of the ecosystem.

To establish the functioning of marine ecosystems and to predict their responses to diverse environmental and anthropogenic stress, such as oil spills, it is relevant to use food web models, which provide integrated and concise information on the cycling of materials and flow of energy (Forest et al., 2011; Thompson et al., 2012; Meddeb et al., 2019). Indeed, these models include field data on different planktonic compartments (i.e. bacteria, phytoplankton size fractions, protozooplankton and metazooplankton), non-living compartments (i.e. dissolved organic carbon and detritus) and take into account the interactions between these compartments (Joint and Morris, 1982; Landry et al., 2020). Several modelling methods have been developed to characterize marine food webs. The linear inverse model (LIM), as defined by (Vézina and Piatt, 1988a), is a useful method in the study of marine ecosystem functioning that allows the estimation of unknown trophic flows among different compartments of food web (Niquil et al., 2011; Pacella et al., 2013; Taffi et al., 2015; Hines et al., 2018). This method was innovated into the LIM Markov Chain Monte Carlo method (LIM-MCMC; Van den Meersche et al., 2009) which is nowadays considered among the most accurate approaches, allowing to estimate the uncertainties associated to each flow.

The inverse food web models have been previously used in order to assess environmental or human pressures on the structure and function of the planktonic food web. They were applied in evaluating the impact of climate change, polychlorinated biphenyls bioaccumulation (PCBs) and even cumulative impacts such as offshore wind farms combined with climate change (Forest et al., 2011; Taffi et al., 2015; Nogues et al., 2021). Meddeb et al., 2018 have also used the LIM-MCMC analysis to depict change in ecosystem functioning in three Mediterranean coastal regions with different anthropogenic pressure. However, few studies have used this integrative method in a pollution context. Recently, Chkili et al. (submitted), based on trophic

models combined with ecological nethwork analysis, showed that the structural and functional properties of the ecosystem change according to the phosphogypsum pollution in the Gulf of Gabès (South-astern Mdietrranean). Thus, it is clear that food-web models could constitute a powerful approach to analyze consequence of oil spill on the entire ecosystem

The "Bizerte City" oil spill occurred on 4 October 2018 due to the cracking of a crude oil tank belonging to the Tunisian Society of Refining Industries (STIR) that released 7 tons oil. This accident caused significant contamination of water and sediment by PAHs. The spill impact extended to 5 km away from to the source of oil leak, and the oil slick has been directed towards the Channel of Bizerte and then entered to the Bizerte Lagoon (Figure.V A1). A planktonic community monitoring was carried out during 4 days from the 1st day after the oil spill to the 18th day. A previous study (Grami et al., submitted) looked at the short (i.e. 1, 4 and 8 days) and long-term (i.e. 18 days) responses of natural phytoplankton community to this oil accident. Results showed that biomass of picophytoplankton largely increased but that of large phytoplankton decrease after few days of oil leak, whereas in long-term, biomasses of all size fractions were enhanced. Furthermore, this enhancement was associated with a shift in species composition of large phytoplankton. In the present study, we assess effects of this oil contamination on the community structure of protozooplankton and its grazing activity, as well as phytoplankton growth on the same days. Also, the study tries for the first time to describe how the planktonic food web evolves during the various days of an oil spill, by integrating observed change of phytoplankton production and protozooplankton feeding into inverse models of carbon flux.

2. Materials and Methods

2.1. Water sampling and analyses

Water sampling was carried out in a station (37°16'07.9"N 9°52'44.7"E ; maximal depth 7 m) located in the Bizerte Channel, which was affected by the oil slick (Fig. S1), during different days (D01, D04, D08 and D18) after the oil spill. The Bizerte Channel connects the Lagoon to the Mediterranean Sea and harbors eutrophicated waters (34.40 N µM, 1.30 P µM, 1.20 Si µM and 6.20 mg Chl *a* m^{-3}, Sahraoui et al., 2012). Chemical contamination by several metals (notably Zn, Cr and Pb, 85-228 mg g^{-1} dry sediment) and PAHs (21-772 µg g^{-1} dry sediment) was also reported for the Channel (Pringault et al., 2016b). During our study,

concentrations of PAHs in seawater of the sampling station were measured after 8 days of the oil spill. Details of the analytical method can be found in Grami et al. (Submitted). Seawater was collected over the water column with a submersible pump and then filtered through 200 µm mesh screen (to remove meta- and macroplankton).and stored in polyethylene containers. Water temperature and salinity were measured *in situ* with microprocessor conductivity meter (LF 196). pH was measured *in situ* with a multi-probe sensor (Multi 1970i, WTW) while turbidity was determined using a turbidimeter (Turb350IR). Value of these environmental parameters were reported in Table V. 3. Samples for phytoplankton and protozooplankton analyses were also taken.

Table V. 3. Environmental parameters and phytoplankton biomasses during different days following the "Bizerte City" oil spill (Mean ± SD, N = 12)

	D01	**D04**	**D08**	**D18**
Water temperature (ºC)	22.00 ± 0.45	24.37 ± 0.31	24.57 ± 0.25	23.27 ± 0.31
Salinity	37.20 ± 0.02	37.33 ± 0.05	37.47 ± 0.05	37.30 ± 0.1
pH	8.20 ± 0.10	8.27 ± 0.12	8.26 ± 0.15	8.83 ± 0.11
Turbidity (NTU)	4.22 ± 0.04	3.64 ± 0.04	3.28 ± 0.08	2.27 ± 0.08

Samples (2 mL, in triplicates) for picophytoplankton (< 2 µm) were analyzed using the CyFlow® Space flow cytometer method (Partec). Prior to analysis, samples were filtered through 30 µm pore filters and enriched with 1 and 2 µm diameter fluorescent beads (Polysciences, Inc) as internal cell size standards. Trucount™ beads were also added to accurately estimate the volume of each sample (BD-Biosciences). Picoprokaryotes and picoeukaryotes were identified and counted based on their relative forward scatter (FSC) and phycoerythrin orange fluorescence (at 488 nm) and Chl *a* red fluorescence (at 638 nm), respectively. Cell volumes were determined using equivalent diameters estimated from flow cytometry. Cell carbon of picophytoplankton (pg C $cell^{-1}$) was determined using the conversion carbon factors of 0.22 pg C μm^{-3} for prokaryotes and 0.22 pg C $cell^{-1}$ for eukaryotes (Sakka Hlaili et al., 2008). Biomass of picophytoplankton (mg C m^{-3}) was estimated by multiplying their cell carbon by their abundance. Samples (100 mL, in triplicate) of phytoplankton (i.e. nano-sized cells: 2-10 µm and micro-sized cells: > 10 µm) were preserved with 3% acid Lugol solution (Parsons et al., 1984) and stored away from light. Phytoplankton abundances were determined under an inverted microscope (100× objectives) on 100 mL settled volumes (H. Utermöhl, 1931). At least 500 cells in each sample were counted. Cell volumes of nano- and

microphytoplankton were calculated after measuring the cell dimension and applying standard geometric formulae to each taxon, as proposed by (Hillebrand et al., 1999). For diatoms, the plasma volume (Vp) was estimated by subtracting the vacuole volume assuming a layer thickness of 1 µm, and the C content was obtained using the formula of pg C $cell^{-1}$ = 0.288 × $Vp^{0.811}$ (Menden-Deuer and Lessard, 2000). For autotrophic flagellates, after estimating the cell volume (Vf, μm^3), the C content was calculated as follows: pg C $cells^{-1}$ = 0.216 × $Vf^{0.939}$ (Menden-Deuer and Lessard, 2000). Carbon biomasses (mg C m^{-3}) of nano- and microphytoplankton was then determined by multiplying the carbon content of different taxa by their respective abundances. For each phytoplankton size fraction, carbon biomass (mg C m^{-3}) was multiplied by the depth of the station to get the biomass expressed in mg C m^{-2}.

For protozooplankton analysis, samples (100 mL, in triplicate) were preserved with 4% basic Lugol solution (Sherr and Sherr, 1993) and stored at room temperature in the dark. Protozooplankton abundance was determined under an inverted microscope (100 x objectives) on 100 ml decanted volumes (Lund et al., 1958). At least 200 cells in each sample were counted. In our study, protozooplankton was composed by heterotrophic nanoflagellates (HNF), heterotrophic ciliates (i.e. loricate and aloricate organisms) and dinoflagellates (i.e. heterotrophic and mixotrophic organisms) according to previous studies (Sakka Hlaili et al., 2007; Jeong et al., 2010b; Boutrup et al., 2016).

2.2. Estimation of protozooplankton grazing

In parallel with sampling, dilution experiments (Landry and Hassett, 1982) were conducted in the same station in order to estimate the impacts of protozooplankton grazing on size fractioned phytoplankton, following different days after the oil spill (i.e. D01, D04, D08 and D18). The dilution technique is very useful, since it provides simultaneous estimations of growth and grazing rates and requires few manipulations of planktonic communities. It is widely used in different areas and contexts (i.e. coastal waters, polluted waters, open sea waters, etc. (Sakka Hlaili et al., 2008; Grinienė et al., 2016; Mejri Kousri et al., 2023) and even under influence of petroleum pollutants (Tang and Buskey, 2022b). Seawater was collected, as described for sampling, filtered through a 200 µm mesh screen and stored in polyethylene containers. A fraction of the collected seawater was filtered by gravity on sterile 0.2 µm filter capsule (polycap 75 AS) to prepare free-particle seawater. This latter was then mixed with the <200 µm prescreened seawater to obtain four dilutions factors (25, 50, 75, and 100% of < 200 µm filtered seawater). Triple 2 L polycarbonate bottles (Nalgene®) were used for each dilution factor, and all bottles were incubated *in situ* for one day (t = 1 d). Subsamples were taken from each dilution

bottle at the beginning and the end of incubation to determine initial and final phytoplankton abundances, which were converted into carbon biomasses (C_0 and C_t), as detailed above. No nutrient was added to the dilution bottles since seawater from the study site is rich by N and P year-round (Meddeb et al., 2019), and previous work in this area reported that nutrients have no effects of phytoplankton growth during dilution experiments (Sakka Hlaili et al., 2007, 2008; Meddeb et al., 2018).

The apparent growth rate of phytoplankton (r, day^{-1}) was calculated from the changes in carbon biomass during the incubation period as:

$$r(d^{-1}) = \ln\left({C_t}/{C_0}\right) \times t^{-1} = k - g$$

where C_0 and C_t are the initial and final carbon biomass (mg C m^{-3}) of size fractioned phytoplankton and *t* is the incubation duration (1 day). The coefficients r were plotted against the dilution factor, and a model I linear regression was used to estimate growth rates k (d^{-1}) (i.e., the y-intercept that represented growth in 100% dilution in the absence of grazers) and the grazing coefficient g (d^{-1}) (i.e., the slope of the regression line) (Landry and Hassett, 1982). The significance of the regression slope was statistically verified (student *t*-test, $p < 0.05$) for each phytoplankton size fraction.

Growth (k) and grazing (g) rates were used to calculate rates of phytoplankton production (P) and consumption (G) according to the following equations (Meddeb et al., 2018; Chkili et al., 2023):

$$P(mg\ C\ m^{-3}\ d^{-1}) = k \times C_0\left[e^{(k-g)t} - 1\right]/(k - g \times t)$$

and

$$G\,(mg\ C\ m^{-3}\ d^{-1}) = g \times C_0\left[e^{(k-g)t} - 1\right]/(k - g \times t)$$

The production and consumption rates (P and G, mg C m^{-3} d^{-1}) were multiplied by the sampling depth to determine the depth-integrated production and grazing rates (Pc and Gc, mg C m^{-2} d^{-1}).

The percentage of production consumed is estimated as:

$$\%Pgrazed\ d^{-1} = \left({Gc}/{Pc}\right) \times 100$$

2.3. Model development

All models were built with R software using the LIM MCMC approach (Van den Meersche et al., 2009). This approach is based on four steps: (i) building an a priori model, (ii) setting up the equalities, (iii) setting up the inequalities, and (iv) calculating the possible solutions for each flux.

2.3.1. *A priori* model

The *a priori model* represents the planktonic compartments and all possible carbon fluxes (known and unknown) between them. Eight compartments were included in each day: BAC (bacteria), PIC (picophytoplankton), NAN (nanophytoplankton), MIC (microphytoplankton), PRO (mainly protozoans < 200 µm: HNF, dinoflagellates and ciliates), MET (mainly metazoans > 200 µm), DOC (dissolved organic carbon) and DET (detritus). The model included thirty-four flows between the compartments and the outside, except for days D08 and D18, for which we added a flow from PIC to LOS which was considered as a loss of PIC by advection (Figure V. 8), in order to balance the flows (because all PIC production could not possibly be maintained inside the planktonic system).

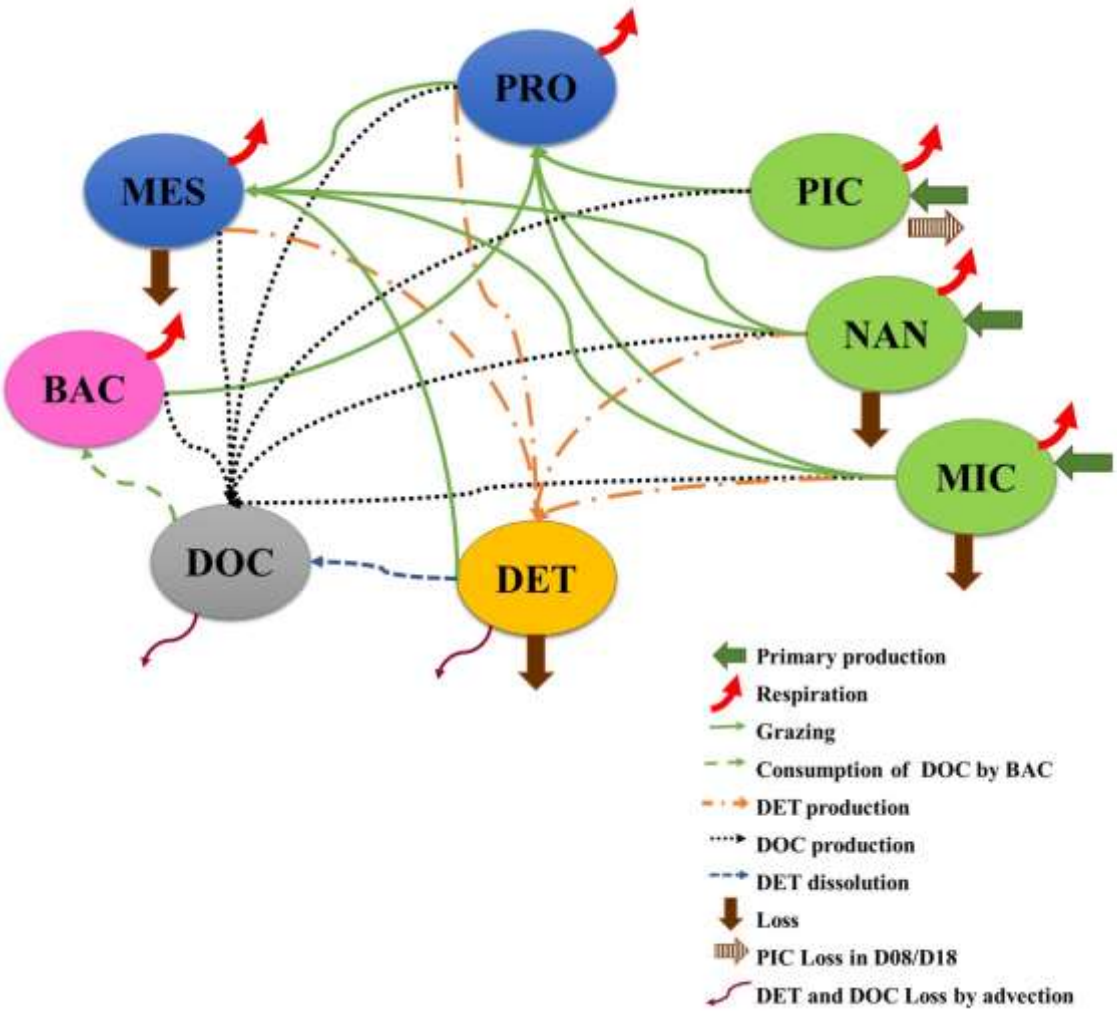

Figure V. 8. *A priori model* used to build the planktonic food web systems during different days after the oil spill. Heterotrophic bacteria = BAC, picophytoplankton < 2 µm = PIC, nanophytoplankton, 2–10 µm = NAN, microphytoplankton 20–200 µm = MIC, protozooplankton < 200 µm = PRO, metazooplankton >200 = MET, dissolved organic carbon = DOC and detritus = DET.

The only source of carbon input to the network is the gross primary production (GPP) of the three phytoplankton size fractions (PIC, NAN and MIC). This carbon could be lost by respiration of all living compartments and sinking of most compartments except BAC, PIC and PRO. The consideration that the very small size of PIC and BAC does not allow them to generate a downward flow is assumed. We made an exception on days D08 and D18, with potential loss of PIC by advection of the non-consumed production. Dissolution of detritus, exudation of phytoplankton and excretion of zooplankton (i.e. PRO and MET) contribute to DOC production. All living compartments, except PIC and BAC, contributed to the generation of DET through mortality, production of faecal pellets by MET and sloppy feeding by

zooplankton. Concerning trophic interactions, BAC and all phytoplankton size fractions were consumed by PRO, while MET only consume NAN and MIC, because smaller cells (i.e. BAC and PIC) are inefficiently captured by MET (Fortier et al., 1994). PRO and DET contribute also to food source for MET. MET production is lost, consumed by organisms which are not planktonic.

2.3.2. Equalities and inequalities

The setting up of the equalities is an essential phase to establish the mass balances of the network. If the mass of the compartment is constant, or its variation negligible, during the period under consideration, the sum of the fluxes into the compartment should be equal to the sum of the fluxes out. Here, the daily variations of the biomass with respect to the daily flux values were neglected. A mass balance equation is written for each compartment (Table S1). The subsequent step is to impose ecological limits (maximum and/or minimum) for each unknown flux, which allows to reduce the range of possible solutions. The inequalities used are of two types of ranges. The first range considered the average value of the fluxes measured in field (i.e. production rates of BAC, PIC, NAN and MIC; grazing rates by PRO and MET, and vertical sinking of particles) (Table S2). These average values allowed the model to estimate the fluxes with uncertainty. For this reason, we proposed to define the minimum and the maximum value for each flux by considering as a confidence interval around the field data, the minimum and maximum of the mean value of each flux. A total of 13 inequalities derived from field measurements were considered for the four stations of the Gulf (Table S2). A second group of constraints was adopted from the literature to constrain the unknown fluxes (Vézina and Piatt, 1988a; Steinberg et al., 2000; Vézina and Pahlow, 2003). These inequalities include the lower and/or upper limits of several processes: such as respiration of all living compartments; DOC production by phytoplankton, PRO, MET and BAC; production and dissolution of DET; growth efficiency of BAC, PRO and MET and assimilation efficiency of PRO and MET. For preferential ingestion of MET, we used diet constraints, based on the assumption that MET feeding depends on the availability of their prey, i.e., the abundance of a prey relative to other prey. Where prey and consumer are the biomass of the prey and consumer, respectively. The selection coefficient (SC) is set up to1 when there is no selection, 1.4 when we assume positive selection, and 0.6 when the selection is assumed negative (Table S3) (Haraldsson et al., 2018). Twenty six inequalities from this second group were applied in the model at four stations (Table S3).

2.3.3. Solutions

The calculation of the unknown fluxes is the last step of the inverse analysis. The LIM-MCMC method was applied using the xsample function of the LimSolve R package, based on the mirror technique defined by (Van den Meersche et al., 2009). It allows the estimation of a sample of values for each unknown flux. A jump value of 10 mg C m^{-2} d^{-1} and 300,000 iterations were adopted to run the models to optimize the coverage of all possible solutions

2.4. Food web typology ratio

To describe the different interactions between compartments and identify the type of trophic pathway, (Sakka Hlaili et al., 2014) provided operational criteria based on Carbon flux ratios that can be easily estimated in the field. In our study, food web typology ratio R7 (picophytoplankton net production divided by total phytoplankton net production) which discriminates between herbivorous (R7 ≤ 0.1), multivorous (R7: 0.1–0.6) and microbial food (R7: ≥ 0.6) was calculated from the flux data obtained by the models.

2.5. Statistical analysis

Statistical analyses were done using SPSS 18.0 statistical software for Windows. One-way ANOVA was used, after checking the normality of the distributions (Kolmogorov-Smirnov test) of the data as well as the homogeneity of variances (Bartlett-Box test), to compare rates (k, g), phytoplankton primary production, abundance and diet of proto and meta-zooplankton communities and carbon throughput among Phytoplankton size fractions and sampling days.

3. Results and discussion

3.1. Oil spills effect on phytoplankton

PAHs levels measured on D08 following the “Bizerte City” oil spill were reported in Grami et al. (submitted). Briefly, sampling station contained PAHs (mainly chrysene) in the water column with ~130 ng PAHs L^{-1}. The oil leak induced different effects on phytoplankton growth and biomass depending on the size fraction (Figure V.9), confirming that cell size is the main factor influencing the phytoplankton response to oil and PAH contamination (Othman et al., 2012; Bretherton et al., 2020a). On D01, nano- and microphytoplankton had similar growth

rates (~1 d^{-1}) (ANOVA, $p > 0.05$, Figure V.9a). After a few days (i.e. D04 and D08), these rates significantly decreased (by 1.5 - 2 folds relative to D01) (ANOVA, $p<0.05$, N = 9) while after 18 days, both size fractions showed regrowth with high rates (1.26 and 1.3 d^{-1}, respectively). Similarly, carbon biomasses for both size fractions fell from D01 to D08 and increased in D18 (Figure V.9b). These results confirmed those of Grami et al. (submitted), showing a decrease of Chl *a* and abundance for large phytoplankton from D01 to D08 and an increase on D18. Several authors have also showed a short-term inhibition and long-term outbreaks for large phytoplankton species, following oil spills (Pan et al., 2012; Ozhan et al., 2014). The short-term inhibition of growth for large phytoplankton could be due to direct negative effect of PAHs on the photosynthetic activity (Aksmann and Tukaj, 2008; Ben Othman et al., 2023), or to indirect effect of reduction in light penetration into water column caused by the petroleum slick after a few days of the oil leak (Fig. S1). The regrowth of nano- and microphytoplankton on D18 could be related to the attenuation of negative effect of oil (direct or indirect), since the oil was dispersed and seawater has recovered its color and smell before the spill (Grami et al. submitted).

Unlike nano- and micro-sized cells, growth rate of picophytoplankton was enhanced leading to increased carbon biomass from D01 to D08 (Figure V. 9). Others studies also reported a proliferation of small phytoplankton after oil spills (González et al., 2009; Huang et al., 2011) as well as their dominance, which is due to increased growth rate relatively to large cells (Quigg et al., 2021). On D18, there was an accumulation of picophytoplankton biomass (by 3-5 folds relatively to D04 and D08), despite that growth rate decreased. This suggest a reduction in top-down control of picophytoplankton by protozooplankton, as was stated in previous studies (Almeda et al., 2018; Gemmell et al., 2018; Deppeler et al., 2019).

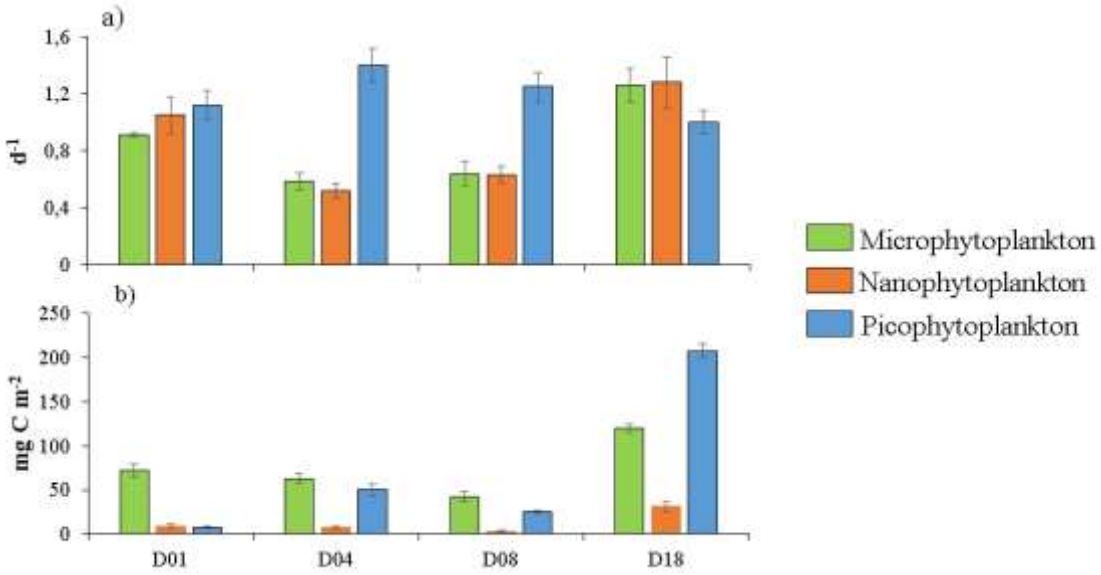

Figure V. 9. Growth rates (a) and biomasses (b) of size-fractioned phytoplankton during different days following the "Bizerte City" oil spill (Mean ± SD, N = 12)

3.2. Oil spill effect on protozooplankton community structure

Protozooplankton displayed significant changes in abundance (ANOVA, $p<0.01$, N = 12) and community structure following the oil spill (Figure V. 10), confirming the high sensitivity of these organisms to oil and PAHs at the cellular and subcellular levels (Pillai et al., 2003; Gomiero et al., 2013; Nogueira et al., 2017; Han et al., 2019). Moreover, the marked changes of total protozooplankton were observed after a few days of the oil leak (i.e. From D01 to D08), with strong decrease in total abundance (by 2 - 3.5 folds) and shift in community composition (Figure V. 10). This agrees with others works, reporting rapid response of protozooplankton to oil pollution and to PAHs (Almeda et al., 2013, 2014b; Pančić et al., 2019a). Protozooplankton community was composed by dinoflagellates, ciliates and HNF, which exhibited different oil responses among days after the oil leak.

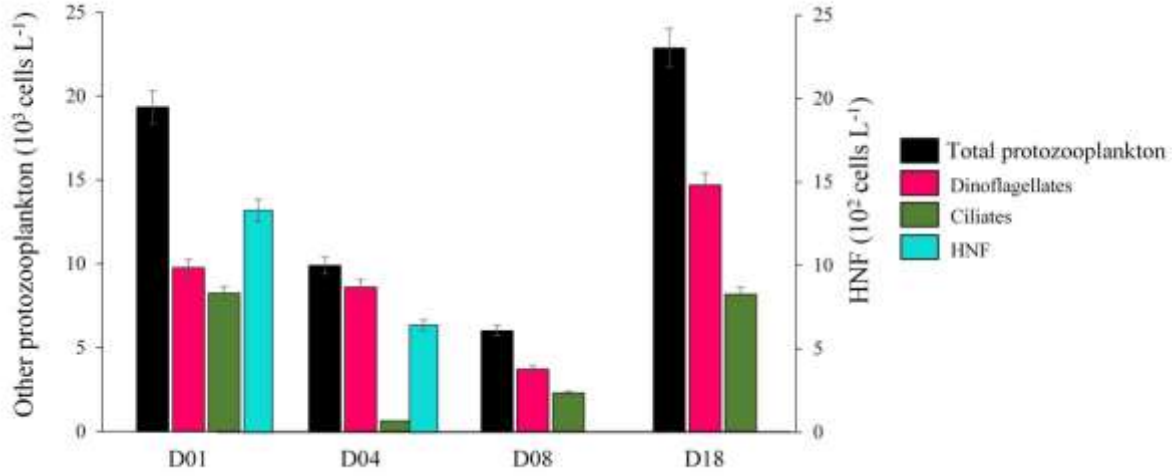

Figure V. 10. Abundances of total protozooplankton and taxonomic groups during differents days following the "Bizerte City" oil spill (Mean ± SD, N = 12)

Dinoflagellates were the dominant group from D01 to D08. They exhibited increased contribution to protozooplankton community from D01 (50%) to D04 (87%), i.e. during the contamination of the station water by oil (Fig. S1), while their abundance significantly decreased only on D08 (by 2.5 folds relatively to D01) (Figure V. 10). The dominance of dinoflagellates following short periods (1- 3 days) of oil spills has been observed in previous studies (Almeda et al., 2018; Setta, 2018; Bretherton et al., 2019). (Almeda et al., 2014b, 2018)) stated that these protozoans could tolerate crude oil at the concentrations found in the post-spill water column. The clearest impact within dinoflagellate community, was the strong decrease in abundance of heterotrophic organisms (ANOVA, $p<0.01$, N=9), with 39 - 60% contribution on D01/D04 and only 6% on D08, whereas abundance of mixotrophic organisms was unaffected (ANOVA, $p>0.05$, N=9) (Figure V. 11a). (Almeda et al., 2014b, 2018) showed also that growth of mixotrophic dinoflagellates is either unaffected or stimulated by oil. From a taxonomic point of view, there was a clear shift in the composition of both dinoflagellate groups, suggesting that oil had a direct effect on these protozoans by selecting tolerant species in detriment of sensitive species. The heterotrophic *Gyrodinium* was dominant (43% of dinoflagellate abundance) on D01 (Figure V. 11a), although the large oil presence in the station on this day (Fig. S1). The ability of the species *Gyrodinium spirale* to resist oil spill and to ingest its pollutants was already shown (Almeda et al., 2014b). Thus, the oil could be bio-accumulated inside their bodies and cause damage to their tissues, leading to decrease of their growth (Barron, 2017; Tang and Buskey, 2022b). This could explain to decrease of these species from D01 to D04 (10% of dinoflagellates) and subsequent disappearance on D08 (Fig. 4a). The heterotrophic

Protoperidinium, which was identified as an indicator of water pollution (Effiong et al., 2018) marked a weak presence on D08 (8%) relatively to D01 and D04 (20%) . The high sensitivity of *Protoperidinium sp.* to crude oil toxicity was recently reported by Tang and Buskey (2022). Conversely to heterotrophic dinoflagellates, the mixotrophic species showed increased contribution and became dominant on D08 (93%). This enhancement was mainly driven by species of *Heterocapsa*, with only a 20% contribution on D01, 40% of D04 but ≥ 60% on D08. Bretherton et al. (2020) have reported that *Heterocapsa pygmaea* was oil resistant and stated that mixotrophy favor the resistance of the specie to oil. It seems that under oil contamination, mixotrophs can cope with the oil toxicity on their photosynthesis by relying on source of organic carbon to maintain their growth. Besides the direct oil effect on dinoflagellates, petroleum pollutants could indirectly influence the dinoflagellate community, by modifying the availability and composition of their food items. Mixotrophic dinoflagellates have great nutritional plasticity, since they can consume a large spectrum of preys, from small to larger ones (Jeong et al., 2008, 2010a). Then, mixotrophs can exploit available preys regardless of size, after oil spill, which could give them more advantage than heterotrophic dinoflagellates, whose feeding is mainly based on large cells (Seong et al., 2006b; Jeong et al., 2010a; Bretherton et al., 2020b). Therefore, the decrease of the heterotrophic dinoflagellates (i.e. *Gyrodinium* and *Protoperidinium)* during D01-D08 (Figure V. 11a) could be regarded as a positive response to the inhibition of the growth of their potential large prey (i.e. nano- and microphytoplankton) due to oil spill (Figure V. 9). Recently, Mejri Kousri et al. (2023), assessing to effect of contaminated sediment on protozooplankton community of the Channel and Lagoon of Bizerte, reported also a decrease of heterotrophic *Gyrodinium* and *Protoperidinium* with a concomitant dominance of mixotrophic dinoflagellates. This emphasizes the fact that the mixotrophy is an important trait for the high adaptability of protozooplankton to different environmental stresses (López-Abbate, 2021), including oil pollution.

The oil contamination had a clear negative effect on ciliates and HNF, after a few days of the oil exposition (i.e. D01-D08). Total abundance of ciliates, which were 80 – 90% dominated by aloricate organisms (mainly *Strombidium* spp), showed a remarkable decrease (ANOVA, $p<0.01$, N=9) from D01 to D04 and D08 (by 12 and 4 folds, respectively) (Figure V. 11b). Our results agreed with those of Almeda et al. (2018) reporting a decrease in abundance of ciliates after short-term exposition to crude oil. Moreover, the sensitivity of *Strombidium* spp. to oil was previously observed (Gemmell et al., 2018). It has also been reported that ciliates are more

vulnerable than dinoflagellates to hydrocarbon toxicity (Almeda et al., 2014b). There was also a significant decrease (ANOVA, $p<0.01$, $N=9$) in HNF on D04 relatively to D01 (by 2 folds) with total disappearance on D08 (Figure V. 10). This result agrees with those of Almeda et al.(2018), reporting a diminution of HNF abundance with increasing oil concentration.

On D18, abundance of protozooplankton largely increased relatively to D08 (by 4 folds, Fig. 3). Grami et al. (submitted) reported that the oil was dispersed by hydrodynamical and climatic conditions on D18 and there was a return of environmental conditions before the oil incident. Hence, the negative effect of oil could be attenuated on this day, leading to the enhancement of protozooplankton. The recovery of growth was observed for both groups of dinoflagellates (mixotrophs and heterotrophs) and ciliates (aloricate and loricates) (Figure V. 11). On D18, there was significant increase in growth and biomass of nano- and microphytoplankton, which are potential prey for these protozoans. This may partially explain the stimulation of protozooplankton, since protozoan growth is known to be regulated by the availability of food items (Sobczak et al., 2002; Mejri Kousri et al., 2023). Unlike the others groups, HNF did not appear on D18, testifying to their high sensitivity to oil or their great exploitation by growing ciliate and dinoflagellates. These observations are in conflict with the study of Pančić et al.(2019) which showed that after 14 days of monitoring, chemically dispersed oil resulted in increased growth of bacteria and HNF, but decreased growth of dinoflagellates and ciliates.

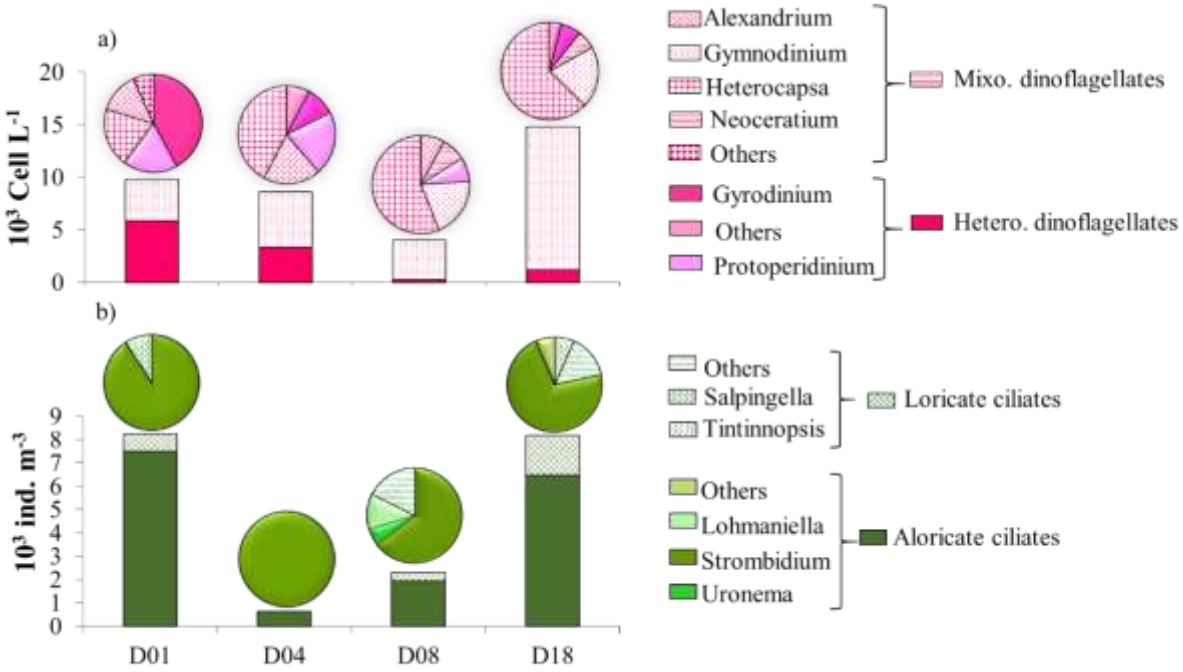

Figure V. 11. Compositions of dinoflagellates (mixotrophic and heterotrophic organisms) (a) and ciliates (aloricate and loricate organisms) (b) during differents days following the "Bizerte City" oil spill.

3.3. Oil spill effect on grazing activity of protozooplankton

Protozooplankton, are distinguished by their great ability to feed on various types of prey and their rapid response to changes in food availability (Strom and Morello, 1998; Hansen and Calado, 1999). It was a major consumer of phytoplankton production in several marine ecosystems (Strom et al., 2001; Calbet and Landry, 2004; Sakka Hlaili et al., 2014). Thereby, protozooplankton grazing represents a critical process in the structuring of the food web given its crucial role in the transfer of biogenic carbon to metazoan and higher trophic levels (Calbet and Saiz, 2005; Laender et al., 2010; Zeldis and Décima, 2020). So assessing the impact of oil contamination on protozooplankton feeding would be of great significance.

During our study, protozooplankton were able to exert significant grazing pressure on various phytoplankton prey throughout days after the oil spill, with rates ranging from 0.1 to 1 d^{-1}. Contrary to our work, Tang and Buskey (2022) observed a strong inhibition of protozooplankton feeding with negative grazing rates following oil exposition. In our study, protozooplankton was sampled from the Channel of Bizerte, which is highly impacted by PAHs

(Barhoumi et al., 2014) since it supports the oil tankers traffic, suggesting that the Channel protozoans are well adapted to the oil compounds. These grazers could be negatively affected by oil but they can keep their growth and physiologic activity at lower rates without total inhibition.

Oil contamination induced different effects on grazing activity of protozooplankton according to the prey and the day (Figure V. 12). For nano- and microphytoplankton, the grazing mortality rates significantly decreased after a few days of oil spill and re-increased on D18. A positive trophic feedback between growth of prey and their grazing is generally found (Sakka Hlaili et al., 2007; Chen et al., 2009; Mejri Kousri et al., 2023). In our study, the grazing mortality rates for the two size fractions showed indeed a temporal evolution post- spill similar to that of their growth rates (Figure V. 9). During our sampling, the community structure of protozooplankton was shifted following the oil leak, with a sharp decrease, from D01 to D08, in dinoflagellates and particularly for heterotrophic *Gyrodinium* and *Protoperidinium* (Figure V. 11) which are known to feed on large prey. Accordingly, grazing of protozooplankton on large phytoplankton decreased during this short period. Tang and Buskey (2022) have reported a decrease in grazing of *Protoperidinium* on large cells (such as diatoms) when exposed to crude oil. The oil pollutants can have detrimental consequences on the physiological status and nutritional quality of nano- and microphytoplankton, thereby reducing their edibility by the protozooplankton. On D18, large cell-consumers, such as loricate ciliates and heterotrophic/mixotrophic dinoflagllates, significantly increased (Figure V. 11), so probably increasing their grazing pressure on nano- and microphytoplankton.

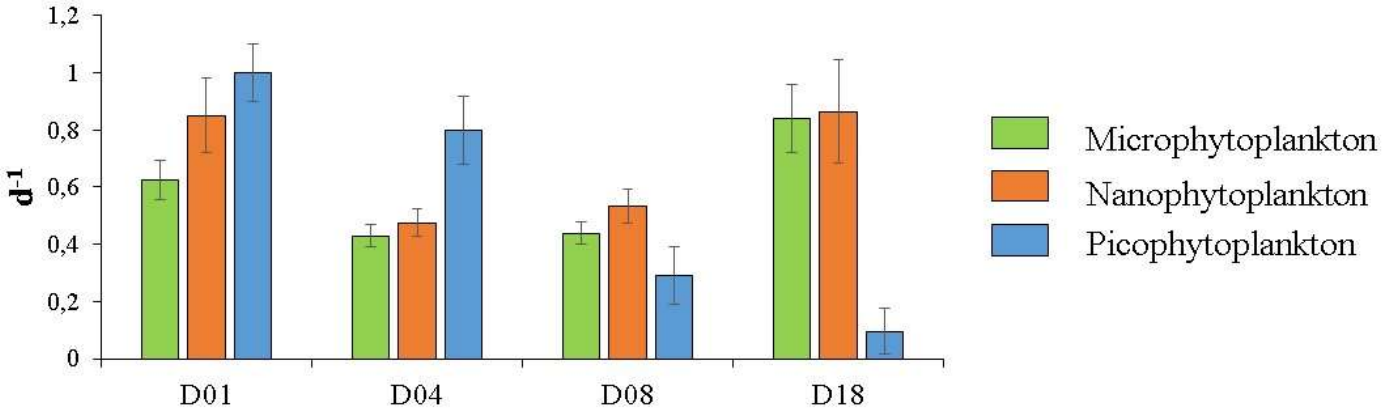

Figure V. 12. Grazing rates on size-fractioned phytoplankton during different days following the "Bizerte City" oil spill (Mean ± SD, N = 12)

Protozooplankton grazing on picophytoplankton decreased gradually from D01 to D18, when it reached very low rate, despite the picoalgal growth displayed significant increase from D01 to D08 (Figure V. 9). The low grazing pressure on picophytopalnkton could be related to the total disappearance of HNF from D08 (Figure V. 10), recalling that HNF are known as major consumers of pico-sized preys (Azam et al., 1983; Caron, 1990). Accordingly, there was an accumulation of picophytoplankton biomass on D18 (Figure V. 9). Several authors have effectively stated that release from grazing is a major cause for the increase of phytoplankton biomass following an oil spill event (Ozhan et al., 2014; Almeda et al., 2018; Cadaillon, 2018; Cederwall et al., 2020) Also, Tang and Buskey (2022) reported that a de-coupling between phytoplankton growth and protozooplankton grazing following oil contamination can promote phytoplankton biomass.

3.4. Oil spill effect on the planktonic food web

Our results showed that oil pollution have different effects on growth and biomass of phytoplankton size fractions, which would influence their carbon production rates. Moreover, protozooplankton groups exhibited various oil responses, with the replacement of vulnerable taxa by tolerant organisms, which have different functional role and feeding selectivity. This provoked significant modification in grazing rates on size-fractioned phytoplankton that can produce cascading impacts on trophic interactions. So the observed oil-induced changes in phytoplankton production rates and their consumption rates by protozooplankton were

integrated in carbon flows models in order to give the first insight on the impact of oil spill on the functioning of food webs and possible consequence on the carbon export. Estimated flows by the LIM-MCMC analysis are given in Table V. 4. Evolution of carbon production (inputs), loss (outputs) and throughput as well as zooplankton feeding during different days after the oil spill are summarized in Figure V. 13.

Table V. 4. Mean values of the fluxes estimated by the LIM-MCMC analysis for each sampling day after the "Bizerte city" oil spill (Mean value± SD).

Flow description	Symbol	Interfered value (mg C m^{-2} d^{-1})			
		D01	D04	D08	D18
Microphytoplankton gross primary production	GPP-MIC	64.51 ± 9.1	59.08 ±8.4	45.91 ±6.5	179.57 ±25
Nanophytoplankton gross primary production	GPP-NAN	7.06 ±1.0	5.03 ±0.7	2.49 ±0.4	60.46 ±8.6
Picophytoplankton gross primary production	GPP-PIC	2.78 ±0.4	78.00 ±11	49.10 ±6.9	396.22 ±56
Microphytoplankton respiration	MIC-RES	5.35 ±0.8	4.87 ±0.7	3.03 ±0.4	17.73 ±2.5
Microphytoplankton dissolved organic carbon exudation	MIC-DOC	8.30 ±1.2	7.37 ±1.0	4.99 ±0.7	27.15 ±3.8
Microphytoplankton net production	MIC-DET	2.54 ±0.4	2.43 ±0.3	0.73 ±0.1	8.15 ±1.2
Microphytoplankton grazing by protozooplankton	MIC-PRO	29.21 ±4.1	35.25 ±5.0	22.69 ±3.2	120.8 ±17.1
Microphytoplankton grazing by metazooplankton	MIC-MET	17.23 ±2.4	7.46 ±1.1	13.81 ±2.0	31.27 ±4.4
Microphytoplankton sinking	MIC-LOS	1.95 ±0.3	1.74 ±0.2	0.66 ±0.1	6.60 ±0.9
Nanophytoplankton respiration	NAN-RES	0.52 ±0.1	0.35 ±0.05	0.19 ±0.03	5.42 ±0.8
Nanophytoplankton dissolved organic carbon exudation	NAN-DOC	0.81 ±0.1	0.57 ±0.1	0.29 ±0.04	7.81 ±1.1
Nanophytoplankton detritus production	NAN-DET	0.16 ±0.02	0.09 ±0.01	0.06 ±0.01	2.30 ±0.33
Nanophytoplankton grazing by protozooplankton	NAN-PRO	5.23 ±0.7	3.85 ±0.5	1.82 ±0.3	35.86 ±5.1
Nanophytoplankton grazing by metazooplankton	NAN-MET	0.17 ±0.02	0.09 ±0.01	0.06 ±0.01	7.36 ±1.04
Nanophytoplankton sinking	NAN-LOS	0.16 ±0.02	0.09 ±0.01	0.06 ±0.01	2.15 ±0.30
Picophytoplankton respiration	PIC-RES	0.17 ±0.02	18.17 ±2.57	13.06 ±1.85	75.95 ±10.74
Picophytoplankton dissolved organic carbon exudation	PIC-DOC	0.29 ±0.04	21.05 ±2.98	10.70 ±1.51	86.95 ±12.30
Picophytoplankton grazing by protozooplankton	PIC-PRO	17.72 ±2.5	57.91 ±8.2	12.03 ±1.7	34.09 ±4.8
Picphytoplankton sinking	PIC- LOS	-	-	12.08 ±1.7	185.4 ±26.2
Protozooplankton respiration	PRO-RES	15.72 ±2.2	39.25 ±5.6	16.29 ±2.3	82.74 ±11.7
Protozooplankton dissolved organic carbon excretion	PRO-DOC	8.66 ±1.2	21.83 ±3.1	9.01 ±1.3	49.85 ±7.0
Protozooplankton detritus production	PRO-DET	7.43 ±1.1	21.34 ±3.0	7.77 ±1.1	42.53 ±6.0
Protozooplankton consumption by MET	PRO-MET	13.83 ±2.0	37.90 ±5.4	14.79 ±2.1	117.7 ±16.6
Metazooplankton respiration	MET-RES	10.89 ±1.5	23.45 ±3.3	10.03 ±1.4	60.54 ±8.6
Metazooplankton dissolved organic carbon excretion	MET-DOC	5.91 ±0.8	12.55 ±1.8	5.38 ±0.8	33.30 ±4.7
Metazooplankton detritus production	MET-DET	5.13 ±0.7	12.08 ±1.7	4.71 ±0.7	28.95 ±4.1
Metazooplankton sinking	MET-LOS	11.06 ±1.6	23.12 ±3.3	10.16 ±1.4	61.15 ±8.6
Bacterial respiration	BAC-RES	16.53 ±2.3	33.42 ±4.7	18.65 ±2.6	107.12 ±15.1
Bacterial dissolved organic carbon production	BAC-DOC	8.41 ±1.2	17.77 ±2.5	9.64 ±1.4	61.04 ±8.6
Bacterial grazing by protozooplankton	BAC-PRO	8.87 ±1.3	23.31 ±3.3	11.32 ±1.6	102.11 ±14.4
Dissolved organic carbon uptake by bacteria	DOC-BAC	33.81 ±4.8	74.49 ±10.5	39.62 ±5.6	270.27 ±38.2
Dissolved organic carbon output	DOC-LOS	7.11 ±1.0	12.51 ±1.8	7.54 ±1.1	30.52 ±4.3
Detritus dissolution	DET-DOC	8.55 ±1.2	5.89 ±0.8	7.14 ±1.0	34.69 ±4.9
Detritus consumption by metazooplankton	DET-MET	1.74 ±0.2	25.73 ±3.6	1.61 ±0.2	27.59 ±3.9
Detritus sinking	DET-LOS	4.97 ±0.7	4.31 ±0.6	4.51 ±0.6	19.64 ±2.8

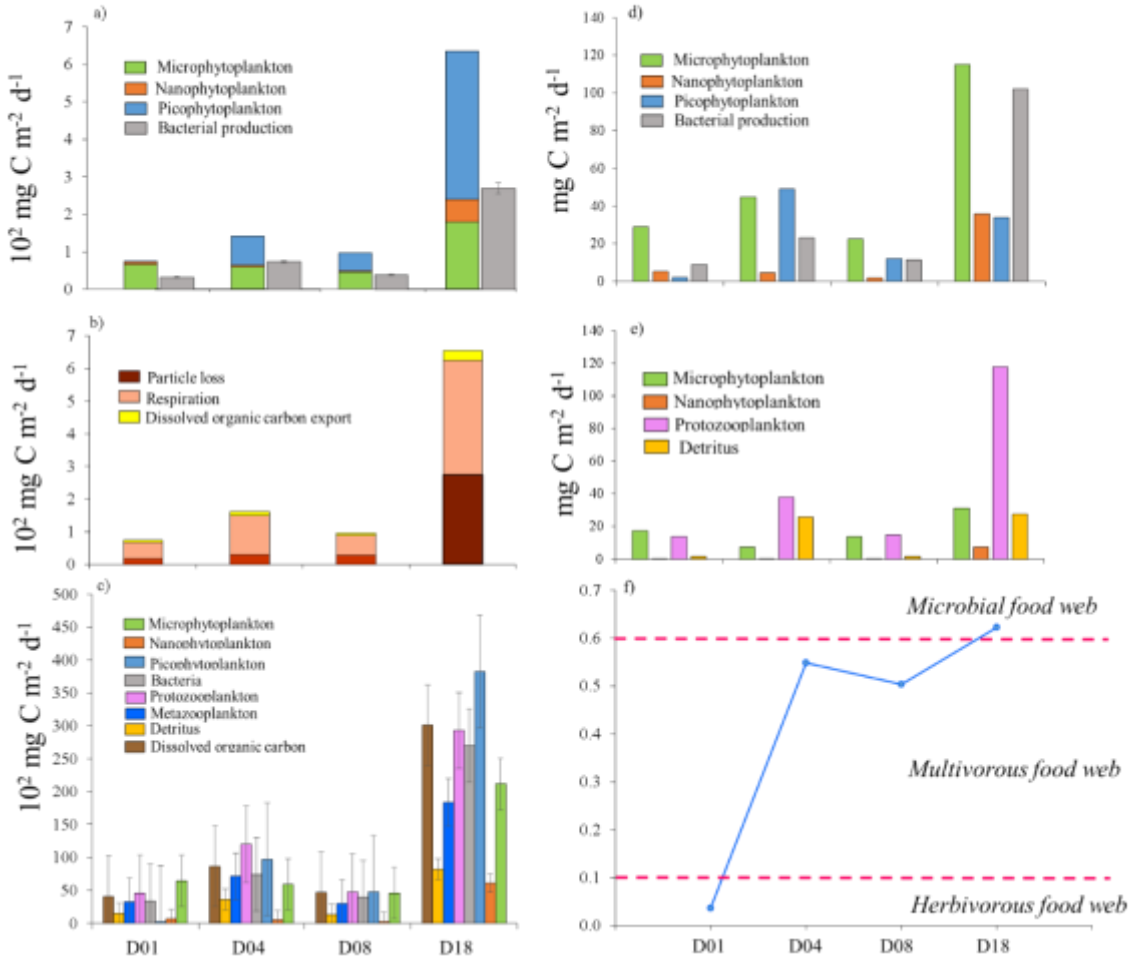

Figure V. 13. Evolution of food web characteristics (carbon production (a), carbon loss (b), carbon throughput (c), diet of protozooplankton(d) and diet of metazooplankton (e)) and typology (R7 ratio(f)) during different days following the "Bizerte City" oil spill

During all days, food web was only powered by the phytoplankton primary production (PP), which showed significant variations among sampling days (ANOVA, $p<0.01$, N=12). PP was low on D01 (75 mg C m^{-2} d^{-1}), increased by 1.5 – 2 folds on D04/D08 (98-142 mg C m^{-2} d^{-1}) and reached 8 folds higher value in D18 (636 mg C m^{-2} d^{-1}) (Figure V. 13a). Previous modelling works, conducted in the Bizerte Channel and Lagoon have showed also that the photosynthetic carbon input was sufficient to support the functioning of food-web during fall and other seasons (Grami et al., 2008a; Meddeb et al., 2019). However, these studies have found

much higher primary production values (358-1872 mg C m^{-2} d^{-1}) than our estimated values from D01 to D08. This suggests a short-term negative effect of oil spill on primary production, as expected. PP measured on D18 was similar to what is usually found during non-oil spill condition in fall. It was therefore clear that the negative oil effect faded in the long-term, as it was observed for the phytoplankton growth and biomass (Figure V. 9). The size composition of PP has also changed following the oil spill. Microphytoplankton largely dominated the PP on D01 (87%), while PP was roughly shared between micro- and picophytoplankton on D04 and D08. In the opposite, picophytoplankton was the main primary producers on D18 (63%). Bacterial production (BP) responded to oil exposure similarly to PP (Figure V. 13a), since bacterial growth tightly depends on the phytoplankton dissolved organic carbon (DOC) exudation (Van den Meersche et al., 2004; Thornton, 2014). Rates of BP measured on all sampling days (34 – 270 mg C m^{-2} d^{-1}) were in the range of estimations during non-oil contamination condition (34-288 mg C m^{-2} d^{-1}, (Grami et al., 2008a); 34 - 189, mg C m^{-2} d^{-1}, (Meddeb et al., 2018). This indicates that bacteria were unaffected by the petroleum hydrocarbons, which can serve as source of carbon to bacterial growth. Several studies have reported that bacterial communities are able to rapidly adapt to oil spills through the selective development of strains that degrade oil (Bælum et al., 2012; Kimes et al., 2014; Bacosa et al., 2015; Wanjohi et al., 2015). (Coral and Karagoz, 2005) revealed the use of carbon-rich oil by bacteria to satisfy their cell growth and energy requirements. In addition, (Wanjohi et al., 2015)) reported that certain bacteria, which are capable of degrading petroleum, can be used to remediate the environment of petroleum contaminants. In our study, the average BP/BP ratio was 0.43 for most days, which was close to the global scale value (0.3; (Cole et al., 1988).

During each day, carbon outputs were mainly driven by respiration of all organisms (44 – 69%) and particle loss (24 – 50%). These flows were low from D01 to D08 (74- 161 mg C m^{-2} d^{-1}) but largely increased on D18 (655 mg C m^{-2} d^{-1}) (ANOVA, $p<0.05$, N=12, Figure V. 13b). In short-term, oil contamination negatively affected phytoplankton, protozooplankton (Figures V. 9,10) and probably metazooplankton, as shown by several previous studies (El-Serehy and Al-Darmaky, 2003; Jiang et al., 2012; Almeda et al., 2013). It is therefore normal that the respiration of these organisms and their loss (mainly by sinking), were low. These output flows increased on D18 in response to the regrowth of phytoplankton and protozooplankton and probably of metazooplankton.

Carbon throughput, which indicated the activity of each compartment, displayed also significant change among sampling days for all compartments (ANOVA, $p<0.05$, N=12, Figure V. 13c), with higher value on D18 relatively to other days. On D01, the most active compartments was microphytoplankton, followed by protozooplankton, bacteria and metazooplankton, suggesting their important role, as producers and grazers. However, picophytoplankton had the lowest throughput, which was consistent with its low production and respiration (Table V. 4). During the other days, the activity of picophytoplankton increased, as did its production rate (Figure V. 13a) and became similar to that of others living compartments. Although protozooplankton was highly active compartment during the entire study period, its consumption rates on different prey significantly varied among days (ANOVA, $p<0.01$, N=12, Table V. 4), which means that its functional role, as microbivore (i.e. small-cells consumer) or herbivore (i.e. large-cells consumer) fluctuated. Consumption rate of metazooplankton on each food item displayed also large variation among days (ANOVA, $p<0.01$, N=12, Table V. 4), indicating that herbivory, carnivory or detritivory of metazoans should play different role in channeling carbon. To elucidate the real role of each grazer's group in the food web during days after the oil spill, the compositions of their diets were analyzed.

On D01, the protozooplankton feeding was mainly based on herbivory, since microphytoplankton represented the main prey consumed, forming 64% of its diet (Figure V. 13d). On this day, we also found high consumption rate on microphuytoplankton (Table V. 4), which could be mainly assigned to the dominant heterotrophic dinoflagellates (i.e. *Gyrodinium* and *Protoperidinium*, Figure V. 11a). Nanophytoplankton and bacteria formed 11% and 19% of the total consumption of protozooplankton, while picophytopalnkton contributed only 5%. On D04 and D08, the feeding of protozooplankton has changed, with an increased contribution of picophytoplankton (25 – 40%) to its diet, but its herbivory remained quite significant, as microphytoplankton formed 38 – 48% of the consumed carbon. Bacteria were also potential prey for protozooplankton, forming 19 – 23 % of its diet, while nanophytoplankton represented only 4%. During both days, mixotrophs, such as *Gymnodinium* and *Heterocapsa*, which are known to feed on variety of sized-items, were dominant (Figure V. 11a). On D18, the herbivory played also a significant role in the feeding of protozooplankton, half of whose food was provide by micro- and nanophytoplankton. This coincided with a resumption of mixotrophic/heterotrophic dinoflagellates and ciliates, including large loricate organisms (Figure V. 11). In contrast, picophytoplankton formed only 12% of

protozooplankton diet, since the small protozoans, such as HNF, had disappeared (Figure V. 10). Despite this, 40% of protozooplankton feeding was based on the bacterivory, which could be related to the high proliferation of *Strombidium*. These ciliates are reported as important bacterivorous (Bernard and Rassoulzadegan, 1990; Mari et al., 2004; W.-L. Chen et al., 2020). In fact, food item size is a selective criterion for protozooplankton, but the physiological state of prey can also influence their grazing. Recently, prey selectivity by *Strombidium* has already been reported by (W.-L. Chen et al., 2020) who showed that this genus feeds mainly on bacteria when the relative concentration of algae is low. Bacteria, especially hydrocarbon-degrading species, are generally stimulated by oil spills (Bælum et al., 2012; Kimes et al., 2014; Wanjohi et al., 2015) , which can increase their nutritional quality thereby enhancing their selectivity and consumption by small protozooplankton (such as *Strombidium*) relatively to other small prey.

Diet of metazooplankton also showed a clear change after oil exposure (Figure V. 13e). These grazers fed mainly on microphytoplankton and protozooplankton during most days, with increasing contribution of protozooplankton from D01 to D18, parallel to the proliferation and the dominance of the mixotroph *Heterocapsa* (Figure V. 11a). (Almeda et al., 2014a) reported also that *Heterocapsa sp.* was the main species used as food by metazoans in dispersed crude oil conditions. metazooplankton have been identified as a useful sentinel organism for oil pollution (Carls et al., 2006). They act as a conductor for the movement of oil-derived contamination and other persistent organic pollutants through the marine food web (Sobek et al., 2006; Hallanger et al., 2011). Therefore, disturbance of metazooplankton can have a significant impact on the entire food web by transferring harmful effects to higher trophic levels in polluted ecosystems.

To highlight the change in trophic pathways from D01 to D18, we use a typology ratio (R7 ratio: picophytoplankton net production divided by total phytoplankton net production), proposed by (Sakka Hlaili et al., 2014) as an operational criterion to discriminate between herbivorous ($R7 \leq 0.1$), multivorous ($0.1 < R7 < 0.6$), and microbial food webs. ($R7 \geq 0.6$). As expected, the oil spill was followed by clear modification in food web structure along the evolution of the oil spill (Figure V. 13f). On D01, carbon seemed to be channelled through herbivorous food web ($R7 = 0.04$). After a few days (i.e. D04 and D08), the carbon transfer pathway was acting as multivorous ($R7 = 0.50$), while it evolved into microbial food web on

D18 (R7 = 0.63). The disruption in the structuring of food web was firstly due to different oil-induced changes in phytoplankton community, since the sensitivity or tolerance to oil and PAHs was widely specie- and size-dependent (Ozhan et al., 2014; Bretherton et al., 2018, 2020a; Ben Othman et al., 2023). Secondly, the rapid response of protozooplankton at structural and functional levels, as shown in our study and previous one (Almeda et al., 2014b; Pančić et al., 2019b; González et al., 2022; Tang and Buskey, 2022b), can obviously induce significant change in trophic interactions. The changes in the food web structure following different days of oil spill suggest that the biogenic carbon would be channeled to higher consumers with different efficiencies. Indeed, herbivorous and multivorous pathways can channel a large amount of carbon to higher consumers, while microbial food web is less efficient, since most carbon can be lost and remineralised (Legendre and Gosselin, 1989; Legendre and Rassoulzadegan, 1995; Sakka Hlaili et al., 2008).

Interestingly, (Meddeb et al., 2019), based on LIM-MCMC analysis, found a microbial food web in the Bizerte Channel during the same period as our study but under non-oil spill condition. One could therefore ask whether 18 days were sufficient for the system to recover its stability and balance state or not? Figure V. 14. presents a comparative diagram between trophic interactions within the microbial food web found by (Meddeb et al., 2019) under non-oil spill accident (non-spill) and by our study on D18 (D_{18}-spill). For both microbial pathways, carbon production showed the same trend, with dominance of production of picophytoplankton (225- 382 mg C m^{-2} d^{-1}) followed by bacteria (172-270 mg C m^{-2} d^{-1}) and lower rates for microphytopalnkton (144-212 mg C m^{-2} d^{-1}) and nanophytoplankton (5-61 mg C m^{-2} d^{-1}). However, protozooplankton displayed differential role between the two microbial food webs. Under non-spill condition, small protozooplankton, including both aloricate ciliates and HNF, fed more on picophytoplankton relative to bacteria, while nano- and microphytoplankton undergone a weak top-down control by protozoopla nkton. In contrast, in our D_{18}-spill food web, the microbivory was carried particularly on bacteria, since picophytoplankton was weakly consumed in spite of its high production. Moreover, nano- and microphytoplan kton contributed more to the consumption of protozooplankton that during non-spill condition. It is therefore clear, that microbial food web observed on D18 after the oil spill did not really correspond to that observed during non-spill period. The D_{18}-spill food web was based on the consumption of bacteria and microphytoplan kton, while picophytoplankton biomass was accumulated due to a de-coupling between its growth rate and grazing. The difference of the two microbial food webs

(i.e. non-spill and D_{18}-spill) may indicate that the system could still be disturbed and has not found its initial equilibrium state, i.e. its stability.

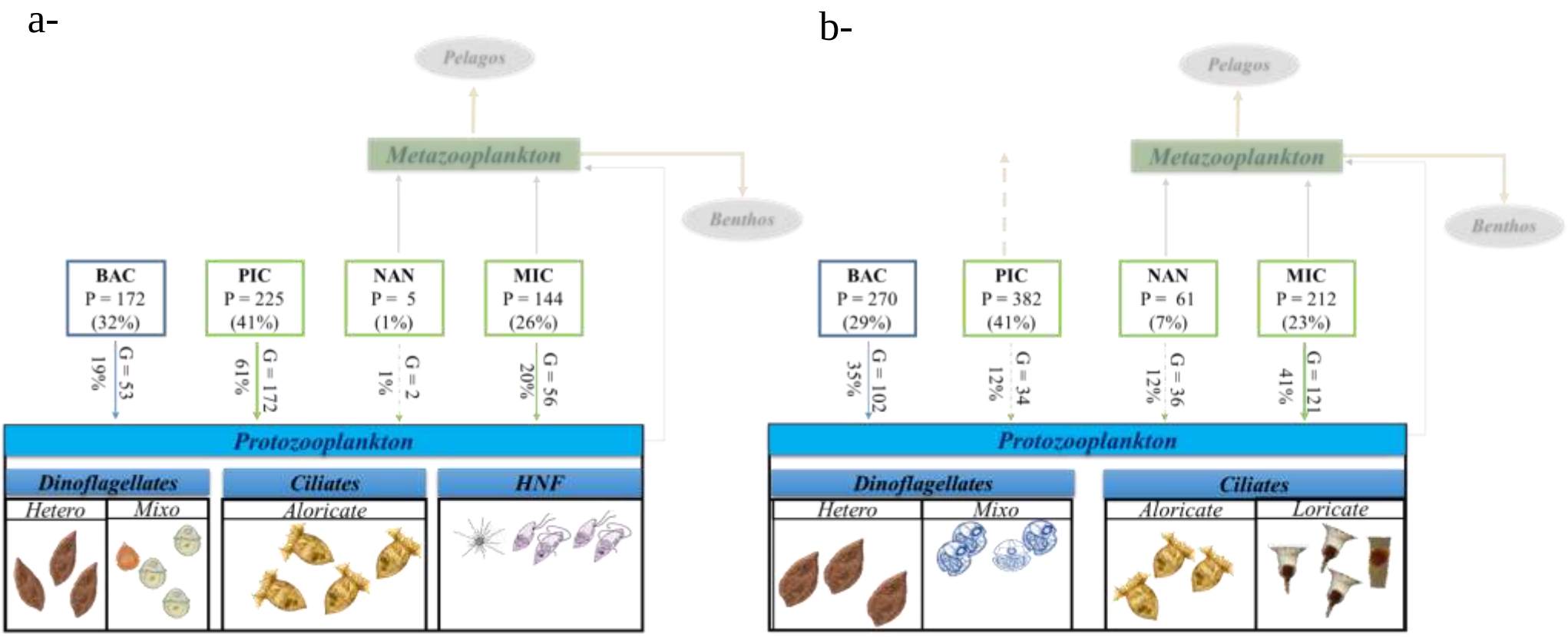

Figure V. 14. Comparative diagram of two microbial food webs found under non-spill condition (from Meddeb et al. 2019) (a) and after 18 days (b) of the "Bizerte City" oil spill. % in the boxes: percentage of carbon production; % next to the arrows: percentage of carbon consumed.

4. Conclusion

Our study clearly showed that oil spill had signiifcnat effects on phytoplankton growth, protozooplank structure and feeding activity from early stage to longer period after the spill. These effect were followed by significant changes on rates of primary production and consumption of phytoplankton by protozooplankton. Integrate these oil-modified rates into inverse carbon flux models allowed us to demonstrate a clear shift in food web structure from herbivores (D01) to multivores (D04/D08) and microbial pathway (D18), implying different carbon export efficiencies throughout the oil spill. In general, the stability of an ecosystem can be expressed either by its resistance to change or by its resilience, which is related to the capacity to recover after a perturbation. Therefore, to go further, a second step of the analysis could use ecological analyses (ENA and Typology ratios) in order to characterize the resistance and resilience of the ecosystem and understand its functional response to a punctual disruption, such as the petroleum accident.

Références (voir références bibliographiques)

Annexes

Field study on natural phytoplankton throughout "Bizerte City" oil spill on the south-western Cost of the Mediterranean Sea

Grami Boutheina [a,b], Oumayma Chkili [a,c,e], Melliti Ben Garali Sondes [a,c], Mejri Kousri Kaouther[a,d], Meddeb Marouan[a], Lassaad Chouba[d], Nathalie Niquil[e], Sakka Hlaili Asma [a,c,*]

Table S1. Average dissimilarity in community composition of microphytoplankton and nanophytoplankton among days following the oil spill of Bizerte.

	Microphytoplankton			Nanophytoplankton		
	D04	**D08**	**D18**	**D04**	**D08**	**D18**
D01	54% ± 3.5	58% ± 4.7	64% ± 3.4	51% ± 2.1	51% ± 3.8	64% ± 3.3
D04		44% ± 1.5	62% ± 1.8		41% ± 1.6	66% ± ??1.3
D08			69% ± 1.7			65% ± 1.9

Novel insight into the oil impact on the protozooplankton, trophic interactions and food web structure: field and modelling study

Oumayma Chkili[1,2,3], Sondes Melliti Ben Garali[1,2], Kaouther Mejri Kousri[1], Marouan Meddeb[1,2], Nathalie Niquil[3], Asma Sakka Hlaili[1,2*]

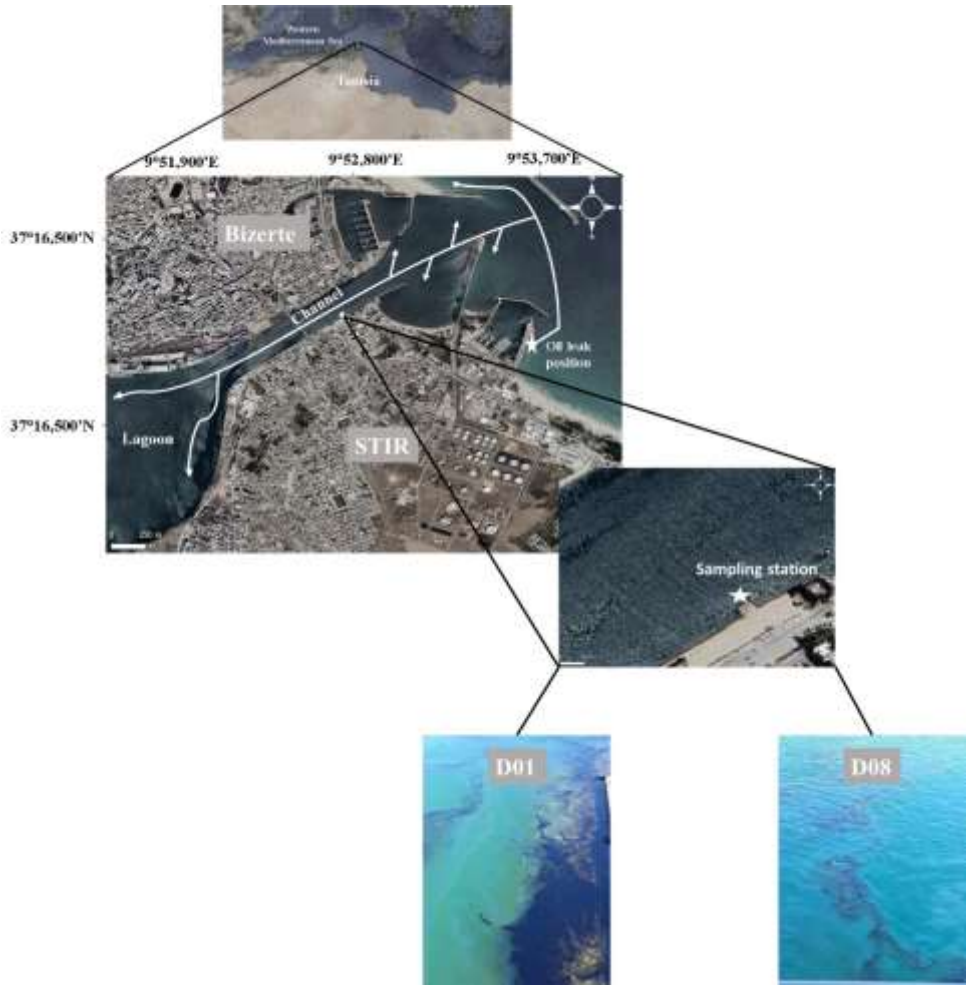

Fig. S1. Position of the oil leak from the Tunisian Society of Refining Industries (STIR) and location of the sampling station in the Bizerte Channel (North of Tunisia). Arrows illustate the trajectory of oil spread. Photos show the oil slick on D01 and D08

Table S1. Mass equilibrium defining the linear equations used for the inverse LIM-MCMC analysis. Each flow is composed of the first three-letter code of the original compartment followed by the first three-letter code of the destination compartment. Abbreviations: GPP, gross primary production; RES, respiration; LOS, loss for the considered system. The PIC-LOS flow marked in thick blue is added only in the equations of two models D08 and D18.

Mass balance equation for each compartment	Equations of the four models
Mass balance for picophytoplankton (PIC)	GPP-PIC – (PIC-RES + PIC-DOC + PIC-PRO(**+PIC-LOS)**) = 0
Mass balance for nanophytoplankton (NAN)	GPP-NAN – (NAN-RES + NAN-DOC + NAN-DET + NAN-PRO + NAN-MET + NAN-LOS) = 0
Mass balance for microphytoplankton (MIC)	GPP-MIC – (MIC-RES + MIC-DOC + MIC-DET + MIC-PRO + MIC-MET + MIC-LOS) = 0
Mass balance for protozooplankton (PRO)	(PIC-PRO + NAN-PRO + MIC-PRO + BAC-PRO) – (PRO-RES + PRO-DOC + PRO-DET + PRO-MET) = 0
Mass balance for metazooplankton (MET)	(NAN-MET + MIC-MET + PRO-MET + DET-MET) − (MET-RES + MET-DOC + MET-DET + MET-LOS) = 0
Mass balance for bacterioplankton (BAC)	DOC-BAC – (BAC-RES + BAC-DOC + BAC-PRO) = 0
Mass balance for dissolved organic carbon (DOC)	(PIC-DOC + NAN-DOC + MIC-DOC + PRO-DOC + MET-DOC + BAC-DOC + DET-DOC) - (DOC-BAC + DOC-LOS) = 0
Mass balance for detritus (DET)	(NAN-DET + MIC-DET + PRO-DET + MET-DET) – (DET-DOC + DET-MET + DET-LOS) = 0

Table S2. Minimum and maximum flows (mg C m^{-2} d^{-1}) estimated in the field and used as inequalities for the networks of four days of monitoring in the channel of bizerte.

Fluxes	**D01**		**D04**		**D08**		**D18**	
	Min	max	min	max	min	max	min	max
GPP-MIC	54.66	66.80	50.02	61.14	40.47	46.68	179.3	219.1
GPP-NAN	5.93	7.24	4.49	5.13	2.12	2.56	51.86	63.38
GPP-PIC	2.30	2.81	87.63	107.11	44.19	54.01	340.7	416.4
MIC-PRO	27.36	33.45	33.33	40.74	21.99	26.27	113.00	138.1
NAN-PRO	5.17	6.20	3.76	4.31	1.76	2.14	33.69	41.17
PIC-PRO	2.30	2.81	50.84	62.14	10.44	12.76	30.45	35.79

Table S3. Constraints used on different planktonic food web networks

Process		Bound	Description	Equation	Reference
Respiration	**PIC NAN MIC**	Upper and lower	Autotrophic respiration ranges between 5% and 30% of their GPP	5% GPP < R < 30% GPP	Vézina and Platt (1988)
	BAC	Lower	Bacterial respiration (R') is higher than 20% of the total uptake of DOC (U_{DOC})	20% U_{DOC} < R'	Vézina and Savenkoff (1999)
	PRO MET	Lower	Zooplankton respiration (R'') is at least 20% of their total ingestion (ΣIng) and does not exceed its maximum specific respiration	20% ΣIng < R''	Vézina and Savenkoff (1999)
DOC production	**PIC NAN MIC**	Upper and lower	Phytoplankton DOC exudation (E) ranges between 10% and 55% of net primary production (NPP)	10% NPP < E < 55% NPP	Vézina and Savenkoff (1999)
	PRO MET	Upper and lower	Zooplankton excretion of DOC (EX) is at least 10% of their total ingestion (ΣIng) and does not exceed its respiration (R'')	10% ΣIng < EX < R"	Vézina and Platt (1988) Vézina and Pace (1994)
	BAC	Upper	Bacterial DOC release (RE) is lower than respiration (R')	RE<R'	Vézina and Pace (1994)
Growth efficiency	**PRO MET**	Upper and lower	Growth efficiency is at least 25% and no more than 50% of total ingestion (ΣIng)	25% ΣIng < ΣIng -(R" + EX +DET) < 50% ΣIng	Vézina and Pahlow (2003)
	BAC	Upper and lower	Growth efficiency of bacterioplankton ranges between 5% and 50% of their total ingestion	0.5 U_{DOC} < U_{DOC} - (r'' + re) < 0.50U_{DOC}	Vézina and Pahlow (2003)
Assimilation efficiency	**PRO MET**	Upper and lower	Assimilation efficiency of zooplankton ranges between 50% and 90% of their total ingestion (ΣIng)	50% ΣIng < Ing -DET < 90% ΣIng	Vézina et al. (2000)
Detritus production	**PRO MET**	Upper and lower	Zooplankton DET production (zoo-DET) is no more than 42% of their combined DET production and respiration (zoo-RES) and is at least 5% of it	5% (zoo-DET + zoo-RES) < zoo-DET < 42% (zoo-DET + zoo-RES)	Steinberg et al. (2000)
Detritus dissolution	**DET**	Upper	The upper bound of DET dissolution (DET-DOC) is 10% of net primary production (NPP)	10% NPP < DET-DOC	Pace et al.(1984)
		lower	DET dissolution (DET-DOC) is at least 10% of DET production	10% DET production <DET-DOC	
Preferential ingestion of MET		Upper	Ingestion of e.g., nanophytoplankton by metazooplankton does not exceed the estimated maximum prey availability	NAN-MET < NANMET.A(t) × Ing-MET MIC-MET < MICMET.A(t) × Ing-MET PRO-MET < PROMET.A(t) × Ing-MET DET-MET < DETMET.A(t) × Ing-MET	Haraldsson et al. (2018)

Discussion Générale

Cette discussion a pour objectif de faire le point sur les progrès réalisés au cours des trois années de la thèse, mais aussi de proposer de nouvelles réflexions pour aller plus loin dans l'étude de l'état de santé des écosystèmes marins et de l'effet de la contamination chronique et pulsée sur leurs fonctionnements et structures.

L'objectif de la thèse était de caractériser l'état de santé des écosystèmes côtiers sud méditerranéens anthropisés à partir du fonctionnement du réseau trophique planctonique en situation de contamination chronique ou pulsée. La thèse a permis d'analyser les facteurs environnementaux ainsi que les communautés planctoniques en termes qualitatif et quantitatif (composition, stock de carbone, flux de carbone) dans ces deux situations. La modélisation des flux de carbone a permis de caractériser le fonctionnement écologique de chaque site, en appliquant des indicateurs écologiques (ratios de typologie et indices fonctionnels ENA). Le but final était alors de sélectionner les indicateurs permettant de caractériser l'état de santé de l'écosystème afin de les proposer comme indicateurs holistiques aux gestionnaires de l'environnement marin.

Pour répondre à ces objectifs, une grande variété d'approches a été appliquée : échantillonnage sur le terrain, suivi par des incubations et expérimentations *in situ*, modélisation et analyses numérique des réseaux trophiques.

La première partie fut l'occasion d'évaluer le fonctionnement de réseau trophique planctonique dans un écosystème côtier soumis à des perturbations permanentes principalement causées par l'industrie du phosphate implanté dans le Golfe depuis les années 70 et de décrire l'état écologique de cet écosystème en se basant sur des indicateurs écologiques (**chapitres III et IV**). Une deuxième partie de travail de thèse a été menée au niveau du Canal de Bizerte lors d'une contamination pulsée due à une fissure dans le réservoir de la société tunisienne STIR causant une fuite de 7 tonnes de pétrole brute (marée noire) (**chapitres V**) afin de savoir comment le réseau trophique planctonique répond à ce type de contamination.

1. Changement de la structure en taille et de la production du phytoplancton en cas de contamination chronique et pulsée: implication pour les réseaux trophiques planctoniques

La structure de taille des communautés de phytoplancton est un élément crucial dans l'écologie qui détermine la direction et la grandeur des flux d'énergie et de carbone dans les réseaux alimentaires pélagiques marins (Riegman et al., 1993; Legendre & Rassoulzadegan, 1995), affectant ainsi la productivité de l'écosystème. Généralement, les grandes cellules (tels que les diatomées) sont responsables de la forte accumulation de la biomasse phytoplanctonique et dominent les

systèmes côtiers eutrophes, tandis que les petites cellules sont représentatives des systèmes oligotrophes (Siokou-Frangou et al., 2010; Šolić et al., 2010). Toutefois, il est possible de trouver des exceptions à cette théorie générale, où la biomasse phytoplanctonique élevée est associée à des cellules de petite taille (Zingone et al., 2011). La structure de taille et la production du phytoplancton peuvent rapidement changer en réponse aux perturbations environnementales et anthropiques tels que le régime de mélange vertical, les fluctuations de lumière et de température, la salinité, la disponibilité des nutriments et les rejets industriels, urbains et agricoles. Ces changements sont évidemment suivies par des modifications dans la composition et la structure des communautés du zooplancton et de leur activité de broutage (Legendre and Rassoulzadegan, 1995b; Kiørboe et al., 1996; Horňák et al., 2005; Bel Hassen et al., 2008; Drira et al., 2018), ce qui pourrait avoir des effets importants sur la structure du réseau trophique marin (Froneman, 2004; Legendre and Rassoulzadegan, 1995; Vargas and González, 2004; Decembrini et al., 2009; Meddeb et al., 2019).

Dans la première partie de notre étude (chapitres III et IV), la dynamique spatiale des communautés planctoniques, de la production primaire et des flux de carbone a été investiguée le long d'un gradient hydrodynamique et nutritif au niveau du Golfe de Gabès, un site soumis à la fois à une courantologie complexe et une contamination chronique. Ce travail a donné une description détaillée des modifications dans les communautés du phytoplancton (taille, composition, biomasse, production), du zooplancton (composition, abondance, activité de broutage) et des voies trophiques (Figure 1a). Les résultats ont montré l'existence de trois types de réseaux en fonction du gradient ascendant de nutriments. Les eaux les moins eutrophes (station S1 la plus vers le Nord) étaient caractérisées par la production primaire la moins élevée (1815 mg C m^{-2} j^{-1}), qui était dominait par le picophytoplancton (78%). Ceci a été associée à une forte microbivorie du protozooplancton (*Strombidium spp.*) representant 76% du transfert de carbone et conduisant ainsi à un réseau trophique microbien. Ce résultat diverge de la vision traditionnelle concernant la dominance de la voie microbienne dans les eaux oligotrophes (Christaki et al., 2011; Zaccone et al., 2018; Decembrini et al., 2021b). Toutefois, certains auteurs ont signalé l'importance du réseau microbien dans des eaux côtières eutrophes (Grami et al., 2008; Viñas et al., 2013; Paklar et al., 2020). La situation a changé dans les eaux ayant des concentrations intermédiaires en nutriments (i.e. stations S2 et S3), puisque la production primaire a augmenté (2170- 2773 mg C m^{-2} j^{-1}) et était composée par le nano- et le microphytoplancton (21-7% et 55-78% ; respectivement) et aussi le picophytoplancton (24-15%). Cette production est transférée vers les niveaux supérieurs par le biais de la microbivorie (20-25% de transfert du carbone) et de l'herbivorie (75-80% du transfert ducarbone) du zooplancton, conduisant donc à un réseau trophique multivore (Figure 1a). Ce type

de réseau a été déjà observé dans d'autres eaux productives (Vargas and González, 2004; Siokou-Frangou et al., 2010; Masclaux et al., 2015; Meddeb et al., 2018). Dans les eaux les plus eutrophes (i.e. station S4), la forte production primaire (3899 mg C m^{-2} j^{-1}) était soutenue par le phytoplancton de grande taille (92%) et principalement acheminée vers les niveaux trophique supérieurs *via* l'herbivorie du protozooplancton (45%) et du metazooplankton (24%), ce qui conduit à un réseau trophique herbivore. Cette voie a été signalée dans plusieurs eaux côtières riches en nutriments et avec une abondance de diatomées (Masclaux et al., 2015; Meddeb et al., 2018; Sakka Hlaili et al., 2008; D'Alelio et al., 2022).

Nos résultats ont montré aussi que ces différents réseaux ont acheminé le carbone biogène vers les consommateurs supérieurs avec des efficacités différentes comme signalé par Legendre & Rassoulzadegan (1995). De plus, en se basant sur l'analyse factorielle multiple (AFM, chapitre IV), les nutriments sont apparus comme des facteurs environnementaux discriminants significatifs des différentes structures trophiques, dans lesquelles phytoplancton de petit et de grand taille jouent des rôles différents dans la production de carbone biogénique. D'ailleurs, les éléments nutritifs sont toujours considérés comme le principal facteur affectant le spectre de taille des producteurs primaires, qui à leur tour influencent l'organisation du réseau trophique (Legendre and Rassoulzadegan, 1995; Sakka Hlaili et al., 2008; Filiz et al., 2020; Hardikar et al., 2021). D'une façon générale, la modification de la structure en taille peut refléter la réponse du phytoplancton aux perturbations de l'environnement, avec des implications pour le fonctionnement de l'écosystème. En effet, l'augmentation du phytoplancton de grande taille par rapport aux petites cellules pourrait être indicateur d'eutrophisation (Bell and Elmetri, 1995; Garmendia et al., 2011; Machado et al., 2023).

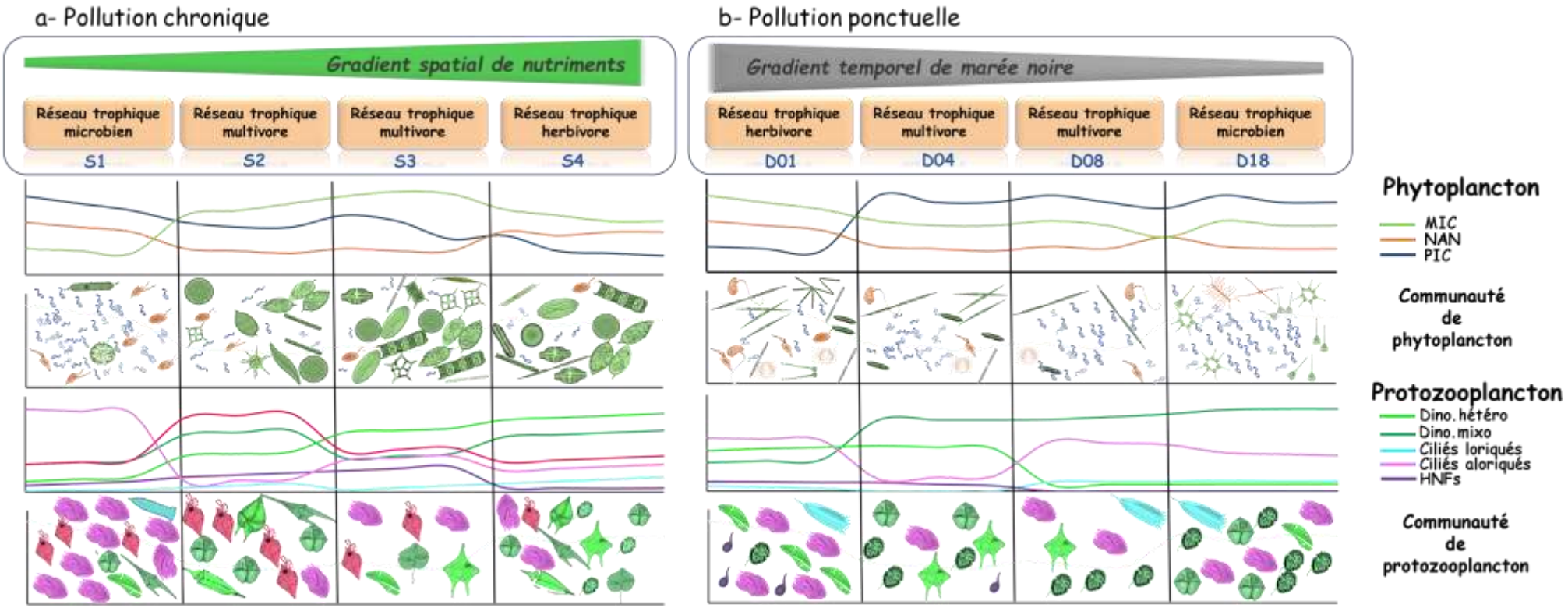

Figure.1. Schéma récapitulatif illustrant la dynamique spatiale lors de la contamination chronique (a) et la dynamique temporelle lors de la contamination pulsée (b) des communautés du phytoplancton et du protozooplancton au sein des différentes structures trophiques.

La structure en taille du phytoplancton peut également changer rapidement en réponse à différents types de contamination (Song et al., 2022; Tesán-Onrubia et al., 2023). Par exemple, les recherches sur les déversements de pétrole dans le système marin ont indiqué que la taille du phytoplancton est une propriété clé déterminant la sensibilité des espèces aux composés pétroliers, puisque les seuils de toxicité des hydrocarbures individuels dépendent de la taille des cellules phytoplanctoniques (Echeveste et al., 2010; Urakawa et al., 2012; Ben Othman et al., 2012, 2023) à part la concentration de pétrole dans l'eau et sa dissolution (Zaghden et al., 2014; Fourati et al., 2018). Généralement, les cellules de petites tailles, ayant un rapport surface: volume élevé, sont plus sensibles que le gros phytoplancton aux hydrocarbures et au pétrole. Par conséquent, les effets des composés pétroliers sur la structure en taille des producteurs primaires peuvent se répercuter sur les niveaux trophiques supérieurs et avoir un impact sur la structure et la dynamique des réseaux trophiques. Comme le phytoplancton, de nombreuses espèces du zooplancton sont sensibles aux substances chimiques contenues dans le pétrole (Suchanek, 1993; Abbriano et al., 2011). Les protozoaires forment des éléments clés de la communauté du plancton marin et des importants brouteurs des biomasses bactériennes et phytoplanctoniques (Poulsen and Reuss, 2002; Calbet and Landry, 2004; Kosiba and Krztoń, 2022; Pecqueur et al., 2022). Par ailleurs, plusieurs études ont déclaré l'intérêt d'appréhender les interactions entre le pétrole et le protozooplancton afin de mieux comprendre l'impact écologique des déversements de pétrole sur les réseaux alimentaires marins (Almeda et al., 2014b, 2018; Klotz et al., 2018; Tang and Buskey, 2022; González et al., 2022).

Dans ce contexte, la deuxième partie de notre étude (chapitres V) a évalué, les réponses rapides (i.e. 1- 8 jours) et à plus long terme (i.e. 18 jour) des communautés du phytoplancton (structure en taille, biomasse, composition et croissance**)** et du protozooplancton (abondance, composition et activité de broutage) à la marée noire survenue dans la région de Bizerte. L'évolution du type du réseau trophique planctonique à la suite de cet accident a été également caractérisée. C'est la première fois que l'on détermine le devenir de ce réseau par rapport à l'état normal de l'écosystème (c'est-à-dire avant l'accident).

Les résultats ont montré que la biomasse et l'abondance du picophytoplancton ont augmenté au fil des jours, jusqu'à où ce petit phytoplancton devenait dominant, avec une forte accumulation de sa biomasse au 18ème jour, malgré que son taux de croissance a diminué à ce jour. Cette augmentation du picophytoplancton semble être due à une réduction de son contrôle par le protozooplancton, comme démontré par d'autres études (Almeda et al., 2018; Gemmell

et al., 2018; Deppeler et al., 2019). D'ailleurs les nanoflagéllés hétérotrophes, les brouteurs potentiels des pico-organismes (Azam et al., 1983; Caron t al., 1990), ont été négativement affectés par le pétrole et ont disparu dès le 8ème jour. En outre, l'abondance des ciliés aloriqués (i.e. *Strombidium*) a remarquablement chuté du 1ier au 8ème jour, ce qui est en accord avec d'autres études rapportant la sensibilité de ces espèces au pétrole (Almeda et al., 2018; Gemmell et al., 2018). Par ailleurs, le taux de broutage du picophytoplancton a graduellement diminué du 1ier au 18ème jour, malgré que sa croissance ait été stimulée du 1ier au 8ème jour. De nombreux auteurs considèrent que la diminution du contrôle « top-down », due à la contamination des brouteurs sensibles aux hydrocarbures, est un facteur majeur contribuant à l'augmentation de la population et à la diversification du phytoplancton marin à la suite d'une marée noire (Johansson et al., 1980; Hjorth et al., 2007; Gemmell et al., 2018). Tang and Buskey (2022) ont rapporté que le découplage entre la croissance du phytoplancton et le broutage du protozooplancton, suite à une contamination par le pétrole, peut favoriser la biomasse phytoplanctonique. Contrairement au picophytoplancton, la croissance et la biomasse du nano- et microphytolancton ont diminué quelques jours après le déversement de pétrole, tandis qu'au 18ème jour, il y eu une re-croissance des deux groupes phytolanctoniques. Plusieurs auteurs ont également montré une inhibition à court terme et une efflorescence à long terme pour les grandes espèces phytoplanctoniques, suite à des marées noires (Pan et al., 2012; Ozhan et al., 2014). L'inhibition a court-terme peut être due à l'effet négatif direct des hydrocarbures sur l'activité photosynthétique (Aksmann & Tukaj, 2008; Ben Othman et al., 2023) ou à l'effet indirecte de la réduction de la lumière dans la colonne d'eau causée par la présence de la nappe de pétrole à la surface de l'eau. Au 18ème jour, le pétrole s'est dispersé et l'eau de mer a retrouvé sa couleur et son odeur avant le déversement, et donc il y aurait une atténuation de l'effet négatif du pétrole (directe et indirecte) sur le gros phytoplancton qui a montré une reprise de croissance. Les taux de broutage du nano- et microphytoplancton ont montré une évolution temporelle similaire à leurs taux de croissance, puisque un feedback trophique positive existe souvent entre ces deux taux (Sakka Hlaili et al., 2007; Chen et al., 2009). De plus, la variation du taux de broutage du gros phytoplancton peut être liée au changement dans la communauté du protozooplancton qui a été observé rapidement après la fuite du pétrole, confirmant la grande sensibilité de ces brouteurs au polluant du pétrole (Gomiero et al., 2013; Nogueira et al., 2017; Han et al., 2019; Pančić et al., 2019). Il y a une forte inhibition des dinoflagellés herbivores (i.e. *Gyrodinium* et *Protoperidinium*), se nourrissant sur les cellules de grande taille, au détriment des mixotrophes (i.e. *Heterocapsa*), ayant une grande plasticité nutritionnelle en consommant

des proies avec une large gamme de taille (Jeong et al., 2008, 2010). A plus long terme (i.e. 18ème jour), les ciliés loriqués (*Tintinnopsis*, *Salpingella*) et les dinoflagellés herbivores (*Hétérocapsa*, *Gyrodinium*) sont devenus plus abondant et probablement ont augenté leur pression de broutage sur les cellules phytoplanctoniques de grande taille.

Les différents effets, causés à court- et long termes par la contamination par le pétrole, sur la croissance et la biomasse des différentes fractions de taille du phytoplancton ont été suivis par une modification de la production primaire (i.e. son taux et sa composition). De même, les diverses réponses des groupes protozooplanctoniques, qui ont des différents rôles fonctionnels et sélectivités alimentaires, ont provoqué des modifications des taux de consommation des fractions de taille du phytoplancton induisant donc des effets par cascade sur la voie de transfert de carbone. Les changements, induits par le pétrole, dans la production du phytoplanctonn et de sa consommation ont été intégrés dans des modèles inverses des flux de carbone afin de donner un premier aperçu de l'impact d'un déversement de pétrole sur le réseau trophique et des onséquenes possible sur l'exportation du carbone biogène.

Comme attendu, il y a eu une nette modification de la structure de la voie trophique tout au long de l'évolution de la marée noire (Figure 1b). Le réseau herbivore a dominé au 1ier jour, alors qu'après quelques jours (i.e. au 4ème et 8ème jour) le carbone était transféré par la voie multivore qui a évolué en réseau microbien au 18ème jour. Ce changement de réseau trophique implique que le carbone serait acheminé aux grands consommateurs avec différentes efficacités (Legendre & Gosselin, 1989; Legendre & Rassoulzadegan, 1995; Sakka Hlaili et al., 2008).

Meddeb et al. (2019), en se basant aussi sur l'analyse inverse, ont trouvé un réseau microbien dans le Canal de Bizerte pendant la même période que notre étude mais en sans déversement de pétrole. La comparaison du réseau microbien observé au 18ème jour après la fuite de pétrole, avec celui de Meddeb et al. (2019) a montré que ces deux voies ne sont pas similaires. La principale différence est due au protozooplancton, qui a montré une composition et un rôle fonctionnel différents entre les deux voies microbiennes, témoignant que 18 jours ne seraient pas suffisants pour que le système retrouve sa stabilité initiale.

A l'issu de nos résultats, il est claire que le phytoplancton, principalement sa structure en taille, est un bon indicateur du changement induit par une contamination chronique ou pulsée. Il est aussi pertinent de considérer les changements du protozooplancton face à ces perturbations. D'ailleurs l'importance d'étudier les réponses du protozooplancton aux

changements environnementaux a été déjà signalée dans plusieurs études (Calbet & Landry 2004; Poulsen & Reuss, 2011; Pecqueur et al., 2022; Kosiba & Krzton, 2022; Drira et al., 2018). Le taux de croissance rapide du protozooplancton, son abondance, sa biomasse et sa diversité peuvent être utilisés comme indicateurs de la contamination organique et toxique et de la qualité de l'eau (Gomes et al., 2007; Naselli-Flores, 2008; Downing, 2010; Buholce et al., 2015; Drira et al., 2018).

2. Typologie des réseaux trophiques planctoniques et propriétés émergentes associées: choix d'indicateurs de l'état écologique des écosystèmes perturbés

Une analyse du fonctionnement trophique basée sur des indicateurs écologiques a été considérée dans la contamination chronique (Chapitre IV) et la contamination pulsée (discussion générale). Parmi les approches utilisées pour comprendre le fonctionnement des écosystèmes perturbés, on trouve la typologie des réseaux trophiques planctoniques qui se base sur l'étude des relations trophiques entre les différentes composantes planctoniques. Legendre & Rassoulzadegan (1995) ont proposé six ratios de typologie afin d'identifier des groupes de stations similaires et ont interprété les valeurs caractéristiques des rapports dans chaque groupe en termes de dominance d'une voie trophique donnée. Dans notre cas, on a considéré les ratios R7 (Production nette de picophytoplancton divisée par la production nette totale de phytoplancton) et R8 (Taux de consommation du phytoplancton total par protozooplancton divisé par le taux de consommation du phytoplancton total par proto et méta-zooplancton) qui ont été proposés par Legendre & Rassoulzadegan (1995) et définis numériquement par Sakka hlaili et al., (2014) pour distinguer le réseau trophique prépondérant. Ces auteurs ont aussi proposé six autres ratios liés au protozooplancton, dont R4 (Production nette totale de phytoplancton divisée par la production nette de nourriture potentielle de protozooplancton) et R6 (Production nette de COD et de DET divisée par la production nette de nourriture potentielle de protozooplancton), qu'on a utilisé dans le cas du Golfe de Gabès et du Canal de Bizerte.

2.1. Cas du Golfe de Gabès

La variation spatiale du type de réseau dans le Golfe de Gabès a été confirmée par le ratio R7, avec la dominance du réseau trophique microbien à la station S1 ($R7 = 0,7 > 0,6$), tandis que la voie multivore était prédominante aux stations S2 et S3 ($0,1 < R7 = 0,2\text{-}0,12 < 0,6$), mais le réseau trophique à la station S4 était herbivore ($R7 = 0,06 < 0,1$). En se basant sur le ratio R8, le phytoplancton était majoritairement consommé par le protozooplancton dans le réseau

microbien (i.e. station S1) mais co-exploité par le proto- et le méta-zooplancton, lorsque les voies multivore (i.e. stations S2 et S3) et herbivore (i.e. station S4) régnaient. Les ratios R4 et R6 ont dévoilé que le phytoplancton total a contribué considérablement à la nourriture du protozooplancton dans les réseaux microbien et herbivore, alors que la contribution des détritus et du COD dans le réseau multivore était un peu plus élevée que celle de phytoplancton.

De plus à chaque type de réseau une ou plusieurs propriétés émergentes pourraient être attribuées. Par exemple, en décrivant la stabilité d'un écosystème, Legendre & Rassoulzadegan (1995) ont déclaré que le réseau herbivore, qui constitue un système peu stable et de nature transitoire, domine le plus souvent les écosystèmes stressés par les forts apports en nutriments. En revanche, les réseaux microbien et multivore ont une plus grande stabilité et sont donc plus durables, dominant dans la plus des écosystèmes océaniques. D'autres études se basant sur les indices ENA ont proposé des théories liant la structure du réseau trophique aux propriétés émergentes. Par exemple, Finn (1976) a suggéré que le débit total du système quantifié par l'indice TST pourrait être utilisé pour quantifier le niveau d'activité de l'écosystème de la même manière que la productivité primaire ou la respiration de la communauté. Plusieurs travaux ont montré que des valeurs élevées de TST correspondent à des écosystèmes productifs, tels que les zones côtières influencées par des remontées d'eau riches en nutriments ou des apports fluviaux et des plateaux continentaux productifs (Coll et al., 2007; Grami et al., 2008; Corrales et al., 2015; Meddeb et al., 2018). Dans notre étude menée dans le Golfe de Gabès, le réseau trophique herbivore identifié dans les eaux les plus eutrophes était effectivement le plus actif que les réseaux trophiques microbien et multivore, trouvés dans les eaux à moindre richesse nutritive. Un système stable est supposé maximiser son recyclage, qui peut être estimé par l'indice de recyclage de Finn (FCI, Finn, 1976) et la longueur moyenne des voies trophiques (APL). Ces deux indices sont souvent considérés comme des indicateurs possibles de stress (Odum, 1985; Scharler & Baird 2005; Tecchio et al., 2015; Pezy et al., 2018). En effet, une baisse du nombre de cycles (FCI) et de leur longueur moyenne (APL) indique une diminution du stress (Baird & Ulanowicz, 1989). Les deux indices ont montré une évolution spatiale similaire, avec des valeurs les plus faibles dans le réseau herbivore de la station S4, indiquant que le système de S4 était moins stable que les voies multivore et microbienne observées dans les autres stations. De plus le niveau de stress important (i.e. FCI et APL les plus élevés) était observé dans le réseau multivore de la station S2, qui était la plus exposée à la principale source de perturbation dans le Golfe (i.e. le complexe chimique). Ainsi, l'augmentation du recyclage

et de la diversité des flux semble conférer au système une certaine résistance à la forte perturbation que le réseau trophique a subie àla station S2. Meddeb et al. (2018) ont aussi trouvé une activité élevée dans le réseau trophique herbivore (Baie de Bizerte) qui coïncidait avec une faible stabilité alors que les réseaux multivore ou microbien (Canal et lagune de Bizerte) étaient les plus stables et matures. Le degré d'organisation et la spécialisation de l'écosystème peuvent aussi être estimées à partir de deux autres indices, à savoir l'ascendance relative (A/C) et l'information mutuelle moyenne (AMI) (Ulanowicz, 1997; Patrício et al., 2004). Ces indices ont montré que les réseaux trophiques multivore (i.e. aux stations S2 et S3) et microbien (i.e. à la station S1) étaient les plus organisés et les plus spécialisés, avec probablement des voies d'acheminement du carbone plus directes. De plus, le rapport détritivorie/ herbivorie (indice D/H) peut être utile puisqu'il peut fournir des informations sur le transfert de carbone aux consommateurs *via* les détritus et/ou les autotrophes (Kay et al., 1989; Ulanowicz, 1992; Chrystal & Scharler, 2014; Niquil et al., 2014; Fath et al., 2019; Safi et al., 2019). Cet indice a montré une variation spatiale significative dans le Golfe de Gabès, indiquant un passage de systèmes basés sur la production phytoplanctonique pour les réseaux herbivore et microbien à des systèmes basés sur un équilibre entre le phytoplancton et les détritus pour le réseau trophique multivore. Nos résultats corroborent avec la théorie suggérant que les environnements riches en nutriments favorisent l'herbivorie par rapport à la détritivorie (Luong et al., 2014), puisque la valeur de D/H la plus faible a coïncidé avec le réseau herbivore présent dans la station la plus eutrophe (i.e. S4).

Les indices ENA sont des outils potentiellement puissants dans la modélisation permettant d'examiner la structure et les flux de matière dans les écosystèmes (Wulf et al., 1989; Christensen & Pauly, 1993; Fath & Patten, 1999) afin d'évaluer la santé des écosystèmes (Niquil et al., 2014). Ces indices sont sensibles aux différents impacts sur les écosystèmes marins (Baird et al., 2009; Tecchio et al., 2016; Pezy et al., 2017). Cependant, ils ne peuvent que partiellement capturer les niveaux de stress anthropogéniques ou naturels des différents types de réseaux trophiques dans les écosystèmes aquatiques (Tecchio et al., 2016). Ainsi, les modèles d'écosystèmes sont de plus en plus utilisés pour conseiller la politique pour l'eau et le milieu marin dans les pays de l'Union Européenne. (par exemple, Heymans et al., 2020), mais vu la complexité des interactions au sein d'un écosystème (Fath et al., 2007; Baird et al 2009) et vu que les résultats des modèles représentent des projections de la réalité sous forme numérique, l'utilisation et la compréhension de ces modèles sont difficiles pour les non-experts.

Récemment Fath et al., (2019) ont rapporté que les indices ENA sont importants, mais ils sont pour l'instant difficilement compréhensibles pour les non-spécialistes et donc difficilement communicables. Les ratios de typologie pourraient être plus pratiques aussi bien pour les experts que pour les non-experts. Ainsi l'identification de la voie trophique dominante dans un assemblage planctonique pourrait être effectuée à partir de ces ratios qui peuvent être calculés à partir de valeurs de flux relativement faciles à estimer sur le terrain, comme la production nette du picophytoplancton divisée par la production totale du phytoplancton et le taux de consommation du phytoplancton total par le protozooplancton divisé par le taux de consommation total par le proto- et le métazooplancton (Figure 2). De même, la détermination de la matière sur laquelle le système est basé pourrait être faite en utilisant des critères calculés à partir des flux estimés sur le terrain, à savoir, la production totale du phytoplancton divisée par la production de nourriture potentielle du protozooplancton et la production du COD et des détritus divisée par la production de nourriture potentielle pour le protozooplancton (Figure 2) (Sakka Hlaili et al., 2014). Ceci faciliterait la prise de décision pour l'écosystème étudié.

D'un point de vue planctonique, les deux indices TST et D/H (Figure 3), souvent recommandés par plusieurs auteurs (Ulanowicz, 2004; Bodini et al., 2012; Fath et al., 2019; Safi et al., 2019), pourraient être couplés avec les ratios de typologie trophique (i.e. R4, R6, R7 et R8) afin de mieux comprendre le fonctionnement des différentes structures du réseau planctonique sous la pression anthropique. L'analyse AFM a montré en effet que ces indicateurs écologiques (i.e. TST, D/H, R4, R6, R7 et R8) étaient les plus structurants dans les systèmes étudiés.

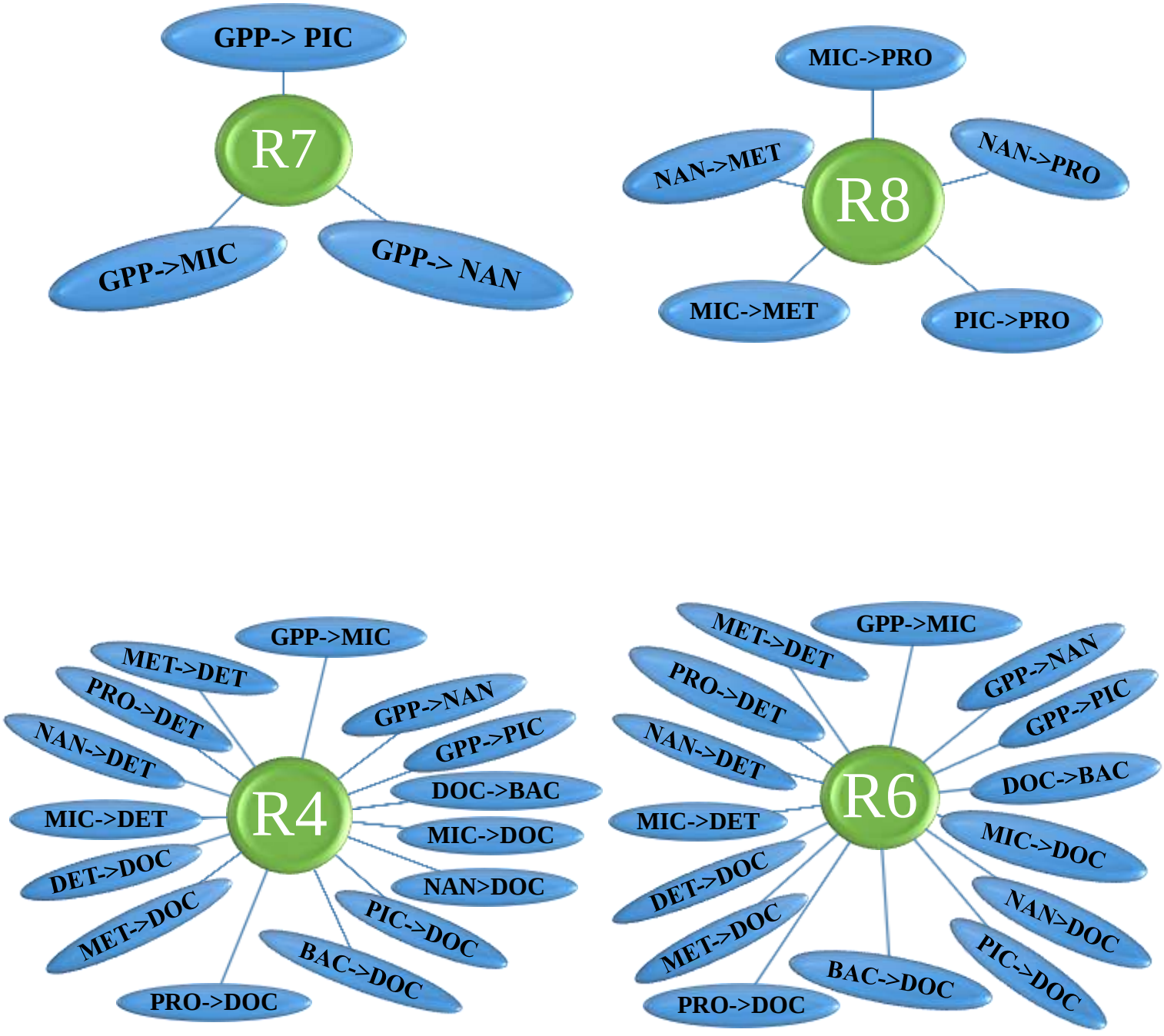

Figure. 2. Schéma illustrant les différents flux impliqués dans l'estimation des ratios de typologie trophique. La description de chaque flux est détaillée dans le Tableau 2 du chapitre IV

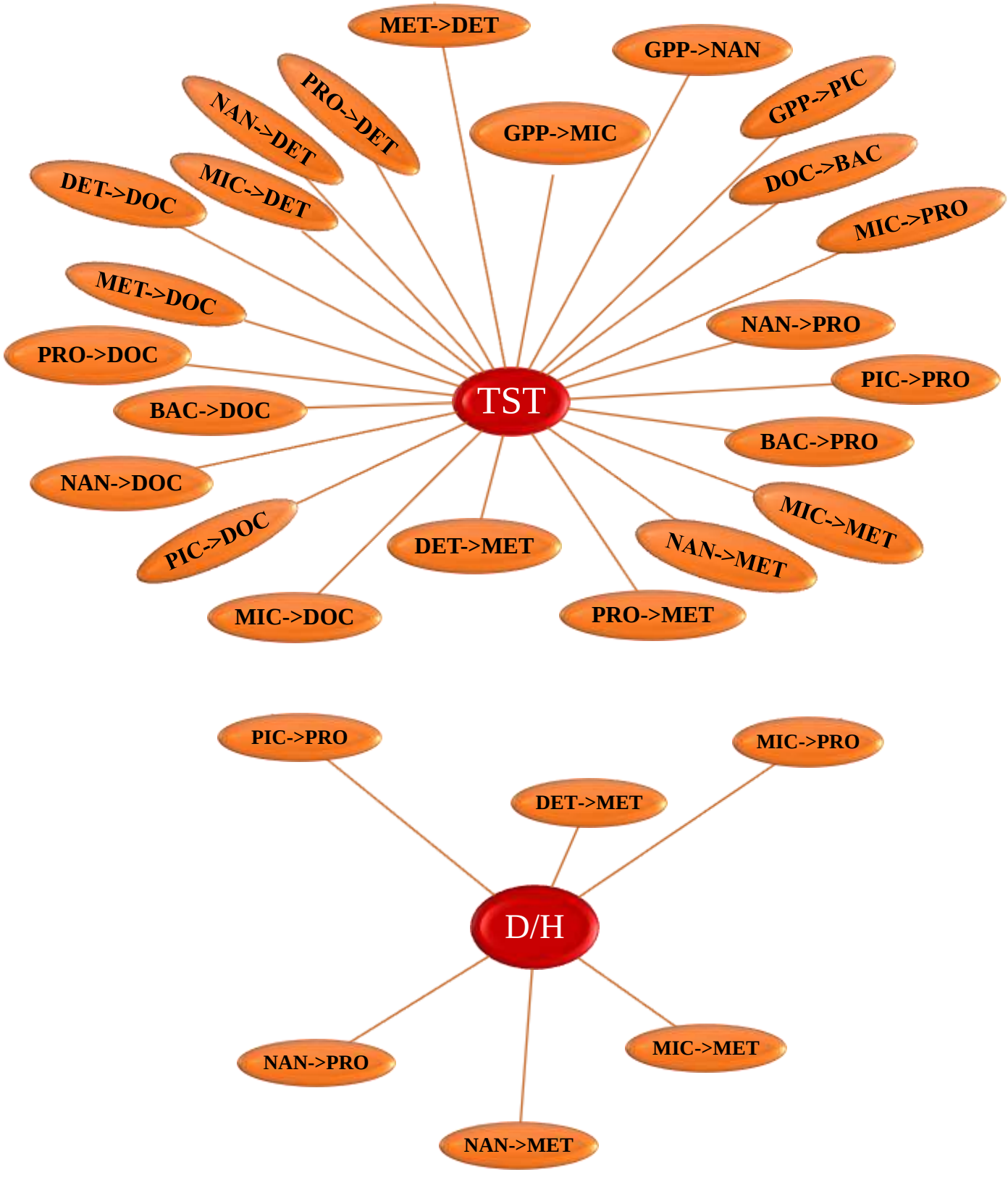

Figure 3. Schéma illustrant les différents flux impliqués dans l'estimation de débit de carbone total (TST) et la détritivorie par rapport à l'herbivorie (D/H). La description de chaque flux est détaillée dans leTtableau 2 du chapitre IV

2.2. Cas du Canal de Bizerte

Les indicateurs écologiques qu'on a proposé étaient testés dans le cas du Golfe de Gabès qui est soumis à une contamination chronique. Les écosystèmes sont non seulement complexes mais leurs dynamiques et fonctionnements changent selon le type de contamination. Il est logique de tester ainsi les indicateurs dans différents types de contamination pour savoir s'ils répondent de la même façon ou non et pour une application plus large dans la gestion des écosystèmes sous différents types de contamination.

Une analyse simplifiée des ratios de typologie et des indices ENA a été effectué dans la présente discussion pour le cas de la marée noire afin de savoir si ces indicateurs répondent de la même façon que dans le cas d'une contamination chronique. Bien qu'un grand intérêt ait été porté à l'effet des déversements de pétrole sur les communautés planctoniques (bactéries, phytoplancton et zooplancton), leurs interactions ainsi que leur impact indirect sur le réseau trophique (Gonzalez et al., 2009; Almeda et al., 2013, 2014, 2016, 2018; Severin et al., 2016; Bretherton et al., 2020; Quigg et al., 202), la proposition d'indicateurs pour les gestionnaires sur l'effet de la contamination par le pétrole sur le réseau trophique planctonique est inexistante. Dans la présente étude, les ratios de typologie ont montré la même tendance que celle révélée dans la contamination chronique (Figure 4). A court et à long termes les valeurs de R7 ont bien discriminé le réseau herbivore (R7<0.1) (au 1^{ier} jour), le réseau multivore (0.1<R7<0.6) (aux 4ème et 8ème jours) et le réseau microbien (R>0.6) au 18ème jour. Ce ratio est le 1er critère proposé par Sakka Hlaili et al. (2014) aux chercheurs et aux gestionnaires afin d'identifier quantitativement la voie trophique qui domine un assemblage planctonique. Ainsi, son application dans l'étude des réseaux trophiques pourrait être utile pour tous les types de contamination. On a également révélé, que les différents réseaux se sont basés sur le phytoplancton (R4 élevé). Le transfert de carbone vers les niveaux supérieurs a été principalement due aux proto- et métazooplancton pour le réseau herbivore (R8 faible) mais aux protozoaires seulement pour les réseaux multivore et microbien (R8 plus au moins élevé).

Contrairement aux ratios de typologie, une différence a été notée pour les indices ENA, puisque l'information a changé pour un même type de réseau entre la contamination chronique et pulsée. L'activité de système indiqué par TST (Figure 5) semble être la plus sensible aux changements de flux du réseau face aux perturbations. Contrairement à la contamination chronique ou le réseau herbivore a montré l'activité la plus élevée, la contamination pulsée a

révélé que le réseau trophique microbien est le plus actif (TST élevé). Ce débit élevé du système semble être associé à l'accumulation de biomasse du picophytoplancton dans le système. Ceci contredit l'idée que le réseau trophique herbivore est plus actif que les réseaux trophiques microbien et multivore (Meddeb et al., 2019; Decembrini et al., 2021). De plus, la comparaison du réseau trophique microbien observé à long terme avec celui observé dans des conditions normales (i.e. avant la marée noire, Meddeb et al., 2019), a montré que le système peut encore être perturbé et qu'il n'a pas trouvé son état d'équilibre initial, c'est-à-dire sa stabilité.

L'indice D/H a légèrement varié au fil des jours après la marée noire et a montré la valeur la plus forte dans le réseau microbien qui s'est installé au 18ème jour. Ceci est différent de ce qu'on a signalé dans la contamination chronique où le réseau multivore a présenté une forte détritivorie. Ceci pourrait être lié à l'effet de pétrole sur la communauté planctonique car il a déjà été signalé que certains détritivores hétérotrophes, en digérant le pétrole, deviennent la principale source de carbone alors que le phytoplancton est décimé (TCO Spill, 2010).

L'analyse AFM a donné aussi des résultats opposés à ceux trouvés par la même analyse pour la contamination chronique. Ainsi, contrairement à la corrélation négative révélé dans la contamination chronique (r= - 0,39 ; *p-value* <<0,05), une corrélation positive entre la production de picophytoplanton, R7 et TST a été bien observée (r= 0,7 ; *p-value* < 0,01 ; Figure 6). Cette corrélation pourrait nous permettre de constater que même si le TST n'a pas montré la même tendance que dans la contamination chronique vis-à-vis les différentes structures trophiques, le couplage de cet indice TST pourrait être applicable dans le cas de contamination pulsée car, comme déjà indiqué, les ratios R7 et R8 permettent de fournir des informations indirectes sur la quantité de production primaire dans le système, ce qui a un effet sur l'activité de l'écosystème mesurée par le TST (Finn, 1976; Ulanowicz, 1986; Borrett & Scharler, 2019). Pour le D/H, comme pour la contamination chronique, il est fortement discriminant. Ceci est bien visible sur l'AFM où cet indice est positivement corrélé à R6 (r= 0,39 ; *p-value* <<0,05) et négativement corrélé à R4 (r= -0,55 ; *p-value* <0,05) sur l'axe 2. Donc son couplage avec les ratios de typologie R4 et R6 est recommandé pour savoir le type de matière sur laquelle le système est basé.

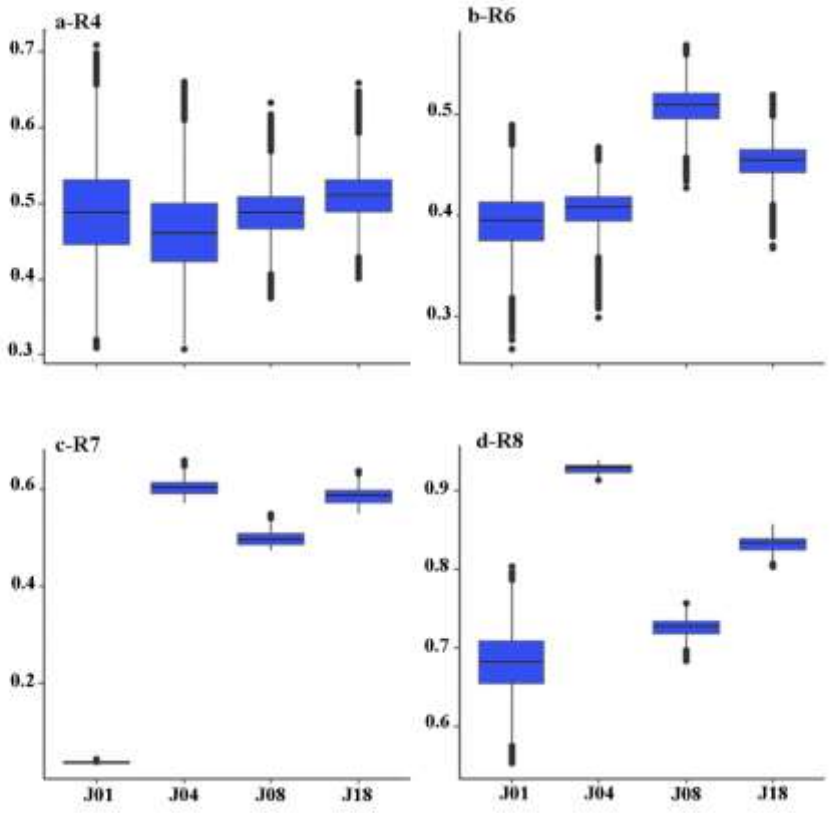

Figure.4 Variation des ratios de la typologie du réseau trophique au cours des différents jours après le déversement de pétrole.

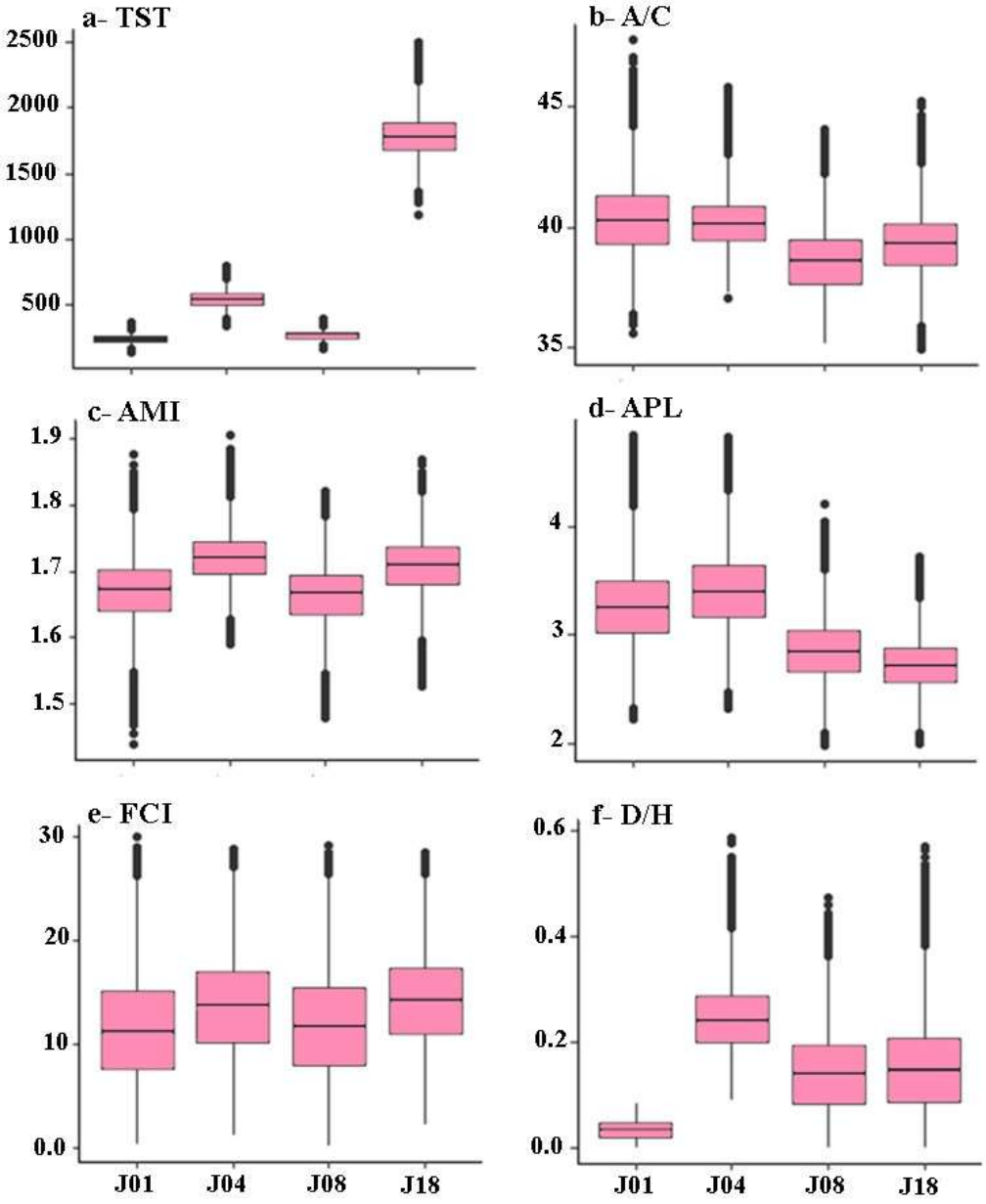

Figure. 5 Variation temporelle des indices ENA calculés pour les réseaux trophiques planctoniques dans la contamination pulsée de Bizerte. Débit total du système (TST ; mg C m^{-2} j^{-1}), ascendance relative (A/C ; %), information mutuelle moyenne (AMI ; bits), longueur moyenne des voies trophiques (APL), indice de recyclage (FCI ; %), et détritivorie/herbivorie (D/H).

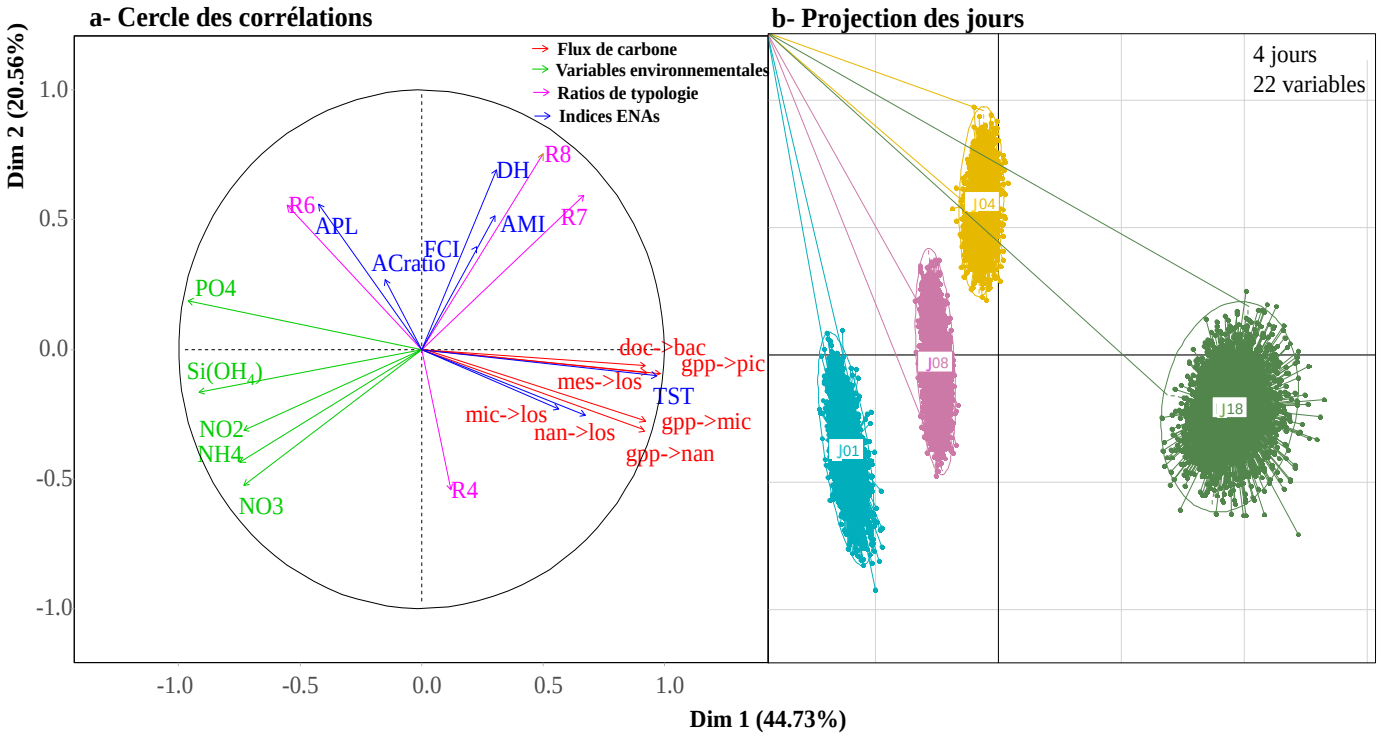

Figure. 6 Analyse factorielle multiple (AFM) montrant les relations entre les indicateurs écologiques (ratios de typologie trophique et indices ENA), les variables environnementales (nutriments inorganiques et organiques : Ninorg, Pinorg, Siinorg, Norg, Porg) et les flux de carbone [GPP de PIC (GPP->PIC), NAN (GPP->NAN) et MIC (GPP->MIC), production bactérienne (DOC->BAC) et enfoncement de NAN (NAN->LOS), MIC (MIC->LOS) et MET (MET->LOS)].

Les ENA sont des outils sensibles de caractérisation de l'état de santé des écosystèmes qui ont été utilisés à plusieurs reprises pour évaluer l'impact des pressions naturelles et anthropiques sur les écosystèmes marins côtiers (Niquil et al., 2014; Pezy et al., 2017; Tecchio et al., 2016; de la Vega et al., 2018a, b; Safi et al., 2019; Fath et al., 2019). Johnson et al. (2009) ont signalé également la sensibilité des ENA aux spécificités environnementales et aux paramètres physiques. Ce qui rend difficile la comparaison des valeurs ENA entre différents écosystèmes. A l'échelle planctonique, l'évaluation de ces indices écologiques dans différents cas de contamination ainsi n'a jamais été faite auparavant, ni leur association aux ratios de typologie trophique. Les rares études qui ont considéré les ENAs dans le réseau trophique planctonique, ne se sont pas concentrées sur la comparaison entre différents facteurs de contamination (Grami et al., 2011; Tortajada et al., 2012; Meddeb et al., 2018).

Les indices ENA ont été utilisés par les conventions de mer régionales, telles que HELCOM, OSPAR et la Convention de Barcelone (Safi et al., 2017, 2019; McQuatters-Gollop et al., 2022) afin de définir et mettre en œuvre une stratégie de maintien du bon état écologique (Rombouts et al., 2013; Safi et al., 2017, 2019; Arroyo et al., 2019). Cependant, leur application dans les réseaux trophiques planctoniques fait généralement défaut. C'est pourquoi nous avons appliqué une approche combinant les ENA et les ratios typologiques afin de mieux comprendre le fonctionnement des différentes structures des réseaux alimentaires planctoniques. En complément des ENA, nous pouvons proposer aux chercheurs et gestionnaires de nouveaux critères (basés sur les ratios typologiques de Sakka Hlaili et al., (2014)), qui pourraient utiliser pour identifier quantitativement les différentes structures du réseau. L'avantage de ces ratios est que si l'on considère certains d'entre eux, on peut accéder directement aux flux spécifiques sans avoir calculer tous les flux de l'ensemble du réseau, comme c'est le cas pour les ENA. Les résultats des ENA permettent de mieux comprendre le fonctionnement des différentes structures du réseau trophique planctonique sous la pression anthropique à savoir son activité (TST) et l'importance des détritus par rapport à la production phytoplanctonique (D/H) dans le système.

3. Limite de l'étude et difficultés rencontrées

Comme pour de nombreuses études portant sur les relations pressions-état, la principale limite de ce travail est le manque de données quantitatives sur les pressions (anthropiques et naturelles) à l'échelle des stations étudiées dans le Golfe de Gabès. Ainsi, les nutriments ne sont pas les seules responsables de la forte contamination dans cet écosystème. De nombreux autres

facteurs pourraient également entrer en ligne de compte tels que les éléments traces métalliques (ETMs) (Chouba & MzouchiAguir, 2006), les HAPs (Zaghdem et al 2022), etc. La quantité et la qualité de ces polluants rejetés peuvent avoir une influence irréversible sur la communauté planctonique. Evaluer la variabilité inhérente des polluants dans la colonne d'eau nécessiterait par ailleurs un plan d'échantillonnage complexe. De plus, la variation spatiale de la communauté planctonique a été bien étudiée. Or les caractéristiques hydrodynamiques et hydrologiques dans le Golfe changent au fil des saisons, ce qui peut avoir un impact sur la dynamique du plancton (Bel Hassen et al. 2008, 2009 ; Makhlouf Belkahia et al. 2021) ainsi que les interactions planctoniques au sein de l'écosystème. La prise en compte des variations saisonnières dans les études ultérieures est importante afin de mieux comprendre le fonctionnement global de cette zone méditerranéenne très dynamique et productive.

De même pour le Canal de Bizerte, bien que les réponses des communautés des producteurs et consommateurs au déversement de pétrole ait été caractérisés, il reste encore beaucoup d'inconnues. Malgré les nombreuses études réalisées au cours de la dernière décennie, les raisons qui sous-tendent la tolérance relativement élevée des dinoflagellés et des diatomées aux hydrocarbures et aux dispersants, ainsi que les effets stimulants de ces polluants sur la croissance et la production de toxines chez certaines espèces formant des efflorescences, sont inconnues. Ainsi en se basant sur l'effet des hydrocarbures sur la croissance et la photosynthèse des espèces sensibles et résistantes, la taille des cellules a été considérée comme le facteur le plus important pour déterminer la réponse de la biomasse du phytoplancton aux hydrocarbures (Bretherton et al., 2020). Ainsi le changement d'échelle entre la réaction d'une espèce donnée au niveau individuel et les changements observés au niveau de la communauté est encore mal connu. Les interactions entre les différentes composantes planctoniques à savoir phytoplancton-phytoplancton, phytoplancton-bactéries et phytoplancton-zooplancton peuvent jouer un rôle important dans le destin d'une espèce donnée lors d'une marée noire.

Conclusion & Perspectives

Conclusion Générale

Ce travail de thèse s'est intéressé principalement (i) à l'identification des différents types de réseaux trophiques planctoniques dominants au niveau des deux sites d'études à partir des dynamiques des communautés planctoniques et (ii) à l'impact des contaminations chronique et soudaine sur leurs propriétés structurales et émergentes fonctionnelles. Le but ultime est de chercher des indicateurs écologiques utiles et efficaces, pour l'évaluation de l'état de santé de l'écosystème, et qui sont facilement applicables par les experts et les non experts, pour une gestion durable des écosystèmes marins. Les différents résultats issus de ce travail peuvent améliorer la compréhension de la dynamique des réseaux trophiques marins, aussi bien dans les écosystèmes fortement touchés par les apports de nutriments anthropogéniques que les systèmes affectés par des marées noires accidentelles.

La première partie du travail a investigué la dynamique des réseaux trophiques planctoniques dans le Golfe de Gabès, un site caractérisé par un hydrodynamisme actif et une forte productivité, mais perturbé en permanence (chapitre III). La combinaison de l'analyse des réseaux écologiques (indices ENA) et des ratios de typologie nous a permis de mieux comprendre le fonctionnement de l'écosystème face à cette perturbation chronique (chapitre IV). Nos résultats ont modifié la vision traditionnelle concernant la dominance de la voie herbivore dans les zones hautement productives et au contraire ils ont mis en évidence la présence d'un continuum de voies trophiques. Ainsi, différents types de réseaux, dans lesquels le petit et le gros phytoplancton, le protozooplancton et le métazooplancton jouaient divers rôles fonctionnels, ont été décrits le long d'un gradient de richesse nutritive qui semble lui-même causé par la circulation complexe dans le Golfe :

► Le réseau microbien a dominé dans la zone la moins riche en nutriments. Il se caractérisait par une production élevée du picophytoplancton et une forte microbivorie du protozooplancton qui était la principale voie de transfert du carbone. Dans ce réseau, le débit total était le plus faible, alors que l'ascendance relative et le recyclage étaient importants, suggérant que le système avait une faible activité mais une organisation et une stabilité élevées. Le carbone qui circulait dans ce système provenait principalement du phytoplancton, puisque le détritivorie/herbivorie était faible.

► L'augmentation de la richesse nutritive a été suivie par une modification du réseau vers une voie multivore, dans laquelle le gros et le petit phytoplancton ainsi que les composants non vivants (détritus et COD) jouaient un rôle important dans la production du carbone organique. La microbivorie (du protozooplancton) ainsi que l'herbivorie (du proto- et métazooplancton) participaient ensemble dans l'exportation du carbone. Ce réseau, ayant la détritivorie/herbivorie la plus élevée, un recyclage, une ascendance et un débit total relativement importants, était un système organisé, le plus stable avec une activité importante.

► Le réseau herbivore était présent dans les eaux les plus riches en nutriments. Le carbone biogène, principalement produit par le microphytoplancton, était acheminé vers les niveaux trophiques supérieurs par le protozooplancton et le métazooplancton herbivore. Ce réseau, avec un débit total du système le plus élevé et une ascendance relative et un recyclage les plus faibles, était le système le plus actif mais le moins organisé et stable. La détritivorie/ herbivorie était la plus faible indiquant que la source de carbone dans ce système était basée plus sur le phytoplancton que sur la matière inerte.

La deuxième partie de la thèse a porté sur l'étude des effets, à court et à plus long terme, d'une marée noire sur les communautés naturelles du phytoplancton et des consommateurs protozoaires et les conséquences résultantes sur le réseau trophique planctonique dans le Canal de Bizerte (chapitre V et discussion générale). Cette étude a souligné l'importance de l'échantillonnage *in situ* à différents stades de la marée noire, puisque le phytoplancton et le protozooplancton ont réagi différemment tout au long de l'évolution de l'incident pétrolier. Pour le phytoplancton, la croissance, la biomasse, la structure de taille et la composition, observées quelques jours après la fuite du pétrole étaient nettement différentes de celles rapportées à plus long terme. De plus, la contamination pétrolière avait des effets différentiels sur les espèces et les fractions de taille du phytoplancton, ce qui a influencé les taux de production primaire. Concernant le protozooplancton, les différents groupes taxonomiques ont présenté diverses réponses au pétrole, avec le remplacement des taxons vulnérables par des organismes tolérants, qui ont des rôles fonctionnels et des sélectivités alimentaires variables. Cela a provoqué une modification significative des taux de consommation du protozooplancton avec un impact ressenti au niveau de tout le réseau planctonique. En effet, l'utilisation combinée des ratios de typologie trophique et des indices fonctionnels ENA a permis d'identifier différents types de réseaux au cours de l'évolution de la marée noire :

► Un jour après la fuite du pétrole, le réseau herbivore a été décelé avec le microphytoplancton comme principal producteurs, dont la production était transférée vers les niveaux supérieurs *via* l'herbivorie du proto- et métazooplancton. Ce réseau, a montré le débit total et la détritivorie/herbivorie les plus faibles, indiquant un système peu actif basé sur le phytoplancton.

► Après quelques jours du rejet du pétrole (4ème et 8ème jour), la voie multivore s'est installait où la production a été grossièrement partagé entre le micro et le picophytoplancton à J04 et J08 (R7 plus au moins forte R4>R6). Cette production est transférée vers les niveaux supérieurs via la microbivorie et l'herbivorie de PRO ainsi que l'herbivorie de MET (R8 plus au moins fort). Le débit total (TST) était plus au moins faible ces les deux jours et la détritivorie par l'herbivorie était plus importante dans le 4ème jour que le 8ème. Ce qui indique un réseau plus au moins actif et basé sur la matière inerte le 4ème jour et le phytoplankton le 8ème jour.

► A plus long terme (18ème jour), le système était dominait par la voie microbienne caractérisée par une production élevée du picophytoplancton et un rôle important du protozooplancton, à travers sa microbivorie et herbivorie, dans l'acheminement du carbone. Ce système était très actif et basé surtout sur le phytoplancton, puisqu'il possédait un débit total élevé et une faible détritivorie/herbivorie. La comparaison de ce réseau microbien avec la voie microbienne généralement observée dans les conditions normales (i.e. en absence de marée noire) à la même période que notre étude (Meddeb et al., 2019) a révélé que malgré que le même type de réseau fonctionnait, le système était encore perturbé et qu'il n'a pas retrouvé son état d'équilibre initial, c'est-à-dire sa stabilité.

Les résultats des deux études nous permettent de conclure que l'évaluation de la santé des écosystèmes peut se faire en se basant sur une combinaison d'indicateurs écologiques, incluant des indices de typologie trophique et des indices fonctionnels ENA. Cette combinaison a permis d'évaluer la structure, le fonctionnement et les propriétés émergentes des écosystèmes soumis à la pression anthropique, chronique et accidentelle. Ces indicateurs peuvent constituer des outils efficaces applicables dans un contexte de gestion des écosystèmes pollués (Figure 1).

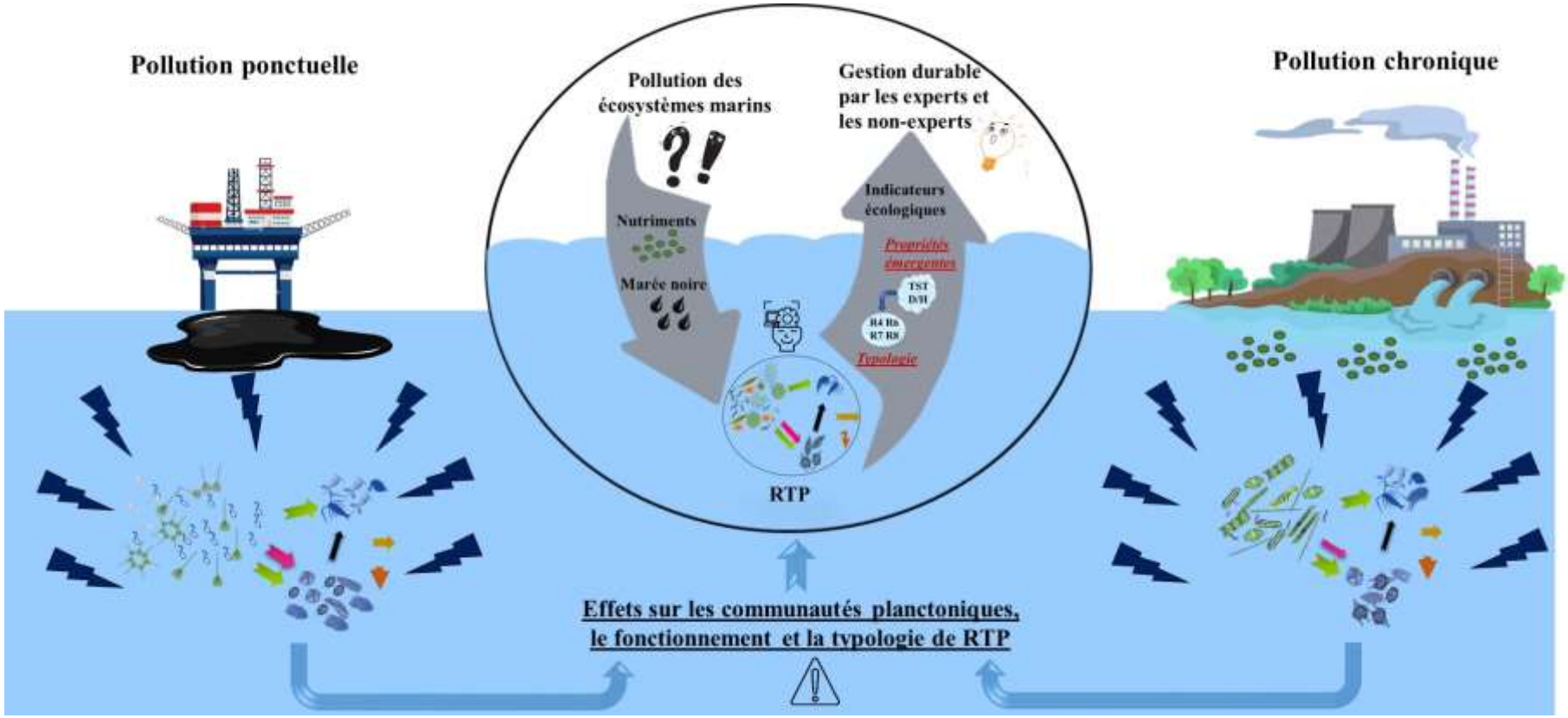

Figure 1. Schéma de synthèse illustrant l'effet de différents types de contamination sur le fonctionnement et la typologie de réseau trophique planctonique (RTP) (un réseau microbien au 18ème jour après la marée noire et un réseau herbivore dans les eaux les plus riches en nutriments) ainsi que les indicateurs écologiques les plus appropriés pour une gestion durable de l'écosystème

Perspectives

À l'issu de cette thèse, certaines perspectives sont inéluctables à développer. Les perspectives proposées ont un aspect fondamental et pratique.

I. Perspectives fondamentales: Mieux comprendre le fonctionnement des réseaux trophiques planctoniques

Perspective 1 : Approfondir la compréhension du rôle de la mixotrophie au sein du réseau planctonique

La présente étude a montré l'importance des mixotrophes aussi bien dans les réseaux soumis à une contamination chronique (cas du Golfe de Gabès) que pulsée (cas de la marée noire). On a signalé que les mixotrophes étaient abondants dans les eaux les plus eutrophes et qu'ils étaient non affectés et même stimulés par le pétrole. En fait, la mixotrophie est facteur de complexité qui retient de plus en plus l'attention. En général, les mixotrophes semblent être plus adaptés aux habitats planctoniques (Laybourn-Parry, 1992), car ils ont certains avantages par rapport aux autotrophes ou hétérotrophes (Veen, 1991; Jones, 1994; Li et al., 1999, 2000; Burkholder et al., 2008). Ward & Followres (2015) ont révélé que la mixotrophie favorise le transfert de la biomasse vers des classes de taille plus grandes, ce qui entraîne une augmentation de la taille moyenne des organismes à l'échelle mondiale et une augmentation de ~35 % du flux de carbone qui sédimente. DeAngelis (1992) a signalé l'effet stabilisateur de la mixotrophie dans les écosystèmes planctoniques océaniques, ce qui tend à surmonter l'effet déstabilisateur général causé par un recyclage étroit de nutriments. Jost et al. (2004) ont émis également l'hypothèse d'un lien mixotrophique qui renforce la stabilité dans le système planctonique. Il semble donc important d'approfondir l'étude de la mixotrophie au sein de la communauté planctonique pour mieux comprendre la réponse et le fonctionnement réseau trophique planctonique face aux perturbations.

Perspective 2 : Approfondir la compréhension du rôle des bactéries hétérotrophes au sein du réseau trophique planctonique

Notre étude a révélé que les hydrocarbures pétroliers peuvent servir une source de carbone pour les bactéries favorisant leurs croissances (chapitre V). Les bactéries hétérotrophes jouent un rôle crucial dans les processus de recyclage, de décomposition et de minéralisation de la matière organique dans les réseaux trophiques (Cunha et al., 2010). Ce sont des producteurs

majeurs de CO_2 dans les cycles biogéochimiques du carbone qui contribuent à la respiration des communautés planctoniques de 10 à 90% (Biddanda et al., 2001; Robinson, 2008). Plusieurs études ont souligné l'importance des bactéries dans les déversements de pétrole (Coral et al 2005; Kostka et al., 2011; Baelum et al., 2012; Kimes et al., 2014; Wanjohi et al., 2015; Bacosa et al., 2015, 2016). La majorité de ces études ont rapporté que les communautés bactériennes sont capables de s'adapter rapidement aux marées noires par le développement sélectif de souches qui dégradent le pétrole ce qui leurs permet d'être utilisées pour assainir l'environnement des contaminants pétroliers (Wanjohi et al., 2015) . Coral et al. (2005) ont révélé l'utilisation par les bactéries du pétrole, riche en carbone, pour satisfaire leur croissance cellulaire et leurs besoins énergétiques. Ainsi en se basant sur des expériences de dégradation de pétrole (Spring, 1994; Wanjohi et al., 2015), les bactéries pourraient être utilisées comme des indicateurs de disparition du pétrole du système. Il serait donc intéressant d'approfondir le rôle joué par les bactéries au sein de réseau trophique dans les eaux riches en nutriments ainsi que lors de suivi de l'évolution de pétrole qui pourrait être considéré par la suite comme un indicateur de l'état de santé de l'écosystème face à une perturbation.

II. Perspectives pratiques: vers l'utilisation des approches omiques pour l'étude des réseaux trophiques planctoniques

En tenant compte de la grande diversité des communautés planctoniques, la dynamique du plancton au cours des perturbations peut être évaluée efficacement en utilisant les technologies méta-omiques (i.e. transcriptomique, protéomique et/ou métabolomique). Ces techniques représentent des outils privilégiés pour améliorer notre connaissance de l'évolution des composantes planctoniques, et ces informations peuvent être traduites en connaissance de l'état de santé du réseau trophique planctonique (Stec et al., 2017; D'Alelio et al., 2019). Les mesures omiques fournissent une grande quantité de données sur la distribution du plancton. Ces méthodes sont d'excellents outils qui permettent par exemple de caractériser les espèces et les communautés en termes de taxonomie et de diversité et d'éclairer les processus fonctionnels qui les caractérisent (*via* les méthodes omiques associés à l'eDNA) (Havermans et al., 2022). Elles permettent également l'identification de plusieurs taxons à partir de l'ensemble de l'ADN d'un échantillon environnemental (Taberlet et al., 2012) et de décrire le lien entre la diversité du plancton et la structure du réseau trophique (Russo et al., 2023) (*via* la méthode le DNA metaB). En plus, les progrès rapides de la modélisation permettent d'améliorer le niveau de précision biologique des modèles écologiques en intégrant les nombreux aspects de la mixotrophie du plancton dans les modèles biogéochimiques (D'Alelio et al., 2016; Ghyoot et

al., 2017). L'identification des réseaux génétiques dédiés à la régulation de la mixotrophie dans les populations naturelles est un autre défi central de la métaomique de nouvelle génération(Mitra et al., 2016; D'Alelio et al., 2019). D'autres efforts fournis par ces mesures omiques permet d'obtenir des informations de départ pour mieux caractériser les interactions entre les espèces de plancton dans le but de façonner les réseaux trophiques : par exemple, les protistes peuvent manger soit des procaryotes, soit d'autres protistes, soit les deux types de proies, les métazoaires peuvent manger des proies unicellulaires ou multicellulaires, ou les deux, et ils peuvent être sélectifs ou non sélectifs (D'Alelio et al., 2016, 2019). Il serait donc intéressant d'utiliser les analyses omiques dans les différents cas de contamination afin d'apporter une analyse complémentaire aux résultats obtenus. Ainsi, les interactions proie-consommateur étudiées dans le présent travail de thèse pourraient être prisent en considération pour avoir plus de récision sur la sélection préférentielle face à aux différents types de perturbations afin de mieux comprendre la différence dans la structuration et le fonctionnement de réseau trophique planctonique.

Références Bibliographiques

-A-

Abbriano, R.M., Carranza, M.M., Hogle, S.L., Levin, R.A., Netburn, A.N., Seto, K.L., Snyder, S.M., Franks, P.J.S., 2011. DEEPWATER HORIZON OIL SPILL: A Review of the Planktonic Response. Oceanography 24, 294–301.

Abdennadher J., Boukthir M., 2006. Numerical simulation of the barotropic tides in the Tunisian Shelf and the Strait of Sicily. J Mar Syst 63:162–182. https://doi.org/10.1016/j.jmarsys.2006.07.001

Aberle N., Lengfellner K., Sommer U., 2007. Spring bloom succession, grazing impact and herbivore selectivity of ciliate communities in response to winter warming. Oecologia 150:668–681. https://doi.org/10.1007/s00442-006-0540-y

Adrian, R., Schneider-Olt, B., 1999. Top-down effects of crustacean zooplankton on pelagic microorganisms in a mesotrophic lake. Journal of Plankton Research 21, 2175–2190. https://doi.org/10.1093/plankt/21.11.2175

Agasild, H., Zingel, P., Karus, K., Kangro, K., Salujõe, J., Nõges, T., 2013. Does metazooplankton regulate the ciliate community in a shallow eutrophic lake? Freshwater Biology 58, 183–191. https://doi.org/10.1111/fwb.12049

Agawin, N.S.R., Duarte, C.M., Agustí, S., 2000. Nutrient and temperature control of the contribution of picoplankton to phytoplankton biomass and production. Limnology and Oceanography 45, 591–600. https://doi.org/10.4319/lo.2000.45.3.0591

Akcay I., Tugrul S., Ozhan K., 2022. Effects of river inputs on particulate organic matter composition and distributions in surface waters and sediments of the Mersin Bay, Northeastern Mediterranean Sea. Reg Stud Mar Sci 52:102316. https://doi.org/10.1016/j.rsma.2022.102316

Aksmann, A., Tukaj, Z., 2008. Intact anthracene inhibits photosynthesis in algal cells: A fluorescence induction study on Chlamydomonas reinhardtii cw92 strain. Chemosphere 74, 26–32. https://doi.org/10.1016/j.chemosphere.2008.09.064

Allen JI., Somerfield PJ., Siddorn J., 2002. Primary and bacterial production in the Mediterranean Sea: a modelling study. J Mar Syst 33–34:473–495. https://doi.org/10.1016/S0924-7963(02)00072-6

Allesina, S., Tang, S., 2012. Stability criteria for complex ecosystems. Nature 483, 205–208. https://doi.org/10.1038/nature10832

Almeda, R., Wambaugh, Z., Chai, C., Wang, Z., Liu, Z., Buskey, E.J., 2013. Effects of Crude Oil Exposure on Bioaccumulation of Polycyclic Aromatic Hydrocarbons and Survival of Adult and Larval Stages of Gelatinous Zooplankton. PLOS ONE 8, e74476. https://doi.org/10.1371/journal.pone.0074476

Almeda, R., Baca, S., Hyatt, C., Buskey, E.J., 2014a. Ingestion and sublethal effects of physically and chemically dispersed crude oil on marine planktonic copepods. Ecotoxicology 23, 988–1003. https://doi.org/10.1007/s10646-014-1242-6

Almeda, R., Connelly, T.L., Buskey, E.J., 2014b. Novel insight into the role of heterotrophic dinoflagellates in the fate of crude oil in the sea. Sci Rep 4, 7560. https://doi.org/10.1038/srep07560

Almeda, R., Harvey, T.E., Connelly, T.L., Baca, S., Buskey, E.J., 2016. Influence of UVB radiation on the lethal and sublethal toxicity of dispersed crude oil to planktonic copepod nauplii. Chemosphere 152, 446–458. https://doi.org/10.1016/j.chemosphere.2016.02.129

Almeda, R., Cosgrove, S., Buskey, E.J., 2018. Oil Spills and Dispersants Can Cause the Initiation of Potentially Harmful Dinoflagellate Blooms ("Red Tides"). Environ. Sci. Technol. 52, 5718–5724. https://doi.org/10.1021/acs.est.8b00335

Antajan, E., Gasparini, S., 2004. Assessment of Cryptophyceae ingestion by copepods using alloxanthin pigment: a caution. Marine Ecology Progress Series 274, 191–198. https://doi.org/10.3354/meps27419 1

Arrigo, K.R., 2005. Marine microorganisms and global nutrient cycles. Nature 437, 349–355. https://doi.org/10.1038/nature04159

Arroyo, N.-L., Safi, G., Vouriot, P., López-López, L., Niquil, N., Le Loc'h, F., Hattab, T., Preciado, I., 2019. Towards coherent GES assessments at sub-regional level: signs of fisheries expansion processes in the Bay of Biscay using an OSPAR food web indicator, the mean trophic level. ICES Journal of Marine Science 76, 1543–1553. https://doi.org/10.1093/icesjms/fsz023

Arts, M.T., 1958-, Brett, M.T., Kainz, M.J., 2009. Lipids in aquatic ecosystems. Springer.

Ashok A, Agusti S (2022). Contrasting sensitivity among oligotrophic marine microbial communities to priority PAHs. Chemosphere, 309, 136490. https://doi.org/10.1016/j.chemosphere.2022.136490

Ayadi, N., Aloulou, F., Bouzid, J., 2015. Assessment of contaminated sediment by phosphate fertilizer industrial waste using pollution indices and statistical techniques in the Gulf of Gabes (Tunisia). Arab J Geosci 8, 1755–1767. https://doi.org/10.1007/s12517-014-1291-4

Ayata, S.-D., Irisson, J.-O., Aubert, A., Berline, L., Dutay, J.-C., Mayot, N., Nieblas, A.-E., D'Ortenzio, F., Palmiéri, J., Reygondeau, G., Rossi, V., Guieu, C., 2018. Regionalisation of the Mediterranean basin, a MERMEX synthesis. Progress in Oceanography, Special issue of MERMEX project: Recent advances in the oceanography of the Mediterranean Sea 163, 7–20. https://doi.org/10.1016/j.pocean.2017.09.016

Azam, F., Fenchel, T., Field, J., Gray, J., Meyer-Reil, L., Thingstad, F., 1983. The Ecological Role of Water-Column Microbes in the Sea. Marine Ecology Progress Series 10, 257–263. https://doi.org/10.3354/meps010257

~B~

Bacosa, H.P., Erdner, D.L., Liu, Z., 2015. Differentiating the roles of photooxidation and biodegradation in the weathering of Light Louisiana Sweet crude oil in surface water from the Deepwater Horizon site. Marine Pollution Bulletin 95, 265–272. https://doi.org/10.1016/j.marpolbul.2015.04.005

Bacosa, H.P., Liu, Z., Erdner, D.L., 2015. Natural Sunlight Shapes Crude Oil-Degrading Bacterial Communities in Northern Gulf of Mexico Surface Waters. Frontiers in Microbiology 6.

Bacosa, H.P., Thyng, K.M., Plunkett, S., Erdner, D.L., Liu, Z., 2016. The tarballs on Texas beaches following the 2014 Texas City "Y" Spill: Modeling, chemical, and microbiological studies. Marine Pollution Bulletin 109, 236–244. https://doi.org/10.1016/j.marpolbul.2016.05.076

Bælum, J., Borglin, S., Chakraborty, R., Fortney, J.L., Lamendella, R., Mason, O.U., Auer, M., Zemla, M., Bill, M., Conrad, M.E., Malfatti, S.A., Tringe, S.G., Holman, H.-Y., Hazen, T.C., Jansson, J.K., 2012. Deep-sea bacteria enriched by oil and dispersant from the Deepwater Horizon spill. Environmental Microbiology 14, 2405–2416. https://doi.org/10.1111/j.1462-2920.2012.02780.x

Bagstad, K.J., Semmens, D.J., Waage, S., Winthrop, R., 2013. A comparative assessment of decision-support tools for ecosystem services quantification and valuation. Ecosystem Services 5, 27–39. https://doi.org/10.1016/j.ecoser.2013.07.004

Baird, D., Ulanowicz, R.E., 1989. The Seasonal Dynamics of The Chesapeake Bay Ecosystem. Ecological Monographs 59, 329–364. https://doi.org/10.2307/1943071

Baird, A.H., Guest, J.R., Willis, B.L., 2009. Systematic and biogeographical patterns in the reproductive biology of scleractinian corals. Annual Review of Ecology, Evolution, and Systematics 40, 551–571. https://doi.org/10.1146/annurev.ecolsys.110308.120220

Baird, D., McGlade, J.M., Ulanowicz, R.E., 1991. The comparative ecology of six marine ecosystems. Philosophical Transactions of the Royal Society of London. Series B: Biological Sciences 333, 15–29. https://doi.org/10.1098/rstb.1991.0058

Bancon-Montigny C., Gonzalez C., Delpoux S., Avenzac M., Spinelli S, Mhadhbi T., Mejri K., Sakka Hlaili A., Pringault O., 2019. Seasonal changes of chemical contamination in coastal waters during sediment resuspension. Chemosphere, 235, 651-661. https://doi.org/10.1016/j.chemosphere.2019.06.213

Banse, K., 1995. Zooplankton: Pivotal role in the control of ocean production: I. Biomass and production. ICES Journal of Marine Science 52, 265–277. https://doi.org/10.1016/1054-3139(95)80043-3

Barhoumi B., LeMenach K., Devier MH., Ameur WB., Etcheber H., Budzinski H., Cachot J., Driss MR., 2014. Polycyclic aromatic hydrocarbons (PAHs) in surface sediments from the Bizerte Lagoon, Tunisia: levels, sources, and toxicological significance. Environ Monit Assess, 186, 2653-2669. https://doi.org/10.1007/s10661-013-3569-5

Barhoumi, B., Clérandeau, C., Gourves, P.-Y., Le Menach, K., El Megdiche, Y., Peluhet, L., Budzinski, H., Baudrimont, M., Driss, M.R., Cachot, J., 2014. Pollution biomonitoring in the Bizerte lagoon (Tunisia), using combined chemical and biomarker analyses in grass goby, Zosterisessor ophiocephalus (Teleostei, Gobiidae). Marine Environmental Research 101, 184–195. https://doi.org/10.1016/j.marenvres.2014.07.002

Barron, M.G., 2012. Ecological Impacts of the Deepwater Horizon Oil Spill: Implications for Immunotoxicity : Toxicologic Pathology and the Immune System. Toxicologic pathology 40, 315–320.

Barron, M.G., 2017. Photoenhanced Toxicity of Petroleum to Aquatic Invertebrates and Fish. Arch Environ Contam Toxicol 73, 40–46. https://doi.org/10.1007/s00244-016-0360-y

Bec, B., Ratréma Husseini, J., Collos, Y., Philippe, S., André, V., 2005. Phytoplankton seasonal dynamics in a Mediterranean coastal lagoon: Emphasis on the picoeukaryote community. Journal of plankton research (0142-7873) (Oxford university press), 2005-09 , Vol. 27 , N. 9 , P. 881-894 27. https://doi.org/10.1093/plankt/fbi061

Beg Paklar, G., Vilibić, I., Grbec, B., Matić, F., Mihanović, H., Džoić, T., Šantić, D., Šestanović, S., Šolić, M., Ivatek-Šahdan, S., Kušpilić, G., 2020. Record-breaking salinities in the middle Adriatic during summer 2017 and concurrent changes in the microbial food web. Progress in Oceanography 185, 102345. https://doi.org/10.1016/j.pocean.2020.10234

Béjaoui B., Raïs S., Koutitonsky V., 2004. Modélisation de la dispersion du phosphogypse dans le golfe de Gabès. Modelisation of the phosphogypsum spreading in the gulf of Gabes. Bull. Inst. Natn. Scien. Tech. Mer de Salammbô, Vol. 31.

Béjaoui, B., Ben Ismail, S., Othmani, A., Ben Abdallah-Ben Hadj Hamida, O., Chevalier, C., Feki-Sahnoun, W., Harzallah, A., Ben Hadj Hamida, N., Bouaziz, R., Dahech, S., Diaz, F., Tounsi, K., Sammari, C., Pagano, M., Bel Hassen, M., 2019. Synthesis review of the Gulf of Gabes (eastern Mediterranean Sea, Tunisia): Morphological, climatic, physical oceanographic, biogeochemical and fisheries features. Estuarine, Coastal and Shelf Science 219, 395–408. https://doi.org/10.1016/j.ecss.2019.01.006

Bel Hassen M., Drira Z., Hamza A., Ayadi H., Akrout F., Issaoui H., 2008. Summer phytoplankton pigments and community composition related to water mass properties in the Gulf of Gabes. Estuar Coast Shelf Sci 77:645–656. https://doi.org/10.1016/j.ecss.2007.10.027

Bel Hassen, M.B., Hamza, A., Drira, Z., Zouari, A., Akrout, F., Messaoudi, S., Aleya, L., Ayadi, H., 2009. Phytoplankton-pigment signatures and their relationship to spring–summer stratification in the Gulf of Gabes. Estuarine, Coastal and Shelf Science 83, 296–306. https://doi.org/10.1016/j.ecss.2009.04.002

Belgrano, A., Scharler, S.E.R.C.U.M., Scharler, U.M., Dunne, J., Ulanowicz, R.E., 2005. Aquatic Food Webs: An Ecosystem Approach. OUP Oxford.

Bell, P.R.F., Elmetri, I., 1995. Ecological indicators of large-scale eutrophication in the Great Barrier Reef lagoon. Oceanographic Literature Review 12, 1145.

Bellinger, B.J., Cocquyt, C., O'Reilly, C.M., 2006. Benthic diatoms as indicators of eutrophication in tropical streams. Hydrobiologia 573, 75–87. https://doi.org/10.1007/s10750-006-0262-5

Ben Brahim, M., Hamza, A., Hannachi, I., Rebai, A., Jarboui, O., Bouain, A., Aleya, L., 2010. Variability in the structure of epiphytic assemblages of Posidonia oceanica in relation to human interferences in the Gulf of Gabes, Tunisia. Marine Environmental Research 70, 411–421. https://doi.org/10.1016/j.marenvres.2010.08.005

Ben Haj, S., 1992. CONTRIBUTION A L'ETUDE BIOGEOLOGIQUE DES PALOURDES (RUDITAPES) (Thèse Doctorat). Université de Nantes, 1962-2021, France.

Ben Ismail S., Sammari C., Pietro Gasparini G., Beranger K., Brahim M, Aleya L., 2012. Water masses exchanged through the Channel of Sicily: Evidence for the presence of new water masses on the Tunisian side of the channel. Deep Sea Research Part I: Oceanographic Research Papers Vol 63, May 2012, Pages 65-81. https://doi.org/10.1016/j.dsr.2011.12.009

Ben Ismail S., Sammari C., Béranger K., 2015. Surface Circulation Features along the Tunisian Coast: Central Mediterranean Sea. 26th IUGG General Assembly, Prague. Czech Republic June 22 – July 2.

Ben Lamine Y., Pringault O., Aissi M, Ensibi C., Mahmoudi E., Kefi O D Y., Yahia M N D., 2015. Environmental controlling factors of copepod communities in the Gulf of Tunis (south western Mediterranean Sea). Cah Biol Mar 56:213–229

Ben Ltaief, T., Drira, Z., Hannachi, I., Bel Hassen, M., Hamza, A., Pagano, M., Ayadi, H., 2015. What are the factors leading to the success of small planktonic copepods in the Gulf of Gabes, Tunisia? J. Mar. Biol. Ass. 95, 747–761. https://doi.org/10.1017/S0025315414001507

Ben Ltaief T., Drira Z., Devenon J L., Hamza A., Ayadi H., Pagano M 2017. How could thermal stratification affect horizontal distribution of depth-integrated metazooplankton communities in the Gulf of Gabes (Tunisia)?. Mar. Biol. Res. 13: 3. https://www.tandfonline.com/doi/abs/10.1080/17451000.2016.1248847

Ben Othman H., Leboulanger C., Le Floc'h E., Mabrouk HH., Hlaili AS., 2012. Toxicity of benz (a) anthracene and fluoranthene to marine phytoplankton in culture: does cell size really matter? J Hazard Mater, 243: 204-211. https://doi.org/10.1016/j.jhazmat.2012.10.020

Ben Othman H., Pringault O., Louati H., Hlaili AS., Leboulanger C., 2017. Impact of contaminated sediment elutriate on coastal phytoplankton community (Thau lagoon, Mediterranean Sea, France). J Exp Mar Biol Ecol, 486: 1-12. https://doi.org/10.1016/j.jembe.2016.09.006

Ben Othman H., Lanouguère É., Got P., Hlaili AS., Leboulanger C., 2018. Structural and functional responses of coastal marine phytoplankton communities to PAH mixtures. Chemosphere, 209, 908-919. https://doi.org/10.1016/j.chemosphere.2018.06.153

Ben Othman, H., Pick, F.R., Sakka Hlaili, A., Leboulanger, C., 2023. Effects of polycyclic aromatic hydrocarbons on marine and freshwater microalgae – A review. Journal of Hazardous Materials 441, 129869. https://doi.org/10.1016/j.jhazmat.2022.129869

Benzouaï S., Louanchi F., Smara Y., 2020. Phytoplankton phenology in algerian continental shelf and slope waters using remotely sensed data. Estuar Coast Shelf Sci 247:107070. https://doi.org/10.1016/j.ecss.2020.107070

Berggreen U., Hansen B., Kiørboe T., 1988. Food size spectra, ingestion and growth of the copepodAcartia tonsa during development: Implications for determination of copepod production. Mar Biol 99:341–352. https://doi.org/10.1007/BF02112126

Berglund J., Müren U., Båmstedt U., Andersson A., 2007. Efficiency of a phytoplankton-based and a bacterial-based food web in a pelagic marine system. Limnol Oceanogr 52:121–131. https://doi.org/10.4319/lo.2007.52.1.0121

Bernard, C., Rassoulzadegan, F., 1990. Bacteria or microflagellates as a major food source for marine ciliates: possible implications for the microzooplankton. Mar. Ecol. Prog. Ser. 64, 147–155. https://doi.org/10.3354/meps064147

Beske-Janssen, P., Johnson, M.P., Schaltegger, S., 2015. 20 years of performance measurement in sustainable supply chain management – what has been achieved? Supply Chain Management: An International Journal 20, 664–680. https://doi.org/10.1108/SCM-06-2015-0216

Bevilacqua, S., Airoldi, L., Ballesteros, E., Benedetti-Cecchi, L., Boero, F., Bulleri, F., Cebrian, E., Cerrano, C., Claudet, J., Colloca, F., Coppari, M., Di Franco, A., Fraschetti, S., Garrabou, J., Guarnieri, G., Guerranti, C., Guidetti, P., Halpern, B.S., Katsanevakis, S., Mangano, M.C., Micheli, F., Milazzo, M., Pusceddu, A., Renzi, M., Rilov, G., Sarà, G., Terlizzi, A., 2021. Chapter One - Mediterranean rocky reefs in the Anthropocene: Present status and future concerns, in: Sheppard, C. (Ed.), Advances in Marine Biology. Academic Press, pp. 1–51. https://doi.org/10.1016/bs.amb.2021.08.001

Biddanda, B., Ogdahl, M., Cotner, J., 2001. Dominance of bacterial metabolism in oligotrophic relative to eutrophic waters. Limnology and Oceanography 46, 730–739. https://doi.org/10.4319/lo.2001.46.3.0730

Bodini, A., Bondavalli, C., 2002. Towards a sustainable use of water resources: a whole-ecosystem approach using network analysis. International Journal of Environment and Pollution.

Bodini, A., Bondavalli, C., Allesina, S., 2012. Cities as ecosystems: Growth, development and implications for sustainability. Ecological Modelling, 7th European Conference on Ecological Modelling (ECEM) 245, 185–198. https://doi.org/10.1016/j.ecolmodel.2012.02.022

Bopp SK, Lettieri T., 2007. Gene regulation in the marine diatom Thalassiosira pseudonana upon exposure to polycyclic aromatic hydrocarbons (PAHs). Gene, 396(2), 293-302. https://doi.org/10.1016/j.gene.2007.03.013

Borgå, K., Fisk, A.T., Hoekstra, P.F., Muir, D.C.G., 2004. Biological and chemical factors of importance in the bioaccumulation and trophic transfer of persistent organochlorine contaminants in arctic marine food webs. Environmental Toxicology and Chemistry 23, 2367–2385. https://doi.org/10.1897/03-518

Borrett, S.R., Scharler, U.M., 2019. Walk partitions of flow in Ecological Network Analysis: Review and synthesis of methods and indicators. Ecological Indicators 106, 105451. https://doi.org/10.1016/j.ecolind.2019.105451

Bouchouicha Smida, D., Sahraoui, I., Mabrouk, H.H., Sakka Hlaili, A., 2012. Dynamique saisonnière du genre Alexandrium (dinoflagellé potentiellement toxique) dans la lagune de Bizerte (Nord de la Tunisie) et contrôle par les facteurs abiotiques environnants. Comptes Rendus Biologies 335, 406–416. https://doi.org/10.1016/j.crvi.2012.04.007

Bouchouicha Smida D., Lundholm N., Kooistra WH., Sahraoui I., Ruggiero MV., Kotaki Y., Ellegaard M., Lambert C., Hadj Mabrouk H., Hlaili AS., 2014a. Morphology and molecular phylogeny of Nitzschia bizertensis sp. nov.—A new domoic acid-producer. Harmful Algae, 32, 49-63. https://doi.org/10.1016/j.hal.2013.12.004

Bouchouicha Smida D., Sahraoui I., Grami B., Hadj Mabrouk H., Sakka Hlaili A., 2014b. Population dynamics of potentially harmful algal blooms in Bizerte Lagoon, Tunisia. African J Aquat Sci, 39(2), 177-188. https://doi.org/10.2989/16085914.2014.911718

Boudaya, L., Mosbahi, N., Dauvin, J.-C., Neifar, L., 2019. Structure of the benthic macrofauna of an anthropogenic influenced area: Skhira Bay (Gulf of Gabès, central Mediterranean Sea). Environ Sci Pollut Res 26, 13522–13538. https://doi.org/10.1007/s11356-019-04809-8

Boudriga I., Thyssen M., Zouari A., Garcia N., Tedetti M., Bel Hassen M., 2022. Ultraphytoplankton community structure in subsurface waters along a North-South Mediterranean transect. Marine Pollution Bulletin 182:113977. https://doi.org/10.1016/j.marpolbul.2022.113977

Bougis, P., 1974. Ecologie du plancton marin. Paris (France) Masson et Cie.

Boukthir M., Jaber IB., Chevalier C., Abdennadher J., 2019. A high-resolution three-dimensional hydrodynamic model of the gulf of Gabes (Tunisia). In 42nd CIESM Congress.

Boutrup PV., Moestrup Ø., Tillmann U., Daugbjerg N., 2016. Katodinium glaucum (Dinophyceae) revisited: proposal of new genus, family and order based on ultrastructure and phylogeny. Phycologia 55:147–164. https://doi.org/10.2216/15-138.1

Bouvy, M., Ba, N., Ka, S., Sane, S., Pagano, M., Arfi, R., 2006. Phytoplankton community structure and species assemblage succession in a shallow tropical lake (Lake Guiers, Senegal). Aquatic Microbial Ecology 45, 147–161. https://doi.org/10.3354/ame045147

Bradshaw C., Tjensvoll I., Sköld M., Allan IJ., Molvaer J., Magnusson J., Naes K., Nilsson HC., 2012. Bottom trawling resuspends sediment and releases bioavailable contaminants in a polluted fjord. Environ Pollut, 170: 232-241. https://doi.org/10.1016/j.envpol.2012.06.019

Bretherton, L., Williams, A., Genzer, J., Hillhouse, J., Kamalanathan, M., Finkel, Z.V., Quigg, A., 2018. Physiological response of 10 phytoplankton species exposed to macondo oil and the dispersant, Corexit. Journal of Phycology 54, 317–328. https://doi.org/10.1111/jpy.12625

Bretherton L., Setta S., Hillhouse J., Bacosa H., Genzer J., Kamalanathan M., Finkel ZV., Irwin AH., Quigg A., 2019a. Growth dynamics and domoic acid production in Pseudo-nitzschia sp. in response to oil and dispersant exposure. Harmf Algae, 86, 55–63. https://doi.org/10.1016/j.hal.2019.05.008.

Bretherton, L., Kamalanathan, M., Genzer, J., Hillhouse, J., Setta, S., Liang, Y., Brown, C.M., Xu, C., Sweet, J., Passow, U., Finkel, Z.V., Irwin, A.J., Santschi, P.H., Quigg, A., 2019b. Response of natural phytoplankton communities exposed to crude oil and chemical dispersants during a mesocosm experiment. Aquatic Toxicology 206, 43–53. https://doi.org/10.1016/j.aquatox.2018.11.004

Bretherton, L., Hillhouse, J., Kamalanathan, M., Finkel, Z.V., Irwin, A.J., Quigg, A., 2020. Trait-dependent variability of the response of marine phytoplankton to oil and dispersant exposure. Marine Pollution Bulletin 153, 110906. https://doi.org/10.1016/j.marpolbul.2020.110906

Brown SL., Landry MR., Christensen S., et al., 2002. Microbial community dynamics and taxon-specific phytoplankton production in the Arabian Sea during the 1995 monsoon seasons. Deep Sea Res Part II Top Stud Oceanogr 49:2345–2376. https://doi.org/10.1016/S0967-0645(02)00040-1

Bruno, S.F., Staker, R.D., Sharma, G.M., Turner, J.T., 1983. Primary productivity and phytoplankton size fraction dominance in a temperate North Atlantic estuary. Estuaries 6, 200–211. https://doi.org/10.2307/1351512

Brussaard CPD., Peperzak L., Beggah S., Wick LY., Wuerz B., Weber J., Arey SJ., Van Der Burg B., Jonas A., Huisman J., Van Der Meer JR., 2016. Immediate ecotoxicological effects of short-lived oil spills on marine biota. Nat commun, 7(1), 11206. https://doi.org/10.1038/ncomms11206

Buholce, L., Līcīte, V., Boikova, E., Botva, U., 2015. Structural Composition of Protozooplankton Communities in Relation to Environmental Factors in Shallow Lakes and Reservoirs of Rīga, Latvia. Proceedings of the Latvian Academy of Sciences. Section B. Natural, Exact, and Applied Sciences. 69, 105–111. https://doi.org/10.1515/prolas-2015-0015

Burkholder, J.M., Glibert, P.M., Skelton, H.M., 2008. Mixotrophy, a major mode of nutrition for harmful algal species in eutrophic waters. Harmful Algae, HABs and Eutrophication 8, 77–93. https://doi.org/10.1016/j.hal.2008.08.010

Burkill, P.H., Edwards, E.S., Sleight, M.A., 1995. Microzooplankton and their role in controlling phytoplankton growth in the marginal ice zone of the Bellingshausen Sea. Deep Sea Research Part II: Topical Studies in Oceanography 42, 1277–1290. https://doi.org/10.1016/0967-0645(95)00060-4

-C-

Cadaillon, A.M., 2018. Réponses fonctionnelles et structurelles des associations phytoplanctoniques face à une perturbation anthropique : un scénario de déversement d'hydrocarbures (masters). Université du Québec à Rimouski, Rimouski.

Calbet, A., Landry, M.R., 1999. Mesozooplankton influences on the microbial food web: Direct and indirect trophic interactions in the oligotrophic open ocean. Limnology and Oceanography 44, 1370–1380. https://doi.org/10.4319/lo.1999.44.6.1370

Calbet A., Landry MR., Scheinberg RD., 2000. Copepod grazing in a subtropical bay: species-specific responses to a midsummer increase in nanoplankton standing stock. Mar Ecol Prog Ser 193:75–84. https://doi.org/10.3354/meps193075

Calbet, A., Landry, M.R., 2004. Phytoplankton growth, microzooplankton grazing, and carbon cycling in marine systems. Limnology and Oceanography 49, 51–57. https://doi.org/10.4319/lo.2004.49.1.0051

Calbet, A., Saiz, E., 2005. The ciliate-copepod link in marine ecosystems. Aquatic Microbial Ecology 38, 157–167. https://doi.org/10.3354/ame038157

Calbet, A., Carlotti, F., Gaudy, R., 2007. The feeding ecology of the copepod Centropages typicus (Kröyer). Progress in Oceanography, The Biology and Ecology of Centropages typicus 72, 137–150. https://doi.org/10.1016/j.pocean.2007.01.003

Calbet, A., Trepat, I., Almeda, R., Salo, V., Saiz, E., Movilla, J., Alcaraz, M., Yebra, L., Simó, R., 2008. Impact of micro- And nanograzers on phytoplankton assessed by standard and size-

fractionated dilution grazing experiments. Aquatic Microbial Ecology 50, 145–156. https://doi.org/10.3354/ame01171

Callieri C., Stockner JG., 2002. Freshwater autotrophic picoplankton: a review. J Limnol 61:1. https://doi.org/10.4081/jlimnol.2002.1

Camus, T., Zeng, C., 2009. The effects of stocking density on egg production and hatching success, cannibalism rate, sex ratio and population growth of the tropical calanoid copepod Acartia sinjiensis. Aquaculture 287, 145–151. https://doi.org/10.1016/j.aquaculture.2008.10.005

Cardoso, A., Cochrane, S., Doerner, H., Ferreira, J., Galgani, F., Hagebro, C., Hanke, G., Hoepffner, N., Keizer, P., Law, R., Olenin, S., Piet, G., Rice, J., Rogers, S., Swartenbroux, F., Tasker, M., Van, D.B.W., 2010. Scientific Support to the European Commission on the Marine Strategy Framework Directive - Management Group Report [WWW Document]. JRC Publications Repository. https://doi.org/10.2788/86430

Carls, M.G., Short, J.W., Payne, J., 2006. Accumulation of polycyclic aromatic hydrocarbons by Neocalanus copepods in Port Valdez, Alaska. Marine Pollution Bulletin 52, 1480–1489. https://doi.org/10.1016/j.marpolbul.2006.05.008

Caron, D.A., Goldman, J.C., Dennett, M.R., 1988. Experimental demonstration of the roles of bacteria and bacterivorous protozoa in plankton nutrient cycles. Hydrobiologia 159, 27–40. https://doi.org/10.1007/BF00007365

Caron, D., A., 1990. Protozoan nutrient regeneration. Ecology of Marine Protozoa.

Caroppo C., Stabili L., Aresta M., Corinaldesi C., Danovaro R., 2006. Impact of heavy metals and PCBs on marine picoplankton. Environ Toxicol 21:541–551. https://doi.org/10.1002/tox.20215

Caroppo C., Roselli L., Di Leo A., 2018. Hydrological conditions and phytoplankton community in the Lesina lagoon (southern Adriatic Sea, Mediterranean). Environ Sci Pollut Res 25:1784–1799. https://doi.org/10.1007/s11356-017-0599-5

Carpenter, S.R., Mooney, H.A., Agard, J., Capistrano, D., DeFries, R.S., Díaz, S., Dietz, T., Duraiappah, A.K., Oteng-Yeboah, A., Pereira, H.M., Perrings, C., Reid, W.V., Sarukhan, J., Scholes, R.J., Whyte, A., 2009. Science for managing ecosystem services: Beyond the Millennium Ecosystem Assessment. Proc. Natl. Acad. Sci. U.S.A. 106, 1305–1312. https://doi.org/10.1073/pnas.0808772106

Casotti R., Landolfi A., Brunet C., D'Ortenzio F., Mangoni O., Ribera d'Alcalà M., Denis M., 2003. Composition and dynamics of the phytoplankton of the Ionian Sea (eastern Mediterranean). J Geophys Res Oceans 108:. https://doi.org/10.1029/2002JC001541

Cederwall, J., Black, T.A., Blais, J.M., Hanson, M.L., Hollebone, B.P., Palace, V.P., Rodríguez-Gil, J.L., Greer, C.W., Maynard, C., Ortmann, A.C., Rooney, R.C., Orihel, D.M., 2020. Life under an oil slick: response of a freshwater food web to simulated spills of diluted bitumen

in field mesocosms. Can. J. Fish. Aquat. Sci. 77, 779–788. https://doi.org/10.1139/cjfas-2019-0224

Cerino F., Bernardi Aubry F., Coppola J., et al., 2012. Spatial and temporal variability of pico-, nano- and microphytoplankton in the offshore waters of the southern Adriatic Sea (Mediterranean Sea). Cont Shelf Res 44:94–105. https://doi.org/10.1016/j.csr.2011.06.006

Cermeño P., Marañón E., Pérez V., Serret P., Fernández E., Castroc CG., 2006. Phytoplankton size structure and primary production in a highly dynamic coastal ecosystem (Ría de Vigo, NW-Spain): Seasonal and short-time scale variability. Estuar Coast Shelf Sci 67:251–266. https://doi.org/10.1016/j.ecss.2005.11.027

Chaalali, A., Saint-Béat, B., Lassalle, G., Le Loc'h, F., Tecchio, S., Safi, G., Savenkoff, C., Lobry, J., Niquil, N., 2015. A new modeling approach to define marine ecosystems food-web status with uncertainty assessment. Progress in Oceanography 135, 37–47. https://doi.org/10.1016/j.pocean.2015.03.012

Chaalali, A., Beaugrand, G., Raybaud, V., Lassalle, G., Saint-Béat, B., Le Loc'h, F., Bopp, L., Tecchio, S., Safi, G., Chifflet, M., Lobry, J., Niquil, N., 2016. From species distributions to ecosystem structure and function: A methodological perspective. Ecological Modelling 334, 78–90. https://doi.org/10.1016/j.ecolmodel.2016.04.022

Change, M.E. on C. and environmental, Change (MedECC), M.E. on C. and environmental, Lionello, P., Cherif, S., Drobinski, P., Fader, M., Hassoun, A.E.R., Giuopponi, C., Koubi, V., Lange, M., Llasat, M.C., Moncada, S., Mrabet, R., Snoussi, M., Toreti, A., Vafeidis, A.T., Xoplaki, E., 2020. Climate and Environmental Change in the Mediterranean Basin – Current Situation and Risks for the Future. First Mediterranean Assessment Report. MedECC.

Chen D., Guo C., Yu L., Lu Y., Sun J., 2020. Phytoplankton growth and microzooplankton grazing in the central and northern South China Sea in the spring intermonsoon season of 2017. Acta Oceanol Sin 39:84–95. https://doi.org/10.1007/s13131-020-1593-1

Chen, B., Liu, H., Landry, M.R., DaI, M., Huang, B., Sune, J., 2009. Close coupling between phytoplankton growth and microzooplankton grazing in the western South China Sea. Limnology and Oceanography 54, 1084–1097. https://doi.org/10.4319/lo.2009.54.4.1084

Chen, W.-L., Chiang, K.-P., Tsai, S.-F., 2020. Neglect of Presence of Bacteria Leads to Inaccurate Growth Parameters of the Oligotrich Ciliate Strombidium sp. During Grazing Experiments on Nanoflagellates. Frontiers in Marine Science 7.

Chisholm, S.W., 1992. Phytoplankton Size, in: Falkowski, P.G., Woodhead, A.D., Vivirito, K. (Eds.), Primary Productivity and Biogeochemical Cycles in the Sea, Environmental Science Research. Springer US, Boston, MA, pp. 213–237. https://doi.org/10.1007/978-1-4899-0762-2_12

Chkili, O., Meddeb, M., Mejri Kousri, K., Melliti Ben Garali, S., Makhlouf Belkhahia, N., Tedetti, M., Pagano, M., Belaaj Zouari, A., Belhassen, M., Niquil, N., Sakka Hlaili, A., 2023. Influence of Nutrient Gradient on Phytoplankton Size Structure, Primary Production and Carbon Transfer Pathway in a Highly Productive Area (SE Mediterranean). Ocean Sci. J. 58, 6. https://doi.org/10.1007/s12601-023-00101-6

Chkili O., Melliti Ben Garali S., Mejri Kousri K., Meddeb. M. Niquil N., Sakka Hlaili A. Novel insight into the oil impact on the protozooplankton, trophic interactions and food web structure: field and modelling study. (Submitted in Science of The Total Environment Journal).

Chouba, L., Mzoughi-Aguir, N., 2006. Les metaux traces (Cd, Pb, Hg) et les hydrocarbures totaux dans les sediments superficiels de la frange cotiere du golfe de Gabes. INSTM Bulletin : Marine and Freshwater Sciences 33, 93–100.

Christaki, U., Van Wambeke, F., Lefevre, D., Lagaria, A., Prieur, L., Pujo-Pay, M., Grattepanche, J.-D., Colombet, J., Psarra, S., Dolan, J.R., Sime-Ngando, T., Conan, P., Weinbauer, M.G., Moutin, T., 2011. Microbial food webs and metabolic state across oligotrophic waters of the Mediterranean Sea during summer. Biogeosciences 8, 1839–1852. https://doi.org/10.5194/bg-8-1839-2011

Christensen, V., 1995. Ecosystem maturity — towards quantification. Ecological Modelling 77, 3–32. https://doi.org/10.1016/0304-3800(93)E0073-C

Christensen, V., Walters, C., Pauly, D., 2005. Ecopath with Ecosim: A User's Guide. Fisheries Centre, University of British Columbia, Vancouver, Canada and ICLARM, Penang, Malaysia 12.

Christian, R.R., Brinson, M.M., Dame, J.K., Johnson, G., Peterson, C.H., Baird, D., 2009. Ecological network analyses and their use for establishing reference domain in functional assessment of an estuary. Ecological Modelling, Special Issue on Cross-Disciplinary Informed Ecological Network Theory 220, 3113–3122. https://doi.org/10.1016/j.ecolmodel.2009.07.012

Chrystal, R.A., Scharler, U.M., 2014. Network analysis indices reflect extreme hydrodynamic conditions in a shallow estuarine lake (Lake St Lucia), South Africa. Ecological Indicators 38, 130–140. https://doi.org/10.1016/j.ecolind.2013.10.025

Cibic T., Cerino F., Karuza A., Fornasaro D., Comici C., Cabrini M., 2018. Structural and functional response of phytoplankton to reduced river inputs and anomalous physical-chemical conditions in the Gulf of Trieste (northern Adriatic Sea). Science of The Total Environment 636:838–853. https://doi.org/10.1016/j.scitotenv.2018.04.205

Ciglenečki I, Vilibić I, Dautović J, Vojvodić V, Ćosović B, Zemunik P, Mihanović H (2020) Dissolved organic carbon and surface active substances in the northern Adriatic Sea: Long-term trends, variability and drivers. Sci Total Environ 730:139104. https://doi.org/10.1016/j.scitotenv.2020.139104

Clayton, J., SP, P., NF, B., 1977. Polychlorinated biphenyls in coastal marine zooplankton: bioaccumulation by equilibrium partitioning. Polychlorinated biphenyls in coastal marine zooplankton: bioaccumulation by equilibrium partitioning.

Cole, J., Findlay, S., Pace, M., 1988. Bacterial Production in Fresh and Saltwater Ecosystems – a Cross-System Overview. Marine Ecology - Progress Series 43, 1–10. https://doi.org/10.3354/meps043001

Coll, M., Santojanni, A., Palomera, I., Tudela, S., Arneri, E., 2007. An ecological model of the Northern and Central Adriatic Sea: Analysis of ecosystem structure and fishing impacts. Journal of Marine Systems 67, 119–154. https://doi.org/10.1016/j.jmarsys.2006.10.002

Coral, G., Karagoz, S., 2005. Isolation and characterization of phenanthrene-degrading bacteria from a petroleum refinery soil. Ann. microbiol 55, 255–259.

Corradino GL., Schnetzer A., 2022. Grazing of a heterotrophic nanoflagellate on prokaryote and eukaryote prey: ingestion rates and gross growth efficiency. Mar Ecol Prog Ser 682:65–77. https://doi.org/10.3354/meps13921

Corrales, X., Coll, M., Tecchio, S., Bellido, J.M., Fernández, Á.M., Palomera, I., 2015. Ecosystem structure and fishing impacts in the northwestern Mediterranean Sea using a food web model within a comparative approach. Journal of Marine Systems 148, 183–199. https://doi.org/10.1016/j.jmarsys.2015.03.006

Costanza, R., Norton, B.G., Haskell, B.D., 1992. Ecosystem Health: New Goals for Environmental Management. Island Press.

Cotano, U., Uriarte, I., Villate, F., 1998. Herbivory of nanozooplankton in polyhaline and euhaline zones of a small temperate estuarine system (Estuary of Mundaka): seasonal variations. Journal of Experimental Marine Biology and Ecology 227, 265–279. https://doi.org/10.1016/S0022-0981(97)00275-X

Courboulès J., Vidussi F., Soulié T., Mas S., Pecqueur D., Mostajir B., 2021. Effects of experimental warming on small phytoplankton, bacteria and viruses in autumn in the Mediterranean coastal Thau Lagoon. Aquat Ecol 55:647–666. https://doi.org/10.1007/s10452-021-09852-7

Cunha, A., Almeida, A., Coelho, F., Gomes, N., Oliveira, V., Santos, A., 2010. Bacterial Extracellular Enzymatic Activity in Globally Changing Aquatic Ecosystems. Current Research, Technology and Education Topics in Applied Microbiology and Microbial Biotechnology 1.

Cushing, D.H., 1989. A difference in structure between ecosystems in strongly stratified waters and in those that are only weakly stratified. Journal of Plankton Research 11, 1–13. https://doi.org/10.1093/plankt/11.1.1

~Ð~

D'Alcalà MR., Conversano F., Corato F., Licandro P., Mangoni O., Marino D., Mazzocchi MG., Modigh M., Montresor M., Nardella M., Saggiomo V., Sarno D., Zingone A., 2004. Seasonal patterns in plankton communities in a pluriannual time series at a coastal Mediterranean site (Gulf of Naples): an attempt to discern recurrences and trends. Sci Mar 68:65–83. https://doi.org/10.3989/scimar.2004.68s165

D'Alelio, D., Montresor, M., Mazzocchi, M.G., Margiotta, F., Sarno, D., d'Alcalà, M.R., 2016. Plankton food-webs: to what extent can they be simplified? Advances in Oceanography and Limnology 7. https://doi.org/10.4081/aiol.2016.5646

D'Alelio, D., Eveillard, D., Coles, V.J., Caputi, L., Ribera d'Alcalà, M., Iudicone, D., 2019. Modelling the complexity of plankton communities exploiting omics potential: From present challenges to an integrative pipeline. Current Opinion in Systems Biology, • Systems biology of model organisms • Systems ecology and evolution 13, 68–74. https://doi.org/10.1016/j.coisb.2018.10.003

D'Alelio, D., Russo, L., Del Gaizo, G., Caputi, L., 2022. Plankton under Pressure: How Water Conditions Alter the Phytoplankton–Zooplankton Link in Coastal Lagoons. Water 14, 974. https://doi.org/10.3390/w14060974

D'Costa, P.M., D'Silva, M.S., Naik, R.K., 2017. Impact of Pollution on Phytoplankton and Implications for Marine Econiches, in: Naik, M.M., Dubey, S.K. (Eds.), Marine Pollution and Microbial Remediation. Springer, Singapore, pp. 205–222. https://doi.org/10.1007/978-981-10-1044-6_13

D'Ortenzio, F., Ribera d'Alcalà, M., 2009. On the trophic regimes of the Mediterranean Sea: a satellite analysis. Biogeosciences 6, 139–148. https://doi.org/10.5194/bg-6-139-2009

Dale, T., 1987. Oil pollution and plankton dynamics. II. Abundance pattern of ciliates inside and outside enclosures and the responses of ciliates to oil during the 1980 spring bloom in lindåspollene, Norway. Sarsia 72, 197–202. https://doi.org/10.1080/00364827.1987.10419717

Dale, T., 1988. Oil pollution and plankton dynamics. Sarsia 73, 179–191. https://doi.org/10.1080/00364827.1988.10413405

Dalsgaard, J., St. John, M., Kattner, G., Müller-Navarra, D., Hagen, W., 2003. Fatty acid trophic markers in the pelagic marine environment, in: Advances in Marine Biology. Academic Press, pp. 225–340. https://doi.org/10.1016/S0065-2881(03)46005-7

Dam HG., Peterson WT., 1988. The effect of temperature on the gut clearance rate constant of planktonic copepods. J Exp Mar Biol Ecol 123:1–14. https://doi.org/10.1016/0022-0981(88)90105-0

Danovaro, R., 2003. Pollution threats in the Mediterranean Sea: An Overview. Chemistry and Ecology - CHEM ECOL 19, 15–32. https://doi.org/10.1080/0275754031000081467

Danovaro, R., Fanelli, E., Aguzzi, J., Billett, D., Carugati, L., Corinaldesi, C., Dell'Anno, A., Gjerde, K., Jamieson, A.J., Kark, S., McClain, C., Levin, L., Levin, N., Ramirez-Llodra, E., Ruhl, H., Smith, C.R., Snelgrove, P.V.R., Thomsen, L., Van Dover, C.L., Yasuhara, M., 2020. Ecological variables for developing a global deep-ocean monitoring and conservation strategy. Nat Ecol Evol 4, 181–192. https://doi.org/10.1038/s41559-019-1091-z

David, V., Sautour, B., Chardy, P., 2007. Successful colonization of the calanoid copepod Acartia tonsa in the oligo-mesohaline area of the Gironde estuary (SW France) – Natural or anthropogenic forcing? Estuarine, Coastal and Shelf Science 71, 429–442. https://doi.org/10.1016/j.ecss.2006.08.018

De Brabandere, L., Iny, A., 2012. Thinking in New Boxes, in: Own the Future. John Wiley & Sons, Ltd, pp. 279–283. https://doi.org/10.1002/9781119204084.ch38

De Jonge, V.N., Schückel, U., 2021. A comprehensible short list of ecological network analysis indices to boost real ecosystem-based management and policy making. Ocean & Coastal Management 208, 105582. https://doi.org/10.1016/j.ocecoaman.2021.105582

De la Vega, C., Horn, S., Baird, D., Hines, D., Borrett, S., Jensen, L.F., Schwemmer, P., Asmus, R., Siebert, U., Asmus, H., 2018a. Seasonal dynamics and functioning of the Sylt-Rømø Bight, northern Wadden Sea. Estuarine, Coastal and Shelf Science 203, 100–118. https://doi.org/10.1016/j.ecss.2018.01.021

De la Vega, C., Schückel, U., Horn, S., Kröncke, I., Asmus, R., Asmus, H., 2018b. How to include ecological network analysis results in management? A case study of three tidal basins of the Wadden Sea, south-eastern North Sea. Ocean & Coastal Management 163, 401–416. https://doi.org/10.1016/j.ocecoaman.2018.07.019

De Laender, F., Van Oevelen, D., Soetaert, K., Middelburg, J., 2010. Carbon transfer in a herbivore- and microbial loop-dominated pelagic food webs in the southern Barents Sea during spring and summer. Mar. Ecol. Prog. Ser. 398, 93–107. https://doi.org/10.3354/meps08335

DeAngelis, D.L., 1992. Dynamics of Nutrient Cycling and Food Webs. Springer Science & Business Media.

Deasi SR., Verlecar XN., Ansari ZA., Jagtap TG., Sarkar A., Vashistha D., Dalal SG., 2010. Evaluation of genotoxic responses of Chaetoceros tenuissimus and Skeletonema costatum to water accommodated fraction of petroleum hydrocarbons as biomarker of exposure. Water Res, 44 (7): 2235-2244. https://doi.org/10.1016/j.watres.2009.12.048

Debenest T., Pinelli E., Coste M., Silvestre J., Mazzella N., Madigou C., Delmas F., 2009. Sensitivity of freshwater periphytic diatoms to agricultural herbicides. Aquat Toxicol, 93(1), 11-17. https://doi.org/10.1016/j.aquatox.2009.02.014

Decembrini, F., Caroppo, C., Azzaro, M., 2009. Size structure and production of phytoplankton community and carbon pathways channelling in the Southern Tyrrhenian Sea (Western Mediterranean). Deep Sea Research Part II: Topical Studies in Oceanography, Multi-disciplinary forays into the south Tyrrhenian Sea - 2005 CIESM/SUB cruises 56, 687–699. https://doi.org/10.1016/j.dsr2.2008.07.022

Decembrini, F., Caroppo, C., Caruso, G., Bergamasco, A., 2021. Linking Microbial Functioning and Trophic Pathways to Ecological Status in a Coastal Mediterranean Ecosystem. Water 13, 1325. https://doi.org/10.3390/w13091325

Deppeler, S., Schulz, K.G., Hancock, A., Pascoe, P., McKinlay, J., Davidson, A., 2019. Ocean acidification reduces growth and grazing of Antarctic heterotrophic nanoflagellates (preprint). Biodiversity and Ecosystem Function: Marine. https://doi.org/10.5194/bg-2019-224

Derouiche, A., Sanda, Y.G., Driss, M.R., 2004. Polychlorinated Biphenyls in Sediments from Bizerte Lagoon, Tunisia. Bull Environ Contam Toxicol 73, 810–817. https://doi.org/10.1007/s00128-004-0499-5

DGPA, 2015. Annuaires statistiques [WWW Document]. URL http://www.ispab.agrinet.tn/index.php/fr/documents-utiles/annuaires-statistiques.html (accessed 5.28.23).

Djomo JE., Dauta A., Ferrier V., Narbonne JF., Monkiedje A., Njine T., Garrigues P., 2004. Toxic effects of some major polyaromatic hydrocarbons found in crude oil and aquatic sediments on Scenedesmus subspicatus. Water res, 38(7), 1817-1821. https://doi.org/10.1016/j.watres.2003.10.023

Dokulil, M.T., Qian, K., 2021. Photosynthesis, carbon acquisition and primary productivity of phytoplankton: a review dedicated to Colin Reynolds. Hydrobiologia 848, 77–94. https://doi.org/10.1007/s10750-020-04321-y

Dolan JR, Pierce RW, Yang EJ, Kim SY (2012) Southern Ocean Biogeography of Tintinnid Ciliates of the Marine Plankton. J Eukaryot Microbiol 59:511–519. https://doi.org/10.1111/j.1550-7408.2012.00646.x

Domingues RB., Barreto M., Brotas V., et al., 2021. Short-term effects of winter warming and acidification on phytoplankton growth and mortality: more losers than winners in a temperate coastal lagoon. Hydrobiologia 848:4763–4785. https://doi.org/10.1007/s10750-021-04672-0

Dong Y., Li QP., Wu Z., Shuai Y., Liu Z., Ge Z., Zhou W., Chen Y., 2021. Biophysical controls on seasonal changes in the structure, growth, and grazing of the size-fractionated phytoplankton community in the northern South China Sea. Biogeosciences 18:6423–6434. https://doi.org/10.5194/bg-18-6423-2021

Dong Y, Li QP., Wu Z., Shuai Y., Liu Z., Ge Z., Zhou W., Chen Y., 2021. Biophysical controls on seasonal changes in the structure, growth, and grazing of the size-fractionated phytoplankton community in the northern South China Sea. Biogeosciences 18:6423–6434. https://doi.org/10.5194/bg-18-6423-2021

Dopheide A., Lear G., Stott R., Lewis G., 2011. Preferential Feeding by the Ciliates Chilodonella and Tetrahymena spp. and Effects of These Protozoa on Bacterial Biofilm Structure and Composition. Appl Environ Microbiol 77:4564–4572. https://doi.org/10.1128/AEM.02421-10

Drira Z., Hamza A., Belhassen M., Ayadi H., Bouaïn A., Aleya L., 2008. Dynamics of dinoflagellates and environmental factors during the summer in the Gulf of Gabes (Tunisia, Eastern Mediterranean Sea). Sci Mar 72:59–71. https://doi.org/10.3989/scimar.2008.72n159

Drira Z, Hassen MB, Hamza A, Rebai A, Bouain A, Ayadi H, Aleya L., 2009. Spatial and temporal variations of microphytoplankton composition related to hydrographic conditions in the Gulf of Gabès. J Mar Biol Assoc U K 89:1559–1569.https://doi.org/10.1017/S002531540900023X

Drira, Z., Hassen, M., Ayadi, H., Hamza, A., Zarrad, R., Bouaïn, A., Aleya, L., 2010. Copepod Gabès (Tunisia, eastern Mediterranean Sea). Journal of the Marine Biological Association of the United Kingdom 90, 145–157. https://doi.org/10.1017/S0025315409990403

Drira Z., Bel Hassen M., Ayadi H., Aleya L., 2014. What factors drive copepod community distribution in the Gulf of Gabes, Eastern Mediterranean Sea? Environ Sci Pollut Res 21:2918–2934. https://doi.org/10.1007/s11356-013-2250-4

Drira Z., Kmiha-Megdiche S., Sahnoun H., Hammami A., Allouche N., Tedetti M., Ayadi H., 2016. Assessment of anthropogenic inputs in the surface waters of the southern coastal area of Sfax during spring (Tunisia, Southern Mediterranean Sea). Mar Pollut Bull 104:355–363. https://doi.org/10.1016/j.marpolbul.2016.01.035

Drira Z., Chaari D., Hamza A., Hassen MB., Pagano M., Ayadi H., 2017. Diazotrophic cyanobacteria signatures and their relationship to hydrographic conditions in the Gulf of Gabes, Tunisia. J Mar Biol Assoc U K 97:69–80. https://doi.org/10.1017/S0025315415002210

Drira, Z., Kmiha-Megdiche, S., Sahnoun, H., Tedetti, M., Pagano, M., Ayadi, H., 2018. Copepod assemblages as a bioindicator of environmental quality in three coastal areas under contrasted anthropogenic inputs (Gulf of Gabes, Tunisia). Journal of the Marine Biological Association of the United Kingdom 98, 1889–1905. https://doi.org/10.1017/S0025315417001515

Du Yoo, Y., Jeong, H.J., Kim, M.S., Kang, N.S., Song, J.Y., Shin, W., Kim, K.Y., Lee, K., 2009. Feeding by Phototrophic Red-Tide Dinoflagellates on the Ubiquitous Marine Diatom Skeletonema costatum. Journal of Eukaryotic Microbiology 56, 413–420. https://doi.org/10.1111/j.1550-7408.2009.00421.x

Duan, L.J., Li, S.Y., Liu, Y., Moreau, J., Christensen, V., 2009. Modeling changes in the coastal ecosystem of the Pearl River Estuary from 1981 to 1998. Ecological Modelling 220, 2802–2818. https://doi.org/10.1016/j.ecolmodel.2009.07.016

Duarte CM., Agustí S., Agawin NSR., 2000. Response of a Mediterranean phytoplankton community to increased nutrient inputs: a mesocosm experiment. Mar Ecol Prog Ser 195:61–70. https://doi.org/10.3354/meps195061

Duda D., Wawruch R., 2017. The impact of Major Maritime accidents on the development of international regulations concerning safety of navigation and protection of the environment. Sci J Pol Nav Acad, 4 (111): 23-44. http://doi.org/10.5604/01.3001.0010.6741

Dupuy, C., Gall, S.L., Hartmann, H.J., Bréret, M., 1999. Retention of ciliates and flagellates by the oyster Crassostrea gigas in French Atlantic coastal ponds: protists as a trophic link between bacterioplankton and benthic suspension-feeders. Marine Ecology Progress Series 177, 165–175. https://doi.org/10.3354/meps177165

Durrieu de Madron, X., Guieu, C., Sempéré, R., Conan, P., Cossa, D., D'Ortenzio, F., Estournel, C., Gazeau, F., Rabouille, C., Stemmann, L., Bonnet, S., Diaz, F., Koubbi, P., Radakovitch, O., Babin, M., Baklouti, M., Bancon-Montigny, C., Belviso, S., Bensoussan, N., Bonsang, B., Bouloubassi, I., Brunet, C., Cadiou, J.-F., Carlotti, F., Chami, M., Charmasson, S., Charrière, B., Dachs, J., Doxaran, D., Dutay, J.-C., Elbaz-Poulichet, F., Eléaume, M., Eyrolles, F., Fernandez, C., Fowler, S., Francour, P., Gaertner, J.C., Galzin, R., Gasparini, S., Ghiglione, J.-F., Gonzalez, J.-L., Goyet, C., Guidi, L., Guizien, K., Heimbürger, L.-E., Jacquet, S.H.M., Jeffrey, W.H., Joux, F., Le Hir, P., Leblanc, K., Lefèvre, D., Lejeusne, C., Lemé, R., Loÿe-Pilot, M.-D., Mallet, M., Méjanelle, L., Mélin, F., Mellon, C., Mérigot, B., Merle, P.-L., Migon, C., Miller, W.L., Mortier, L., Mostajir, B., Mousseau, L., Moutin, T., Para, J., Pérez, T., Petrenko, A., Poggiale, J.-C., Prieur, L., Pujo-Pay, M., Pulido-Villena, Raimbault, P., Rees, A.P., Ridame, C., Rontani, J.-F., Ruiz Pino, D., Sicre, M.A., Taillandier, V., Tamburini, C., Tanaka, T., Taupier-Letage, I., Tedetti, M., Testor, P., Thébault, H., Thouvenin, B., Touratier, F., Tronczynski, J., Ulses, C., Van Wambeke, F., Vantrepotte, V., Vaz, S., Verney, R., 2011. Marine ecosystems' responses to climatic and anthropogenic forcings in the Mediterranean. Progress in Oceanography 91, 97–166. https://doi.org/10.1016/j.pocean.2011.02.003

-e-

Eastwood, P.D., Mills, C.M., Aldridge, J.N., Houghton, C.A., Rogers, S.I., 2007. Human activities in UK offshore waters: an assessment of direct, physical pressure on the seabed. ICES Journal of Marine Science 64, 453–463. https://doi.org/10.1093/icesjms/fsm001

Echeveste P., Dachs J., Berrojalbiz N., Agustí S., 2010a. Decrease in the abundance and viability of oceanic phytoplankton due to trace levels of complex mixtures of organic pollutants. Chemosphere, 81(2): 161-168. https://doi.org/10.1016/j.chemosphere.2010.06.072

Echeveste P., Agustí S., Dachs J., 2010b. Cell size dependent toxicity thresholds of polycyclic aromatic hydrocarbons to natural and cultured phytoplankton populations. Environ pollut, 158(1): 299-307. https://doi.org/10.1016/j.envpol.2009.07.006

Echeveste P., Agustí S., Dachs J., 2011. Cell size dependence of additive versus synergetic effects of UV radiation and PAHs on oceanic phytoplankton. Environ Pollut, 159(5): 1307-1316. https://doi.org/10.1016/j.envpol.2011.01.023

Effiong, K.S., Inyang, A.I., Robert, U.U., 2018. Spatial distribution and diversity of phytoplankton community in Eastern Obolo River Estuary, Niger Delta. JOMS 9, 1–14. https://doi.org/10.5897/JOMS2016.0139

El Kateb, Claudio Stalder, Andres Rüggeberg, Christoph Neururer, Jorge E. Spangenberg,, Silvia Spezzaferri, 2018. Impact of industrial phosphate waste discharge on the marine environment in the Gulf of Gabes (Tunisia). PloS one, 13(5), e0197731. https://doi.org/10.1371/journal.pone.0197731

El Zrelli, R., Courjault-Radé, P., Rabaoui, L., Castet, S., Michel, S., Bejaoui, N., 2015. Heavy metal contamination and ecological risk assessment in the surface sediments of the coastal area surrounding the industrial complex of Gabes city, Gulf of Gabes, SE Tunisia. Marine Pollution Bulletin 101, 922–929. https://doi.org/10.1016/j.marpolbul.2015.10.047

El-Fadel M., Abdallah R., Rachid G., 2012. A modeling approach toward oil spill management along the Eastern Mediterranean. J Environ Manage, 113: 93-102. http://doi.org/10.1016/j.jenvman.2012.07.035

El-Serehy, H.A., Al-Darmaky, M.M., 2003. The effect of the Banton 300 oil-spill accident on marine life in Umm Al-Quwain in the Arabian Gulf (northern United Arab Emirates). Egyptian Journal of Biology 5. https://doi.org/10.4314/ejb.v5i1.29980

Enajjar, S., Saïdi, B., Bradai, M., 2015. The Gulf of Gabès (Central Mediterranean Sea): a nursery area for sharks and batoids (Chondrichthyes: Elasmobranchs). Cahiers de Biologie Marine 56, 143–150.

Escofier, B., Pagès, J., 1990. Analyses factorielles simples et multiples : objectifs, méthodes et interprétation. Dunod.

European Commission, 2010. Commission Decision of 1 September 2010 on criteria and methodological standards on good environmental status of marine waters (notified under document C(2010) 5956) (Text with EEA relevance) (2010/477/EU). https://doi.org/10.25607/OBP-820

~F~

Fath, B.D., Patten, B.C., 1999. Review of the Foundations of Network Environ Analysis. Ecosystems 2, 167–179. https://doi.org/10.1007/s100219900067

Fath, B.D., Asmus, H., Asmus, R., Baird, D., Borrett, S.R., de Jonge, V.N., Ludovisi, A., Niquil, N., Scharler, U.M., Schückel, U., Wolff, M., 2019. Ecological network analysis metrics: The need for an entire ecosystem approach in management and policy. Ocean & Coastal Management 174, 1–14. https://doi.org/10.1016/j.ocecoaman.2019.03.007

Ferland, J., Gosselin, M., Starr, M., 2011. Environmental control of summer primary production in the Hudson Bay system: The role of stratification. Journal of Marine Systems, The Hudson Bay System 88, 385–400. https://doi.org/10.1016/j.jmarsys.2011.03.015

Filiz, N., Işkın, U., Beklioğlu, M., Öğlü, B., Cao, Y., Davidson, T.A., Søndergaard, M., Lauridsen, T.L., Jeppesen, E., 2020. Phytoplankton Community Response to Nutrients, Temperatures, and a Heat Wave in Shallow Lakes: An Experimental Approach. Water 12, 3394. https://doi.org/10.3390/w12123394

Finkel ZV., Liang Y., Nanjappa D., Bretherton L., Brown CM., Quigg A., Irwin AJ., 2020. A ribosomal sequence-based oil sensitivity index for phytoplankton groups. Mar Pollut Bull, 151, 110798. https://doi.org/10.1016/j.marpolbul.2019.110798

Finn, J.T., 1976. Measures of ecosystem structure and function derived from analysis of flows. Journal of Theoretical Biology 56, 363–380. https://doi.org/10.1016/S0022-5193(76)80080-X

Fiori, E., Servadei, I., Piermattei, V., Bonamano, S., Madonia, A., Guerrini, F., Marcelli, M., Pistocchi, R., 2016. A new approach to assess the effects of oil spills on phytoplankton community during the "Serious Game" experiment (MEDESS-4MS Project). Deep Sea Research Part II: Topical Studies in Oceanography, Physical, chemical and biological observations and modelling of oil spills in the Mediterranean Sea 133, 76–87. https://doi.org/10.1016/j.dsr2.2016.05.026

Forest, A., Tremblay, J.-É., Gratton, Y., Martin, J., Gagnon, J., Darnis, G., Sampei, M., Fortier, L., Ardyna, M., Gosselin, M., Hattori, H., Nguyen, D., Maranger, R., Vaqué, D., Marrasé, C., Pedrós-Alió, C., Sallon, A., Michel, C., Kellogg, C., Deming, J., Shadwick, E., Thomas, H., Link, H., Archambault, P., Piepenburg, D., 2011. Biogenic carbon flows through the planktonic food web of the Amundsen Gulf (Arctic Ocean): A synthesis of field measurements and inverse modeling analyses. Progress in Oceanography 91, 410–436. https://doi.org/10.1016/j.pocean.2011.05.002

Fortier, L., Le Fèvre, J., Legendre, L., 1994. Export of biogenic carbon to fish and to the deep ocean: the role of large planktonic microphages. Journal of Plankton Research 16, 809–839. https://doi.org/10.1093/plankt/16.7.809

Fourati, R., Tedetti, M., Guigue, C., Goutx, M., Zaghden, H., Sayadi, S., Elleuch, B., 2018. Natural and anthropogenic particulate-bound aliphatic and polycyclic aromatic hydrocarbons in surface waters of the Gulf of Gabès (Tunisia, southern Mediterranean Sea). Environ Sci Pollut Res 25, 2476–2494. https://doi.org/10.1007/s11356-017-0641-7

Froneman, P.W., 2004. Food web dynamics in a temperate temporarily open/closed estuary (South Africa). Estuarine, Coastal and Shelf Science 59, 87–95. https://doi.org/10.1016/j.ecss.2003.08.003

Frontier, S., Pichod-Viale, D., Leprêtre, A., Davoult, D., Luczak, C., 2008. Ecosystèmes. Structure, fonctionnement, évolution. Dunod, 4ème édition, Paris.

Frost, B.W., 1984. Utilization of phytoplankton production in the surface layer, in: Global Ocean Flux Study: Proceedings of a Workshop. National Academy Press Washington, DC, pp. 125–134.

Furse, G.A., 1899. French Ports in Northern Africa. Royal United Services Institution. Journal 43, 1113–1124. https://doi.org/10.1080/03071849909423646

-G-

Gaichas, S.K., 2008. A context for ecosystem-based fishery management: Developing concepts of ecosystems and sustainability. Marine Policy 32, 393–401. https://doi.org/10.1016/j.marpol.2007.08.002

Gallo F., Schulz KG., Azevedo EB., Madruga J., Ramos JB., 2018. Responses of the diatom Asterionellopsis glacialis to increasing sea water CO2 concentrations and turbulence. Mar Ecol Prog Ser, 589, 33-44. https://doi.org/10.3354/meps12450

Garmendia, M., Revilla, M., Bald, J., Franco, J., Laza-Martínez, A., Orive, E., Seoane, S., Valencia, V., Borja, Á., 2011. Phytoplankton communities and biomass size structure (fractionated chlorophyll “a”), along trophic gradients of the Basque coast (northern Spain). Biogeochemistry 106, 243–263. https://doi.org/10.1007/s10533-010-9445-2

Gaudy, R., Youssara, F., Diaz, F., Raimbault, P., 2003. Biomass, metabolism and nutrition of zooplankton in the Gulf of Lions (NW Mediterranean). Oceanologica Acta 26, 357–372. https://doi.org/10.1016/S0399-1784(03)00016-1

Gemmell, B.J., Bacosa, H.P., Dickey, B.O., Gemmell, C.G., Alqasemi, L.R., Buskey, E.J., 2018. Rapid alterations to marine microbiota communities following an oil spill. Ecotoxicology 27, 505–516. https://doi.org/10.1007/s10646-018-1923-7

Ghyoot, C., Flynn, K.J., Mitra, A., Lancelot, C., Gypens, N., 2017. Modeling Plankton Mixotrophy: A Mechanistic Model Consistent with the Shuter-Type Biochemical Approach. Frontiers in Ecology and Evolution 5.

Giannakourou, A., Tsiola, A., Kanellopoulou, M., Magiopoulos, I., Siokou, I., Pitta, P., 2014. Temporal variability of the microbial food web (viruses to ciliates) under the influence of

the Black Sea Water inflow (N. Aegean, E. Mediterranean). Mediterranean Marine Science 769–780. https://doi.org/10.12681/mms.1041

Gifford, D., 1988. Impact of grazing by microzooplankton in the Northwest Arm of Halifax Harbour, Nova Scotia. Mar. Ecol. Prog. Ser. 47, 249–258. https://doi.org/10.3354/meps047249

Gilde K., Pinckney JL., 2012. Sublethal effects of crude oil on the community structure of estuarine phytoplankton. Estuar Coasts, 35(3), 853-861. https://dx.doi.org/10.1007/s12237-011-9473-8

Girault, M., Arakawa, H., Hashihama, F., 2013. Phosphorus stress of microphytoplankton community in the western subtropical North Pacific. Journal of Plankton Research 35, 146–157. https://doi.org/10.1093/plankt/fbs076

GOFS, U., 1986. Global Ocean Flux Study: Report 3. US GOFS Planning Office, Woods Hole, Mass.

Goldman, J.C., Caron, D.A., 1985. Experimental studies on an omnivorous microflagellate: implications for grazing and nutrient regeneration in the marine microbial food chain. Deep Sea Research Part A. Oceanographic Research Papers 32, 899–915. https://doi.org/10.1016/0198-0149(85)90035-4

Goldman, J.C, Caron, D.A, Dennett, M., 1987. Nutrient cycling in a microflagellate food chain: IV. Phytoplankton-microflagellate interactions. Mar. Ecol. Prog. Ser. 38, 75–87. https://doi.org/10.3354/meps038075

Gomes, E.A.T., Santos, V.S. dos, Tenenbaum, D.R., Villac, M.C., 2007. Protozooplankton characterization of two contrasting sites in a tropical coastal ecosystem (Guanabara Bay, RJ). Braz. j. oceanogr. 55, 29–38.

Gomiero, A., Dagnino, A., Nasci, C., Viarengo, A., 2013. The use of protozoa in ecotoxicology: Application of multiple endpoint tests of the ciliate E. crassus for the evaluation of sediment quality in coastal marine ecosystems. Science of The Total Environment 442, 534–544. https://doi.org/10.1016/j.scitotenv.2012.10.023

González, J., Figueiras, F.G., Aranguren-Gassis, M., Crespo, B.G., Fernández, E., Morán, X.A.G., Nieto-Cid, M., 2009. Effect of a simulated oil spill on natural assemblages of marine phytoplankton enclosed in microcosms. Estuarine, Coastal and Shelf Science 83, 265–276. https://doi.org/10.1016/j.ecss.2009.04.001

González, J.J., Viñas, L., Franco, M.A., Fumega, J., Soriano, J.A., Grueiro, G., Muniategui, S., López-Mahía, P., Prada, D., Bayona, J.M., Alzaga, R., Albaigés, J., 2006. Spatial and temporal distribution of dissolved/dispersed aromatic hydrocarbons in seawater in the area affected by the Prestige oil spill. Marine Pollution Bulletin, The Prestige Oil Spill: A Scientific Response 53, 250–259. https://doi.org/10.1016/j.marpolbul.2005.09.039

González, J., Fernández, E., Figueiras, F.G., 2022. Assessing the effect of oil spills on the dynamics of the microbial plankton community using a NPZD model. Estuarine, Coastal and Shelf Science 265, 107734. https://doi.org/10.1016/j.ecss.2021.107734

Gotwals, A.W., Songer, N.B., 2010. Reasoning up and down a food chain: Using an assessment framework to investigate students' middle knowledge. Science Education 94, 259–281. https://doi.org/10.1002/sce.20368

Goutz, HM, Berland B, Leveau M, Bertrand JC (984). Effects of petroleum biodegradation products on phytoplankton growth. Second International Colloquium on Marine Bacteriology, pp. 621-627. IFREMER, Paris, France.

Graeve, M., Kattner, G., Hagen, W., 1994. Diet-induced changes in the fatty acid composition of Arctic herbivorous copepods: Experimental evidence of trophic markers. Journal of Experimental Marine Biology and Ecology 182, 97–110. https://doi.org/10.1016/0022-0981(94)90213-5

Grami, B., Niquil, N., Sakka Hlaili, A., Gosselin, M., Hamel, D., Hadj Mabrouk, H., 2008. The plankton food web of the Bizerte Lagoon (South-western Mediterranean): II. Carbon steady-state modelling using inverse analysis. Estuarine, Coastal and Shelf Science 79, 101–113. https://doi.org/10.1016/j.ecss.2008.03.009

Grami, B., 2009. Dynamique et fonctionnement des réseaux trophiques planctoniques dans la lagune de Bizerte : modélisation par la méthode inverse (These de doctorat). La Rochelle.

Grami, B., Rasconi, S., Niquil, N., Jobard, M., Saint-Béat, B., Sime-Ngando, T., 2011. Functional Effects of Parasites on Food Web Properties during the Spring Diatom Bloom in Lake Pavin: A Linear Inverse Modeling Analysis. PLOS ONE 6, e23273. https://doi.org/10.1371/journal.pone.0023273

Grami B., Chkili O., Melliti Ben Garali S., Mejri Kousri K., Meddeb M., Chouba L., Niquil N., Sakka Hlaili Field study on natural phytoplankton throughout "Bizerte City" oil spill on the south-western Cost of the Mediterranean Sea (Submitted in Archive of Environmental Contamination and Toxicologie).

Grattepanche, J.-D., Vincent, D., Breton, E., Christaki, U., 2011. Microzooplankton herbivory during the diatom–Phaeocystis spring succession in the eastern English Channel. Journal of Experimental Marine Biology and Ecology 404, 87–97. https://doi.org/10.1016/j.jembe.2011.04.004

Grilli, J., Rogers, T., Allesina, S., 2016. Modularity and stability in ecological communities. Nat Commun 7, 12031. https://doi.org/10.1038/ncomms12031

Grinienė, E., Šulčius, S., Kuosa, H., 2016. Size-selective microzooplankton grazing on the phytoplankton in the Curonian Lagoon (SE Baltic Sea). Oceanologia 58, 292–301. https://doi.org/10.1016/j.oceano.2016.05.002

Gueroun, S.M., Molinero, J.-C., Piraino, S., Dali Yahia, M.N., 2020. Population dynamics and predatory impact of the alien jellyfish Aurelia solida (Cnidaria, Scyphozoa) in the Bizerte Lagoon (southwestern Mediterranean Sea). Mediterranean Marine Science 21, 22–35.

Guerrero, F., Rodriguez, V., 1998. Existence and significance of Acartia grani resting eggs (Copepoda: Calanoida) in sediments of a coastal station in the Alboran Sea (SE Spain). Journal of Plankton Research 20, 305–314. https://doi.org/10.1093/plankt/20.2.305

Gugliermetti, F., Cinquepalmi, F., Astiaso Garcia, D., 2007. The use of environmental sensitivity indices (ESI) maps for the evaluation of oil spill risk in Mediterranean coastlines and coastal waters, in: Sustainable Development and Planning III. Presented at the SUSTAINABLE DEVELOPMENT 2007, WIT Press, Algarve, Portugal, pp. 593–600. https://doi.org/10.2495/SDP070572

Gutiérrez-Rodríguez, A., Latasa, M., Scharek, R., Massana, R., Vila, G., Gasol, J.M., 2011. Growth and grazing rate dynamics of major phytoplankton groups in an oligotrophic coastal site. Estuarine, Coastal and Shelf Science 95, 77–87. https://doi.org/10.1016/j.ecss.2011.08.008

~H~

Hallanger, I.G., Ruus, A., Warner, N.A., Herzke, D., Evenset, A., Schøyen, M., Gabrielsen, G.W., Borgå, K., 2011. Differences between Arctic and Atlantic fjord systems on bioaccumulation of persistent organic pollutants in zooplankton from Svalbard. Science of The Total Environment 409, 2783–2795. https://doi.org/10.1016/j.scitotenv.2011.03.015

Halouani, G., Abdou, K., Hattab, T., Romdhane, M.S., Ben Rais Lasram, F., Le Loc'h, F., 2016. A spatio-temporal ecosystem model to simulate fishing management plans: A case of study in the Gulf of Gabes (Tunisia). Marine Policy 69, 62–72. https://doi.org/10.1016/j.marpol.2016.04.002

Hamdi, I., Denis, M., Bellaaj-Zouari, A., Khemakhem, H., Bel Hassen, M., Hamza, A., Barani, A., Bezac, C., Maalej, S., 2015. The characterisation and summer distribution of ultraphytoplankton in the Gulf of Gabès (Eastern Mediterranean Sea, Tunisia) by using flow cytometry. Continental Shelf Research 93, 27–38. https://doi.org/10.1016/j.csr.2014.10.002

Han, J., Park, J.C., Kang, H.-M., Byeon, E., Yoon, D.-S., Lee, M.-C., Sayed, A.E.-D.H., Hwang, U.-K., Lee, J.-S., 2019. Adverse effects, expression of defense-related genes, and oxidative stress-induced MAPK pathway in the benzo[α]pyrene-exposed rotifer Brachionus rotundiformis. Aquatic Toxicology 210, 188–195. https://doi.org/10.1016/j.aquatox.2019.03.004

Hannachi, I., Drira, Z., Belhassen, M., Hamza, A., Ayadi, H., Bouain, A., Aleya, L., 2008. Abundance and Biomass of the Ciliate Community during a Spring Cruise in the Gulf of Gabes (Eastern Mediterranean Sea, Tunisia). Acta Protozoologica 14.

Hansen, P.J., Calado, A.J., 1999. Phagotrophic Mechanisms and Prey Selection in Free-living Dinoflagellates1. Journal of Eukaryotic Microbiology 46, 382–389. https://doi.org/10.1111/j.1550-7408.1999.tb04617.x

Haraldsson, M., Gerphagnon, M., Bazin, P., Colombet, J., Tecchio, S., Sime-Ngando, T., Niquil, N., 2018. Microbial parasites make cyanobacteria blooms less of a trophic dead end than commonly assumed. ISME J 12, 1008–1020. https://doi.org/10.1038/s41396-018-0045-9

Hardikar, R., C.k., H., Ram, A., Parthipan, V., 2021. Distribution of size-fractionated phytoplankton biomass from the anthropogenically stressed tropical creek (Thane creek, India). Regional Studies in Marine Science 41, 101577. https://doi.org/10.1016/j.rsma.2020.101577

Hargraves, P.E., 2002. The ebridian flagellates Ebria and Hermesinum. Plankton Biology and Ecology, 49(1), 9-16.

Harrison PJ., Cochlan WP., Acreman JC., Parsons TR., Thompson PA., Dovey HM., Xiaolin C., 1986. The effects of crude oil and Corexit 9527 on marine phytoplankton in an experimental enclosure. Mar Environ Res, 18(2), 93-109. https://dx.doi.org/10.1016/0141-1136(86)90002-4

Harrison, W.G., Cota, G.F., 1991. Primary production in polar waters: relation to nutrient availability. Polar Research 10, 87–104. https://doi.org/10.3402/polar.v10i1.6730

Hattab, T., Ben Rais Lasram, F., Albouy, C., Romdhane, M.S., Jarboui, O., Halouani, G., Cury, P., Le Loc'h, F., 2013. An ecosystem model of an exploited southern Mediterranean shelf region (Gulf of Gabes, Tunisia) and a comparison with other Mediterranean ecosystem model properties. Journal of Marine Systems 128, 159–174. https://doi.org/10.1016/j.jmarsys.2013.04.017

Hattour, M.J., Sammari, C., Ben Nassrallah, S., 2010. Hydrodynamique du golfe de Gabès déduite à partir des observations de courants et de niveaux. Revue Paralia 3, 3.1-3.12. https://doi.org/10.5150/revue-paralia.2010.003

Havermans, C., Dischereit, A., Pantiukhin, D., Friedrich, M., Murray, A., 2022. Environmental DNA in an ocean of change: Status, challenges and prospects. Arquivos de Ciencias Do Mar 55, 298–337. https://doi.org/10.32360/acmar.v55iEspecial.78188

He, X., Wang, Z., Bai, Z., Han, L., Chen, M., 2021. Diel Feeding Rhythm and Grazing Selectivity of Small-Sized Copepods in a Subtropical Embayment, the Northern South China Sea. Frontiers in Marine Science 8.

Hemmer MJ., Barron MG., Greene RM., 2011. Comparative toxicity of eight oil dispersants, Louisiana sweet crude oil (LSC), and chemically dispersed LSC to two aquatic test species. Environmental Toxicology and Chemistry 30: 2244–2252. https://doi.org/10.1002/etc.619

Heymans, J.J., Coll, M., Libralato, S., Morissette, L., Christensen, V., 2014. Global Patterns in Ecological Indicators of Marine Food Webs: A Modelling Approach. PLOS ONE 9, e95845. https://doi.org/10.1371/journal.pone.0095845

Hill, S.L., Murphy, E.J., Reid, K., Trathan, P.N., Constable, A.J., 2006. Modelling Southern Ocean ecosystems: krill, the food-web, and the impacts of harvesting. Biological Reviews 81, 581–608. https://doi.org/10.1017/S1464793106007123

Hillebrand, H., Dürselen, C.-D., Kirschtel, D., Pollingher, U., Zohary, T., 1999. Biovolume Calculation for Pelagic and Benthic Microalgae. Journal of Phycology 35, 403–424. https://doi.org/10.1046/j.1529-8817.1999.3520403.x

Hines, D.E., Ray, S., Borrett, S.R., 2018. Uncertainty analyses for Ecological Network Analysis enable stronger inferences. Environmental Modelling & Software 101, 117–127. https://doi.org/10.1016/j.envsoft.2017.12.011

Hjorth, M., Vester, J., Henriksen, P., Forbes, V., Dahllöf, I., 2007. Functional and structural responses of marine plankton food web to pyrene contamination. Marine Ecology Progress Series 338, 21–31. https://doi.org/10.3354/meps338021

Holt, G.J., Holt, S.A., 2000. Vertical distribution and the role of physical processes in the feeding dynamics of two larval sciaenids Sciaenops ocellatus and Cynoscion nebulosus. Marine Ecology Progress Series 193, 181–190. https://doi.org/10.3354/meps193181

Horňák, K., Mašín, M., Jezbera, J., Bettarel, Y., Nedoma, J., Sime-Ngando, T., Šimek, K., 2005. Effects of decreased resource availability, protozoan grazing and viral impact on a structure of bacterioplankton assemblage in a canyon-shaped reservoir. FEMS Microbiology Ecology 52, 315–327. https://doi.org/10.1016/j.femsec.2004.11.013

Huang, Y.-J., Jiang, Z.-B., Zeng, J.-N., Chen, Q.-Z., Zhao, Y., Liao, Y., Shou, L., Xu, X., 2011. The chronic effects of oil pollution on marine phytoplankton in a subtropical bay, China. Environ Monit Assess 176, 517–530. https://doi.org/10.1007/s10661-010-1601-6

~I~

Ikavalko J., Gerdes B., Hiukka R., 2005. Effects of crude oil on arctic sea ice biota: an experimental study. In Phycologia 44(4):48-58. New Business Office, Po Box 1897, Lawrence, KS 66044-8897 USA: Int Phycological Soc.

Irigoien, X., 1998. Gut clearance rate constant, temperature and initial gut contents: a review. Journal of Plankton Research 20, 997–1003. https://doi.org/10.1093/plankt/20.5.997

~J~

Jacobson, D.M., Anderson, D.M., 1986. Thecate Heterophic Dinoflagellates: Feeding Behavior and Mechanisms1. Journal of Phycology 22, 249–258. https://doi.org/10.1111/j.1529-8817.1986.tb00021.x

Jafari, F., Ramezanpour, Z., Sattari, M., 2015. First record of Ebria tripartita (Schumann) Lemmermann, 1899 from south of the Caspian Sea. Caspian Journal of Environmental Sciences 13, 283–288.

James, M.R., Hall, J.A., Laybourn-Parry, J.A., 1998. Protozooplankton and Microzooplankton Ecology in Lakes of the Dry Valleys, Southern Victoria Land, in: Ecosystem Dynamics in a Polar Desert: The Mcmurdo Dry Valleys, Antarctica. American Geophysical Union (AGU), pp. 255–267. https://doi.org/10.1029/AR072p0255

Jeong, H.J., Shim, J.H., Kim, J.S., Park, J.Y., Lee, C.W., Lee, Y., 1999. Feeding by the mixotrophic thecate dinoflagellate Fragilidium cf. mexicanum on red-tide and toxic dinoflagellates. Marine Ecology Progress Series 176, 263–277. https://doi.org/10.3354/meps176263

Jeong, H.J., Yoo, Y.D., Kim, S.T., Kang, N.S., 2004. Feeding by the heterotrophic dinoflagellate Protoperidinium bipes on the diatom Skeletonema costatum. Aquatic Microbial Ecology 36, 171–179. https://doi.org/10.3354/ame036171

Jeong, H.J., Seong, K.A., Yoo, Y.D., Kim, T.H., Kang, N.S., Kim, S., Park, J.Y., Kim, J.S., Kim, G.H., Song, J.Y., 2008. Feeding and Grazing Impact by Small Marine Heterotrophic Dinoflagellates on Heterotrophic Bacteria. Journal of Eukaryotic Microbiology 55, 271–288. https://doi.org/10.1111/j.1550-7408.2008.00336.x

Jeong, H.J., Yoo, Y.D., Kang, N.S., Rho, J.R., Seong, K.A., Park, J.W., Nam, G.S., Yih, W., 2010. Ecology of Gymnodinium aureolum. I. Feeding in western Korean waters. Aquatic Microbial Ecology 59, 239–255. https://doi.org/10.3354/ame01394

Jiang, Z., Huang, Y., Xu, X., Liao, Y., Shou, L., Liu, J., Chen, Q., Zeng, J., 2010. Advance in the toxic effects of petroleum water accommodated fraction on marine plankton. Acta Ecologica Sinica 30, 8–15. https://doi.org/10.1016/j.chnaes.2009.12.002

Jiang, Z., Huang, Y., Chen, Q., Zeng, J., Xu, X., 2012. Acute toxicity of crude oil water accommodated fraction on marine copepods: The relative importance of acclimatization temperature and body size. Marine Environmental Research 81, 12–17. https://doi.org/10.1016/j.marenvres.2012.08.003

Jiao, N., Yang, Y., Hong, N., Ma, Y., Harada, S., Koshikawa, H., Watanabe, M., 2005. Dynamics of autotrophic picoplankton and heterotrophic bacteria in the East China Sea. Continental Shelf Research 25, 1265–1279. https://doi.org/10.1016/j.csr.2005.01.002

Johansson, M., Gorokhova, E., Larsson, U., 2004. Annual variability in ciliate community structure, potential prey and predators in the open northern Baltic Sea proper. Journal of Plankton Research 26, 67–80. https://doi.org/10.1093/plankt/fbg115

Johansson, S., Larsson, U., Boehm, P., 1980. The Tsesis oil spill impact on the pelagic ecosystem. Marine Pollution Bulletin 11, 284–293. https://doi.org/10.1016/0025-326X(80)90166-6

Joint, I., Morris, J., 1982. The role of bacteria in the turnover of organic matter in the sea. The role of bacteria in the turnover of organic matter in the sea.

Jones, R.I., 1994. Mixotrophy in planktonic protists as a spectrum of nutritional strategies. Mar. Microb. Food Webs 8, 87–96.

Jørgensen, S.E., Patten, B.C., Straškraba, M., 2000. Ecosystems emerging:: 4. growth. Ecological Modelling 126, 249–284. https://doi.org/10.1016/S0304-3800(00)00268-4

Jost, C., Lawrence, C.A., Campolongo, F., van de Bund, W., Hill, S., DeAngelis, D.L., 2004. The effects of mixotrophy on the stability and dynamics of a simple planktonic food web model. Theoretical Population Biology 66, 37–51. https://doi.org/10.1016/j.tpb.2004.02.001

Jung, S.W., Kwon, O.Y., Joo, C.K., Kang, J.-H., Kim, M., Shim, W.J., Kim, Y.-O., 2012. Stronger impact of dispersant plus crude oil on natural plankton assemblages in short-term marine mesocosms. Journal of Hazardous Materials 217–218, 338–349. https://doi.org/10.1016/j.jhazmat.2012.03.034

-K-

Kahla, O., Melliti Ben Garali, S., Karray, F., Ben Abdallah, M., Kallel, N., Mhiri, N., Zaghden, H., Barhoumi, B., Pringault, O., Quéméneur, M., Tedetti, M., Sayadi, S., Sakka Hlaili, A., 2021. Efficiency of benthic diatom-associated bacteria in the removal of benzo(a)pyrene and fluoranthene. Science of The Total Environment 751, 141399. https://doi.org/10.1016/j.scitotenv.2020.141399

Kamalanathan, M., Hillhouse, J., Claflin, N., Rodkey, T., Mondragon, A., Prouse, A., Nguyen, M., Quigg, A., 2021. Influence of nutrient status on the response of the diatom Phaeodactylum tricornutum to oil and dispersant. PLOS ONE 16, e0259506. https://doi.org/10.1371/journal.pone.0259506

Kang, J.J., Jang, H.K., Lim, J.-H., Lee, D., Lee, J.H., Bae, H., Lee, C.H., Kang, C.-K., Lee, S.H., 2020. Characteristics of Different Size Phytoplankton for Primary Production and Biochemical Compositions in the Western East/Japan Sea. Frontiers in Microbiology 11.

Karlson, K., Bamstedt, U., 1994. Planktivorous predation on copepods. Evaluation of mandible remains in predator guts as a quantitative estimate of predation. Mar. Ecol. Prog. Ser. 108, 79–89. https://doi.org/10.3354/meps108079

Kase, L., Metfies, K., Kraberg, A.C., Neuhaus, S., Meunier, C.L., Wiltshire, K.H., Boersma, M., 2021. Metabarcoding analysis suggests that flexible food web interactions in the eukaryotic plankton community are more common than specific predator–prey relationships at Helgoland Roads, North Sea. ICES Journal of Marine Science 78, 3372–3386. https://doi.org/10.1093/icesjms/fsab058

Katechakis, A., Stibor, H., Sommer, U., Hansen, T., 2004. Feeding selectivities and food niche separation of Acartia clausi, Penilia avirostris (Crustacea) and Doliolum denticulatum (Thaliacea) in Blanes Bay (Catalan Sea, NW Mediterranean). Journal of Plankton Research 26, 589–603. https://doi.org/10.1093/plankt/fbh062

Kay, J.J., Graham, L.A., Ulanowicz, R.E., 1989. A Detailed Guide to Network Analysis, in: Wulff, F., Field, J.G., Mann, K.H. (Eds.), Network Analysis in Marine Ecology. Springer Berlin Heidelberg, Berlin, Heidelberg, pp. 15–61. https://doi.org/10.1007/978-3-642-75017-5_2

Kchaou, N., Elloumi, J., Drira, Z., Hamza, A., Ayadi, H., Bouain, A., Aleya, L., 2009. Distribution of ciliates in relation to environmental factors along the coastline of the Gulf of Gabes, Tunisia. Estuarine, Coastal and Shelf Science 83, 414–424. https://doi.org/10.1016/j.ecss.2009.04.019

Kennish, M.J., 1996. Practical Handbook of Estuarine and Marine Pollution. CRC Press.

Khammeri, Y., Hamza, I.S., Zouari, A.B., Hamza, A., Sahli, E., Akrout, F., Ben Kacem, M.Y., Messaoudi, S., Hassen, M.B., 2018. Atmospheric bulk deposition of dissolved nitrogen, phosphorus and silicate in the Gulf of Gabès (South Ionian Basin); implications for marine heterotrophic prokaryotes and ultraphytoplankton. Continental Shelf Research 159, 1–11. https://doi.org/10.1016/j.csr.2018.03.003

Khammeri, Y., Bellaaj-Zouari, A., Hamza, A., Medhioub, W., Sahli, E., Akrout, F., Barraj, N., Ben Kacem, M.Y., Bel Hassen, M., 2020. Ultraphytoplankton community composition in Southwestern and Eastern Mediterranean Basin: Relationships to water mass properties and nutrients. Journal of Sea Research 158, 101875. https://doi.org/10.1016/j.seares.2020.101875

Khedhri, I., 2014. First record of Naineris setosa (Verrill, 1900) (Annelida: Polychaeta: Orbiniidae) in the Western Mediterranean Sea. BIR 3, 83–88. https://doi.org/10.3391/bir.2014.3.2.05

Kimes, N.E., Callaghan, A.V., Suflita, J.M., Morris, P.J., 2014. Microbial transformation of the Deepwater Horizon oil spill—past, present, and future perspectives. Frontiers in Microbiology 5.

Kiørboe, T., Hansen, J.L.S., Alldredge, A.L., Jackson, G.A., Passow, U., Dam, H.G., Drapeau, D.T., Waite, A., Garcia, C.M., 1996. Sedimentation of phytoplankton during a diatom bloom : Rates and mechanisms. Journal of Marine Research 54, 1123–1148.

Kleppel, G.S., Pieper, R.E., 1984. Phytoplankton pigments in the gut concents of planktonic copepods from coastal waters off southern California. Mar. Biol. 78, 193–198. https://doi.org/10.1007/BF00394700

Klotz, P., Schloss, I.R., Dumont, D., 2018. Effects of a Chronic Oil Spill on the Planktonic System in San Jorge Gulf, Argentina: A ONE-VERTICAL-DIMENSION MODELING APPROACH. Oceanography 31, 81–91.

Kmiha-Megdiche, S., Rekik, A., Pagano, M., Ayadi, H., Elloumi, J., 2021. The influence of environmental characteristics on the distribution of ciliates in two coastal areas in the Eastern Mediterranean Sea (Gulf of Gabes, Tunisia). Regional Studies in Marine Science 45, 101799. https://doi.org/10.1016/j.rsma.2021.101799

Knights, A.M., Koss, R.S., Robinson, L.A., 2013. Identifying common pressure pathways from a complex network of human activities to support ecosystem-based management. Ecological Applications 23, 755–765. https://doi.org/10.1890/12-1137.1

Koched, W.K., Alemany, F., Ismail, S.B., Benmessaoud, R., Hattour, A., Garcia, A., 2015. Environmental conditions influencing the larval fish assemblage during summer in the Gulf of Gabes (Tunisia: South central Mediterranean). Mediterranean Marine Science 16, 666–681. https://doi.org/10.12681/mms.1158

Kojima, D., Hamao, Y., Amei, K., Fukai, Y., Matsuno, K., Mitani, Y., Yamaguchi, A., 2022. Vertical distribution, standing stocks, and taxonomic accounts of the entire plankton community, and the estimation of vertical material flux via faecal pellets in the southern Okhotsk Sea. Deep Sea Research Part I: Oceanographic Research Papers 185, 103771. https://doi.org/10.1016/j.dsr.2022.103771

Kosiba, J., Wilk-Woźniak, E., Krztoń, W., Strzesak, M., Pociecha, A., Walusiak, E., Pudaś, K., Szarek-Gwiazda, E., 2017. What Underpins the Trophic Networks of the Plankton in Shallow Oxbow Lakes? Microb Ecol 73, 17–28. https://doi.org/10.1007/s00248-016-0833-6

Kosiba, J., Krztoń, W., 2022. Insight into the role of cyanobacterial bloom in the trophic link between ciliates and predatory copepods. Hydrobiologia 849, 1195–1206. https://doi.org/10.1007/s10750-021-04780-x

Kostka, J.E., Prakash, O., Overholt, W.A., Green, S.J., Freyer, G., Canion, A., Delgardio, J., Norton, N., Hazen, T.C., Huettel, M., 2011. Hydrocarbon-Degrading Bacteria and the Bacterial Community Response in Gulf of Mexico Beach Sands Impacted by the Deepwater Horizon Oil Spill. Applied and Environmental Microbiology 77, 7962–7974. https://doi.org/10.1128/AEM.05402-11

Kottuparambil S., Agusti S., 2018. PAHs sensitivity of picophytoplankton populations in the Red Sea. Environ Pollut, 239, 607-616. https://doi.org/10.1016/j.envpol.2018.04.079

Kovač, Ž., Platt, T., Ninčević Gladan, Ž., Morović, M., Sathyendranath, S., Raitsos, D.E., Grbec, B., Matić, F., Veža, J., 2018. A 55-Year Time Series Station for Primary Production in the Adriatic Sea: Data Correction, Extraction of Photosynthesis Parameters and Regime Shifts. Remote Sensing 10, 1460. https://doi.org/10.3390/rs10091460

Kryzevicius, Z., Mickuviene, K., Bucas, M., Vilkiene, M., Zukauskaite, A., 2020. Vertical distribution of polycyclic aromatic hydrocarbons in the brackish sea water column: ex situ experiment. PeerJ 8, e10087. https://doi.org/10.7717/peerj.10087

~ل~

Laender, F.D., Oevelen, D.V., Soetaert, K., Middelburg, J.J., 2010. Carbon transfer in a herbivore- and microbial loop-dominated pelagic food webs in the southern Barents Sea during

spring and summer. Marine Ecology Progress Series 398, 93–107. https://doi.org/10.3354/meps08335

Lafabrie, C., Hlaili, A.S., Leboulanger, C., Tarhouni, I., Othman, H.B., Mzoughi, N., Chouba, L., Pringault, O., 2013. Contaminated sediment resuspension induces shifts in phytoplankton structure and function in a eutrophic Mediterranean lagoon. Knowl. Managt. Aquatic Ecosyst. 05. https://doi.org/10.1051/kmae/2013060

Landry, M.R., Hassett, R.P., 1982. Estimating the grazing impact of marine micro-zooplankton. Marine Biology 67, 283–288. https://doi.org/10.1007/BF00397668

Landry, M.R., Stukel, M.R., Décima, M., 2020. Food-web fluxes support high rates of mesozooplankton respiration and production in the equatorial Pacific. Marine Ecology Progress Series 652, 15–32. https://doi.org/10.3354/meps13479

Larras F., Bouchez A, Rimet F., Montuelle B., 2012. Using bioassays and species sensitivity distributions to assess herbicide toxicity towards benthic diatoms. PloS One 7(8): e44458. https://doi.org/10.1371/journal.pone.0044458

Latham, L.G., Scully, E.P., 2002. Quantifying constraint to assess development in ecological networks. Ecological Modelling 154, 25–44. https://doi.org/10.1016/S0304-3800(02)00032-7

Latham, L.G., 2006. Network flow analysis algorithms. Ecological Modelling 192, 586–600. https://doi.org/10.1016/j.ecolmodel.2005.07.029

Laurenceau-Cornec, E.C., Trull, T.W., Davies, D.M., Bray, S.G., Doran, J., Planchon, F., Carlotti, F., Jouandet, M.-P., Cavagna, A.-J., Waite, A.M., Blain, S., 2015. The relative importance of phytoplankton aggregates and zooplankton fecal pellets to carbon export: insights from free-drifting sediment trap deployments in naturally iron-fertilised waters near the Kerguelen Plateau. Biogeosciences 12, 1007–1027. https://doi.org/10.5194/bg-12-1007-2015

Laybourn-Parry, J., Marchant, H.J., Brown, P.E., 1992. Seasonal cycle of the microbial plankton in Crooked Lake, Antarctica. Polar Biol 12, 411–416. https://doi.org/10.1007/BF00243112

Leblanc, K., Quéguiner, B., Diaz, F., Cornet, V., Michel-Rodriguez, M., Durrieu de Madron, X., Bowler, C., Malviya, S., Thyssen, M., Grégori, G., Rembauville, M., Grosso, O., Poulain, J., de Vargas, C., Pujo-Pay, M., Conan, P., 2018. Nanoplanktonic diatoms are globally overlooked but play a role in spring blooms and carbon export. Nat Commun 9, 953. https://doi.org/10.1038/s41467-018-03376-9

Lee C,I, Kim MC,, Kim HC,. 2009. Temporal variation of chlorophyll a concentration in the coastal waters affected by the Hebei Spirit oil spill in the West Sea of Korea. Mar Pollut Bull, 58(4):496–502. http://doi.org/10.1016/j.marpolbul.2008.12.007

Leflaive J., Ten Hage L., 2009. Chemical interactions in diatoms: role of polyunsaturated aldehydes and precursors. New Phytol, 184(4):794-805. http://doi.org/0.1111/j.1469-8137.2009.03033.x

Legendre and Le Fèvre, L., 1989. Hydrodynamical singularities as controls of recycled versus export production in oceans. productivity of the Ocean : Present and Pasts.

Legendre, L., Gosselin, M., 1989. New production and export of organic matter to the deep ocean: Consequences of some recent discoveries. Limnol. Oceanogr. 34, 1374–1380. https://doi.org/10.4319/lo.1989.34.7.1374

Legendre, L., 1990. The significance of microalgal blooms for fisheries and for the export of particulate organic carbon in oceans. Journal of Plankton Research 12, 681–699. https://doi.org/10.1093/plankt/12.4.681

Legendre, L., Rassoulzadegan, F., 1995. Plankton and nutrient dynamics in marine waters. Ophelia 41, 153–172. https://doi.org/10.1080/00785236.1995.10422042

Legendre, L., Rassoulzadegan, F., 1996. Food-web mediated export of biogenic carbon in oceans:hydrodynamic control. Mar. Ecol. Prog. Ser. 145, 179–193. https://doi.org/10.3354/meps145179

Leguerrier, D., 2005. Construction et étude d'un modèle de réseau trophique de la vasière de Brouage (bassin de marennes Oléron, France). Prise en compte de la saisonnalité et des échanges physiques pour la synthèse constructive des connaissances sur une zone intertidale d'une région tempérée. Université de la Rochelle.

Leruste, A., Pasqualini, V., Garrido, M., Malet, N., De Wit, R., Bec, B., 2019. Physiological and behavioral responses of phytoplankton communities to nutrient availability in a disturbed Mediterranean coastal lagoon. Estuarine, Coastal and Shelf Science 219, 176–188. https://doi.org/10.1016/j.ecss.2019.02.014

LESSARD, E.J., 1991. The trophic role of heterotrophic dinoflagellates in diverse marine environments. Mar. microb. food webs 5, 49–58.

Levin, S.A., 1992. The problem of pattern and scale in ecology. (Ecology). 73, 1943–1967. https://doi.org/10.2307/1941447

Lewis, K.A., Christian, R.R., Martin, C.W., Allen, K.L., McDonald, A.M., Roberts, V.M., Shaffer, M.N., Valentine, J.F., 2022. Complexities of disturbance response in a marine food web. Limnology & Oceanography 67. https://doi.org/10.1002/lno.11790

Li H, Duan, D, Beckingham B, Yang Y, Ran Y, Grathwohl P, 2020. Impact of trophic levels on partitioning and bioaccumulation of polycyclic aromatic hydrocarbons in particulate organic matter and plankton. Mar. Pollut. Bull. 160, 111527 https://doi.org/10.1016/j.marpolbul.2020.111527.

Li P, Cai Q., Lin W., Chen B., Zhang B., 2016. Offshore oil spill response practices and emerging challenges. Mar Pollut Bull, 110: 6–27. https://doi.org/https://doi.org/10.1016/j.marpolbul.2016.06.020

Li, A., Stoecker, D.K., Adolf, J.E., 1999. Feeding, pigmentation, photosynthesis and growth of the mixotrophic dinoflagellate Gyrodinium galatheanum. Aquatic Microbial Ecology 19, 163–176. https://doi.org/10.3354/ame019163

Li, A., Stoecker, D.K., Coats, D.W., 2000. Mixotrophy in Gyrodinium galatheanum (Dinophyceae): grazing responses to light intensity and inorganic nutrients. Journal of Phycology 36, 33–45.

Li, Q., Edwards, K.F., Schvarcz, C.R., Steward, G.F., 2022. Broad phylogenetic and functional diversity among mixotrophic consumers of Prochlorococcus. ISME J 16, 1557–1569. https://doi.org/10.1038/s41396-022-01204-z

Liquete, C., Piroddi, C., Macías, D., Druon, J.-N., Zulian, G., 2016. Ecosystem services sustainability in the Mediterranean Sea: assessment of status and trends using multiple modelling approaches. Sci Rep 6, 34162. https://doi.org/10.1038/srep34162

Liu, Q., Chai, F., Dugdale, R., Chao, Y., Xue, H., Rao, S., Wilkerson, F., Farrara, J., Zhang, H., Wang, Z., Zhang, Y., 2018. San Francisco Bay nutrients and plankton dynamics as simulated by a coupled hydrodynamic-ecosystem model. Continental Shelf Research 161, 29–48. https://doi.org/10.1016/j.csr.2018.03.008

Livanou, E., Lagaria, A., Santi, I., Mandalakis, M., Pavlidou, A., Lika, K., Psarra, S., 2019. Pigmented and heterotrophic nanoflagellates: Abundance and grazing on prokaryotic picoplankton in the ultra-oligotrophic Eastern Mediterranean Sea. Deep Sea Research Part II: Topical Studies in Oceanography, Revisiting the Eastern Mediterranean: Recent knowledge on the physical, biogeochemical and ecosystemic states and trends (Volume I) 164, 100–111. https://doi.org/10.1016/j.dsr2.2019.04.007

López-Abbate, M.C., Molinero, J.C., Barría de Cao, M.S., Silva, R., Negri, R., Guinder, V.A., Hozbor, M.C., Hoffmeyer, M.S., 2019. Eutrophication disrupts summer trophic links in an estuarine microbial food web. Food Webs 20, e00121. https://doi.org/10.1016/j.fooweb.2019.e00121

López-Abbate, M.C., 2021. Microzooplankton Communities in a Changing Ocean: A Risk Assessment. Diversity 13, 82. https://doi.org/10.3390/d13020082

Loureiro S., Jauzein C., Garcés E., Collos Y., Camp J., Vaqué D., 2009. The significance of organic nutrients in the nutrition of Pseudo-nitzschia delicatissima (Bacillariophyceae). J Plankton Res, 31(4), 399-410. https://doi.org/10.1093/plankt/fbn122

Lovejoy, C., Legendre, L., Martineau, M.-J., Bâcle, J., von Quillfeldt, C.H., 2002. Distribution of phytoplankton and other protists in the North Water. Deep Sea Research Part II: Topical

Studies in Oceanography, The International North Water Polynya Study 49, 5027–5047. https://doi.org/10.1016/S0967-0645(02)00176-5

Lund, C. Kipling, E. D. Le Cren, 1958. The inverted microscope method of estimating algal numbers and the statistical basis of estimations by counting | SpringerLink [WWW Document]. URL https://link.springer.com/article/10.1007/BF00007865 (accessed 6.8.22).

Luong, A.D., De Laender, F., Olsen, Y., Vadstein, O., Dewulf, J., Janssen, C.R., 2014. Inferring time-variable effects of nutrient enrichment on marine ecosystems using inverse modelling and ecological network analysis. Science of The Total Environment 493, 708–718. https://doi.org/10.1016/j.scitotenv.2014.06.027

Lv X., Liu X., Hu X., Geng R., Tang C., Xing Q., 2023. The Red Tide Organism Chaetoceros sp. Responding to Exposure to Oil and Dispersant. Sustain Sci, 15(2), 1103. https://doi.org/10.3390/su15021103

~M~

MacArthur, R., 1955. Fluctuations of Animal Populations and a Measure of Community Stability. Ecology 36, 533–536. https://doi.org/10.2307/1929601

Machado, K.B., Bini, L.M., Melo, A.S., Andrade, A.T. de, Almeida, M.F. de, Carvalho, P., Teresa, F.B., Roque, F. de O., Bortolini, J.C., Padial, A.A., Vieira, L.C.G., Dala-Corte, R.B., Siqueira, T., Juen, L., Dias, M.S., Gama Júnior, W.A., Martins, R.T., Nabout, J.C., 2023. Functional and taxonomic diversities are better early indicators of eutrophication than composition of freshwater phytoplankton. Hydrobiologia 850, 1393–1411. https://doi.org/10.1007/s10750-022-04954-1

MacIsaac EA., Stockner JG., 1993. Enumeration of phototrophic picoplankton byautofluorescence microscopy. In Kemp PF, Sherr BF, Sherr EB, Cole JJ, [Ed.],"Handbook of methods in aquatic microbial ecology", Lewis Publishers, pp. 187-197

Magazzu, G., Decembrini, F., 1995. Primary production, biomass and abundance of phototrophic picoplankton in the Mediterranean Sea: a review. Oceanographic Literature Review 12, 1100–1101.

Makhlouf Belkahia, N., Pagano, M., Chevalier, C., Devenon, J.L., Daly Yahia, M.N., 2021. Zooplankton abundance and community structure driven by tidal currents in a Mediterranean coastal lagoon (Boughrara, Tunisia, SW Mediterranean Sea). Estuarine, Coastal and Shelf Science 250, 107101. https://doi.org/10.1016/j.ecss.2020.107101

Mansano AS., Hisatugo KF., Hayashi LH., Regali-Seleghim MH., 2014. The importance of protozoan bacterivory in a subtropical environment (Lobo-Broa Reservoir, SP, Brazil). Braz J Biol 74:569–578. https://doi.org/10.1590/bjb.2014.0081

Mansouri, B., Gzam, M., Souid, F., Telahigue, F., Chahlaoui, A., Ouarrak, K., Kharroubi, A., 2020. Assessment of heavy metal contamination in Gulf of Gabès coastland (southeastern

Tunisia): impact of chemical industries and drift currents. Arab J Geosci 13, 1180. https://doi.org/10.1007/s12517-020-06163-3

Maranon, E., 2010. Phytoplankton Size Structure. Encyclopedia of Ocean Sciences 4249–4256. https://doi.org/10.1016/B978-012374473-9.00661-5

Margalef, R., 1978. Life-forms of phytoplankton as survival alternatives in an unstable environment. Oceanol. Acta 1, 493–509.

Mari, X., Rassoulzadegan, F., Brussaard, C.P.D., 2004. Role of TEP in the microbial food web structure. II. Influence on the ciliate community structure. Marine Ecology Progress Series 279, 23–32. https://doi.org/10.3354/meps279023

Marques, F., Chainho, P., Costa, J.L., Domingos, I., Angélico, M.M., 2015. Abundance, seasonal patterns and diet of the non-native jellyfish Blackfordia virginica in a Portuguese estuary. Estuarine, Coastal and Shelf Science, Coastal systems under change: tuning assessment and management tools 167, 212–219. https://doi.org/10.1016/j.ecss.2015.07.024

Marquis, E., Niquil, N., Delmas, D., Hartmann, H.J., Bonnet, D., Carlotti, F., Herbland, A., Labry, C., Sautour, B., Laborde, P., Vézina, A., Dupuy, C., 2007. Inverse analysis of the planktonic food web dynamics related to phytoplankton bloom development on the continental shelf of the Bay of Biscay, French coast. Estuarine, Coastal and Shelf Science 73, 223–235. https://doi.org/10.1016/j.ecss.2007.01.003

Marshall HG., Lacouture RV., Buchanan C., Johnson JM., 2006. Phytoplankton assemblages associated with water quality and salinity regions in Chesapeake Bay, USA, Estuar Coast Shelf Sci, 69 (1–2): 10-18. https://doi.org/10.1016/j.ecss.2006.03.019.

Martin-Cereceda, M., Novarino, G., Young, J.R., 2003. Grazing by Prymnesium parvum on small planktonic diatoms. Aquatic Microbial Ecology 33, 191–199. https://doi.org/10.3354/ame033191

Marty, J.-C., Chiavérini, J., 2002. Seasonal and interannual variations in phytoplankton production at DYFAMED time-series station, northwestern Mediterranean Sea. Deep Sea Research Part II: Topical Studies in Oceanography, Studies at the DYFAMED (France JGOFS) Time-Series Station, N.W. M editerranean Sea 49, 2017–2030. https://doi.org/10.1016/S0967-0645(02)00025-5

Masclaux, H., Tortajada, S., Philippine, O., Robin, F.-X., Dupuy, C., 2015. Planktonic food web structure and dynamic in freshwater marshes after a lock closing in early spring. Aquat Sci 77, 115–128. https://doi.org/10.1007/s00027-014-0376-1

Mauchline, J., 1998. Adv. Mar. Biol. 33: The biology of calanoid copepods. Advances in Marine Biology.

Mayot, N., D'Ortenzio, F., Taillandier, V., Prieur, L., de Fommervault, O.P., Claustre, H., Bosse, A., Testor, P., Conan, P., 2017. Physical and Biogeochemical Controls of the Phytoplankton Blooms in North Western Mediterranean Sea: A Multiplatform Approach Over a

Complete Annual Cycle (2012–2013 DEWEX Experiment). Journal of Geophysical Research: Oceans 122, 9999–10019. https://doi.org/10.1002/2016JC012052

Mayot, N., Nival, P., Levy, M., 2020. Primary Production in the Ligurian Sea, in: The Mediterranean Sea in the Era of Global Change 1. John Wiley & Sons, Ltd, pp. 139–164. https://doi.org/10.1002/9781119706960.ch6

Mazumder, D., Saintilan, N., Wen, L., Kobayashi, T., Rogers, K., 2017. Productivity influences trophic structure in a temporally forced aquatic ecosystem. Freshwater Biology 62, 1528–1538. https://doi.org/10.1111/fwb.12963

McCann, K.S., 2000. The diversity–stability debate. Nature 405, 228–233. https://doi.org/10.1038/35012234

McQuatters-Gollop, A., Guérin, L., Arroyo, N.L., Aubert, A., Artigas, L.F., Bedford, J., Corcoran, E., Dierschke, V., Elliott, S.A.M., Geelhoed, S.C.V., Gilles, A., González-Irusta, J.M., Haelters, J., Johansen, M., Le Loc'h, F., Lynam, C.P., Niquil, N., Meakins, B., Mitchell, I., Padegimas, B., Pesch, R., Preciado, I., Rombouts, I., Safi, G., Schmitt, P., Schückel, U., Serrano, A., Stebbing, P., De la Torriente, A., Vina-Herbon, C., 2022. Assessing the state of marine biodiversity in the Northeast Atlantic. Ecological Indicators 141, 109148. https://doi.org/10.1016/j.ecolind.2022.109148

McQueen, D.J., Post, J.R., Mills, E.L., 1986. Trophic Relationships in Freshwater Pelagic Ecosystems. Can. J. Fish. Aquat. Sci. 43, 1571–1581. https://doi.org/10.1139/f86-195

Meddeb, M., Grami, B., Chaalali, A., Haraldsson, M., Niquil, N., Pringault, O., Sakka Hlaili, A., 2018. Plankton food-web functioning in anthropogenically impacted coastal waters (SW Mediterranean Sea): An ecological network analysis. Progress in Oceanography 162, 66–82. https://doi.org/10.1016/j.pocean.2018.02.013

Meddeb, M., Niquil, N., Grami, B., Mejri, K., Haraldsson, M., Chaalali, A., Pringault, O., Hlaili, A.S., 2019. A new type of plankton food web functioning in coastal waters revealed by coupling Monte Carlo Markov chain linear inverse method and ecological network analysis. Ecological Indicators 104, 67–85. https://doi.org/10.1016/j.ecolind.2019.04.077

Meersche, K.V. den, Soetaert, K., Oevelen, D.V., 2009. xsample(): An R Function for Sampling Linear Inverse Problems. Journal of Statistical Software 30, 1–15. https://doi.org/10.18637/jss.v030.c01

Mejri Kousri, K., Meddeb, M., Grami, B., Melliti Ben Garali, S., Chkili, O., Sahraoui, I., Gonzalez, C., Montigny, C., Pringault, O., Sakka Hlaili, A., 2023. Effects of experimental sediment resuspension on protozooplankton grazing activity: implication for the planktonic food web structure. Aquat Ecol 57, 165–186. https://doi.org/10.1007/s10452-022-09998-y

Melliti Ben Garali S., Sahraoui I., Ben Othman H, Kouki A., de la Iglesia .P, Diogène J, Lafabrie C., Andree KB., Fernández-Tejedor M., Mejri K., Meddeb M., Pringault O., Sakka Hlaili A., 2021. Capacity of the potentially toxic diatoms Pseudo-nitzschia mannii and Pseudo-

nitzschia hasleana to tolerate polycyclic aromatic hydrocarbons. Ecotoxicol Environ Saf, 214,112082. https://doi.org/10.1016/j.ecoenv.2021.112082

Melliti Ben Garali S., Sahraoui I., de la Iglesia P., Chalghaf M., Diogène J., Ksouri J., Sakka Hlaili A., 2016. Effects of nitrogen supply on Pseudo-nitzschia calliantha and Pseudo-nitzschia cf. seriata: field and laboratory experiments. Ecotoxicol, 25, 1211-1225. https://doi.org/10.1007/s10646-016-1675-1

Melliti Ben Garali S., Sahraoui I., de la Iglesia P., Chalghaf M., Diogène J., Ksouri J., Sakka Hlaili A., 2020. Factors driving the seasonal dynamics of Pseudo-nitzschia species and domoic acid at mussel farming in the SW Mediterranean Sea. C hem Ecol, 36(1), 66-82. https://doi.org/10.1080/02757540.2019.1676417

Menden-Deuer, S., Lessard, E.J., 2000. Carbon to volume relationships for dinoflagellates, diatoms, and other protist plankton. Limnology and Oceanography 45, 569–579. https://doi.org/10.4319/lo.2000.45.3.0569

Méndez, M., García, D., Maestre, F.T., Escudero, A., 2008. More Ecology is Needed to Restore Mediterranean Ecosystems: A Reply to Valladares and Gianoli. Restoration Ecology 16, 210–216. https://doi.org/10.1111/j.1526-100X.2008.00390.x

Mengelt C., Prézelin BB., 2005. A potential novel link between organic nitrogen loading and Pseudo-nitzschia spp. blooms. In California and the World Ocean'02: Revisiting and Revising California's Ocean Agenda (pp. 882-896). https://doi.org/10.1061/40761(175)78

Mercado, J.M., Cortés, D., Gómez-Jakobsen, F., García-Gómez, C., Ouaissa, S., Yebra, L., Ferrera, I., Valcárcel-Pérez, N., López, M., García-Muñoz, R., Ramos, A., Bernardeau, J., Belando, M.D., Fraile-Nuez, E., Ruíz, J.M., 2021. Role of small-sized phytoplankton in triggering an ecosystem disruptive algal bloom in a Mediterranean hypersaline coastal lagoon. Marine Pollution Bulletin 164, 111989. https://doi.org/10.1016/j.marpolbul.2021.111989

Michán, C., Blasco, J., Alhama, J., 2021. High-throughput molecular analyses of microbiomes as a tool to monitor the wellbeing of aquatic environments. Microbial Biotechnology 14, 870–885. https://doi.org/10.1111/1751-7915.13763

Michel, C., Nielsen, T.G., Nozais, C., Gosselin, M., 2002. Significance of sedimentation and grazing by ice micro- and meiofauna for carbon cycling in annual sea ice (northern Baffin Bay). Aquatic Microbial Ecology 30, 57–68. https://doi.org/10.3354/ame030057

Mille G, Asia L., Guiliano M., Malleret L., Doumenq P., 2007. Hydrocarbons in coastal sediments from the Mediterranean Sea (Gulf of Fos area, France). Mar Pollut Bull, 54(5), 566-575. https://doi.org/10.1016/j.marpolbul.2006.12.009

Mishamandani S., Gutierrez T., Berry D., Aitken MD., 2016. Response of the bacterial community associated with a cosmopolitan marine diatom to crude oil shows a preference for the

biodegradation of aromatic hydrocarbons. Environ Microbiol, 18, 1817–1833. https://doi.org/10.1111/1462-2920.12988

Mitra, A., Flynn, K.J., Tillmann, U., Raven, J.A., Caron, D., Stoecker, D.K., Not, F., Hansen, P.J., Hallegraeff, G., Sanders, R., Wilken, S., McManus, G., Johnson, M., Pitta, P., Våge, S., Berge, T., Calbet, A., Thingstad, F., Jeong, H.J., Burkholder, J., Glibert, P.M., Granéli, E., Lundgren, V., 2016. Defining Planktonic Protist Functional Groups on Mechanisms for Energy and Nutrient Acquisition: Incorporation of Diverse Mixotrophic Strategies. Protist 167, 106–120. https://doi.org/10.1016/j.protis.2016.01.003

Moigis and Gocke, 2003. Primary production of phytoplankton estimated by means of the dilution method in coastal waters | Journal of Plankton Research | Oxford Academic [WWW Document]. URL https://academic.oup.com/plankt/article/25/10/1291/1545944 (accessed 6.8.22).

Montagnes, D.J.S., Dower, J.F., Figueiredo, G.M., 2010. The Protozooplankton–Ichthyoplankton Trophic Link: An Overlooked Aspect of Aquatic Food Webs1. Journal of Eukaryotic Microbiology 57, 223–228. https://doi.org/10.1111/j.1550-7408.2010.00476.x

Moran, X.A.G., Estrada, M., 2001. Short-term variability of photosynthetic parameters and particulate and dissolved primary production in the Alboran Sea (SW Mediterranean). Marine Ecology Progress Series 212, 53–67. https://doi.org/10.3354/meps212053

Morsy, A., Ebeid, M., Soliman, A., Halim, A.A., Ali, A.E., Fahmy, M., 2022. Evaluation of the water quality and the eutrophication risk in Mediterranean sea area: A case study of the Port Said Harbour, Egypt. Environmental Challenges 7, 100484. https://doi.org/10.1016/j.envc.2022.100484

Mousseau, L., Klein, B., Legendre, L., Dauchez, S., Tamigneaux, E., Tremblay, J.-E., Ingram, R.G., 2001. Assessing the trophic pathways that dominate planktonic food webs: an approach based on simple ecological ratios. Journal of Plankton Research 23, 765–777. https://doi.org/10.1093/plankt/23.8.765

Nakano, S., Tomaru, Y., Katano, T., Kaneda, A., Makino, W., Nishibe, Y., Hirose, M., Onji, M., Kitamura, S.-I., Takeoka, H., 2004. The dynamics of microbial and herbivorous food webs in a coastal sea with special reference to intermittent nutrient supply from bottom intrusion. Aquatic Ecology 38, 485–493. https://doi.org/10.1007/s10452-004-0441-2

~N~

Naselli-Flores, L., Padisák, J., Albay, M., 2007. Shape and size in phytoplankton ecology: do they matter? Hydrobiologia 578, 157–161. https://doi.org/10.1007/s10750-006-2815-z

Negrete-García, G., Luo, J.Y., Long, M.C., Lindsay, K., Levy, M., Barton, A.D., 2022. Plankton energy flows using a global size-structured and trait-based model. https://doi.org/10.1101/2022.02.01.478546

Niquil, N., Soetaert, K.E.R., Johnson, G.A., Van Oevelen, D., Bacher, C., Saint-Béat, B., Vézina, A.F., 2011. Inverse modelling in modern ecology and application to coastal ecosystems, in: Wolanski, E., Mclusky, D. (Eds.), Estuarine and Coastal Ecosystem Modelling, Treatise on Estuarine and Coastal Science. Elsevier B.V., pp. 115–133. https://doi.org/10.1016/B978-0-12-374711-2.00906-2

Niquil, N., Chaumillon, E., Johnson, G.A., Bertin, X., Grami, B., David, V., Bacher, C., Asmus, H., Baird, D., Asmus, R., 2012. The effect of physical drivers on ecosystem indices derived from ecological network analysis: Comparison across estuarine ecosystems. Estuarine, Coastal and Shelf Science, ECSA 46 Conference Proceedings 108, 132–143. https://doi.org/10.1016/j.ecss.2011.12.031

Niquil, N., Baeta, A., Marques, J.C., Chaalali, A., Lobry, J., Patrício, J., 2014. Reaction of an estuarine food web to disturbance: Lindeman's perspective. Marine Ecology Progress Series 512, 141–154. https://doi.org/10.3354/meps10885

Nogueira, D.J., Mattos, J.J., Dybas, P.R., Flores-Nunes, F., Sasaki, S.T., Taniguchi, S., Schmidt, É.C., Bouzon, Z.L., Bícego, M.C., Melo, C.M.R., Toledo-Silva, G., Bainy, A.C.D., 2017. Effects of phenanthrene on early development of the Pacific oyster Crassostrea gigas (Thunberg, 1789). Aquatic Toxicology 191, 50–61. https://doi.org/10.1016/j.aquatox.2017.07.022

Nogues, Q., Raoux, A., Araignous, E., Chaalali, A., Hattab, T., Leroy, B., Ben Rais Lasram, F., David, V., Le Loc'h, F., Dauvin, J.-C., Niquil, N., 2021. Cumulative effects of marine renewable energy and climate change on ecosystem properties: Sensitivity of ecological network analysis. Ecological Indicators 121, 107128. https://doi.org/10.1016/j.ecolind.2020.107128

~O~

Odum, E.P., 1969. The Strategy of Ecosystem Development. Science 164, 262–270. https://doi.org/10.1126/science.164.3877.262

Odum, E.P., 1985. Trends Expected in Stressed Ecosystems. BioScience 35, 419–422. https://doi.org/10.2307/1310021

Ohman, M.D., Hirche, H.-J., 2001. Density-dependent mortality in an oceanic copepod population. Nature 412, 638–641. https://doi.org/10.1038/35088068

Ohwada K,, Nishimura M,, Wada M,, Nomura H,, Shibata A,, Okamoto K,, ... & Yamada, M., 2003. Study of the effect of water-soluble fractions of heavy-oil on coastal marine organisms using enclosed ecosystems, mesocosms. Mar Pollut Bull, 47(1-6), 78-84. https://doi.org/10.1016/S0025-326X(03)00102-4

Olson, M.B., Strom, S.L., 2002. Phytoplankton growth, microzooplankton herbivory and community structure in the southeast Bering Sea: insight into the formation and temporal persistence of an Emiliania huxleyi bloom. Deep Sea Research Part II: Topical Studies in

Oceanography, Ecology of the SE Bering Sea 49, 5969–5990. https://doi.org/10.1016/S0967-0645(02)00329-6

Othman, H.B., Leboulanger, C., Le Floc'h, E., Hadj Mabrouk, H., Sakka Hlaili, A., 2012. Toxicity of benz(a)anthracene and fluoranthene to marine phytoplankton in culture: Does cell size really matter? Journal of Hazardous Materials 243, 204–211. https://doi.org/10.1016/j.jhazmat.2012.10.020

Othmani, A., Béjaoui, B., Chevalier, C., Elhmaidi, D., Devenon, J.-L., Aleya, L., 2017. High-resolution numerical modelling of the barotropic tides in the Gulf of Gabes, eastern Mediterranean Sea (Tunisia). Journal of African Earth Sciences 129, 224–232. https://doi.org/10.1016/j.jafrearsci.2017.01.007

Ozhan K., Bargu S., 2014. Distinct responses of Gulf of Mexico phytoplankton communities to crude oil and the dispersant Corexit EC9500A under different nutrient regimes. Ecotoxicol 23, 370–384. https://doi.org/10.1007/s10646-014-1195-9 .

Ozhan, K., Parsons, M.L., Bargu, S., 2014. How Were Phytoplankton Affected by the Deepwater Horizon Oil Spill? BioScience 64, 829–836. https://doi.org/10.1093/biosci/biu117

~p~

Pacella, S.R., Lebreton, B., Richard, P., Phillips, D., DeWitt, T.H., Niquil, N., 2013. Incorporation of diet information derived from Bayesian stable isotope mixing models into mass-balanced marine ecosystem models: A case study from the Marennes-Oléron Estuary, France. Ecological Modelling 267, 127–137. https://doi.org/10.1016/j.ecolmodel.2013.07.018

Pan, G., Tang, D., Zhang, Y., 2012. Satellite monitoring of phytoplankton in the East Mediterranean Sea after the 2006 Lebanon oil spill. International Journal of Remote Sensing 33, 7482–7490. https://doi.org/10.1080/01431161.2012.685982

Pančić, M., Köhler, E., Paulsen, M.L., Toxværd, K., Lacroix, C., Le Floch, S., Hjorth, M., Nielsen, T.G., 2019a. Effects of oil spill response technologies on marine microorganisms in the high Arctic. Marine Environmental Research 151, 104785. https://doi.org/10.1016/j.marenvres.2019.104785

Paranjape, M.A., 1990. Microzooplankton herbivory on the Grand Bank (Newfoundland, Canada): A seasonal study. Mar. Biol. 107, 321–328. https://doi.org/10.1007/BF01319832

Parson TR., Maita Y., Lalli CM., 1984. A Manual of Chemical and Biological Methods for Seawater Analysis. Pergamon Press, Oxford, 173 p.

Parsons ML., Brandt AL., Turner RE., Morrison WL., Ralabais NN., 2021. Characterization of common phytoplankton on the Louisiana shelf. Mar Pollut Bull, 168: 112458, https://doi.org/10.1016/j.marpolbul.2021.112458 .

Parsons, M.L., Morrison, W., Rabalais, N.N., Turner, R.E., Tyre, K.N., 2015. Phytoplankton and the Macondo oil spill: A comparison of the 2010 phytoplankton assemblage to baseline

conditions on the Louisiana shelf. Environmental Pollution 207, 152–160. https://doi.org/10.1016/j.envpol.2015.09.019

Parsons, T.R., Harrison, P.J., Acreman, J.C., Dovey, H.M., Thompson, P.A., Lalli, C.M., Lee, K., Guanguo, L., Xiaolin, C., 1984. An experimental marine ecosystem response to crude oil and Corexit 9527: Part 2—Biological effects. Marine Environmental Research 13, 265–275. https://doi.org/10.1016/0141-1136(84)90033-3

Patrício, J., Ulanowicz, R., Pardal, M.A., Marques, J.C., 2004. Ascendency as an ecological indicator: a case study of estuarine pulse eutrophication. Estuarine, Coastal and Shelf Science 60, 23–35. https://doi.org/10.1016/j.ecss.2003.11.017

Pauly, D., Christensen, V., Walters, C., 2000. Ecopath, Ecosim, and Ecospace as tools for evaluating ecosystem impact of fisheries. ICES Journal of Marine Science 57, 697–706. https://doi.org/10.1006/jmsc.2000.0726

Pecqueur, D., Courboulès, J., Roques, C., Mas, S., Pete, R., Vidussi, F., Mostajir, B., 2022. Simultaneous Study of the Growth and Grazing Mortality Rates of Microbial Food Web Components in a Mediterranean Coastal Lagoon. Diversity 14, 186. https://doi.org/10.3390/d14030186

Penela-Arenaz M., Bellas J., Vasquez E., 2009. Chapter five: Effects of the Prestige oil spill on the biota of NW Spain: 5 years of learning. Adv Mar Biol, 56: 365-396. https://doi.org/10.1016/S0065-2881(09)56005-1

Peters F, Arin L, Marrasé C, Berdalet E, Sala MM (2006) Effects of small-scale turbulence on the growth of two diatoms of different size in a phosphorus-limited medium. J Mar Syst 61:134–148. https://doi.org/10.1016/j.jmarsys.2005.11.012

Pezy, J.-P., Raoux, A., Marmin, S., Balay, P., Niquil, N., Dauvin, J.-C., 2017. Before-After analysis of the trophic network of an experimental dumping site in the eastern part of the Bay of Seine (English Channel). Marine Pollution Bulletin 118, 101–111. https://doi.org/10.1016/j.marpolbul.2017.02.042

Pillai, M.C., Vines, C.A., Wikramanayake, A.H., Cherr, G.N., 2003. Polycyclic aromatic hydrocarbons disrupt axial development in sea urchin embryos through a β-catenin dependent pathway. Toxicology 186, 93–108. https://doi.org/10.1016/S0300-483X(02)00695-9

Piroddi, C., Coll, M., Steenbeek, J., Macias Moy, D., Christensen, V., 2015. Modelling the Mediterranean marine ecosystem as a whole: addressing the challenge of complexity. Mar. Ecol. Prog. Ser. 533, 47–65. https://doi.org/10.3354/meps11387

Poulsen, L.K., Reuss, N., 2002. The plankton community on Sukkertop and Fylla Banks Off West Greenland during a spring bloom and post-bloom period: Hydrography, phytoplankton and protozooplankton. Ophelia 56, 69–85. https://doi.org/10.1080/00785236.2002.10409491

Prasad, K.V.H., 2022. Ecosystem Ecology, in: Prasad, K.V.H. (Ed.), Insect Ecology: Concepts to Management. Springer Nature, Singapore, pp. 189–207. https://doi.org/10.1007/978-981-19-1782-0_13

Pringault, O., Lafabrie, C., Avezac, M., Bancon-Montigny, C., Carre, C., Chalghaf, M., Delpoux, S., Duvivier, A., Elbaz-Poulichet, F., Gonzalez, C., Got, P., Leboulanger, C., Spinelli, S., Sakka Hlaili, A., Bouvy, M., 2016. Consequences of contaminant mixture on the dynamics and functional diversity of bacterioplankton in a southwestern Mediterranean coastal ecosystem. Chemosphere 144, 1060–1073. https://doi.org/10.1016/j.chemosphere.2015.09.093

Pringault, O., Bouvy, M., Carre, C., Mejri, K., Bancon-Montigny, C., Gonzalez, C., Leboulanger, C., Hlaili, A.S., Goni-Urriza, M., 2021. Chemical contamination alters the interactions between bacteria and phytoplankton. Chemosphere 278, 130457. https://doi.org/10.1016/j.chemosphere.2021.130457

Psarra, S., Zohary, T., Krom, M.D., Mantoura, R.F.C., Polychronaki, T., Stambler, N., Tanaka, T., Tselepides, A., Frede Thingstad, T., 2005. Phytoplankton response to a Lagrangian phosphate addition in the Levantine Sea (Eastern Mediterranean). Deep Sea Research Part II: Topical Studies in Oceanography, On the Nature of Phosphorus Cycling and Limitation in the Eastern Mediterranean 52, 2944–2960. https://doi.org/10.1016/j.dsr2.2005.08.015

Putt, M., Stoecker, D.K., 1989. An experimentally determined carbon : volume ratio for marine "oligotrichous" ciliates from estuarine and coastal waters. Limnology and Oceanography 34, 1097–1103. https://doi.org/10.4319/lo.1989.34.6.1097

Putzeys, S., Juárez-Fonseca, M., Valencia-Agami, S.S., Mendoza-Flores, A., Cerqueda-García, D., Aguilar-Trujillo, A.C., Martínez-Cruz, M.E., Okolodkov, Y.B., Arcega-Cabrera, F., Herrera-Silveira, J.A., Aguirre-Macedo, M.L., Pech, D., 2022. Effects of a Light Crude Oil Spill on a Tropical Coastal Phytoplankton Community. Bull Environ Contam Toxicol 108, 55–63. https://doi.org/10.1007/s00128-021-03306-4

~Q~

Quigg, A., Parsons, M., Bargu, S., Ozhan, K., Daly, K.L., Chakraborty, S., Kamalanathan, M., Erdner, D., Cosgrove, S., Buskey, E.J., 2021. Marine phytoplankton responses to oil and dispersant exposures: Knowledge gained since the Deepwater Horizon oil spill. Marine Pollution Bulletin 164, 112074. https://doi.org/10.1016/j.marpolbul.2021.112074

~R~

Raimbault, P., Garcia, N., Cerutti, F., 2008. Distribution of inorganic and organic nutrients in the South Pacific Ocean − evidence for long-term accumulation of organic matter in nitrogen-depleted waters. Biogeosciences 5, 281–298. https://doi.org/10.5194/bg-5-281-2008

Rassoulzadegan, F., Laval-Peuto, M., Sheldon, R.W., 1988. Partitioning of the food ration of marine ciliates between pico- and nanoplankton. Hydrobiologia 159, 75–88. https://doi.org/10.1007/BF00007369

Raveh, O., David, N., Rilov, G., Rahav, E., 2015. The Temporal Dynamics of Coastal Phytoplankton and Bacterioplankton in the Eastern Mediterranean Sea. PLOS ONE 10, e0140690. https://doi.org/10.1371/journal.pone.0140690

Raven, A., 1986. Physiological consequences of extremely small size for autotrophic organisms in the sea. Photosynthetic Picoplankton. Can. Bull. Fish. Aquat. Sci. 214, 1–70.

Rekik, A., Denis, M., Maalej, S., Ayadi, H., 2015. Spatial and seasonal variability of pico-, nano- and microphytoplankton at the bottom seawater in the north coast of Sfax, Eastern Mediterranean Sea. Environ Sci Pollut Res 22, 15961–15975. https://doi.org/10.1007/s11356-015-4811-1

Reygondeau, G., Guieu, C., Benedetti, F., Irisson, J.-O., Ayata, S.-D., Gasparini, S., Koubbi, P., 2017. Biogeochemical regions of the Mediterranean Sea: An objective multidimensional and multivariate environmental approach. Progress in Oceanography 151, 138–148. https://doi.org/10.1016/j.pocean.2016.11.001

Riccardi, N., 2010. Selectivity of plankton nets over mesozooplankton taxa: implications for abundance, biomass and diversity estimation. J Limnol 69, 287. https://doi.org/10.4081/jlimnol.2010.287

Richardson, T.L., Jackson, G.A., 2007. Small Phytoplankton and Carbon Export from the Surface Ocean. Science 315, 838–840. https://doi.org/10.1126/science.1133471

Riegman, R., Kuipers, B.R., Noordeloos, A.A.M., Witte, H.J., 1993. Size-differential control of phytoplankton and the structure of plankton communities. Netherlands Journal of Sea Research 31, 255–265. https://doi.org/10.1016/0077-7579(93)90026-O

Riemann, B., Christoffersen, K., 1993. Microbial trophodynamics in temperate lakes. Mar. microb. food webs 7, 69–100.

Riley, G., 1946. Factors controlling phytoplankton populations on Georges Bank. Journal of Marine Research 6.

Robinson, C., 2008. Heterotrophic bacterial respiration, in: Kirchman, D. (Ed.), Microbial Ecology of the Oceans. Wiley, pp. 299–334.

Robinson, C., Steinberg, D.K., Anderson, T.R., Arístegui, J., Carlson, C.A., Frost, J.R., Ghiglione, J.-F., Hernández-León, S., Jackson, G.A., Koppelmann, R., Quéguiner, B., Ragueneau, O., Rassoulzadegan, F., Robison, B.H., Tamburini, C., Tanaka, T., Wishner, K.F., Zhang, J., 2010. Mesopelagic zone ecology and biogeochemistry – a synthesis. Deep Sea Research Part II: Topical Studies in Oceanography, Ecological and Biogeochemical Interactions in the Dark Ocean 57, 1504–1518. https://doi.org/10.1016/j.dsr2.2010.02.018

Romano, J., Kromrey, J., Coraggio, J., 2006. Exploring methods for evaluating group differences on the NSSE and other surveys: Are the t-test and Cohen's d indices the most appropriate choices? In annual meeting of the Southern Association for Institutional Research 1–51.

Rombouts, I., Beaugrand, G., Fizzala, X., Gaill, F., Greenstreet, S.P.R., Lamare, S., Le Loc'h, F., McQuatters-Gollop, A., Mialet, B., Niquil, N., Percelay, J., Renaud, F., Rossberg, A.G., Féral, J.P., 2013. Food web indicators under the Marine Strategy Framework Directive: From complexity to simplicity? Ecological Indicators 29, 246–254. https://doi.org/10.1016/j.ecolind.2012.12.021

Rooney, N., McCann, K., Gellner, G., Moore, J.C., 2006. Structural asymmetry and the stability of diverse food webs. Nature 442, 265–269. https://doi.org/10.1038/nature04887

Ross ON, Fraysse M, Pinazo C, Pairaud I (2016) Impact of an intrusion by the Northern Current on the biogeochemistry in the eastern Gulf of Lion, NW Mediterranean . Estuarine, Coastal and Shelf Science 170: 1-9. https://doi.org/10.1016/j.ecss.2015.12.022

Russo, L., Bellardini, D., Zampicinini, G., Jordán, F., Congestri, R., D'Alelio, D., 2023. From metabarcoding time series to plankton food webs: The hidden role of trophic hierarchy in providing ecological resilience. Marine Ecology n/a, e12733. https://doi.org/10.1111/maec.12733

Rutledge, R.W., Basore, B.L., Mulholland, R.J., 1976. Ecological stability: An information theory viewpoint. Journal of Theoretical Biology 57, 355–371. https://doi.org/10.1016/0022-5193(76)90007-2

~S~

Safi, G., Arroyo, N.L., Heymans, J., Raoux, A., Preciado, I., Schueckel, C., Tecchio, S., Niquil, N., 2017. Addressing gaps in biodiversity indicator development for the OSPAR Region from data to ecosystem assessment: Applying an ecosystem approach to (sub) regional habitat assessments. (report). Deliverable 3.4.2 Ecological Network Analysis indices OSPAR/FW9 indicator cemp guideline.

Safi, G., Giebels, D., Arroyo, N.L., Heymans, J.J., Preciado, I., Raoux, A., Schückel, U., Tecchio, S., de Jonge, V.N., Niquil, N., 2019. Vitamine ENA: A framework for the development of ecosystem-based indicators for decision makers. Ocean & Coastal Management 174, 116–130. https://doi.org/10.1016/j.ocecoaman.2019.03.005

Sahraoui, I., Grami, B., Bates, S.S., Bouchouicha, D., Chikhaoui, M.A., Mabrouk, H.H., Hlaili, A.S., 2012. Response of potentially toxic Pseudo-nitzschia (Bacillariophyceae) populations and domoic acid to environmental conditions in a eutrophied, SW Mediterranean coastal lagoon (Tunisia). Estuarine, Coastal and Shelf Science 102–103, 95–104. https://doi.org/10.1016/j.ecss.2012.03.018

Sahu G., Mohanty AK., Sarangi RK., Satpathy KK., 2022. Asterionellopsis glacialis (Family: Fragilariaceae, Class: Bacillariophyceae, Phylum: Ochrophyta) bloom and its impact on

plankton dynamics at Kalpakkam (Bay of Bengal, Southeast coast of India). Oceanologia, 64(1), 145-159. https://doi.org/10.1016/j.oceano.2021.04.005

Saidi, I., Ben Said, O., Ben Abdelmalek, J., Jouili, S., Chicharo, L., Beyrem, H., 2019. Impact of heavy metals of industrial plant wastewater on benthic communities of Bizerte Lagoon (Tunisia). Chemistry and Ecology 35, 746–774. https://doi.org/10.1080/02757540.2019.1644324

Saint-Béat, B., Baird, D., Asmus, H., Asmus, R., Bacher, C., Pacella, S.R., Johnson, G.A., David, V., Vézina, A.F., Niquil, N., 2015. Trophic networks: How do theories link ecosystem structure and functioning to stability properties? A review. Ecological Indicators 52, 458–471. https://doi.org/10.1016/j.ecolind.2014.12.017

Saint-Béat, B., Dupuy, C., Bocher, P., Chalumeau, J., Crignis, M.D., Fontaine, C., Guizien, K., Lavaud, J., Lefebvre, S., Montanié, H., Mouget, J.-L., Orvain, F., Pascal, P.-Y., Quaintenne, G., Radenac, G., Richard, P., Robin, F., Vézina, A.F., Niquil, N., 2013. Key Features of Intertidal Food Webs That Support Migratory Shorebirds. PLOS ONE 8, e76739. https://doi.org/10.1371/journal.pone.0076739

Saint-Béat, B., Maps, F., Babin, M., 2018. Unraveling the intricate dynamics of planktonic Arctic marine food webs. A sensitivity analysis of a well-documented food web model. Progress in Oceanography 160, 167–185. https://doi.org/10.1016/j.pocean.2018.01.003

Saiz, E., Rodriguez, V., Alcaraz, M., 1992. Spatial distribution and feeding rates of Centropages typicus in relation to frontal hydrographic structures in the Catalan Sea (Western Mediterranean). Marine Biology 112, 49–56. https://doi.org/10.1007/BF00349727

Sakka, A., Legendre, L., Gosselin, M., Delesalle, B., 2000. Structure of the oligotrophic planktonic food web under low grazing of heterotrophic bacteria: Takapoto Atoll, French Polynesia. Marine Ecology Progress Series 197, 1–17. https://doi.org/10.3354/meps197001

Sakka Hlaili, A., Grami, B., Hadj Mabrouk, H., Gosselin, M., Hamel, D., 2007. Phytoplankton growth and microzooplankton grazing rates in a restricted Mediterranean lagoon (Bizerte Lagoon, Tunisia). Mar Biol 151, 767–783. https://doi.org/10.1007/s00227-006-0522-y

Sakka Hlaili, A., Grami, B., Niquil, N., Gosselin, M., Hamel, D., Troussellier, M., Hadj Mabrouk, H., 2008. The planktonic food web of the Bizerte lagoon (south-western Mediterranean) during summer: I. Spatial distribution under different anthropogenic pressures. Estuarine, Coastal and Shelf Science 78, 61–77. https://doi.org/10.1016/j.ecss.2007.11.010

Sakka Hlaili, A.S., Niquil, N., Legendre, L., 2014. Planktonic food webs revisited: Reanalysis of results from the linear inverse approach. Progress in Oceanography 120, 216–229. https://doi.org/10.1016/j.pocean.2013.09.003

Sakka Hlaili A., Sahraoui Khalifa I., Bouchouicha-Smida D., Ben Garali S, Ksouri J., Chalghaf M, N., Kooistra WHCF., de la Iglesia P., Diogène J., 2016. Toxic and potentially toxic diatom

blooms in Tunisian (SW Mediterranean) waters: review of ten years of investigations. Adv Environ Res, 48, J.A. Daniels (Ed.), Nova Publisher, New York, NY, 51-70.

Salgado-Hernanz, P.M., Racault, M.-F., Font-Muñoz, J.S., Basterretxea, G., 2019. Trends in phytoplankton phenology in the Mediterranean Sea based on ocean-colour remote sensing. Remote Sensing of Environment 221, 50–64. https://doi.org/10.1016/j.rse.2018.10.036

Sanders, R.W., Berninger, U.-G., Lim, E.L., Kemp, P.F., Caron, D.A., 2000. Heterotrophic and mixotrophic nanoplankton predation on picoplankton in the Sargasso Sea and on Georges Bank. Marine Ecology Progress Series 192, 103–118. https://doi.org/10.3354/meps192103

Sargian P., Mas S., Pelletier E., Demers S., 2007. Multiple stressors on an Antarctic microplankton assemblage: water soluble crude oil and enhanced UVBR level at Ushuaia (Argentina). Polar Biol, 30, 829-841. https://doi.org/10.1007/s00300-006-0243-1

Sautour, B., Artigas, L.F., Delmas, D., Herbland, A., Laborde, P., 2000. Grazing impact of micro- and mesozooplankton during a spring situation in coastal waters off the Gironde estuary. Journal of Plankton Research 22, 531–552. https://doi.org/10.1093/plankt/22.3.531

Scharler, U.M., Baird, D., 2005. A comparison of selected ecosystem attributes of three South African estuaries with different freshwater inflow regimes, using network analysis. Journal of Marine Systems 56, 283–308. https://doi.org/10.1016/j.jmarsys.2004.12.003

Seong, K.A., Jeong, H.J., Kim, S., Kim, G.H., Kang, J.H., 2006. Bacterivory by co-occurring red-tide algae, heterotrophic nanoflagellates, and ciliates. Marine Ecology Progress Series 322, 85–97. https://doi.org/10.3354/meps322085

Setta, S.P., 2018. The Interaction Between Phytoplankton and Bacteria in Response to Oil and Dispersant; Implications for Microbial Mutualism and Carbon Cycling (Thesis).

Severin, T., Bacosa, H.P., Sato, A., Erdner, D.L., 2016. Dynamics of Heterocapsa sp. and the associated attached and free-living bacteria under the influence of dispersed and undispersed crude oil. Letters in Applied Microbiology 63, 419–425. https://doi.org/10.1111/lam.12661

Severin, T., Erdner, D.L., 2019. The Phytoplankton Taxon-Dependent Oil Response and Its Microbiome: Correlation but Not Causation. Frontiers in Microbiology 10.

Shaiek, M., Haj, S.B., Aissi, M., Amer, I.B., 2017. First record of Pachygrapsus maurus (Lucas, 1846) in the Northern Tunisian coast.

Sharp, J.H., Peltzer, E.T., Alperin, M.J., Cauwet, G., Farrington, J.W., Fry, B., Karl, D.M., Martin, J.H., Spitzy, A., Tugrul, S., Carlson, C.A., 1993. Procedures subgroup report. Marine Chemistry, Measurement of Dissolved Organic Carbon and Nitrogen in Natural Waters 41, 37–49. https://doi.org/10.1016/0304-4203(93)90104-V

Sheng YL., Tang DL., Pan G., 2011. Phytoplankton bloom over the Northwest Shelf of Australia after the Montara oil spill in 2009. Geomat Nat Hazards Risk. 2(4):329–347. https://dx.doi.org/10.1080/19475705.2011.564213

Sherr, E., Sherr, B., 1988. Role of microbes in pelagic food webs: A revised concept. Limnology and Oceanography 33, 1225–1227. https://doi.org/10.4319/lo.1988.33.5.1225

Sherr, E.B., Sherr, B.F., 1987. High rates of consumption of bacteria by pelagic ciliates. Nature 325, 710–711. https://doi.org/10.1038/325710a0

Sherr, E.B., Sherr, B.F., 1993. Preservation and Storage of Samples for Enumeration of Heterotrophic Protists, in: Handbook of Methods in Aquatic Microbial Ecology. CRC Press.

Sherr, E.B., Sherr, B.F., 2007. Heterotrophic dinoflagellates: a significant component of microzooplankton biomass and major grazers of diatoms in the sea. Marine Ecology Progress Series 352, 187–197. https://doi.org/10.3354/meps07161

Sherr, E.B., Sherr, B.F., Fallon, R.D., Newell, S.Y., 1986. Small, aloricate ciliates as a major component of the marine heterotrophic nanoplankton1. Limnology and Oceanography 31, 177–183. https://doi.org/10.4319/lo.1986.31.1.0177

Sherr, E.B., Sherr, B.F., Hartz, A.J., 2009. Microzooplankton grazing impact in the Western Arctic Ocean. Deep Sea Research Part II: Topical Studies in Oceanography, The Western Artic Shelf-Basin Interactions (SBI)Project, Vol.2 56, 1264–1273. https://doi.org/10.1016/j.dsr2.2008.10.036

Shevchenko OG., Orlova TY., Hernandez-Becerril DU., 2006. The genus Chaetoceros (Bacillariophyta) from Peter the Great Bay, Sea of Japan. Bot Mar 49, 236–258. https://doi.org/10.1515/BOT.2006.028

Sieburth, J.McN., Smetacek, V., Lenz, J., 1978. Pelagic ecosystem structure: Heterotrophic compartments of the plankton and their relationship to plankton size fractions 1. Limnology and Oceanography 23, 1256–1263. https://doi.org/10.4319/lo.1978.23.6.1256

Silkin VA., Abakumov AI., Pautova LA., Mikaelyan AS., Chasovnikov VK., Lukasheva TA., 2011. Coexistence of non-native and Black Sea phytoplankton species: Discussion of invasion hypotheses. Russ J Biol Invasions, 2(4), 256-264. http://doi.org/10.1134/S2075111711040102

Šimek, K., Bobková, J., Macek, M., Nedoma, J., Psenner, R., 1995. Ciliategrazing on picoplankton in a eutrophic reservoir during the summer phytoplankton maximum: A study at the species and community level. Limnology and Oceanography 40, 1077–1090. https://doi.org/10.4319/lo.1995.40.6.1077

Sime-Ngando, T., 2012. Phytoplankton Chytridiomycosis: Fungal Parasites of Phytoplankton and Their Imprints on the Food Web Dynamics. Frontiers in Microbiology 3.

Sime-Ngando, T., M, G., S, R., Jp, C., 1995. Significance of planktonic ciliated protozoa in the Lower St. Lawrence Estuary: comparison with bacterial, phytoplankton, and particulate organic carbon. Aquatic Microbial Ecology 09, 243–258. https://doi.org/10.3354/ame009243

Sintes, E., Martínez-Taberner, A., Moyà, G., Ramon, G., 2004. Dissecting the microbial food web: structure and function in the absence of autotrophs. Aquatic Microbial Ecology 37, 283–293. https://doi.org/10.3354/ame037283

Siokou-Frangou, I., Christaki, U., Mazzocchi, M.G., Montresor, M., Ribera d'Alcalá, M., Vaqué, D., Zingone, A., 2010. Plankton in the open Mediterranean Sea: a review. Biogeosciences 7, 1543–1586. https://doi.org/10.5194/bg-7-1543-2010

Slaughter, A.M., Bollens, S.M., Bollens, G.R., 2006. Grazing impact of mesozooplankton in an upwelling region off northern California, 2000–2003. Deep Sea Research Part II: Topical Studies in Oceanography, The Role of Wind-Driven Flow in Shelf Productivity 53, 3099–3115. https://doi.org/10.1016/j.dsr2.2006.07.005

Smith, V.H., Joye, S.B., Howarth, R.W., 2006. Eutrophication of freshwater and marine ecosystems. Limnology and Oceanography 51, 351–355. https://doi.org/10.4319/lo.2006.51.1_part_2.0351

Sobczak, W.V., Cloern, J.E., Jassby, A.D., Müller-Solger, A.B., 2002. Bioavailability of organic matter in a highly disturbed estuary: The role of detrital and algal resources. Proceedings of the National Academy of Sciences 99, 8101–8105. https://doi.org/10.1073/pnas.122614399

Sobek, A., Cornelissen, G., Tiselius, P., Gustafsson, Ö., 2006. Passive Partitioning of Polychlorinated Biphenyls between Seawater and Zooplankton, a Study Comparing Observed Field Distributions to Equilibrium Sorption Experiments. Environ. Sci. Technol. 40, 6703–6708. https://doi.org/10.1021/es061248c

Šolić, M., Krstulović, N., Kušpilić, G., Ninčević Gladan, Ž., Bojanić, N., Šestanović, S., Šantić, D., Ordulj, M., 2010. Changes in microbial food web structure in response to changed environmental trophic status: A case study of the Vranjic Basin (Adriatic Sea). Marine Environmental Research 70, 239–249. https://doi.org/10.1016/j.marenvres.2010.05.007

Sommer, U., Adrian, R., De Senerpont Domis, L., Elser, J.J., Gaedke, U., Ibelings, B., Jeppesen, E., Lürling, M., Molinero, J.C., Mooij, W.M., van Donk, E., Winder, M., 2012. Beyond the Plankton Ecology Group (PEG) Model: Mechanisms Driving Plankton Succession. Annual Review of Ecology, Evolution, and Systematics 43, 429–448. https://doi.org/10.1146/annurev-ecolsys-110411-160251

Song Y., Guo Y., Liu H., Zhang G., Zhang X., Thangaraj S., Sun J., 2022. Water quality shifts the dominant phytoplankton group from diatoms to dinoflagellates in the coastal ecosystem of the Bohai Bay. Mar Pollut Bull, 183: 114078. https://doi.org/10.1016/j.marpolbul.2022.114078

Sorgente, R., Olita, A., Oddo, P., Fazioli, L., Ribotti, A., 2011. Numerical simulation and decomposition of kinetic energy in the Central Mediterranean: insight on mesoscale circulation and energy conversion. Ocean Sci. 7, 503–519. https://doi.org/10.5194/os-7-503-2011

Soto LA., Botello AV., Licea-Duran S., Lizarraga-Partida ML., Yanez-Arancibia A., 2014. The environmental legacy of the Ixtoc-I oil spill in Campeche Sound, southwestern Gulf of Mexico. Front Mar Sci. 1:57. https://doi.org/10.3389/fmars.2014.00057

Sreekanth, G.B., Chakraborty, S.K., Jaiswar, A.K., Zacharia, P.U., Mohamed, K.S., 2021. Modeling the impacts of fishing regulations in a tropical Indian estuary using Ecopath with Ecosim approach. Environ Dev Sustain 23, 17745–17763. https://doi.org/10.1007/s10668-021-01410-3

Stec, K.F., Caputi, L., Buttigieg, P.L., D'Alelio, D., Ibarbalz, F.M., Sullivan, M.B., Chaffron, S., Bowler, C., Ribera d'Alcalà, M., Iudicone, D., 2017. Modelling plankton ecosystems in the meta-omics era. Are we ready? Marine Genomics 32, 1–17. https://doi.org/10.1016/j.margen.2017.02.006

Steele, J.H., 1974. The Structure of Marine Ecosystems, in: The Structure of Marine Ecosystems. Harvard University Press. https://doi.org/10.4159/harvard.9780674592513

Steenbeek, J., Corrales, X., Platts, M., Coll, M., 2018. Ecosampler: A new approach to assessing parameter uncertainty in Ecopath with Ecosim. SoftwareX 7, 198–204. https://doi.org/10.1016/j.softx.2018.06.004

Steinberg, D.K., Carlson, C.A., Bates, N.R., Goldthwait, S.A., Madin, L.P., Michaels, A.F., 2000. Zooplankton vertical migration and the active transport of dissolved organic and inorganic carbon in the Sargasso Sea. Deep Sea Research Part I: Oceanographic Research Papers 47, 137–158. https://doi.org/10.1016/S0967-0637(99)00052-7

Steinberg, D.K., Landry, M.R., 2017. Zooplankton and the Ocean Carbon Cycle. Annual Review of Marine Science 9, 413–444. https://doi.org/10.1146/annurev-marine-010814-015924

Stibor, H., Stockenreiter, M., Nejstgaard, J.C., Ptacnik, R., Sommer, U., 2019. Trophic switches in pelagic systems. Current Opinion in Systems Biology, • Systems biology of model organisms • Systems ecology and evolution 13, 108–114. https://doi.org/10.1016/j.coisb.2018.11.006

Stockner, J.G., Antia, N.J., 1986. Algal Picoplankton from Marine and Freshwater Ecosystems: A Multidisciplinary Perspective. Can. J. Fish. Aquat. Sci. 43, 2472–2503. https://doi.org/10.1139/f86-307

Stockner, J.G, Callieri, C., Cronberg, G., 2002. Picoplankton and Other Non-Bloom-Forming Cyanobacteria in Lakes, in: Whitton, B.A., Potts, M. (Eds.), The Ecology of Cyanobacteria: Their Diversity in Time and Space. Springer Netherlands, Dordrecht, pp. 195–231. https://doi.org/10.1007/0-306-46855-7_7

Strom, S.L., Morello, T.A., 1998. Comparative growth rates and yields of ciliates and heterotrophic dinoflagellates. Journal of Plankton Research 20, 571–584. https://doi.org/10.1093/plankt/20.3.571

Strom, S.L., Brainard, M.A., Holmes, J.L., Olson, M.B., 2001. Phytoplankton blooms are strongly impacted by microzooplankton grazing in coastal North Pacific waters. Marine Biology 138, 355–368. https://doi.org/10.1007/s002270000461

Subramaniam, R.C., Corney, S.P., Melbourne-Thomas, J., Péron, C., Ziegler, P., Swadling, K.M., 2022. Spatially explicit food web modelling to consider fisheries impacts and ecosystem representation within Marine Protected Areas on the Kerguelen Plateau. ICES Journal of Marine Science 79, 1327–1339. https://doi.org/10.1093/icesjms/fsac056

Suchanek, T.H., 1993. Oil Impacts on Marine Invertebrate Populations and Communities1. American Zoologist 33, 510–523. https://doi.org/10.1093/icb/33.6.510

Sun L., Chiu MH., Xu C., Lin P., Schwehr KA., Bacosa H., Kamalanathan M., Quigg A., Chin WC., Santschi PH., 2018. The effects of sunlight on the composition of exopolymeric substances and subsequent aggregate formation during oil spills. Mar Chem, 203, 49-54, https://doi.org/10.1016/j.marchem.2018.04.006

Taberlet, P., Coissac, E., Pompanon, F., Brochmann, C., Willerslev, E., 2012. Towards next-generation biodiversity assessment using DNA metabarcoding. Molecular Ecology 21, 2045–2050. https://doi.org/10.1111/j.1365-294X.2012.05470.x

~T~

Taffi, M., Paoletti, N., Liò, P., Pucciarelli, S., Marini, M., 2015. Bioaccumulation modelling and sensitivity analysis for discovering key players in contaminated food webs: The case study of PCBs in the Adriatic Sea. Ecological Modelling, Special Issue: Ecological Modelling for Ecosystem Sustainability: Selected papers presented at the 19th ISEM Conference, 28-31 October 2013, Toulouse, France 306, 205–215. https://doi.org/10.1016/j.ecolmodel.2014.11.030

Tanaka, T., Zohary, T., Krom, M.D., Law, C.S., Pitta, P., Psarra, S., Rassoulzadegan, F., Thingstad, T.F., Tselepides, A., Woodward, E.M.S., Flaten, G.A.F., Skjoldal, E.F., Zodiatis, G., 2007. Microbial community structure and function in the Levantine Basin of the eastern Mediterranean. Deep Sea Research Part I: Oceanographic Research Papers 54, 1721–1743. https://doi.org/10.1016/j.dsr.2007.06.008

Tang D., Sun J., Zhou L., Wang S., Singh RP., Pan G., 2019. Ecological response of phytoplankton to the oil spills in the oceans, Geomatics Nat Hazards Risk, 10(1), 853-872. https://doi.org/10.1080/19475705.2018.1549110

Tang, C.H., Buskey, E.J., 2022a. De-coupled phytoplankton growth and microzooplankton grazing in a simulated oil spill event in mesocosms. Marine Pollution Bulletin 178, 113631. https://doi.org/10.1016/j.marpolbul.2022.113631

Tang, C.H., Buskey, E.J., 2022b. Impaired grazing of marine protozoa in sub-lethal exposure to the water accommodated fraction of crude oil and dispersant. Environmental Pollution 315, 120414. https://doi.org/10.1016/j.envpol.2022.120414

Taş, S., Okuş, E., Ünlü, S., & Altiok, H., 2011. A study on phytoplankton following 'Volgoneft-248' oil spill on the north-eastern coast of the Sea of Marmara. J Mar Biolog Assoc UK, 91(3), 715-725. https://doi.org/10.1017/S0025315410000330

Tecchio, S., Chaalali, A., Raoux, A., Tous Rius, A., Lequesne, J., Girardin, V., Lassalle, G., Cachera, M., Riou, P., Lobry, J., Dauvin, J.-C., Niquil, N., 2016. Evaluating ecosystem-level anthropogenic impacts in a stressed transitional environment: The case of the Seine estuary. Ecological Indicators 61, 833–845. https://doi.org/10.1016/j.ecolind.2015.10.036

Tecchio, S., Rius, A.T., Dauvin, J.-C., Lobry, J., Lassalle, G., Morin, J., Bacq, N., Cachera, M., Chaalali, A., Villanueva, M.C., Niquil, N., 2015. The mosaic of habitats of the Seine estuary: Insights from food-web modelling and network analysis. Ecological Modelling 312, 91–101. https://doi.org/10.1016/j.ecolmodel.2015.05.026

Templado, J., 2014. Future Trends of Mediterranean Biodiversity, in: Goffredo, S., Dubinsky, Z. (Eds.), The Mediterranean Sea. Springer Netherlands, Dordrecht, pp. 479–498. https://doi.org/10.1007/978-94-007-6704-1_28

Ter Braak, 1986. Canonical Correspondence Analysis: A New Eigenvector Technique for Multivariate Direct Gradient Analysis - ter Braak - 1986 - Ecology - Wiley Online Library [WWW Document]. URL https://esajournals.onlinelibrary.wiley.com/doi/abs/10.2307/1938672 (accessed 6.8.22).

Tesán-Onrubia, J.A., Tedetti, M., Carlotti, F., Tenaille, M., Guilloux, L., Pagano, M., Lebreton, B., Guillou, G., Fierro-González, P., Guigue, C., Chifflet, S., Garcia, T., Boudriga, I., Belhassen, M., Zouari, A.B., Bănaru, D., 2023. Spatial variations of biochemical content and stable isotope ratios of size-fractionated plankton in the Mediterranean Sea (MERITE-HIPPOCAMPE campaign). Marine Pollution Bulletin 189, 114787. https://doi.org/10.1016/j.marpolbul.2023.114787

Thomas, C.R., Christian, R.R., 2001. Comparison of nitrogen cycling in salt marsh zones related to sea-level rise. Marine Ecology Progress Series 221, 1–16. https://doi.org/10.3354/meps221001

Thompson, R.M., Brose, U., Dunne, J.A., Hall, R.O., Hladyz, S., Kitching, R.L., Martinez, N.D., Rantala, H., Romanuk, T.N., Stouffer, D.B., Tylianakis, J.M., 2012. Food webs: reconciling the structure and function of biodiversity. Trends in Ecology & Evolution 27, 689–697. https://doi.org/10.1016/j.tree.2012.08.005

Thornton, D.C.O., 2014. Dissolved organic matter (DOM) release by phytoplankton in the contemporary and future ocean. European Journal of Phycology 49, 20–46. https://doi.org/10.1080/09670262.2013.875596

Tomajka J., 1985. The influence of petroleum hydrocarbons on the primary production of the Danube River plankton. Acta Hydrochim Hydrobiol, 13: 615-618.

Tomlinson, S., Arnall, S.G., Munn, A., Bradshaw, S.D., Maloney, S.K., Dixon, K.W., Didham, R.K., 2014. Applications and implications of ecological energetics. Trends in Ecology & Evolution 29, 280–290. https://doi.org/10.1016/j.tree.2014.03.003

Totti, C., Cangini, M., Ferrari, C., Kraus, R., Pompei, M., Pugnetti, A., Romagnoli, T., Vanucci, S., Socal, G., 2005. Phytoplankton size-distribution and community structure in relation to mucilage occurrence in the northern Adriatic Sea. Science of The Total Environment, Mucilages in the Adriatic and Tyrrhenian Seas 353, 204–217. https://doi.org/10.1016/j.scitotenv.2005.09.028

Tréguer P., Bowler C., Moriceau B., Dutkiewicz S., Gehlen M., Aumont O., Bittner L., Dugdale R., Finkel Z., Iudicone D., Jahn O., Guidi L., Lasbleiz M., Leblanc K., Levy M., Pondaven P., 2018. Influence of diatom diversity on the ocean biological carbon pump. Nature Geosci, 11: 27–37. https://doi.org/10.1038/s41561-017-0028-x

Trombetta, T., Vidussi, F., Roques, C., Mas, S., Scotti, M., Mostajir, B., 2021. Co-occurrence networks reveal the central role of temperature in structuring the plankton community of the Thau Lagoon. Sci Rep 11, 17675. https://doi.org/10.1038/s41598-021-97173-y

Trombetta, T., Bouget, F.-Y., Félix, C., Mostajir, B., Vidussi, F., 2022. Microbial Diversity in a North Western Mediterranean Sea Shallow Coastal Lagoon Under Contrasting Water Temperature Conditions. Frontiers in Marine Science 9. https://doi.org/10.3389/fmars.2022.858744

Tseng, L.-C., Kumar, R., Dahms, H.-U., Chen, Q.-C., Hwang, J.-S., 2008. Copepod Gut Contents, Ingestion Rates, and Feeding Impacts in Relation to Their Size Structure in the Southeastern Taiwan Strait. Zoological Studies 15.

Turner, R.E., 2002. Element ratios and aquatic food webs. Estuaries 25, 694–703. https://doi.org/10.1007/BF02804900

-U-

Ulanowicz, R., 1986. PHENOMENOLOGICAL PERSPECTIVE OF ECOLOGICAL DEVELOPMENT. ASTM Special Technical Publication 73–81.

Ulanowicz, R., 1992. Ecosystem health and trophic flow networks. pp. 190–225.

Ulanowicz, R., 1997. Ecology, the Ascendent Perspective. Columbia University Press, New York.

Ulanowicz, R.E., 2004. Quantitative methods for ecological network analysis. Computational Biology and Chemistry 28, 321–339. https://doi.org/10.1016/j.compbiolchem.2004.09.001

Ulanowicz, R.E., Goerner, S.J., Lietaer, B., Gomez, R., 2009. Quantifying sustainability: Resilience, efficiency and the return of information theory. Ecological Complexity 6, 27–36. https://doi.org/10.1016/j.ecocom.2008.10.005

Urakawa, H., Garcia, J.C., Barreto, P.D., Molina, G.A., Barreto, J.C., 2012. A sensitive crude oil bioassay indicates that oil spills potentially induce a change of major nitrifying prokaryotes from the Archaea to the Bacteria. Environmental Pollution 164, 42–45. https://doi.org/10.1016/j.envpol.2012.01.009

Utermöhl, H., 1931. Neue Wege in der quantitativen Erfassung des Plankton.(Mit besonderer Berücksichtigung des Ultraplanktons.). SIL Proceedings, 1922-2010 5, 567–596. https://doi.org/10.1080/03680770.1931.11898492

Utermöhl H., 1958. Zur Vervollkomnung der quantitativen Phytoplankton-Methodik. Mitt int Ver ther angew Limnol, 9: 1-38.

-V-

Van den Meersche, K., Middelburg, J.J., Soetaert, K., van Rijswijk, P., Boschker, H.T.S., Heip, C.H.R., 2004. Carbon-nitrogen coupling and algal-bacterial interactions during an experimental bloom: Modeling a 13C tracer experiment. Limnology and Oceanography 49, 862–878. https://doi.org/10.4319/lo.2004.49.3.0862

Van den Meersche, K., Soetaert, K., Oevelen, D.V., 2009. xsample(): An R Function for Sampling Linear Inverse Problems. Journal of Statistical Software 30, 1–15. https://doi.org/10.18637/jss.v030.c01

Varela M, Bode A., Lorenzo J., Alvarez-Ossorio MT., Miranda A., Patrocinio T., Anadon R., Viesca L., Rodriguez N., Valdés L., Cabal J., Urritia A., Garcia-Soto C., Rodriguez M., Alvarez-Salgado XA., Groom S., 2006. The effect of the 'Prestige' oil spill on the plankton of the N–NW Spanish Coast. Mar Pollut Bull, 53: 272–286. https://doi.org/10.1016/j.marpolbul.2005.10.005

Vargas, C.A., González, H.E., 2004. Plankton community structure and carbon cycling in a coastal upwelling system. II. Microheterotrophic pathway. Aquatic Microbial Ecology 34, 165–180. https://doi.org/10.3354/ame034165

Vargha, A., Delaney, H.D., 2000. A Critique and Improvement of the CL Common Language Effect Size Statistics of McGraw and Wong. Journal of Educational and Behavioral Statistics 25, 101–132. https://doi.org/10.3102/10769986025002101

Varkitzi, I., Psarra, S., Assimakopoulou, G., Pavlidou, A., Krasakopoulou, E., Velaoras, D., Papathanassiou, E., Pagou, K., 2020. Phytoplankton dynamics and bloom formation in the oligotrophic Eastern Mediterranean: Field studies in the Aegean, Levantine and Ionian seas. Deep Sea Research Part II: Topical Studies in Oceanography, Revisiting the Eastern Mediterranean: Recent knowledge on the physical, biogeochemical and ecosystemic states and trends (Volume II) 171, 104662. https://doi.org/10.1016/j.dsr2.2019.104662

Vasconcellos, M., Mackinson, S., Sloman, K., Pauly, D., 1997. The stability of trophic mass-balance models of marine ecosystems: a comparative analysis. Ecological Modelling 100, 125–134. https://doi.org/10.1016/S0304-3800(97)00150-6

Vascotto, I., Mozetič, P., Francé, J., 2021. Phytoplankton Time-Series in a LTER Site of the Adriatic Sea: Methodological Approach to Decipher Community Structure and Indicative Taxa. Water 13, 2045. https://doi.org/10.3390/w13152045

Veen, A., 1991. Ecophysiological studies on the phagotrophic phytoflagellate Dinobryon divergens Imhof (PhD Thesis). Universiteit van Amsterdam.

Verity, P.G., Paffenhofer, G.-A., 1996. On assessment of prey ingestion by copepods. Journal of Plankton Research 18, 1767–1779. https://doi.org/10.1093/plankt/18.10.1767

Verity, P.G., Robertson, C.Y., Tronzo, C.R., Andrews, M.G., Nelson, J.R., Sieracki, M.E., 1992. Relationships between cell volume and the carbon and nitrogen content of marine photosynthetic nanoplankton. Limnology and Oceanography 37, 1434–1446. https://doi.org/10.4319/lo.1992.37.7.1434

Verity, P.G., Wassmann, P., Frischer, M.E., Howard-Jones, M.H., Allen, A.E., 2002. Grazing of phytoplankton by microzooplankton in the Barents Sea during early summer. Journal of Marine Systems, Seasonal C-cycling variability in the open and ice-covered waters of the Barents Sea 38, 109–123. https://doi.org/10.1016/S0924-7963(02)00172-0

Verlecar XN., Desai SR., Sarkar A., Dalal SG., 2006. Biological indicators in relation to coastal pollution along Karnataka Coast, India. Wat Res, 40, 3304-3312. http://doi.org/10.1016/j.watres.2006.06.022

Vézina, A.F., Platt, T., 1987. Small-Scale Variability of New Production and Particulate Fluxes in the Ocean. Can. J. Fish. Aquat. Sci. 44, 198–205. https://doi.org/10.1139/f87-026

Vézina, A.F, Piatt, T., 1988. Food web dynamics in the ocean. I. Best-estimates of flow networks using inverse methods. Mar. Ecol. Prog. Ser. 42, 269–287. https://doi.org/10.3354/meps042269

Vézina, A.F., Pahlow, M., 2003. Reconstruction of ecosystem flows using inverse methods: how well do they work? Journal of Marine Systems, The Use of Data Assimilation in Coupled Hydrodynamic, Ecological and Bio-geo-chemical Models of the Ocean. Selected papers from the 33rd International Liege Colloquium on Ocean Dynamics, held in Liege, Belgium on May 7-11th, 2001. 40–41, 55–77. https://doi.org/10.1016/S0924-7963(03)00013-7

Vidussi, F., Marty, J.-C., Chiavérini, J., 2000. Phytoplankton pigment variations during the transition from spring bloom to oligotrophy in the northwestern Mediterranean sea. Deep Sea Research Part I: Oceanographic Research Papers 47, 423–445. https://doi.org/10.1016/S0967-0637(99)00097-7

Viñas, M.D., Negri, R.M., Cepeda, G.D., Hernández, D., Silva, R., Daponte, M.C., Capitanio, F.L., 2013. Seasonal succession of zooplankton in coastal waters of the Argentine Sea (Southwest Atlantic Ocean): prevalence of classical or microbial food webs. Marine Biology Research 9, 371–382. https://doi.org/10.1080/17451000.2012.745003

~W~

Wanjohi, L., Mwamburi, L., Too, E., Aloo, B., KOSGEI, J., 2015. ISOLATION AND IDENTIFICATION OF BACTERIA WITH BIOREMEDIATION POTENTIAL OF OIL SPILLS IN LAKE NAKURU, KENYA. Asian Journal of Microbiology, Biotechnology and Environmental Sciences 17, 831–838.

Ward, B., Dutkiewicz, S., Jahn, O., follows, michael, 2012. A size-structured food-web model for the global ocean. Limnology and Oceanography 57, 1877–1891. https://doi.org/10.4319/lo.2012.57.6.1877

Ward, B.A., Follows, M.J., 2016. Marine mixotrophy increases trophic transfer efficiency, mean organism size, and vertical carbon flux. Proceedings of the National Academy of Sciences 113, 2958–2963. https://doi.org/10.1073/pnas.1517118113

White, H.K., Hsing, P.-Y., Cho, W., Shank, T.M., Cordes, E.E., Quattrini, A.M., Nelson, R.K., Camilli, R., Demopoulos, A.W.J., German, C.R., Brooks, J.M., Roberts, H.H., Shedd, W., Reddy, C.M., Fisher, C.R., 2012. Impact of the Deepwater Horizon oil spill on a deep-water coral community in the Gulf of Mexico. Proceedings of the National Academy of Sciences 109, 20303–20308. https://doi.org/10.1073/pnas.1118029109

Wickham, S.A., Wenta, P., Sinner, A., Weiss, R., 2022. Microzooplankton grazing and community composition in a high-productivity marine ecosystem. Journal of Plankton Research 44, 414–426. https://doi.org/10.1093/plankt/fbac015

Wirtz KW., Liu X., 2006. Integrating economy, ecology, and uncertainity in an oil spill DSS: the Prestige accident in Spain 2002. Estuar Coast Shelf Sci, 70: 525-532. https://doi.org/10.1016/j.ecss.2006.06.016

Worm, B., Barbier, E.B., Beaumont, N., Duffy, J.E., Folke, C., Halpern, B.S., Jackson, J.B.C., Lotze, H.K., Micheli, F., Palumbi, S.R., Sala, E., Selkoe, K.A., Stachowicz, J.J., Watson, R., 2006. Impacts of Biodiversity Loss on Ocean Ecosystem Services. Science 314, 787–790. https://doi.org/10.1126/science.1132294

~X~

Xiang, Y., Lam, P.J., Burd, A.B., Hayes, C.T., 2022. Estimating Mass Flux From Size-Fractionated Filtered Particles: Insights Into Controls on Sinking Velocities and Mass Fluxes in Recent U.S. GEOTRACES Cruises. Global Biogeochemical Cycles 36, e2021GB007292. https://doi.org/10.1029/2021GB007292

-Y-

Yang, E.J., Choi, J.K., Hyun, J.-H., 2008. Seasonal variation in the community and size structure of nano- and microzooplankton in Gyeonggi Bay, Yellow Sea. Estuarine, Coastal and Shelf Science 77, 320–330. https://doi.org/10.1016/j.ecss.2007.09.034

Yang, J., Wei, H., Yalin, T., Alan, W., Xiaofeng, L., Jiqiu, L., 2019. Combined effects of food resources and exposure to ammonium nitrogen on population growth performance in the bacterivorous ciliate Paramecium caudatum. European Journal of Protistology 71, 125631. https://doi.org/10.1016/j.ejop.2019.125631

Yang, Martin Günter Joachim Löder 4,5 & Karen Helen Wiltshire 4, & David J. S. Montagnes, 2022. Comparing the Trophic Impact of Microzooplankton during the Spring and Autumn Blooms in Temperate Waters | SpringerLink [WWW Document]. URL https://link.springer.com/article/10.1007/s12237-020-00775-4 (accessed 6.8.22).

Yodzis, P., 1988. The Indeterminacy of Ecological Interactions as Perceived Through Perturbation Experiments. Ecology 69, 508–515. https://doi.org/10.2307/1940449

-Z-

Zaccone, R., Azzaro, M., Azzaro, F., Caruso, G., Caroppo, C., Decembrini, F., Diociaiuti, T., Fonda Umani, S., Leonardi, M., Maimone, G., Monticelli, L.S., Paranhos, R., Placenti, F., Cuttitta, A., Patti, B., La Ferla, R., 2018. Trophic structure and microbial activity in a spawning area of Engraulis encrasicolus. Estuarine, Coastal and Shelf Science 207, 215–222. https://doi.org/10.1016/j.ecss.2018.04.008

Zaghden, H., Kallel, M., Elleuch, B., Oudot, J., Saliot, A., Sayadi, S., 2014. Evaluation of hydrocarbon pollution in marine sediments of Sfax coastal areas from the Gabes Gulf of Tunisia, Mediterranean Sea. Environ Earth Sci 72, 1073–1082. https://doi.org/10.1007/s12665-013-3023-6

Zaghden, H., Barhoumi, B., Jlaiel, L., Guigue, C., Chouba, L., Touil, S., Sayadi, S., Tedetti, M., 2022. Occurrence, origin and potential ecological risk of dissolved polycyclic aromatic hydrocarbons and organochlorines in surface waters of the Gulf of Gabès (Tunisia, Southern Mediterranean Sea). Marine Pollution Bulletin 180, 113737. https://doi.org/10.1016/j.marpolbul.2022.113737

Zayen, A., Sayadi, S., Chevalier, C., Boukthir, M., Ben Ismail, S., Tedetti, M., 2020. Microplastics in surface waters of the Gulf of Gabes, southern Mediterranean Sea: Distribution, composition and influence of hydrodynamics. Estuarine, Coastal and Shelf Science 242, 106832. https://doi.org/10.1016/j.ecss.2020.106832

Zehr JP., Kudela RM., 2011. Nitrogen cycle of the open ocean: from genes to ecosystems. Ann Rev Mar Sci, 3:197–225. https://doi.org/10.1146/annurev-marine-120709-142819

Zeldis, J.R., Décima, M., 2020. Mesozooplankton connect the microbial food web to higher trophic levels and vertical export in the New Zealand Subtropical Convergence Zone. Deep Sea Research Part I: Oceanographic Research 155, 103146. https://doi.org/10.1016/j.dsr.2019.103146

Zhang Y., Wang, Tan L., 2019. Characterization of allelochemicals of the diatom Chaetoceros curvisetus and the effects on the growth of Skeletonema costatum. Sci Total Environ, 660, 269-276. https://doi.org/10.1016/j.scitotenv.2019.01.056.

Zhang, S., Liu, H., Ke, Y., Li, B., 2017. Effect of the Silica Content of Diatoms on Protozoan Grazing. Frontiers in Marine Science 4.

Zhu, Z.-Z., Ma, K.-J., Ran, X., Zhang, H., Zheng, C.-J., Han, T., Zhang, Q.-Y., Qin, L.-P., 2011. Analgesic, anti-inflammatory and antipyretic activities of the petroleum ether fraction from the ethanol extract of Desmodium podocarpum. Journal of Ethnopharmacology 133, 1126–1131. https://doi.org/10.1016/j.jep.2010.11.042

Zingone, A., Sarno, D., Siano, R., Marino, D., 2011. The importance and distinctiveness of small-sized phytoplankton in the Magellan Straits. Polar Biol 34, 1269–1284. https://doi.org/10.1007/s00300-010-093

Étude de l'état de santé des écosystèmes côtiers sud méditerranéens anthropisés par application des modèles du réseau trophique planctonique et des indicateurs écologiques en situation de contamination chronique & pulsée.

Résumé

Les écosystèmes côtiers méditerranéens sont considérés parmi les zones les plus perturbées vu qu'elles sont soumises à une importance pression anthropique, qui a conduit à leur eutrophisation et leur contamination par divers types de polluants chimiques. Ces perturbations ont des conséquences sur le fonctionnement de ces écosystèmes, leur état écologique et ultimement sur leurs capacités d'exportation de carbone et de productivité. C'est dans ce contexte que ce travail a été mené visant à étudier l'état de santé des deux écosystèmes côtiers sud méditerranéens anthropisés en caractérisant les réseaux trophiques planctoniques (RTPs) et en appliquant des indicateurs écologiques. Cette étude a concerné le Golfe de Gabès qui est caractérisé par une forte hydrodynamique et une contamination chronique due principalement aux industries du complexe Gannouche-Gabès et le Canal de Bizerte qui a été soumis à une contamination pulsée causée par une fuite de pétrole.

Dans le Golfe de Gabès, la dynamique spatiale du RTP a été étudiée en automne 2017 lors de la campagne MERMEX-MERITE dans quatre stations situées à différentes distances de la principale source de contamination. Des échantillonnages et des incubations in situ ont été conduits à chaque station pour déterminer les conditions environnementales, et nutritives entre autres, les biomasses carbonées des composantes du réseau [carbone organique particulaire et dissous, bactérioplancton, picophytoplancton (< 2 µm), nanophytoplancton (2-10 µm), microphytoplancton (> 10 µm), protozooplancton et métazooplancton (> 200 µm)] et certains flux de carbone (production bactérienne et phytoplanctonique, consommation du protozooplancton et du métazooplancton et sédimentation des particules). Les flux estimés à partir des données de terrain ont été utilisés dans une analyse inverse de Monte Carlo en Chaîne de Markov (LIM-MCMC) pour calculer les flux manquants afin de construire des modèles du RTP de chaque station. Cette analyse inverse était suivie par une analyse des indicateurs écologiques (ENAs et ratios de typologie) afin de dégager les propriétés structurales et fonctionnelles des RTPs. Les résultats ont montré que la circulation hydrodynamique complexe dans le Golfe semble induire un gradient nord-sud et côte-large des concentrations nutritives conduisant à des variations spatiales dans la structuration en taille et la production du phytoplancton ainsi que dans les interactions trophiques. Par conséquent différentes voies trophiques ont été distinguées en fonction du stress nutritif. Le réseau microbien dominait à la station la moins riche en nutriments (la plus au nord) et se caractérisait par la production primaire et l'activité les plus faibles, mais par l'ascendance la plus élevée, reflétant une importante organisation et stabilité. Le système à la station la plus eutrophe (la plus au sud) fonctionnait comme un réseau herbivore et était le plus actif avec une forte production primaire et débit total de carbone, mais restait le moins organisé et le moins stable. Dans les deux autres stations, un réseau multivore s'est développé et était le plus organisé grâce à une importante détritivorie par rapport à l'herbivorie, un fort recycle et une ascendance élevée.

Dans le Canal de Bizerte, les effets d'une marée noire, survenue en octobre 2018, sur les communautés du phytoplancton et du protozooplancton ainsi que leurs interactions trophiques ont été évalués dès les premiers jours suivant le déversement du pétrole et après quelques semaines. L'évolution du RTP au cours des différents jours suivant le déversement a été aussi décrite. Des échantillonnages et des incubations in situ ont été conduits les 1ier, 4ème, 8ème et 18ème jours après la fuite du pétrole. On a noté la présence d'une nappe de pétrole du 1ier au 8ème jour avec une contamination des eaux par les hydrocarbures aromatiques polycycliques (HAPs), principalement le chrysène. Le phytoplankton a montré des différentes réponses au fil du temps. À court terme (du 1er au 8ème jour), la croissance et la biomasse du picophytoplancton ont augmenté, alors que celles du nano- et du microphytoplancton ont diminué, probablement en raison de la sensibilité des certaines grandes espèces aux HAPs. À plus long terme (18ème jour), la dispersion du pétrole et la réduction de son effet négatif se sont accompagnées par une prolifération des grandes cellules avec un changement dans leur composition taxinomique et une forte accumulation de la biomasse du picophytoplancton, causée par la diminution de leur broutage par le protozooplancton. En conséquence, la structure en taille du phytoplancton a évolué tout au long de l'exposition au pétrole, passant d'une prédominance du microphytoplancton après quelques jours à une dominance à long terme du picophytoplancton. La structure de la communauté du protozooplancton a également changé au fil des jours vers une dominance des dinoflagellés mixotrophes (principalement Heterocapsa) au détriment d'une diminution des dinoflagellés hétérotrophes (i.e. *Gyrodinium* and *Protoperidinium*). Les ciliés (principalement *Strombidium*) ont montré une diminution à court terme mais une récupération au 18ème jour, tandis que les nanoflagellés hétérotrophes étaient plus vulnérables à la toxicité du pétrole et ont disparu à partir du 8ème jour. Les taux de production des différentes fractions de taille du phytoplancton ainsi que leurs taux de consommation par le protozooplancton ont largement varié entre les différents jours. L'intégration de ces taux modifiés par la contamination pétrolière dans des modèles linéaires inverses de flux de carbone et le calcul des indicateurs écologiques ont montré un changement clair dans la structure et le fonctionnement du RTP, de la voie herbivore (au 1ier jour), au réseau multivore (4ème et 8ème jour) jusqu'un réseau microbien spécial (au 18ème jour), ce qui implique différentes efficacités dans l'exportation du carbone tout au long de l'évolution de la marée noire.

Cette étude met en évidence l'importance de coupler la typologie des RTPs et les indicateurs écologiques pour mieux décrire l'état écologique des écosystèmes soumis soit à une contamination permanente ou pulsée. Ces approches intégratives peuvent fournir des outils efficaces pour gérer et évaluer la santé des écosystèmes anthropisés.

Mots clés : Structure de la taille du phytoplancton, production primaire, broutage par le zooplancton, réseau trophique planctonique, contamination chronique, marée noire, ratios de typologie, indices ENAs, Sud-ouest de la mer Méditerranée.

Study of the health status of anthropized southern Mediterranean coastal ecosystems by applying planktonic food web models and ecological indicators in situations of chronic & pulsed contamination.

Abstract

Mediterranean coastal ecosystems are considered to be among the most disturbed zones, as they are subject to considerable anthropogenic pressure, which has led to their eutrophication and contamination by various types of chemical pollutants. These disturbances have consequences for the functioning of these ecosystems, their ecological status and ultimately their carbon export and productivity capacities. It is against this backdrop that this study was carried out to investigate the state of health of two anthropized southern Mediterranean coastal ecosystems by characterizing planktonic food webs (PFWs) and applying ecological indicators. The study focused on the Gulf of Gabès, which is characterized by strong hydrodynamics and chronic contamination due mainly to the industries of the Gannouche-Gabès complex, and the Bizerte Channel, which was subjected to pulsed contamination caused by an oil spill.

In the Gulf of Gabès, the spatial dynamics of the PFWs were studied in autumn 2017 during the MERMEX-MERITE campaign at four stations located at different distances from the main source of contamination. Sampling and *in situ* incubation were conducted at each station to determine environmental and nutrient conditions, including carbon biomass of food webcomponents [particulate and dissolved organic carbon, bacterioplankton, picophytoplankton (< 2 µm), nanophytoplankton (2-10 µm), microphytoplankton (> 10 µm), protozooplankton and metazooplankton (> 200 µm)] and certain carbon fluxes (bacterial and phytoplankton production, protozooplankton and metazooplankton consumption and particulate sedimentation). The fluxes estimated from the field data were used in an inverse Markov Chain Monte Carlo (LIM-MCMC) analysis to calculate the missing fluxes in order to build models of the PFW for each station. This inverse analysis was followed by an analysis of ecological indicators (ENAs and typology ratios) to identify the structural and functional properties of the PFWs. The results showed that the complex hydrodynamic circulation in the Gulf appears to induce a north-south and coast-offshore gradient in nutrient concentrations, leading to spatial variations in phytoplankton size structuring and production, as well as trophic interactions. As a result, different trophic pathways were distinguished as a function of nutrient stress. The microbial food web dominated at the least nutrient-rich station (northernmost) and was characterized by the lowest primary production and activity, but the highest ascendancy, reflecting a high degree of organization and stability. The system at the most eutrophic station (southernmost) functioned as an herbivorous food web and was the most active with high primary production and total carbon flow, but remained the least organized and stable. At the other two stations, a multivorous food web developed and was the most organized thanks to high detritivory compared with herbivory, strong recycling and high ascendancy.

In the Bizerte Channel, the effects of an oil spill, which occurred in October 2018, on phytoplankton and protozooplankton communities and their trophic interactions were assessed from the first days after the oil spill and after a few weeks. In situ sampling and incubation were carried out on days 1, 4, 8 and 18 after the oil spill. The presence of an oil slick was noted from days 1 to 8, with water contamination by polycyclic aromatic hydrocarbons (PAHs), mainly chrysene. Phytoplankton showed different responses over time. In the short term (days 1-8), picophytoplankton growth and biomass increased, while those of nano- and microphytoplankton decreased, probably due to the sensitivity of certain large species to PAHs. In the longer term (day 18), the dispersal of oil and the reduction of its negative effect were accompanied by a proliferation of large cells with a change in their taxonomic composition and a strong accumulation of picophytoplankton biomass, caused by reduced grazing by protozooplankton. As a result, the size structure of phytoplankton evolved throughout oil exposure, from a predominance of microphytoplankton after a few days to a long-term dominance of picophytoplankton. The structure of the protozooplankton community also changed over the days towards a dominance of mixotrophic dinoflagellates (mainly *Heterocapsa*) at the expense of a decrease in heterotrophic dinoflagellates (i.e. *Gyrodinium* and *Protoperidinium*). Ciliates (mainly *Strombidium*) showed a short-term decrease but recovery by day 18, while heterotrophic nanoflagellates were more vulnerable to oil toxicity and disappeared by day 8. The production rates of the various phytoplankton size fractions and their consumption rates by protozooplankton varied widely among days. Integrating these oil contamination-modified rates into linear inverse carbon flux models and calculating ecological indicators showed a clear shift in PFW structure and function, from the herbivorous pathway (at day 1), to the multivorous food web (days 4 and 8) to a special microbial food web (at day 18), implying different carbon export efficiencies throughout the evolution of the oil spill.

This study highlights the importance of coupling PFW typology and ecological indicators to better describe the ecological state of ecosystems subjected to either permanent or pulsed contamination. These integrative approaches can provide effective tools for managing and assessing the health of anthropized ecosystems.

Keywords: Phytoplankton size structure, primary production, zooplankton grazing, planktonic food web, chronic contamination, oil spill, typology ratios, ENAs indices, southwestern Mediterranean Sea.